

Modified Celluloses as Multifunctional Excipients in Rapidly Dissolving Immediate Release Tablets

Inauguraldissertation

zur

Erlangung der Würde eines Doktors der Philosophie
vorgelegt der Philosophisch – Naturwissenschaftlichen Fakultät
der Universität Basel

von

Franziska Simone Müller

Aus Oberhofen, Aargau

Basel, 2008

Genehmigt von der Philosophisch – Naturwissenschaftlichen Fakultät

auf Antrag von

Professor Dr. Hans Leuenberger

Dr. Gabriele Betz

und

PD Dr. Peter van Hoogevest

Basel, den 09.12.08

Professor Dr. Eberhard Parlow
Dekan

meiner Familie

Danksagung / Acknowledgments

Mein tiefster Dank geht an Prof. Dr. Hans Leuenberger, der es mir ermöglicht hat, diese Arbeit unter seiner Aufsicht am Institut für Pharmazeutische Technologie durchzuführen. Ich danke ihm dafür, dass er mich immer wieder von neuem herausgefordert hat, aber auch dass er mir immer hilfsbereit zur Seite gestanden hat.

Ich danke Dr. Gabriele Betz für die Dissertationsleitung.

Ich danke PD Dr. Peter van Hoogevest für die Übernahme des Korreferates.

Ich danke Philippe Tschopp von der Firma Pharmatrans Sanaq AG für die unkomplizierte Zusammenarbeit und die Spende der Cellulosen MCC SANAQ 102, MCC SANAQrapid Type I und Type II. Prof. Vijay Kumar von der Universität Iowa danke ich für das Zuverfügungstellen von UICEL-A/102 und UICEL-XL. Finanziell wurde diese Arbeit unterstützt durch die Stiftung zur Förderung des pharmazeutischen Nachwuchs (Senglet-Stiftung) und den Schweizerischen Nationalfonds.

Ein grosses „grazia“ geht an Stefan Winzap, der mich stets unterstützt hat, sei es bei der vorliegenden Arbeit, im Praktikum, aber auch in persönlichen Belangen. Ich danke ihm für seine freundschaftliche Art und seine enorme Hilfsbereitschaft.

Ich danke Katharina Gloor und Maya von Moos, meinen beiden Masterstudentinnen, die mir eine grosse Unterstützung waren bei der Durchführung dieser Arbeit und mit und von denen ich sehr viel gelernt habe.

Ich danke Maxim Puchkov für seine aufmunternde Art und seine prompte Hilfe bei allen mathematischen Problemen und Michael Lanz für seine unkomplizierte Hilfe bei praktischen Problemen.

Ich danke allen Personen mit denen ich in den letzten mehr als drei Jahren zusammengearbeitet habe. Alle aufzuzählen würde den Rahmen dieser Danksagung sprengen, deshalb erwähne ich namentlich all jene, mit denen mich mehr als die Arbeit verbindet. Ein riesiges Dankeschön an David Blaser, Ivana Vejnovic, Marcel Schneider, Murad Ruman, Selma Sehic, Sonja Reutlinger und Thomas Meyer. Ich danke auch den Mitarbeitern der MolSysTox, die mir im letzten Jahr viel Gesellschaft geleistet haben.

Ganz herzlich möchte ich all jenen Personen danken, die mich zum Teil seit meiner Kindheit treu und mit viel Freundschaft begleiten.

Zu guter Letzt und mit grösster Freude danke ich meinen Eltern und Geschwistern, jenen Menschen also, die mich immer unterstützt haben, und die mich zu dem Menschen werden liessen, der ich bin. Für die Dankbarkeit, die Francesco Corona verdient hat, fehlen mir die Worte: *„E va bene così... senza parole... senza parole...“* (Vasco Rossi).

Table of Contents

SYMBOLS, ABBREVIATIONS, AND COMMENTS	V
1 SUMMARY	1
2 INTRODUCTION	5
2.1 General Considerations	5
2.2 Aims of the Study	7
3 THEORETICAL SECTION	8
3.1 Polymorphism	8
3.2 Cellulose	9
3.2.1 Types of Cellulose and Their Production	9
3.2.2 Polymorphism of Cellulose	11
3.2.3 Comparison of Cellulose Modifications	12
3.2.4 Application of Cellulose Modifications	13
3.3 Granulation	14
3.3.1 Granules	14
3.3.2 Methods of Granulation	14
3.3.3 Granulation Mechanisms	15
3.4 Compaction	17
3.4.1 Introduction	17
3.4.2 Direct Compaction versus Granulation	17
3.4.3 Tableting Process and Bonding Mechanisms	17
3.4.4 Compact Properties	19
3.4.5 Methods of Classification	21
3.4.5.1 Heckel Equation and Modified Heckel Equation	21
3.4.5.2 Leuenberger Equation	22
3.4.5.3 Modified Van der Waals Equation of the State	23
3.4.6 Dilution Capacity	24

TABLE OF CONTENTS

3.5	Liquid - Solid Interactions	26
3.5.1	Introduction	26
3.5.2	Water Uptake	27
3.5.3	Disintegration	30
3.5.3.1	Definition and Relevance of Disintegration	30
3.5.3.2	Mechanisms of Disintegration	30
3.5.3.3	Disintegrants	33
3.5.4	Dissolution	34
3.5.4.1	Definition, Significance, and Developments	34
3.5.4.2	Mathematical Models	36
3.6	Percolation Theory	40
3.6.1	Historical Development and Theoretical Background	40
3.6.2	Application in Powder Technology	42
4	MATERIAL AND METHODS	45
4.1	Material	45
4.1.1	Storage	45
4.1.2	Model Drug	45
4.1.3	Excipients	45
4.1.3.1	Celluloses	45
4.1.3.2	Magnesium Stearate	46
4.1.3.3	PVP	46
4.1.4	Powder Characterisation	47
4.1.4.1	Structure Analysis with X-Ray	47
4.1.4.2	Scanning Electron Microscopy (SEM)	48
4.1.4.3	Particle Size Determination	48
4.1.4.4	Densities	50
4.1.4.5	Hausner Factor and Carr's Index	51
4.1.4.6	Moisture Content	51
4.1.4.7	Solubility	53
4.1.4.8	Water Uptake Rate	53
4.2	Granulation	54
4.2.1	Preparation	54
4.2.2	Granules Characterisation	55
4.2.2.1	Scanning Electron Microscopy (SEM)	55
4.2.2.2	Particle Size Determination	55
4.2.2.3	Densities	56

TABLE OF CONTENTS

4.2.2.4	Hausner Factor and Carr's Index	56
4.2.2.5	Moisture Content	57
4.2.2.6	Drug Content	57
4.3	Tablet Compaction	58
4.3.1	Single Substance Compaction	58
4.3.2	Compaction of Binary Mixtures of two Excipients with a Constant Compaction Force	58
4.3.3	Compaction of Binary Mixtures of two Excipients to a Constant Relative Density	58
4.3.4	Ternary Mixture Compaction	58
4.3.5	Compaction for Granulation Studies	59
4.3.5.1	Tablets Made From Granules Compacted with a Constant Compression Pressure	59
4.3.5.2	Tablets Made From Powders	59
4.3.5.3	Tablets Made From Granules Compacted to a Constant Relative Density	59
4.4	Tablet Characterisation	60
4.4.1	Tablet Storage	60
4.4.2	Relative Density	60
4.4.3	Elastic Recovery	60
4.4.4	Crushing Strength and Tensile Strength	60
4.4.5	Compaction Models	60
4.4.6	Water Uptake Rate	61
4.4.7	Disintegration Time	62
4.4.8	Dissolution	62
4.4.8.1	Dissolution Models	62
4.4.9	Statistical Analysis	63
5	RESULTS AND DISCUSSION	64
5.1	Compressibility and Compactibility	64
5.1.1	Single Substances	64
5.1.2	Binary Mixtures	73
5.1.2.1	Mixtures of Two Excipients	73
5.1.2.2	Mixtures of Proquazone and Excipients	80
5.1.3	Ternary Mixtures	88
5.1.4	Dilution Capacity	91
5.1.5	Elastic Recovery	95
5.2	Liquid - Solid Interactions	101
5.2.1	Water Uptake	101
5.2.2	Disintegration	105

TABLE OF CONTENTS

5.2.3	Dissolution	112
5.2.3.1	Influence of the Relative Density	112
5.2.3.2	Influence of the Drug Load	123
5.2.3.3	Influence of the Load of Modified Cellulose	136
5.2.4	Dissolution Models	147
5.2.4.1	Model independent approach	148
5.2.4.2	Model dependent approach	150
5.2.5	Disintegrant Comparison based on a Model Independent and a Model Dependent Approach	154
5.3	Relation between Mechanical Resistance and Liquid - Solid Interactions	157
5.4	Granulation versus Direct Compaction	162
5.4.1	Compressibility and Compactibility	162
5.4.2	Liquid - Solid Interactions	166
5.5	Quality of Fit	174
6	CONCLUSIONS AND OUTLOOK	179
6.1	Selection and Comparison of Models	179
6.2	Compressibility and Compactibility	180
6.3	Liquid - Solid Interactions	183
6.4	Granulation	186
6.5	Evaluation of Cellulose Types	188
6.6	Outlook	190
7	REFERENCES	192
8	CURRICULUM VITAE	199

Symbols, Abbreviations, and Comments

Symbols

γ_t	pressure susceptibility
$\varepsilon, \varepsilon_c$	porosity, critical porosity
ρ_{app}	apparent density
ρ_c	critical relative density
ρ_r	relative density
ρ_t	true density
σ	compaction pressure
$\sigma_t, \sigma_{t\ max}$	tensile strength, maximum possible tensile strength
σ_y	mean yield pressure
a	scale parameter (Weibull)
b	shape parameter (Weibull)
A_V, B_V, C_V	Van der Waals - coefficients
C	constant (from modified Heckel equation)
D	Diameter
F	crushing force or strength
f_1	Difference factor
f_2	Similarity factor
h, h_{min}	height, minimal height
K	constant (from Heckel equation)
k_1	dissolution rate constant (first order)
k_2	dissolution rate constant (Hixson-Crowell cubic root law)
k_3	dissolution rate constant (Higuchi equation)
M_0, W_0	total amount of drug in the formulation (= drug load)
M_t	accumulated drug amount at time t
p	probability
p_c	percolation threshold (critical probability, critical concentration)
r	radius
r^2	coefficient of determination
$t_{10\%} / t_{50\%} / t_{90\%}$	time to dissolve 10%, 50%, or 90% drug load, respectively
V_a	apparent volume of the compact
V_t	true volume of the substance
W_t	remaining drug amount at time t

SYMBOLS, ABBREVIATIONS, AND COMMENTS

Abbreviations

ANOVA	Analysis of Variance
AV	average
API	active pharmaceutical ingredient
BCS	Biopharmaceutical Classification System
CI	Carr's Index
DT	disintegration time
EMA	European Medicines Agency
ER	elastic recovery
FDA	Food and Drug Administration
HCl	hydrochloric acid
HPLC	high pressure liquid chromatography
IR	immediate release
MANOVA	Multivariate Analysis of Variance
MCC	microcrystalline cellulose
NaOH	Sodium hydroxide
PAT	Process Analytical Technology
PVP	polyvinylpyrrolidone
QbD	Quality by Design
RCF	resulting compaction force
rH	relative humidity
RPM	rotations per minute
RSD	relative standard deviation
SC	sink conditions
SD	standard deviation
SEM	scanning electron microscope
SQ	sum of squares
UICEL	University of Iowa Cellulose
WUR	water uptake rate

Comments

Percentages [%] are generally given in mass fractions [% (m/m)]. Exceptions are emphasized.

1 Summary

Polymorphism is common in pharmaceutical sciences, about 50% of all APIs appear to have multiple polymorphic forms, but this phenomenon is also known in excipients. Polymorphism in pharmaceutical ingredients may influence physical, chemical, and technological properties. To avoid problems, effects of polymorphism should be evaluated in an early stage of the product development. Cellulose is a fibrous, tough, and water-insoluble substance which is found for the most part in plants. Also cellulose exhibits polymorphism, the most prevalent form in nature is modification I, even though modification II is more stable. Celluloses used in pharmaceutical sciences are prepared by chemical and mechanical treatment. Powdered cellulose and microcrystalline cellulose which show modification I are widely accepted, inert, and show a wide range of applications in pharmaceutical technology. Celluloses with modification II, e.g. UICEL-A/102 and UICEL-XL, are considered as multifunctional excipients for direct compaction with good disintegration properties.

Six different celluloses were investigated. They were classified in four different groups; class 1 are cellulose I modifications (MCC 102), class 2 are partially converted cellulose II modifications (Type I), class 3 are fully converted cellulose II modifications (UICEL S, Type II, and UICEL B), and class 4 are cross-linked cellulose II modifications (UICEL-XL). The compressibility of all six substances was determined with the Heckel equation, the modified Heckel equation, and the recently introduced modified van der Waals equation of the state. Compactibility was assessed with the Leuenberger equation. Furthermore, the resulting compaction force and the tensile strength of binary and ternary mixtures consisting of proquazone as a model drug substance and one or two celluloses were determined. Dilution capacity was calculated according to Kuentz, Lanz, and the rule of thumb of Lanz based on three different relative densities. Furthermore, the elastic recovery of the celluloses was investigated.

The second part of this work is attended to liquid-solid interactions, where water uptake, disintegration, and dissolution were studied. Dissolution profiles were determined and compared with different model independent and model dependent approaches as the FDA requirements for rapidly dissolving immediate release formulations, ANOVA, difference and similarity factor, Weibull equation, first order kinetics, Hixson-Crowell cubic root law, and Higuchi release model.

Finally, two formulations were granulated by fluidised bed method. Additionally, powder mixtures of the same composition were prepared. Tablets made from granules and powder

SUMMARY

mixtures were investigated with the same methods as in the previous two sections with the goal to assess the influence of granulation on the cellulose properties.

From the different compressibility and compactibility models applied, the use of the Leuenberger equation was selected as the most appropriate approach. This approach was superior to the compressibility models, since the hardness of the tablet is included. The findings of the Leuenberger equation agreed with the results of tensile strength in cellulose-controlled binary and ternary mixtures. However, the Leuenberger equation based on tensile strength values was limited in case of very plastic materials; the use of the Brinell hardness is preferred. Amongst the models of compressibility, the Heckel equation was favoured due to the simple evaluation by linear regression, whereas modified Heckel equation and modified van der Waals equation required non-linear regression. A good correlation was found between the Heckel equation and the modified Heckel equation, the correlation between the Heckel equation and the modified van der Waals approach could not be proved. Resulting compaction force or Carr's Index were not suitable to determine compressibility, but both parameters might be interesting in production and quality control. The rule of thumb according to Lanz was selected as the best model for dilution capacity; it allows a rough estimation of the critical concentration without a lot of additional work. A linear relationship between the load of modified cellulose in binary and ternary mixtures and the elastic recovery as well as the tensile strength was found. The influence of the relative density on the tensile strength could be confirmed.

The determination of water uptake rates which are considered as the first step in all liquid - solid interactions was not a very sensitive method. The modification of the cellulose increased indeed the water uptake rate, but a significant difference was only found for Type II. No correlation between water uptake rate and disintegration and dissolution was found. Disintegration was strongly affected by the method. The use of disks reduced disintegration times. A better correlation was found when no disks were used, but a delay between disintegration and complete dissolution was still observed. This was referred to the physical-chemical properties of the active ingredient, but also to the disintegrant efficiency of the filler. Dissolution testing was the most appropriate approach to detect differences between materials. The qualitative assessment of dissolution profiles allowed a first estimation and required no further tools, but the meaningfulness was small. Model independent approaches were fairly simple to use but they lacked of kinetic background. Model dependent approaches were more complex in implementation and comparison, but, with exception of the Weibull model, they explained the physical background. The comparison of models was generally done based on the coefficient of determination (r^2). To

rule out a possible error, especially when different methods or transformed data were used, it is advised to study the residual sum of squares and the residual distribution which should randomly scatter around zero. Two model profiles were selected and the analysis was repeated based on the residual sum of squares in the non-transformed space. The previously selected model based on r^2 was confirmed in both cases by this approach.

No clear favourite model for the evaluation and comparison of drug release profiles was found. ANOVA was favoured amongst the model independent approaches, since more than two profiles might be compared at the same time. The most appropriate model dependent approach was the Weibull equation. The decisive advantage of this approach is the wide applicability on profiles with different release kinetics. Negative, on the other hand, is clearly the lack of scientific background and the insignificance of the fitted parameters, a and b . To increase the significance it is advised to use these parameters only as an intermediate for further calculations such as $t_{90\%}$. The first order model was very suitable for all formulations which were rapidly dissolving, but it was influenced by the stirring rate and the sink conditions. The Hixson-Crowell equation was appropriate, if the drug was dominating and no tablet break up occurred. Formulations with MCC 102 and Type I and a small drug load showed release kinetics described by the square root of time law of Higuchi. Dissolution was dependent on the method, increased paddle speed accelerated drug release. In general, no linear relationship between disintegration times and $t_{90\%}$ was found. Only low drug load formulations of MCC 102 and Type I showed this linearity at different relative densities. Since the composition of the formulations influences the release kinetics, as shown in this study, it is always advised to study drug release. At low drug loads, when the drug is embedded in the excipient, the cellulose takes responsibility for the dissolution, at very high drug loads, where the excipient is embedded in the drug, the later controls dissolution. In the intermediate range, both ingredients are involved and contribute to the drug release.

The evaluation of granulation experiments was complicated because of the differences in the relative density of tablets. Tensile strength was not clearly influenced by granulation. No effect was found concerning water uptake, but the disintegration time of the granulated MCC 102 formulation was reduced. The effect on UICEL SM was less clear since disintegration was anyway very fast. The drug release of all tablets followed first order kinetics.

Class 1 (MCC 102) and Class 2 (Type I) were not suitable as fillers in rapidly dissolving immediate release formulations. Both showed less efficient disintegrant properties and were influenced by the drug load and the relative density, hence the cohesive forces. Concerning the rapid dissolution, Class 3 and 4 substances are preferred. All four

SUMMARY

celluloses of these two classes showed good disintegrant properties, this might be related to the developed swelling force. Furthermore, they were independent of drug load and relative density of the tablets. A minimal amount of 22.5% of UICEL S and UICEL B were determined to obtain rapidly dissolving immediate release formulations. Type II which was used in even smaller amounts showed this critical mass fraction at 4.5%; higher amounts did not influence the disintegration time anymore. Type II, due to its fibrous structure, showed advantages in compaction and water uptake rates; it was slightly more sensitive on the relative density compared to UICEL-A/102. No negative effect due to the smaller crystallinity was established. UICEL-XL was studied in a smaller extent, but a comparable behaviour to class 3 substances is supposed. Compared to class 3, UICEL-XL showed increased compactibility with comparable disintegration behaviour.

The degree of conversion influenced, additionally to the disintegration behaviour, also the compactibility, which was significantly reduced for fully converted cellulose II products. Furthermore, the elastic recovery was increased after modification.

The improved drug release after granulation may be related to a hydrophilizing effect of PVP when it is fine distributed through the whole tablet. This is only the case after granulation. The distribution of PVP may also affect the tablet hardness by influencing the electrostatic forces such as the van der Waals forces. It is fairly difficult to give evidence on a process based on only four formulations. Further studies are certainly required.

The initial idea to study modified celluloses as multifunctional single excipients was abandoned in favour of studying the properties of binary mixtures with cellulose I products such as MCC 102. These mixtures combine the high mechanical resistance of cellulose I and the very good disintegrant properties of cellulose II. Modified celluloses are preferred compared to other disintegrants due to their chemical similarity to MCC 102 showing the same properties, such as inertness and the fibrous structure. UICEL-XL may be used as a multifunction excipient due to its improved compactibility, but no clear advantage compared to mixtures of MCC 102 and a class 3 cellulose can be established.

2 Introduction

2.1 General Considerations

Pharmacy is the science of physical-chemical properties of active principles, their extraction, their analytics, and their formulations which include excipients and dedicated processes to achieve a dosage form, such as tablets or creams; in special cases case of active ingredients, e.g. active principles of plant origin also their biosynthesis and the plants themselves have to be considered. [1]

An active ingredient is not directly a medicine which can be sold to clients. The procedure from new chemical entity to the product sold in the pharmacy requires many steps which are related to pharmaceutical technology. Pharmaceutical technologists are involved (1) in preformulation, where the physical-chemical properties of the drug and compatibility between active and inactive ingredients are studied, (2) in formulation development, where the formulation is developed and optimized with respect to quality and safety, or in other words, where ingredients and processes are quantitatively and qualitatively selected, (3) in scale-up, where formulation and process are adapted to the production scale, and (4) in production, where the final product is prepared in large scale. [2, 3]

From tablet intake to systemic action, an active ingredient has to pass many barriers. Chemical modification as well as proper selection of the route of administration, dosage form, and formulation may promote the passage and increases the dose locally at the site of action. Prerequisite for a systemic action is the absorption of the drug into the systemic circulation. Absorption is mainly determined by the solubility and permeability of the active ingredient. The biopharmaceutical classification system (BCS) is based on these two parameters. [4] Permeability is a drug – body interaction and cannot directly be influenced by pharmaceutical technology; however, solubility can be increased by various methods. The main interest of formulation scientists focuses on class II drugs with a poor solubility but high permeability.

Tablets, from the technological point of view, are single dose dosage forms, produced by compaction of powders or granules. With respect to physics, tablets are considered as disperse systems (gaseous state/solid state). [5]

Tablets are the most frequently used dosage forms, reasons for that are (1) safe and ease intake, hence better compliance, (2) high dosing accuracy, (3) wide variety of shapes,

INTRODUCTION

colours, and taste, (4) control of the drug release by formulation and/or production technology, (5) economical large scale production from almost all solid active ingredients, and (6) long shelf life, easy packaging, easy storage, and transport. [2, 5]

Additionally to active ingredients, a tablet contains minimally one excipient. Excipients are responsible for tablet properties with respect to robustness, manufacturing feasibility, stability, safety, and bioavailability. They have to be inert, i.e. without pharmacological or toxicological activity, and have to be compatible with all ingredients in the mixture. [2, 5] The use of an all-in-one excipient, i.e. of a multifunctional excipient, reduces the components, and, at the same time, the risk of incompatibilities.

Microcrystalline cellulose is widely used as a binder/diluent in oral tablet formulations where it is used in wet granulation and direct compaction processes. Furthermore, MCC shows properties of a lubricant or disintegrant. [6] Polymorphic changes of the crystal lattice, degree of crystallinity, and degree of polymerisation of cellulose results in different properties and suitability as excipients. UICEL and UICEL-XL are excipients suitable as a binder, filler, and/or disintegrant in solid dosage forms. Compared to MCC, UICEL shows improved flow, but is less ductile and more elastic. UICEL-XL, however, is better compressible and compactable compared to UICEL. [7-11]

Product development is expensive. Approximately 30% to 35% of the total cost of bringing a new drug on the market is spent for product development. [12] To improve quality and hence reduce time to market and the related increased costs, formulations and processes should be developed in the framework of Process Analytical Technology (PAT) and Quality by Design (QbD). The scope of PAT is to built-in quality into a product or, furthermore, being quality by design. [13] Important tools in context of QbD are design space, i.e. the multidimensional combination and interaction of input variables as material attributes and process parameters that have been demonstrated to provide assurance of quality, and furthermore, control space, i.e. the region inside the design space within which the company will try to operate. [14] Working within the design space is not considered as change. Movement out of the design space is considered to be a change and would normally initiate a regulatory post-approval change process. [15] Proper evaluation and definition of these spaces ensure the quality of the product and accelerate the product development, registration, and finally introduction to market.

2.2 Aims of the Study

Material properties are potentially important in solid dosage form design. Beside proper evaluation of the active ingredient, the focus should also be on the selection of excipients. Accurate investigations on excipient properties may reduce later problems in large scale production and product quality.

An ideal formulation contains an active ingredient and a minimal amount of ideally multifunctional excipients to reduce the risk of incompatibilities. Cellulose is widely accepted, inert, and shows a wide range of applications, it is therefore particularly suitable in direct compaction, but also in dry and wet granulation. The formulation coming from development is robust, i.e. allows technical and formulation changes without influencing the final product.

The aims of this study include the evaluation of six different celluloses of different polymorphic form, different degree of conversion, and different producers. All celluloses were investigated on (1) their compressibility and compactibility behaviour, (2) their liquid – solid interactions, and (3) the influence of major process changes as granulation, always with respect to rapidly dissolving immediate release formulations according to the FDA. [16]

Compressibility and compactibility are important parameters for product quality regarding storage, transport, and further processing. This work includes four different models as Heckel equation, modified Heckel equation, Leuenberger equation, and the modified van der Waals equation of the state; the most suitable model should be evaluated and validated. The most suitable model to calculate dilution capacity should be determined.

Liquid – solid interactions are investigated with different methods as water uptake rate, disintegration time, and drug release studies. The most appropriate method should be evaluated. Furthermore, this work should focus on drug release with respect to model independent approaches, such as the FDA approach for rapidly dissolving immediate release formulations, ANOVA, difference factor and similarity factor, and model dependent approaches, e.g. the Weibull equation, first order release kinetics, Hixson-Crowell cubic root law, and if advised further models, to describe release profiles and compare them.

Tablets made from granules and from direct compaction should be studied with the methods evaluated in the first two sections. Advantages and disadvantages of granulation on the performance of celluloses should be assessed.

3 Theoretical Section

3.1 Polymorphism

Polymorphism is defined as a property of substance to exhibit in more than one crystal structure. The polymorphic forms show different crystal lattices and thus different physical and chemical properties. [17] Examples of polymorphism in nature are the carbon modifications of diamond and graphite. Unless it is not correct, amorphous forms and pseudopolymorphs are occasionally regarded as polymorphs. Amorphous substances are highly disordered therefore have zero crystallinity. [18] Glass, the amorphous form of SiO_2 and derivatives, is a typical example of an amorphous substance. Pseudopolymorphism is related to hydrates and solvates in which the molecules of the solvent are incorporated in the crystal lattice. [17]

Polymorphism can have a negative impact on the physical, chemical and technological properties of a substance. Different polymorphic modifications show different melting points, solubility, rate of dissolution, or hygroscopicity. The maybe most significant consequence is the possible difference in bioavailability. Even though no significant difference in bioavailability exists, the different crystal habits of the polymorphic forms can influence the compressibility and the flow properties. [19]

Polymorphism in pharmaceutical sciences is common, about 50% of all APIs appear to have multiple polymorphic forms. [17] Singhal and Curatolo reviewed 94 publications in the field of drug polymorphism. [20] Two considerable examples of importance thereof were selected. In 1998 the supply of Norvir® was threatened due to a new less soluble crystal form of ritonavir, which was detected in in vitro dissolution test. [21] The influence on the bioavailability was reported by Aguiar and co-workers [22], they showed a significantly greater absorption of chloramphenicol palmitate polymorph B than of polymorph A in humans.

Polymorphism does not only appear in active ingredients, but is also known in excipients. Sorbitol, for example, exists in four polymorphic forms (α , β , γ , and δ), whereof modification γ shows the highest compressibility. In case of Mannitol, the modification B shows the highest compressibility, whereas modification C is preferred for lyophilisation. [23] Apart from excipients used in solid dosage forms, cacao butter (oleum cacao) exists in four polymorphic forms. To achieve the most stable β -form, the substance should not be heated up more than 33°C . [5]

It can be said that polymorphism influences the properties of the active ingredient as well as the dosage form. Accurate evaluation of the active ingredient and proper selection of excipients and dosage form are essential in dosage form design.

3.2 Cellulose

3.2.1 Types of Cellulose and Their Production

Cellulose is a long-chain polymeric polysaccharide composed of β -1,4-linked poly-anhydroglucopyranose (see Figure 1). [24] It is a fibrous, tough, and water-insoluble substance, which is found in the protective cell walls of plants, particularly in stalks, stems, trunks, and all woody portions of the plant tissue. [25] A large proportion of the industrially manufactured cellulose comes from cotton and different types of wood. Raw cotton contains about 85-90% cellulose compared with 40-60% in wood. [24]

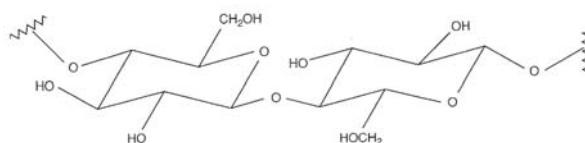


Figure 1: Repeating unit of a cellulose chain.

Cellulose for pharmaceutical use is gained by dispersing the cellulose pulp in a 17.5% sodium hydroxide (NaOH) solution. The non-dissolved α -cellulose can be removed. This white residue is sold after washing and mechanically pulverization as powdered cellulose. The degree of crystallization is low, the degree of polymerization lies between 100 and 1300. [24]

THEORETICAL SECTION

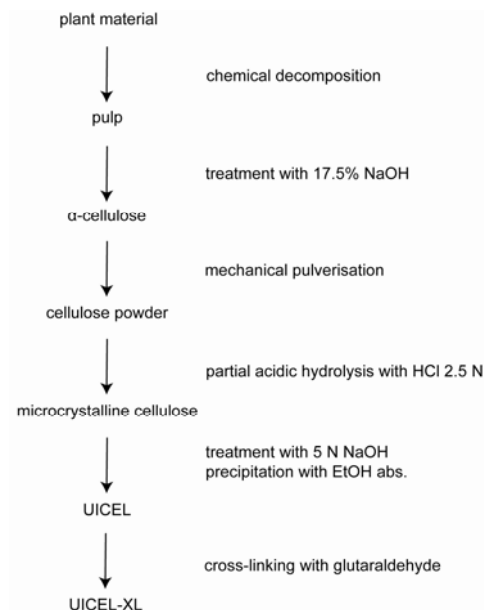


Figure 2: Production and modification of cellulose.

Microcrystalline cellulose is produced by treating powdered cellulose with an aqueous solution of hydrochloric acid (HCl). Due to this partial acid hydrolysis a cellulose with higher crystallinity and lower degree of polymerization (200-300) is created. [24] UICEL (University of Iowa Cellulose) is a mercerized form of cellulose. Pulp, cotton linter, α-cellulose [7, 26], or microcrystalline cellulose [11, 27] is used as starting material which is treated with an aqueous solution of sodium hydroxide (5 M) with constant stirring. The resultant gel is precipitated with 95% (v/v) ethanol. The consequential white powder is washed with water to purify and neutralize and afterwards dried. This mercerized substance shows a Cellulose II lattice and compared with MCC a lower degree of polymerisation and lower crystallinity. [7] When UICEL is produced from Avicel PH-102 or comparable product it is called UICEL-A/102. [11] A further modification starting from Cellulose II was described by Kumar et al. [8] and Reus Medina and Kumar [10]. They investigated the cross-linking of cellulose II with glutaraldehyde to improve the binder properties of cellulose II powders while maintaining their rapidly disintegration characteristics. Figure 2 summarizes the stages of production.

3.2.2 Polymorphism of Cellulose

As described above, polymorphism is found in active ingredients as well as in excipients. For the semi-crystalline cellulose four main polymorphic forms were found (I, II, III, and IV). Figure 3 demonstrates the different modifications and their conversion.

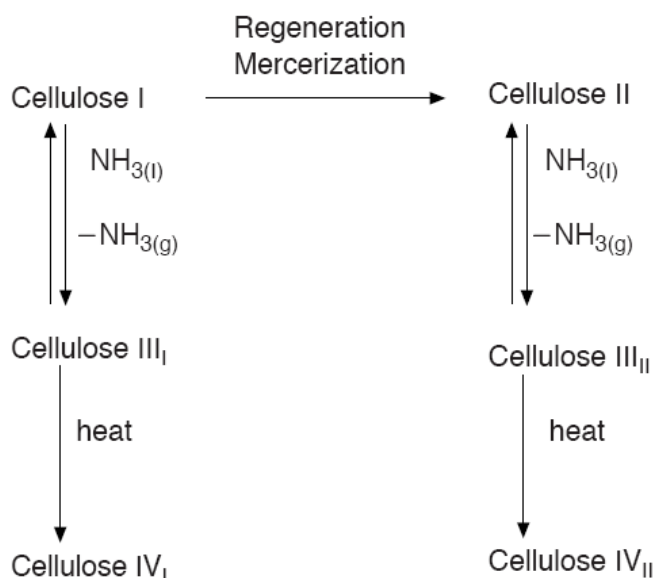


Figure 3: Interconversion of the polymorphs of cellulose by regeneration or mercerization, treatment with liquid or gaseous ammonia, and heat. [25]

The most prevalent polymorphic form of cellulose in nature is modification I, even though it is not the most stable form. Within cellulose I modifications, two further differentiations were found called I α and I β . Cellulose produced by primitive organisms as bacteria has a higher proportion of I α than cellulose from higher plants, where I β dominates. [25]

The thermodynamically more favourable cellulose II is rarely found in nature. Only one mutant strain of *Glucanoacetobacter xylinum* was found to produce it and the alga *Halicystis* seems to contain it natively. Considering the polymorphic forms of cellulose, only cellulose I and cellulose II are important from a technical and commercial point of view. [28] Cellulose II may be obtained by either regeneration or by mercerization. Regeneration includes solubilization of cellulose I in a solvent followed by precipitation by dilution in water, whereas mercerization is the process of swelling the fibres in concentrated sodium hydroxide followed by removal of the swelling agent. [7, 25]

THEORETICAL SECTION

Cellulose III_I and Cellulose III_{II} are reversibly formed by treating cellulose I or cellulose II, respectively, with liquid ammonia. The fourth polymorphic form is prepared by heating cellulose III to 206°C in glycerol. [25]

3.2.3 Comparison of Cellulose Modifications

Due to denser packing and stronger hydrogen bonds, cellulose II shows different physical and chemical properties compared with Cellulose I. Additionally to the influence of the polymorphic form, crystallinity as well as the degree of polymerisation can influence the cellulose properties. [24] Crystallinity values found in literature are listed in Table 1. The wide range of crystallinity within the types of cellulose is influenced by the different methods of calculation, e.g. peak height or peak area, but also by brand-to-brand and batch-to-batch variabilities. However, a tendency is detectable. The crystallinity of powdered cellulose is smaller than of microcrystalline cellulose. UICEL is less crystalline than MCC [7] and UICEL-XL [10]. In many publications a low degree of crystallinity is correlated with poor compressibility and poor compactibility [11, 27, 29], but also the opposite was observed [30]. An additional important effect of the low crystallinity is increased tendency of moisture sorption [27, 29, 31], which can have a negative impact on the stability of a product. The tendency to absorb water decreases with a higher crystallinity. [31]

Table 1: Degree of crystallinity determined with X-Ray analysis.

Type	Crystallinity	References
native cellulose	60 – 70%	[24, 32]
powdered cellulose	26 – 73%	[29, 32]
microcrystalline cellulose	53 – 85%	[29, 32]
UICEL	47 – 68% 35 – 100%	[7, 8, 26]
UICEL-XL	≥ 75%	[8]

The degree of polymerization depends on the origin of the pulp and can vary from 15'000 (cotton) to 5'000 – 9'000 (wood). [24] An increased degree of polymerization results in

higher water sorption, increased compressibility and compactibility, and reduced elastic deformation. [33] In case of conversion from cellulose I to cellulose II, the starting material influences the final product. [34]

The degrees of polymerization of different types of cellulose are listed in Table 2.

Table 2: Degree of polymerization.

Type	Degree of Polymerization	References
native cellulose	5000 – 15000	[24, 25, 28]
powdered cellulose	440 – 2250	[35]
microcrystalline cellulose	≤ 350	[7, 28, 35]
UICEL	74 – 350	[7, 26]
UICEL-XL	~ 79	[10]

3.2.4 Application of Cellulose Modifications

So far, origin, production, and physical and chemical differences between different types of cellulose were discussed. This chapter focuses on the application of different celluloses and their advantage in solid dosage form design.

Powdered cellulose, as a pure substance, shows poor flowability and reduced binding properties compared with microcrystalline cellulose and is therefore not suitable for direct compression. Prior to compaction granulation is advantageous. [36]

Microcrystalline cellulose is widely used in pharmaceuticals, primarily as a binder/diluent in oral tablet and capsule formulations where it is used in both wet granulation and direct-compression processes. It is also used as a binder/diluent with properties of a lubricant or disintegrant. [6]

UICEL is an excipient suitable as a binder, filler, and/or disintegrant in solid dosage forms. [7] Compared with MCC, UICEL shows improved flow, but is less ductile and more elastic. The suitability of UICEL as an efficient disintegrant can compensate for the reduced compactibility. [7, 11]

UICEL-XL is also suitable as an all-in-one binder, filler, and disintegrant. Compared with UICEL, it is better compressible and compactable, i.e. it is a stronger binder. The disin-

THEORETICAL SECTION

tegration efficiency of UICEL-XL is indeed more sensitive on the compaction pressure, but shows still very short disintegration times. [8-10]

3.3 Granulation

3.3.1 Granules

Granules are agglomerates of small powder particles with an irregular shape and a rough surface. The particle size is between 200 and 500 μm for granules used as an intermediate in capsule or tablet production. There are several reasons for granulation [5, 37]:

- prevention of segregation by “freezing” the mix in the correct proportion in each granule
- improve of flow properties by increasing the particle size and hereby the decrease of the specific surface area
- improve of compaction characteristics
- optimization of the surface properties as wettability, porosity, solubility, or disintegration time.

3.3.2 Methods of Granulation

Granulation is classified by the technology of production. Granules can be produced by dry granulation or wet granulation. The dry method may be used for moist sensitive drugs or in case of reduced compressibility after wet granulation. The most common method is wet granulation because of the wide and easy application. The advantages and disadvantages of the different technologies are given in Table 3.

Particle shape, intraparticle porosity, and granule strength are strongly depending on the manufacturing process. Particles can show cylindrical, spherical, or angular shape. The method of granulation may also influence the granule density. Fluidised bed granulation results in particles with the highest porosity, intermediate density is obtained with a two stage process, i.e. wet agglomeration in a high shear mixer with a subsequent drying step in a fluidised bed dryer, and the densest granules are manufactured by dry granulation. Fluidised bed granules show better dissolution properties [38, 39], and this wet granulation method is fast and economical since mixing, granulation, and drying takes place in one pot. [5]

Table 3: Advantages and disadvantages of granulation methods. [39]

	Advantages	Disadvantages
Wet granulation	<ul style="list-style-type: none"> ▪ physical properties of active ingredients and excipients are less important ▪ voluminous and fine powders can be handled ▪ good distribution of low dose active ingredients ▪ suitable for all tablet types ▪ good plasticity 	<ul style="list-style-type: none"> ▪ multistage process, therefore time and cost expensive ▪ loss of material ▪ heat and moist sensitive substances are not suitable ▪ decreased dissolution rate possible (depending on the binder amount)
Dry granulation	<ul style="list-style-type: none"> ▪ no wetting and drying of the mixtures ▪ applicable for heat and moist sensitive substances 	<ul style="list-style-type: none"> ▪ wide particle size distribution ▪ high compaction pressures needed (heat development) ▪ not suitable for voluminous substances ▪ loss of material
Direct compaction	<ul style="list-style-type: none"> ▪ no wetting and drying of the mixtures ▪ fast method ▪ little loss of material 	<ul style="list-style-type: none"> ▪ only possible with expensive excipients ▪ less suitable for high dose products ▪ inappropriate for voluminous and fine powders ▪ segregation possible, hence problems with content uniformity

3.3.3 Granulation Mechanisms

Granules need bonds between powder particles. These bonds have to be strong enough to resist later handling. Bonds formed by liquid bridges of the granulation liquid in wet granulation are a result of different stages given below. [5, 37, 38] The process is illustrated in Figure 4.

- Phase I No liquid bridges are formed between the powder particles; the powder mixture is wetted without agglomeration.
- Phase II Start of agglomeration by forming liquid bridges; the particles are hold together by points of contact of liquid. (pendular state, Figure 4 A)
- Phase III Region of optimal wetting, the interparticular voids are partially filled with granulation liquid. (funicular state, Figure 4 B)

THEORETICAL SECTION

- Phase IV The voids are totally filled with granulation liquid; the powder mixture is over wetted. ("liquid-in-solid" or capillary state, Figure 4 C)
- Phase V Change from over wetted powder mixture to suspension. ("solids-in-liquid" or droplet state, Figure 4 D)

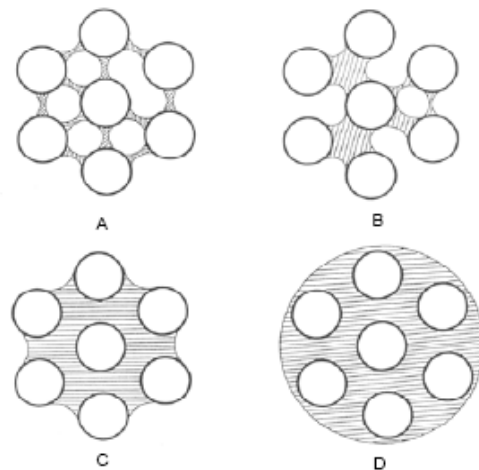


Figure 4: Stages in the development of moist granules: pendular stage (A), funicular state (B), capillary state (C), and droplet state (D). [40]

At the end of the wet granulation process, the granulating liquid is removed by drying. The granules are still kept together by different mechanisms as solid bridges, attractive (van der Waals) forces between solid particles, or mechanical interlocking. [37]

Solid bridges can be formed by partial melting, hardening of the binder, or crystallization of dissolved substances. Hardening of the binder is the common mechanism in pharmaceutical wet granulation. The liquid will form liquid bridges and the binder will harden or crystallize on drying to form solid bridges to bind the particles. This effect is known for PVP, cellulose derivatives, and pregelatinized starch. Crystallization does not only derive from binder solution, but can derive from any soluble substance in the granule formulation.

Attractive (van der Waals) forces between solid particles are important in dry granulation. Weak electrostatic forces may contribute to the initial forming of agglomerates during mixing. More important are the stronger Van der Waals forces that contribute significantly to the granule strength. [37]

Mechanical interlocking of bulky or fibrous particles occurs under pressure. It complements the other attractive forces. [5]

3.4 Compaction

3.4.1 Introduction

Tabletting is the conversion of a loose powder bed into a coherent compact of defined shape and strength. It involves compressibility and compactibility. Compressibility is the ability of a powder to decrease in volume under pressure; compactibility may therefore be defined as the ability of a powder to be compressed into a tablet of specified strength. Compressibility is only an indirect measure of a material's ability to form tablets, compactibility however is clearly measurable, e.g. by crushing force or hardness. [41]

3.4.2 Direct Compaction versus Granulation

Tablets are produced from granules or directly compressed powders. Direct compaction offers many advantages. It requires less production steps and therefore less equipment, less process time, etc.. [36] The ease of manufacture and the economical advantages favour direct compaction, but it shows also some limitations. Powder mixtures for direct compaction require sufficient plastic deformation, good flow properties, and no de-mixing tendencies. A further disadvantage of direct compaction is the high cost of direct compressible fillers (e.g. microcrystalline cellulose or directly compressible starch). [36] If a powder or powder mixture cannot meet the requirements, its properties can be improved by granulation. Advantages and disadvantages of granulation methods and direct compaction are discussed above (see Table 3).

3.4.3 Tabletting Process and Bonding Mechanisms

Conversion from powder or granules to a tablet needs external forces. According to Train [42], the compaction process can be divided into four sequential steps. In the first step (I), the force is used to overcome the friction between the particles. The apparent volume is reduced by interparticulate slippage, therefore a dense packing of the particles is obtained. In the next step (II), within the material, columns, vaults, and bridges are built. The material starts to withstand the imposed load. Increased force leads to particle deformation (III), first in a reversible elastic manner followed by an irreversible brittle or plastic deformation. In

THEORETICAL SECTION

the last stage of compaction (IV), a strong structure is formed. The behaviour of this compact depends on the characteristics of the material. Figure 5 depicts these stages of compaction as a result of the applied force.

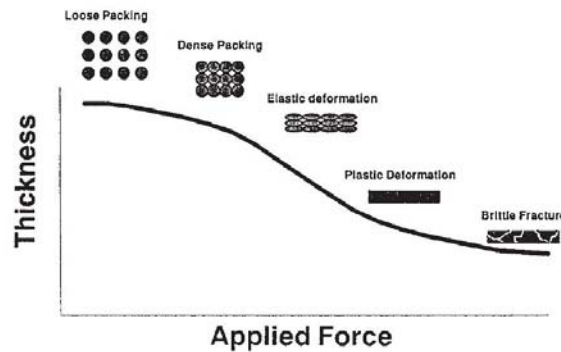


Figure 5: Stages of compaction according to Rudnic [43].

Rumpf [44] classified the general bonding mechanisms in five types.

- Solid bridges (sintering, melting, crystallization, chemical reactions, and hardened binders);
- bonding due to movable liquids (capillary and surface tension forces);
- non freely movable binder bridges (viscous binders and adsorption layers);
- attraction between solid particles (molecular and electrostatic forces);
- shape related bonding (mechanical interlocking).

Führer [45] extracted the three main bonding mechanisms in dry powder compaction. Table 4 lists these types with the corresponding dissociation energies and the maximum attraction forces.

Table 4: Some specifications of bonding mechanisms in compacted dry powders (adapted from Nyström et al. [46]).

Type	Dissociation energy [kcal/mol]	Maximum attraction distance [Å]
Solid bridges	50 – 200	< 10
Intermolecular forces	1 – 10	100 – 1000
Mechanical interlocking		

Intermolecular forces act between surfaces over a small distance and include van der Waals forces, electrostatic forces, and hydrogen bondings. [47] Nyström and co-authors [46] account for the intermolecular forces as the dominating mechanism for pharmaceutical materials.

Solid bridges that contribute to the overall compact strength can be defined as areas of real contact at an atomic level, hence the distance maximum attraction distance is much smaller.

Mechanical interlocking describes the hooking and twisting together of the packed material, therefore the particles have to be in direct contact.

Compacts hold together predominantly by intermolecular forces show a fast disintegration time, while solid bridges e.g. sinter bridges or binder bridges tend to increase the disintegration time. [5]

3.4.4 Compact Properties

Compact properties directly related to the compaction are the relative density ρ_r and the tablet strength. The relative density, or solid fraction, is dependent on the applied pressure and is calculated according to Equation 1. The apparent density ρ_{app} is the density of the tablet including all pores and is calculated from mass (m), tablet height (h), and tablet radius (r). The true density ρ_t corresponds to the density of the material without any pores and is therefore a specific material property.

$$\rho_r = \frac{\rho_{app}}{\rho_t} = \frac{m}{\rho_t \cdot h \cdot r^2 \cdot \pi} \quad \text{Equation 1}$$

The porosity ε is defined as the ratio of gas volume to total volume and is calculated according to Equation 2.

$$\varepsilon(\%) = (1 - \rho_r) \cdot 100 \quad \text{Equation 2}$$

The relative density is significantly involved in tablet strength and tablet disintegration and is therefore very important in solid dosage form design. [38] Tablet strength can be quantified by different methods as indentation hardness, crushing strength, bending strength, tensile strength, or friability. [38] Tablet hardness and crushing strength are frequently used synonymously by mistake. The indentation hardness of a material is

THEORETICAL SECTION

defined as the resistance which it presents to a penetrating object. A well known method is the Brinell hardness test, where a steel sphere is pressed against the surface of a tablet for a specified time. The indentation produced is depending upon the plasticity of the material. [41] Crushing strength is easier to perform and therefore often used in routine controls together with friability. It is defined as the force needed to crush the tablet under radial load. [35] Tensile strength σ_t is used to make tablets of different shape comparable. The crushing strength F is normalised by the tablet diameter (D) and height (h) (see Equation 3). A favourable tensile strength of tablets is in the range of 1.5 – 2.5 MPa. [38]

$$\sigma_t = \frac{2 \cdot F}{\pi \cdot D \cdot h} \quad \text{Equation 3}$$

Tablet characteristics like relative density or tensile strength can be used to investigate material properties. Metals and other materials possessing a high crystalline order or homogenous structure show a clear relationship between material deformation and applied stress. With an increased applied stress, the material first deforms always elastically, followed by plastic deformation and/or fragmentation due to brittle behaviour. Most pharmaceutical materials do not follow this simple model. High tablet strength is primarily produced by materials possessing a low elastic component and having a high bonding surface area that could develop intermolecular forces. [46] Figure 6 depicts the behaviour of brittle and ductile materials under load. Substances with a high fragmentation propensity or plastic deformation increase the surface area and thereby the contact points. Tablets with low fragmentation propensity need to form strong interparticulate attraction forces (e.g. solid bridges) to get strong tablets.

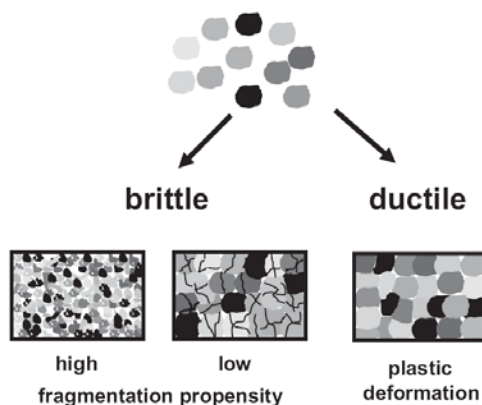


Figure 6: Behaviour of brittle and ductile substances under load. [48]

3.4.5 Methods of Classification

3.4.5.1 Heckel Equation and Modified Heckel Equation

To describe the compression characteristics of powders, the most frequently used equation was postulated by Heckel [49, 50] and was originally developed for metallic powders.

The Heckel equation (Equation 4) describes the relationship between the porosity of a compact and the applied pressure and is based on the assumption that the densification of the bulk powder in-die follows first order kinetics.

$$\ln \frac{1}{1-\rho_r} = K \cdot \sigma + A \quad \text{Equation 4}$$

ρ_r is the relative density of the compact at pressure σ . The constants K and A are determined analytically from the slope and the intercept of the extrapolated linear region of a plot of $\ln(1/(1-\rho_r))$ versus σ . The intercept A is related to a starting density ρ_0 . The mean yield pressure σ_y is the reciprocal of constant K (Equation 5).

$$\sigma_y = \frac{1}{K} \quad \text{Equation 5}$$

At lower pressures, a curved region can always be shown, resulting from particle movement and rearrangement processes before interparticle bonding becomes appreciable.

To describe the powder behaviour under very low compression pressures, Kuentz and Leuenberger [51] postulated a modified Heckel equation which allows the description of the transition between the state of a powder and the state of a tablet. It considers that the pressure susceptibility γ_t which is defined as the decrease of porosity ϵ under pressure can only be defined below a critical porosity ϵ_c or above the corresponding critical relative density ρ_c , because a rigid structure exists there. Taking this into account Equation 6 was defined, where γ_t is the pressure susceptibility, ρ_r is the relative density, ρ_c is the critical relative density and C is a constant.

$$\gamma_t \propto \frac{C}{\rho_r - \rho_c} \quad \text{Equation 6}$$

THEORETICAL SECTION

The new density versus pressure relationship can be described in the modified Heckel equation (Equation 7).

$$\sigma = \frac{1}{C} \left[\rho_c - \rho_r - (1 - \rho_c) \ln \left(\frac{1 - \rho_r}{1 - \rho_c} \right) \right] \quad \text{Equation 7}$$

Constant K and its reciprocal value σ_y from the Heckel equation as well as constant C from the modified Heckel equation can be used to describe material properties. Well compressible, soft, and ductile powders have higher values than poor compressible, hard, and brittle powders.

ρ_c is the relative density where a rigidity starts to evolve and a negligible mechanical resistance between the punches is produced. [51]

3.4.5.2 Leuenberger Equation

Whereas the Heckel equation and the modified Heckel equation handle the compressibility, i.e. the ability of a powder to decrease in volume under pressure, the Leuenberger equation includes the compactibility, i.e. the ability of the powdered material to be compressed into a tablet of specific strength. [41]

As it is more important in pharmaceutical sciences to get a compact of defined strength rather than of defined volume reduction, the use of the Leuenberger equation (Equation 8) is a good model where compressibility as well as compactibility is included. [52]

$$\sigma_t = \sigma_{t \max} \left(1 - e^{-\gamma_t \cdot \sigma \cdot \rho_r} \right) \quad \text{Equation 8}$$

Originally, the indentation hardness (or Brinell hardness) was used in this equation [41], but as supposed by Blattner and co-authors, Equation 8 can be applied using the tensile strength σ_t , the relative density ρ_r , and the compaction pressure σ to fit the maximum possible tensile strength $\sigma_{t \max}$ at zero porosity and the pressure susceptibility γ_t

The maximum tensile strength $\sigma_{t \max}$ is a degree for the compactibility. It will never be exceeded at infinite pressure σ_∞ and can be used to classify powders. A low $\sigma_{t \max}$ value corresponds to a relative poor compactibility, while high γ_t refer to good compressibility.

3.4.5.3 Modified Van der Waals Equation of the State

A new compression equation, developed by Lanz [27], is derived from the Van der Waals equation of the state. The fundamental principle of this approach is based on the observation that gaseous as well as particulate systems are compressible and can undergo a phase transition, i.e. from the gaseous to the liquid state or from a disperse particulate state to a solid such as a tablet.

The ideal gas law (Equation 9) describes the state of an amount of gas and is determined by its pressure, volume, and temperature. Compared with Equation 9, the Van der Waals equation (Equation 10) describes the state of a real gas and is one of the most used equations to predict it. Van der Waals modified the ideal gas law by introducing two terms. The first modification ($a n^2/V^2$) accounts for the attractive forces between gas molecules, the second modification ($n b$) accounts for the volume of the gas molecules. The pressure can also be written as the sum of the repulsive and attractive terms (Equation 11).

$$p \cdot V = n \cdot R \cdot T \quad \text{Equation 9}$$

$$\left(p + \frac{a \cdot n^2}{V^2} \right) (V - n \cdot b) = n \cdot R \cdot T \quad \text{Equation 10}$$

$$p = \frac{n \cdot R \cdot T}{V - n \cdot b} - \frac{a \cdot n^2}{V^2} = p_{\text{rep}} + p_{\text{attr}} \quad \text{Equation 11}$$

where:

p	pressure [Pa]	P_{rep}	repulsive term [Pa]
V	volume [m ³]	P_{attr}	attractive term [Pa]
n	number of moles [mol]	a	material constant, accounts for attraction [m ⁶ ·Pa/mol ²]
R	universal gas constant: 8.3145 J/(mol·K)	b	material constant, measures for the molecular volume; accounts for incompressibility [m ³ /mol]
T	absolute temperature [K]		

To make the Van der Waals equation applicable on powders some more modifications are introduced (Equation 12). Because the thermal energy is supposed to play a minor role, i.e. the compression takes place at an approximately constant temperature; the term $n \cdot R \cdot T$ is

THEORETICAL SECTION

substituted by the constant C_V . The terms $n \cdot b$ and $a \cdot n^2$ are also replaced by the parameters B_V and A_V , respectively. Furthermore, volume V corresponds to the apparent volume V_a , the ratio of the true volume V_t to the relative density ρ_r .

$$\sigma = \frac{C_V}{\underbrace{V_a - B_V}_{P_{rep}}} - \frac{A_V}{\underbrace{V_a^2}_{P_{attr}}} = \frac{C_V}{V_t \left(\frac{1}{\rho_r} - \frac{B_V}{V_t} \right)} - \frac{A_V}{V_t^2} \cdot \rho_r^2 \quad \text{Equation 12}$$

where:

σ	compression pressure [MPa]	A_V	“van-der-Waals” coefficient [$\text{cm}^6 \cdot \text{MPa}$]
C_V	“van-der-Waals” coefficient [$\text{cm}^3 \cdot \text{MPa}$]	V_t	true volume of the substance [cm^3]
V_a	apparent volume of the compact ($V_a = V_t / \rho_r$) [cm^3]	ρ_r	relative density
B_V	“van-der-Waals” coefficient [cm^3]		

Compared with the well known Heckel equation and its modification, this new approach has the advantage, that it is applicable to the full pressure range including the initial stage of particle rearrangement and fragmentation.

C_V correlates with the mean yield pressure σ_y of the Heckel equation. Small mean yield pressures correspond to small values for C_V , which is characteristic for ductile substances. B_V has a clear physical meaning. It equals the volume at infinite pressure and corresponds to the true volume of all particles. A_V can also be related to the mean yield pressure.

In the thesis of Lanz [27], a difference between V_t and B_V is observable, this is due to data used for the evaluation. Lanz worked with in-die-data, working with out-of-die data should reduce this difference.

3.4.6 Dilution Capacity

As mentioned above, direct compaction is limited to a certain amount of drug in the formulation. The majority of the active ingredients are poorly compactable, high drug load is therefore mostly not possible. The maximum amount of drug is limited to the dilution potential of the filler. Wells and Langridge [53] defined the dilution potential (or dilution capacity) as the proportion of a non or poorly compactable drug B which can be incorporated into a well compactable substance A to produce “satisfactory tablets”. The term “satisfactory tablets” can be related to various properties such as the friability or tensile strength.

Kuentz and Leuenberger [54] were the first authors who proposed an equation for the calculation of the dilution capacity (Equation 13). The slightly modified Equation 14 developed by Lanz [27] is easier to apply, but it has to be pointed out that this equation is just strictly valid if the effect of B on the tensile strength can be neglected, i.e. only the matrix formed by substance A determines the strength of the tablets.

$$X_{c(A)1/2} = -\frac{\Phi}{2} \pm \sqrt{\left(\frac{\Phi}{2}\right)^2 - \phi}$$

with

Equation 13

$$\phi \equiv \frac{-2 \cdot \rho_{c(A)} \cdot \rho_{t(A)} - \rho_{t(B)}}{\rho_{c(A)} \cdot (\rho_{t(A)} + \rho_{t(B)})} \text{ and } \Phi \equiv \frac{\rho_{t(A)}}{\rho_{t(A)} + \rho_{t(B)}}$$

$X_{c(A)}$ corresponds to the minimal amount of filler required. For the value of $\rho_{c(A)}$, the percolation threshold for the 100% of the well compactable substance A is used. $\rho_{t(A)}$ and $\rho_{t(B)}$ are the true densities of substance A and B.

$$X_{c(A)} = \frac{\rho_{t(A)}}{\rho_{t(B)}} \cdot \left(\frac{1}{\frac{\rho_{t(A)}}{\rho_{t(B)}} + \frac{1}{\rho_{c(A)}} - 1} \right)$$

Equation 14

To get a rough estimation of the dilution capacity, Kuentz and Leuenberger [54] proposed to work with the relative bulk density $\rho_{r \text{ bulk}}$. Because $\rho_{c(A)}$ is usually very close to the relative tap density and to be on the safe side the calculation should involve the relative tap density $\rho_{r \text{ tap}}$. If the true densities of substance A and B are similar, the dilution capacity $X_{c(B)}$ equals approximately the difference $1 - \rho_{c(A)}$. Equation 15 is only applicable when the true densities of both substances are very similar. [27]

$$X_{c(B)} = 1 - \rho_{r \text{ tap}}$$

Equation 15

3.5 Liquid - Solid Interactions

3.5.1 Introduction

A systemically acting drug has to be in solution before its uptake over the biological membrane into the blood stream. All steps, from intact tablet to systematic action, are depicted in Figure 7. Water uptake is always the first step; it brings the dissolution media into the tablet. Since dissolution from the surface of the intact tablet is assumed to be small, disintegration is needed to increase the surface area from which the drug can dissolve. [55] Drug release will be the rate-limiting factor in bioavailability if it is slower than the absorption rate. In this case, the release characteristics of the dosage form will determine the drug blood-level profile. This effect is used for sustained-release preparations, where prolonged drug levels in the body are desired. [56]

When a fast onset of action is required, immediate release (IR) dosage forms are designed. The FDA defines an IR product to be rapidly or fast dissolving when no less than 85% of the labelled drug amount dissolves within 30 minutes. [16]

As mentioned by Krämer et al. [55], disintegration of the tablet is required for fast release of the drug. This can be obtained by adding a disintegrant to the formulation.

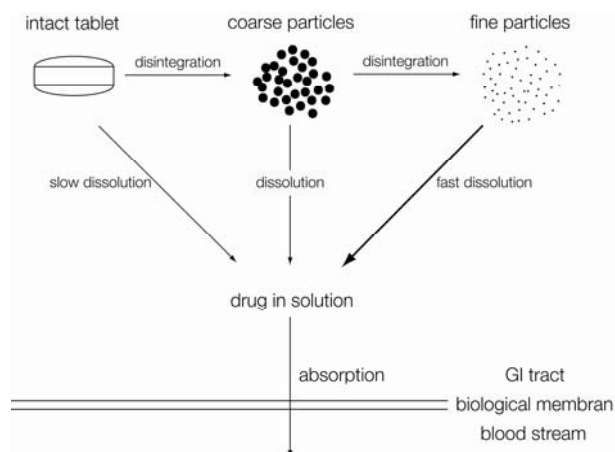


Figure 7: From intact tablet to systemic action.

Bioavailability is not only a question of the formulation and its release properties, but also of the active ingredient. The Biopharmaceutical Classification System (BCS) (Table 5) categorizes all active ingredients based on their aqueous solubility and intestinal permeability. [16]

Dissolution, solubility, and intestinal permeability are three major factors that govern the rate and extent of drug absorption from immediate release (IR) solid dosage forms. [4]

Table 5 The Biopharmaceutical Classification System (BCS).

Class I: high solubility high permeability	Class II: low solubility high permeability
Class III: high solubility low permeability	Class IV: low solubility low permeability

The detailed mechanism and models of water uptake, disintegration, and dissolution are described in the following chapters.

3.5.2 Water Uptake

Water uptake is the first step in the disintegration mechanism of tablets and is therefore also of importance for drug release.

There are two main mechanisms of action for water uptake into the tablet (Figure 8 A and B). In the first case, the water diffuses through a porous network. Low hydrophobicity and good wettability are therefore a pre-requisite for capillary diffusion (A). In the second case, the water diffuses through a solid network of disintegrant particles (B). Diffusion through the disintegrant particle network is possible by default, because disintegrants are assumed to be hydrophilic and water conductive. In practice it is possible that both cases are present within a tablet due to the not perfect mixing. [57]

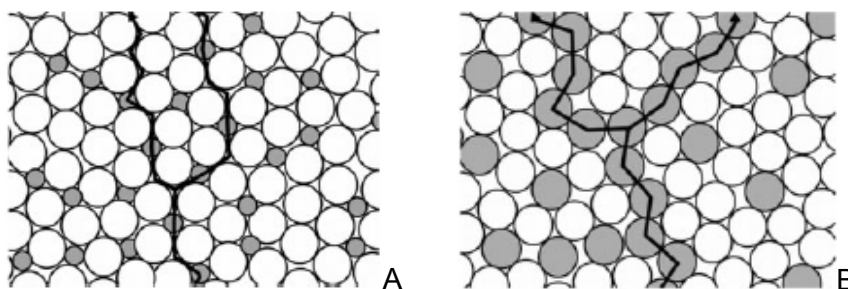


Figure 8: Routes of water uptake through a porous network (A) or through a solid network of disintegrant particles. [57]

THEORETICAL SECTION

For water uptake measurements, it is assumed that the tablet is a system of continuous pores. The penetration rate in a porous system is influenced by the positive capillary forces and the opposite high-viscous inhibiting forces. The capillary attraction is influenced by the pore structure and the liquid. The behaviour of the liquid is important for surface tension and wetting. In contact of the compact with the liquid, the liquid raises into the capillary system of the tablet. Wicking is dependent on the disintegrant properties. An ideal disintegrant particle is fibrous, resistant to collapse, does not swell, and shows a small contact angle. [58] For the quantitative determination of the water uptake into powders and tablets, different methods are applied.

In 1933 Enslin [59] published a method to determine water uptake into a powder bed. This method was static and very imprecise and sensitive; hence the Enslin method was modified several times. In 1986 Van Kamp et al. [60] substituted the volumetric pipette for an analytical balance. The change from volumetric to gravimetric measurements allowed to record data with a computer. The water uptake kinetic was now easier to determine. The nowadays used devices, e.g. the Krüss Tensiometer K 100 used in this study, are based on this Van Kamp equipment.

To evaluate the water uptake kinetics, different equations are applied. The most frequently applied equations are Weibull equation [61], Hill equation [62], and Washburn equation [63]. Ferrari et al. [64] apply the Weibull equation on different tablet systems, where in most cases, the fitting is satisfactory. Only when the tablets show an irregular pattern of water uptake, e.g. kinks or biphasic water uptake, the fitting to Weibull equation is less good. In a later work published in 1991 Ferrari et al. introduced a new model based on the Hill equation. The “maximum effect model” can be applied as a single exponential or as the sum of two or more exponentials, depending on the water uptake pattern. The disadvantage of these two models is the lack of physical meaning.

Equation 16 shows the original Washburn equation. This model gives the relationship between capillary height or pore length (L) and time t. This physical meaning makes it more appropriate than the above mentioned Weibull and Hill equations.

$$L^2(t) = \frac{2 \cdot r \cdot \sigma \cdot \cos\Theta}{k_0 \cdot \eta} \cdot t$$

Equation 16

Further parameters influencing water uptake rate are mean pore radius (r), surface tension between pore wall and liquid (σ), contact angle (Θ), dynamic viscosity of the liquid (η), and a constant accounting for the tablet porosity (k_0).

Unfortunately the classical Washburn equation does not correlate mass and time; using mass is more convenient and more accurate determinable with modern measuring instruments. Introducing mass requires some modifications.

With the average pore radius (r) and the assumption that water has the density 1, following relation between wicked water amount [$Q(t)$] at time t and corresponding height of the liquid column [$L(t)$] in a tablet is found.

$$Q(t) = \pi \cdot r^2 \cdot L(t) \tag{Equation 17}$$

Equation 18 resulting from the combination of Equation 16 and Equation 17 allows the quantification of the amount of water (Q) absorbed in relation to the time.

$$Q^2(t) = \frac{2 \cdot \pi^2 \cdot r^5 \cdot \sigma \cdot \cos \Theta}{k_0 \cdot \eta} \cdot t \tag{Equation 18}$$

Provided that mean pore radius (r), dynamic viscosity (η), contact angle (Θ) and surface tension (σ) are constant over the whole experiment, Equation 19 can be denoted as the modified Washburn equation, where [$Q(t)$] is the amount of water absorbed, (K) the water uptake rate and t the time.

$$Q(t) = K \cdot \sqrt{t} \tag{Equation 19}$$

Guyot-Hermann [65] and Luginbühl [66] listed some limitations of the application of the modified Washburn equation (Equation 19), where some assumptions have to be done. The pore radius (r) is provided to be constant. In reality, the pore structure can break up and can get wider or narrower due to swelling of particles. In consequence, the water uptake is increased or decreased, respectively. The porosity of the tablet, expressed as (k_0) in Equation 16, is supposed to be constant. Pores, in fact, are more or less irregular and show some tortuosity. In case of soluble, mucilaginous disintegrants, the dynamic viscosity (η) is increased over time and the resulting penetration rate is reduced. The variation of

THEORETICAL SECTION

contact angle (Θ) and surface tension (σ) is small and has to be considered as result of increased viscosity. Considering all those limitations, the modified Washburn equation is only applicable in the initial phase of water uptake.

3.5.3 Disintegration

3.5.3.1 Definition and Relevance of Disintegration

Disintegration is the process by which a solid dosage form breaks up when it comes in contact with an aqueous medium. As discussed before, in most cases disintegration is required for drug release. To obtain a fast bioavailability, disintegration is absolute necessary. [65] Even though disintegration and dissolution are treated in two different chapters and therefore appear to be consecutive, they occur simultaneously. Disintegration dominates the early stages, dissolution the later ones. [56]

During compaction interparticle bondings like mechanical interlocking, liquid bridges, intermolecular bonding, or solid bridges are built (see Chapter 3.4.3 Tableting Process and Bonding Mechanisms). In order that the tablet can disintegrate, those bondings have to be overcome. There are various theories describing the process of disintegration.

3.5.3.2 Mechanisms of Disintegration

Disintegration is a complex interplay of different mechanisms. Figure 9 gives a short overview of the mechanisms included. The thickness of the arrow signifies the importance in disintegration. The common factor of all mechanisms is the requirement of water uptake into the system.

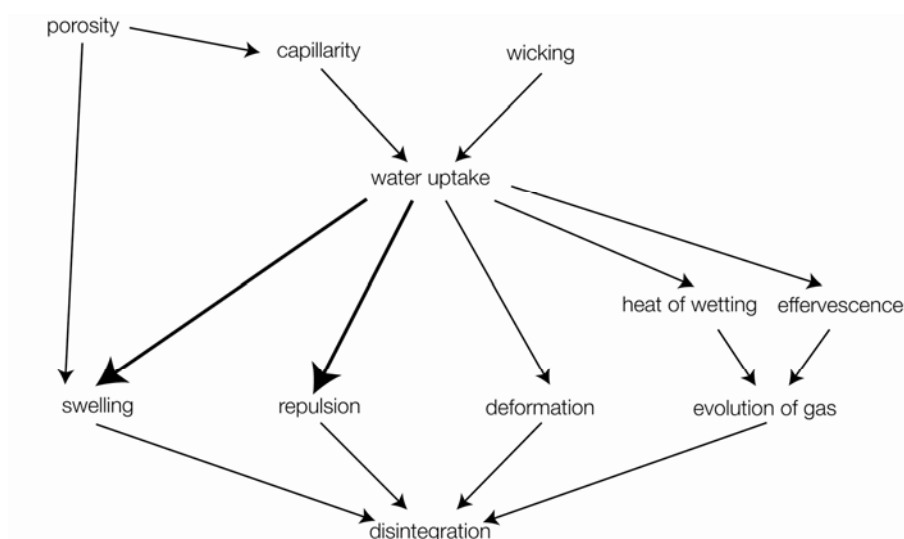


Figure 9: Mechanisms of disintegration.

Water uptake

The mechanism of water uptake is discussed in detail above. In summary, water uptake is promoted by capillarity or wicking. Capillarity is depending on the porosity of the tablet and capillary wall properties, whereas wicking is dependent on the disintegrant properties.

Swelling

Kanig and Rudnic [67] and Guyot-Hermann [65] reviewed many publications related to disintegration properties. They considered swelling as a main mechanism in disintegration. After penetration of water disintegrant particles swell, cause a localized stress, and break up the matrix from within. [68] This can occur only when the tablet matrix does not accommodate to the swelling of the particles by elastic behaviour. [67] The connection between swelling and porosity is nicely summarized by Lowenthal; highly porous tablets with a large void volume show a slow disintegration, because the swelling of the disintegrant particle does not exert enough pressure on the tablet matrix, very dense tablets on the other hand have a decreased ability of water uptake and hence disintegration is slow. [58] This leads to the assumption that the minimal disintegration time is related to a critical relative density.

Even though swelling is perhaps the most widely accepted general mechanism of action, there are also contradictory arguments. List and Muazzam [69] summarize some of the arguments against swelling as a significant disintegration process, e.g. the slowness of the swelling process compared with the quickness of some effective disintegrants, the small volume increase of some effective disintegrants, and the lack of energy release.

THEORETICAL SECTION

Repulsion

However, disintegration cannot be totally explained by swelling. A further widely accepted hypothesis is the particle repulsion theory. Particle repulsion requires water penetration to annihilate cohesion forces between particles resulting in development of repulsion forces and then disintegration. [65] The dissociation of interparticle bondings can be considered as the opposite of compaction, where interparticle bondings are built.

Deformation

Deformation plays rather a minor role in disintegration. Particles deformed under stress of tableting return to their normal size and shape when exposed to moisture. This leads to localized stresses as known from swelling followed by breaking up of the matrix. [68]

Evolution of gas

Moreover, the development of gas within the tablet can lead to disintegration. This happens either due to effervescent ingredients or to expanded air as a result of heat development in contact with water. [65] The latter mechanism of action has to play a minor role, otherwise tablets would fall apart because of heat development during compaction and ejection from tablet press. [58]

Figure 10 summarizes the main mechanisms of disintegration according to Kanig and Rudnic [67].

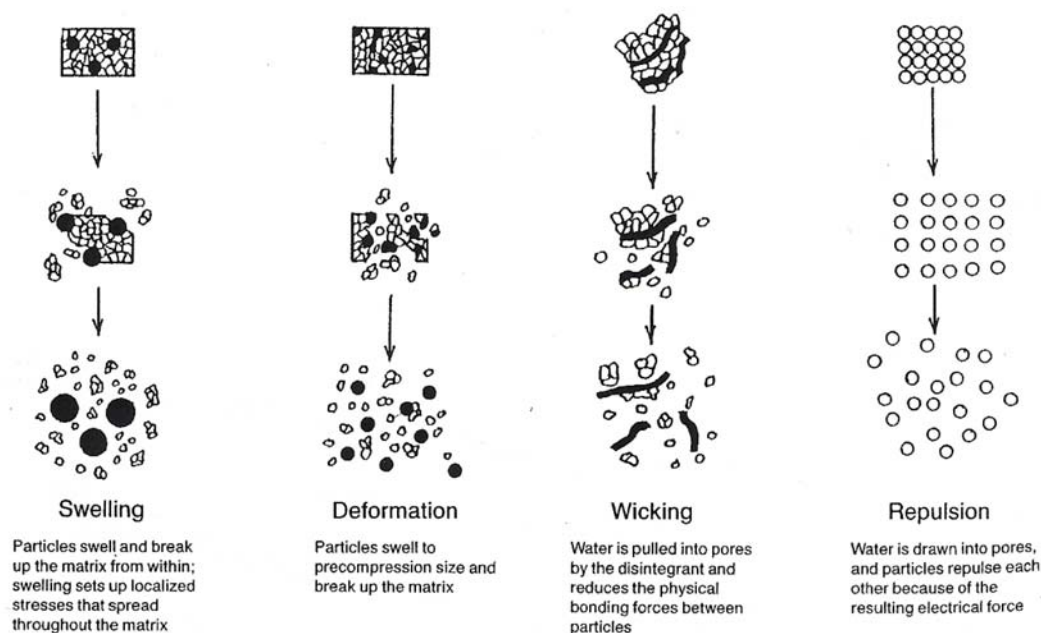


Figure 10: Summary of the main mechanisms of disintegration. [67]

3.5.3.3 Disintegrants

Disintegrants are substances which accelerate the disintegration process when they are in contact with water or gastric juice.

From the practical point of view two groups of disintegrants can be discerned; native starches and so-called “new disintegrating agents”. The problem of starch is the poor compressibility. More efficient disintegrants have been developed therefore. They can be distinguished in following categories [65]:

- modified starches
- cross-linked polyvinylpyrrolidone
- celluloses and modified celluloses
- other types.

Modified starches are basically cross-linked carboxymethyl potato starches which show improved swelling capacity compared with the native starch grains. Two examples of this type are Primojel® and Explotab®. StaRX 1500® is a maize starch physically modified by compaction in presence of water. It contains undamaged maize grains and gelatinized starch particles which swell in contact with water. Additionally to its disintegrating effect, StaRX 1500® shows good flow properties and is well compactable. [65]

Cross-linked PVP is insoluble in water but shows high hydrophilicity. Even though no swelling is observed, it exerts very good disintegration properties already in low concentrations. Examples are Polyplasdone XL® or Kollidon CL®.

Cellulose and modified celluloses enhance water penetration by suction due to their fibrillar structure and the high hydrophilicity. Powdered and microcrystalline cellulose are superficially used as binders but show small disintegrating properties. [36] To increase the hydrophilicity of cellulose, sodium or calcium substitution, carboxymethylation, and cross-linking known from starch modifications were introduced. Ac-di-Sol® is an example for cross-linked sodium carboxy methylcellulose. Compared to the soluble hydroxyl propylcellulose (HPC), the low-substituted hydroxyl propylcellulose (L-HPC) is extremely insoluble. [65] Moreover, excipient properties can be determined by the extent of the modification.

Kumar and co-workers work on new cellulose-based tableting excipients. In 2002 they introduced a cellulose II modification called UICEL, which is a direct compactable excipient with improved disintegration properties. [7] A further development was the cross-linking of UICEL referred to as UICEL-XL, which shows improved compactibility and maintained disintegration behaviour compared to UICEL. [10]

THEORETICAL SECTION

To the last group of disintegrants count cation exchange resins, alginic acid and derivatives, gums and derivatives, mixtures of silicates, pectins, Smecta, and synthetic materials. [65]

Among all those substances, native starches remain highly suitable and the most widely used disintegrant. Problems can arise when very short disintegration times are aspired and hence poorly compressible starch is required in high amounts. In that case the above mentioned disintegrants can be a good alternative. [65]

As pointed out by Hüttenrauch and Keiner [70] the main properties of a good disintegrant are:

- strong hydrophilicity
- weak hydrosolubility
- weak mucilaginous behaviour in contact with water
- high binding power and capacity for plastic deformation and hydrogen bond formation
- good flowability and good compressibility.

Guyot-Hermann [65] reviewed those properties. High hydrophilicity is required for fast water suction inside the tablet. This can be determined by either measuring the mass increase after storage at 100% rH or by water uptake. Disintegrants should be water insoluble to support water uptake by wicking and capillarity. These mechanisms are again hindered by increased viscosity due to mucilaginous behaviour. Flowability, compressibility, and compactibility are more important for production and product quality. Every component in the formulation can influence the product at the end. Disintegrants, particularly when they are used in large portions, can decrease the mechanical stability of the tablet. A good alternative to obtain fast disintegration time without markedly reduced compaction properties is the use of “super-disintegrants”, i.e. disintegrants that are efficient in an amount less than 5%. [71]

3.5.4 Dissolution

3.5.4.1 Definition, Significance, and Developments

Dissolution, i.e. the solubilization of the drug from the intact tablet or from fine particles, was already discussed above. This chapter focuses on the development and importance of dissolution testing and approaches of dissolution profile evaluation.

Even if the first dissolution models were already applied at the end of the 19th century, it took a long time until dissolution testing became compendial. Initially, pharmacopoeias focussed on disintegration time measurements. In 1934 the first official disintegration test was published in the Swiss Pharmacopoeia (Figure 11) [72], followed by the British Pharmacopoeia in 1945 and the USP in 1950. [55] In the early 1950s scientists became aware of the limits of disintegration and the importance of dissolution testing.

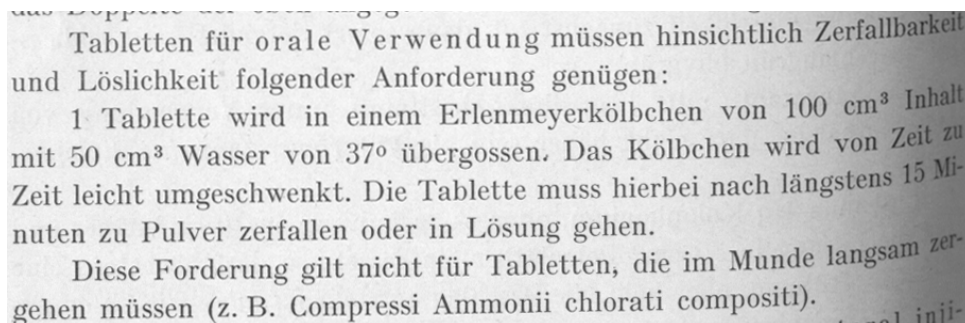


Figure 11: Disintegration test published in Pharmacopoea Helvetica V. [73]

In 1970 the first dissolution test was introduced in USP and NF. [72] Switzerland followed in 1986 with the entry in the 7th edition of Swiss pharmacopoeia. [74] In the following years, the importance of dissolution testing increased and in 1985 a general chapter on drug release was published in USP. [72] Until the early 1970s dissolution was mainly related to in vivo – in vitro correlations (IVIVC), but in the years between 1970 and 1975 dissolution testing became important in formulation research and product quality control. [55]

Nowadays, dissolution testing plays a major role at several stages of the development process. Formulation scientist use dissolution to evaluate the dissolution properties of the drug itself and thereby select appropriate excipients for the formulation. Clinical scientists rely on dissolution tests to establish IVIVC with the goal to minimize clinical studies and thereby costs of product development. Dissolution testing is also routinely used in Quality Control with the focus on batch to batch consistency and detection of manufacturing deviations. [75] The availability of validated, prognostic dissolution methodology would assist the evaluation of preclinical and clinical data by regulatory scientists. In certain cases it may be appropriate and preferred to use dissolution testing to estimate biopharmaceutical implications of a product change. The abdication of bioequivalence studies would save time and costs. [76]

THEORETICAL SECTION

The correlation between in vitro and in vivo studies, not only in the field of oral dosage forms, is the goal of the actual research. To improve the quality of the in vitro – in vivo correlations after oral administration, especially for poorly soluble class II drugs, the use of biorelevant dissolution media was studied. [77] Two dissolution media mimicking the content of the human gastrointestinal tract are called FaSSIF (Fasted State Simulated Intestinal Fluids) and FeSSIF (Fed State Simulated Intestinal Fluids). [78]

3.5.4.2 Mathematical Models

To compare drug release profiles various approaches are possible. The first choice is between model dependent and model independent procedures. Most of the guidelines on dissolution profile comparison recommend model independent methods. [79] They are easy to apply, but they lack scientific justification. [80] Some of those model independent and model dependent approaches are discussed now.

Model independent approach

Costa and Sousa Lobo [80] reviewed model independent approaches and classified them in three groups:

- statistical methods, including single-point comparison with ANOVA and multi-point comparison with MANOVA
- ratio tests, e.g. the ratio of the mean dissolution time or the AUC of two profiles
- pair-wise procedures as difference factor, similarity factor, or Rescigno index [81].

Additionally to the lack of scientific explanation, ratio tests and pair-wise procedures are limited. They allow the comparison of only two different profiles and one of the profiles has to be defined as the reference. Applying simple statistical methods allows at least the comparison of two and more dissolution profiles.

FDA [82] as well as EMEA [83] proposes the application of the similarity factor to compare two dissolution profiles, hence the concepts of difference factor and similarity factor are discussed here.

The FDA [82] defines the difference factor f_1 as follows: “The difference factor (f_1) calculates the percent (%) difference between the two curves at each time point and is measurement of the relative error between the two curves.” The equation to calculate f_1 is

given in Equation 20, where (n) is the number of time points, (R_t) the dissolution value of the reference at the time t, and (T_t) the corresponding value of the test curve.

$$f_1 = \frac{\sum_{t=1}^n |R_t - T_t|}{\sum_{t=1}^n R_t} \quad \text{Equation 20}$$

The similarity factor f_2 (Equation 21) is defined as “the logarithmic reciprocal square root transformation of the sum of squared error and is measurement of the similarity in the percent (%) dissolution between two curves”. [82]

$$f_2 = 50 \cdot \log \left[\left(1 + \frac{1}{n} \cdot \sum_{t=1}^n |R_t - T_t|^2 \right)^{-0.5} \cdot 100 \right] \quad \text{Equation 21}$$

The most suitable dissolution profile comparison is achieved when reference and test products were determined under exactly the same conditions and minimally three to four dissolution points are available. When mean data are used, the relative standard deviation should not be more than 10%, except at the initial stage, where 20% are tolerated. Finally, only one point above 85% of the total drug amount dissolved should be included. When the release of 85% needs less than 15 minutes, the curves can be considered as equal without further mathematical evaluation.

Two curves are considered similar, when f_1 is close to 0 and f_2 is close to 100. f_1 values up to 15 as well as a minimal f_2 value of 50 are required to accept two curves as equal.

Model dependent approach

Model dependent methods are approaches where an equation is fitted to the data of each sample. The received parameters are afterwards compared. These equations have preferably a kinetic background.

The Weibull equation is an empirical equation derived from statistics. Langenbucher adapted it to the dissolution/release profiles. [84] The advantage of Weibull equation is the application to almost all kinds of dissolution curves.

THEORETICAL SECTION

Applied to dissolution rate data, the Weibull equation (Equation 22) expresses the accumulated fraction of the drug (m) in solution at time t .

$$m = \frac{M_t}{M_0} = 1 - e^{-\frac{(t-T)^b}{a}} \quad \text{Equation 22}$$

Furthermore, M_t is the accumulated amount of drug at time t and M_0 is the total amount of the drug in the formulation. In case that the final plateau differs from 1, the fraction is expressed in terms of the actual plateau and the percentages are adjusted accordingly [84] (T) is introduced to the equation considering a possible lag time. For immediate release tablets it is supposed that the drug dissolves immediately after the first contact with the medium, (T) is therefore regarded as zero. The time scale of the process is expressed in the scale parameter a ; the shape parameter b characterizes the curve as follows:

- Case 1 ($b = 1$) exponential curves
- Case 2 ($b > 1$) Sigmoid, S – shaped curves, with upward curvature followed by a turning point
- Case 3 ($b < 1$) parabolic form, with a higher initial slope, followed by the exponential curve

To receive less abstract parameters than a and b , Equation 22, assuming $T = 0$, can be rearranged and modified to Equation 23 which allows the calculation of the more common $t_{10\%}$, $t_{50\%}$, and $t_{90\%}$. M_t is expressed as $x \cdot M_0$, where $x = 0.1, 0.5, \text{ or } 0.9$, respectively.

$$t_{x\%} = \left(-a \cdot \ln \frac{M_0 - M_t}{M_0} \right)^{\frac{1}{b}} \quad \text{Equation 23}$$

As the Weibull model is empirical and is not based on a kinetic fundament, it presents some deficiencies. The lack of parameters related to the intrinsic dissolution as well as the limited use for IVIVC is criticized. The Weibull model can indeed describe the curve, but it does not characterize the dissolution kinetic properties of the drug. [80]

Many models with a kinetic fundament were introduced to the field of dissolution. Costa and Sousa Lobo [80] reviewed various models (Table 6).

Table 6: Dissolution models reviewed by Costa and Sousa Lobo. [80]

Type	Application	Comments
0.Order kinetics	Several types of modified release dosage forms	No disintegration, no change of the area, no equilibrium conditions
1.Order kinetics		Based on Noyes-Whitney equation and further modifications
Higuchi model	Matrix systems	$M_t = k \cdot \sqrt{t}$
Hixson-Crowell model		Solid dimensions diminish proportionally, geometrical form keeps constant
Korsmeyer-Peppas model	Controlled-release polymeric system	
Baker-Lonsdale model	Controlled-release	
Hopfenberg model	Surface-eroding devices with several geometries	

Most of these models are applied on modified release dosage forms. Polli et al. [85] applied different models on immediate release dosage forms. They found Weibull model, first order kinetics, and Hixson-Crowell model the most appropriate.

First order kinetics can ideally be described by Equation 24 which is derived from the Noyes-Whitney equation [86], where M_t is the dissolved amount of drug, M_0 the initial drug load, k the dissolution constant, and t the time.

$$M_t = M_0 \cdot (1 - e^{-k \cdot t})$$

Equation 24

Most of the dissolution profiles do not follow this ideal case, at least not the whole sampling period. Drugs particle on the surface go immediately into solution, this leads to an initial

THEORETICAL SECTION

increase of the dissolution profile. If the tablet is coated or first has to disintegrate, a lag time can be observed.

The Hixson-Crowell equation (Equation 25) accounts for the residual drug instead of the drug released. Hixson and Crowell [87] observed that the particle regular area is proportional to the cubic root of its volume. Due to this link to the cubic root, the model has a second name: “cubic root law”.

$$\sqrt[3]{W_0} - \sqrt[3]{W_t} = k \cdot t \quad \text{Equation 25}$$

The parameters of Equation 25 are the initial drug load W_0 , the remaining amount of drug W_t at time t , and the constant k .

As mentioned in Table 6, the cubic root law as given in Equation 25 is only applicable when the dimensions of the solids, i.e. a tablet or bulk powder, diminish proportionally and the geometrical shape keeps constant. [80]

3.6 Percolation Theory

3.6.1 Historical Development and Theoretical Background

Percolation theory has its origin in the early 1940ies when Flory [88] and Stockmayer [89] studied the gelation and defined it as a process of polymerization. Sixteen years later, Broadbent and Hammersley [90] introduced the term “percolation theory” and established the mathematical fundamentals.

Percolation theory can be applied in very different areas. Stauffer and Aharony [91], in their introduction to percolation theory, mention, for instance, fire propagation in forests. This is a good example to introduce percolation theory.

Considering a forest as a two-dimensional, infinite, square lattice, lattice sites are occupied with trees or not occupied. In Figure 12 a schematic forest is given with two different occupation probabilities (p). Imagine that the fire starts on the left side and it can spread only to a directly neighboured tree. If the forest is sparsely populated with trees (or in other words has a small occupation probability) the fire can penetrate marginally, e.g. in Figure 12 A the fire can destroy only the first group (or finite cluster) of trees. With an increasing amount of trees, the probability of a tree to have a direct neighbour increases. The

occupation probability, where the individual finite clusters merge to one infinite cluster is called the percolation threshold. In the example of Figure 12, the percolation threshold p_c is 0.593. Above this threshold, the fire can spread throughout the whole forest (Figure 12 B). [66, 91]

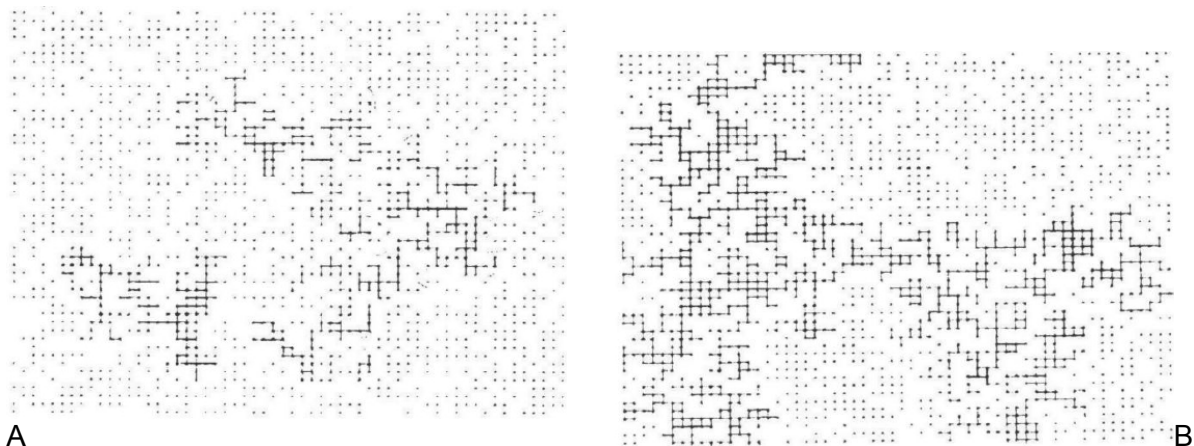


Figure 12: Site percolation in a square lattice; occupation probability 0.5 (A) and occupation probability 0.6 (B). [91]

This mind game is based on a simple two-dimensional square lattice and the phenomenon of site-percolation. In case of a site percolation, each site is randomly occupied with the probability p and empty with the probability $(1-p)$ and clusters are groups of neighbouring occupied sites. [91] These occupied sites may be trees or drug particles and the empty sites glades, pores, or excipients. [92]

Contrary to the site percolation, in bond percolation all lattice sites are occupied from the beginning ($p = 1$). Thus it may be possible to form at random a bond between two particles within the lattice. The cluster size depends on the number of bonds between neighbored particles. [92]

Percolation theory deals not only with the probability of occupation or bonding, but also with different lattice types. In a two dimensional space the square, the honeycomb, and the triangular lattice are important. Diamond, simple cubic, body-centred cubic (BCC), and face-centred cubic (FCC) belong to the three dimensional lattice types. Additionally, there are more complex lattices known, e.g. higher-dimensional lattices or the Bethe lattice which does not belong to the two nor to the three dimensional space. [91] The theoretical values for the percolation threshold can differ depending on the lattice type and the percolation type (bond or site). [91]

THEORETICAL SECTION

In a two-dimensional lattice, only one component can percolate (e.g. trees), whereas in a three dimensional lattice (e.g. a tablet) two components can percolate at the same time and hence two percolation thresholds exist. [92] In a binary system of component A and B, A forms individual clusters in a continuous phase of B when $p < p_{c(A)}$. At the percolation threshold $p_{c(A)}$ component A starts to percolate. Components A and B form now clusters spanning the three-dimensional lattice. With an increasing amount of component A, B is reduced and above a critical concentration ($p_{c(B)}$), B forms only individual clusters in a continuous phase of component A. This phenomenon can be found when A and B differ in their properties. Often multi-component systems can be reduced to binary ones. Table 7 gives an overview of those properties.

Table 7: Properties of components in percolation systems.

A	B
an electrical conductor	an isolator
a hydrophobic powder fraction	a hydrophilic powder fraction
a solid particle	a pore
drug particles	a functional excipient
drug particles	rest of the components

3.6.2 Application in Powder Technology

Percolation theory allows a new insight in the formulation of dosage forms and their properties. The following sub-sections focus on the important concepts used in this work. More applications of the percolation theory in this field can be found in a recommendable review of Leuenberger. [92]

Compressibility

As already described in Chapter 3.4.5.1, compressibility can be described applying Heckel equation and modified Heckel equation.

In words of percolation theory, tablet formation can be described as a combination of site and bond percolation phenomena. Leu and Leuenberger [93] describe these phenomena

as follows. After pouring the particles into the die lattice sites are either empty forming pores or occupied by molecules forming clusters. Under compression, the number of lattice sites is continuously reduced until the final tablet dimension is achieved. First, fine particles are bonded by weak inter-particulate forces, in other words, as soon as the particles are in contact, a bond percolation throughout the powder bed exists (p_{c1}). Under further compression, a relative density is reached at which the particles can not easily be displaced anymore and an important increase of the compression force must be expected (p_{c2}). This is now typical for a site percolation phenomenon with the site percolation threshold. Further increase of the compression force leads to the third threshold (p_{c3}), where the pore system will no longer form a continuous network.

The percolation threshold p_{c2} correlates to the critical relative density of the modified Heckel equation (Equation 7) where rigidity starts to evolve and a negligible mechanical resistance between the punches is produced. [51]

Compact strength

Percolation theory influences also the compact strength of tablets. Considering a well compactable substance A creating adequate strength and a poorly compactable substance B exhibiting no bonding strength, only substance A is relevant for the tensile strength. (If B is regarded as pores in a matrix of A, it will be clear that only A is responsible for the adequate strength.) Beside the percolation threshold of the relative density which was already discussed above and which is also valid for mixtures there exists also a threshold of the mass fraction. [54] The tablet hardness is controlled entirely by the component which percolates the system. [52] The maximal mass fraction of the poorly compactable drug is called dilution capacity. (see also chapter 3.4.6, page 24)

Both models to calculate the dilution capacity (Equation 13 and Equation 14) request the mechanical percolation threshold of the well compactable substance A. [54]

Water uptake, disintegration, and dissolution

Water uptake and sequentially disintegration and dissolution are influenced by percolation phenomena. According to Luginbühl and Leuenberger [68] maximal water uptake rate correlates with minimal disintegration time and maximal dissolution rate.

As already explained in chapter 3.5.2, two main mechanisms of action are responsible for water uptake. In the first case the water diffuses through a porous network, in the second case water is conducted through a solid network of disintegrant particles (Figure 8 A and B). [57] In the first case, where water is conducted by the pores, a continuous network of pores is required, i.e. the relative density has to be lower than the percolation threshold p_{c3} (see above). But also a minimal relative density is necessary to build capillaries. In case

THEORETICAL SECTION

two, where the water is conducted by the disintegrant particles, a critical amount of disintegrant exists. Figure 13 gives a short explanation of the influence of the disintegrant amount on the disintegration time and the link to percolation theory.

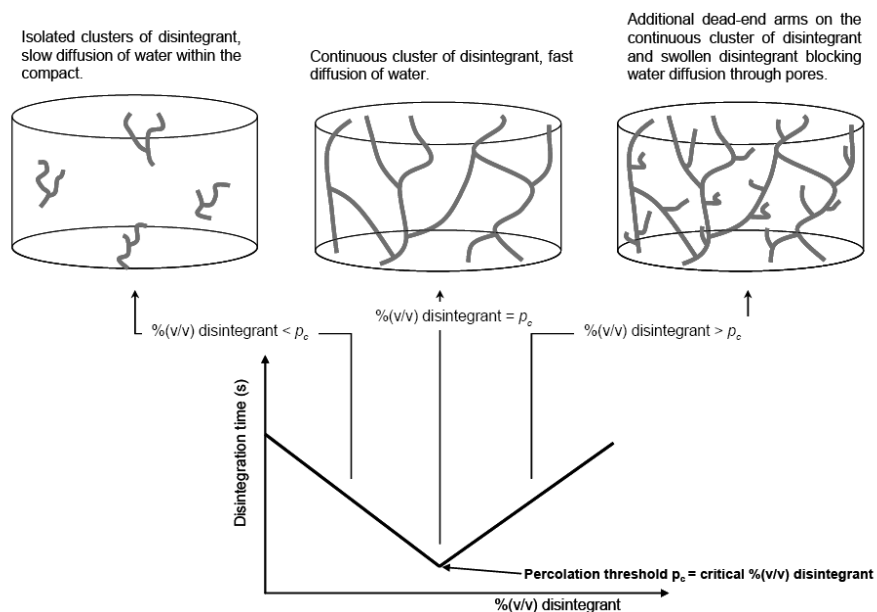


Figure 13: Percolation theory and the influence of the amount of disintegrant on disintegration properties. [94]

Relevance in formulation design

It is known that the critical concentration of a component in a binary or more complex powder mixture is a source of lack of robustness of a formulation. To avoid problems in scale-up and production, the formulations have to be developed carefully. [92] Components should not be used close to the critical concentration, e.g. when dealing with dilution capacity.

4 Material and Methods

4.1 Material

4.1.1 Storage

All powder substances were stored over a saturated solution of potassium chloride (K_2CO_3 , Hanseler AG, Herisau, CH) for at least 14 days. The resulting relative humidity was about 44%. [95]

4.1.2 Model Drug

Proquazone, a quinazolinone derivative and a weak base, is highly lipophilic and shows poor solubility in water. [96] The melting point is 140.0 – 144.0°C. It appears as a yellow, crystalline powder, inodorous or with a weak characteristic odour.

Proquazone is an NSAID that was used in musculoskeletal and joint disorders. [97]

Proquazone: Charge: 87327, supplied from Sandoz AG, Basel, CH (nowadays: Novartis Pharma AG, Basel, CH)

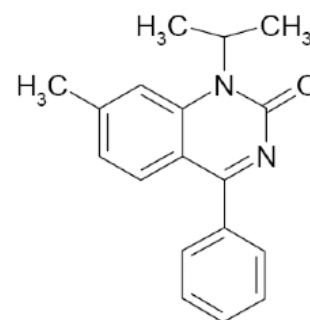


Figure 14: Chemical structure of proquazone.

4.1.3 Excipients

4.1.3.1 Celluloses

The celluloses used can be classified in four different classes. Class 1 are cellulose I modifications, class 2 are partially converted Cellulose II modifications, class 3 are fully converted cellulose II modifications, and Class 4 are cross-linked cellulose II modifications. MCC 102 was used as a standard for cellulose I modifications, UICEL-A/102 (S) as a standard for cellulose II modifications. UICEL-A/102 (SM) that was used for granulation experiments originates from UICEL-A/102 (S) and was milled with a ball mill (Pulverisette, Type 501, Fritsch GmbH, Idar-Oberstein, D). Names, lot numbers, and producers are listed in Table 8.

MATERIAL AND METHODS

Table 8: Celluloses types used in this study.

Class	Name (later referred to as)	Lot and Producer
Class 1	MCC SANAQ 102 (MCC 102)	Lot: 24 03 58 Pharmatrans SANAQ AG, Basel, CH
Class 2	MCC SANAQrapid Type I (Type I)	Lot: 120-T18 Pharmatrans SANAQ AG, Basel, CH
Class 3	UICEL-A/102 (S) (UICEL S)	Lot: MR-II-90-09/903 University of IOWA, IOWA, USA
	MCC SANAQrapid Type II (Type II)	Lot: 126-T03 Pharmatrans SANAQ AG, Basel, CH
	UICEL-A/102 (B) (UICEL B)	Lot: n/a University of Applied Sciences FHNW, MuttENZ, CH
Class 4	UICEL-XL (UICEL-XL)	Lot: MRM-V-43004-114 University of IOWA, IOWA, USA

4.1.3.2 Magnesium Stearate

Magnesium stearate is a mixture of different fatty acids, mainly stearic acid and palmitic acid. It is a white, very fine, bulky, impalpable unctuous powder, tasteless, odourless or with a faint odour of stearic acid. Magnesium stearate is practically insoluble in water and water free ethanol. [35]

Magnesium stearate: Lot: 84808, Novartis Pharma AG, Basel, CH

4.1.3.3 PVP

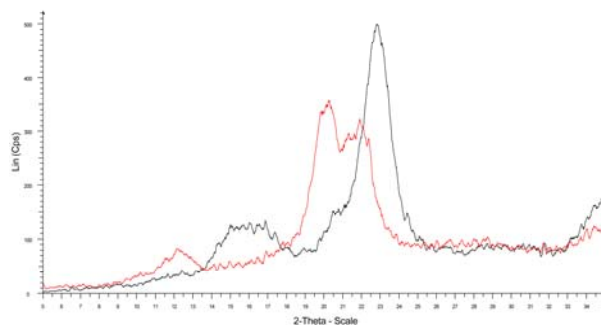
PVP (Polyvinylpyrrolidone) is a fine, white or very slightly cream-coloured, tasteless, matt finished powder, slightly sticky, with a weak characteristic flavour. It is good soluble in water, ethanol 96% and methanol, but poor soluble in acetone. [35]

Kollidon K30 (Art: 26-6952), Lot: 87819, BASF, Ludwigshafen, D

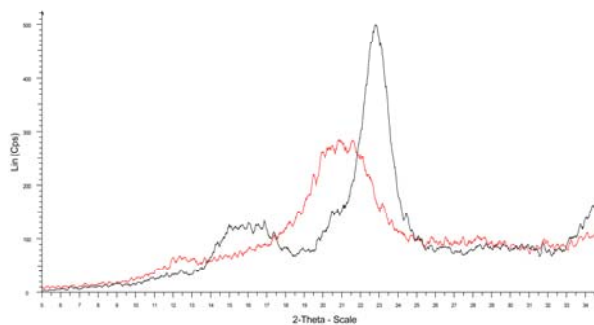
4.1.4 Powder Characterisation

4.1.4.1 Structure Analysis with X-Ray

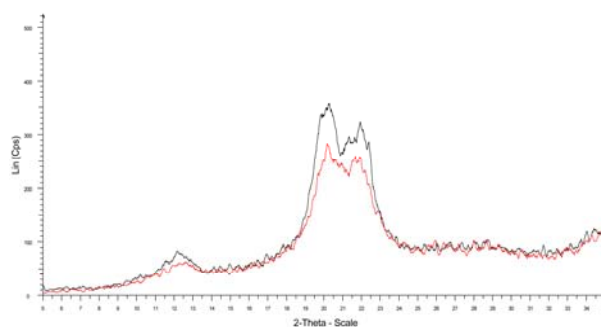
The analysis was performed at the Institute of Mineralogy and Petrography of the University of Basel (X-Ray Diffractometer Siemens D5000, Siemens, München, D).



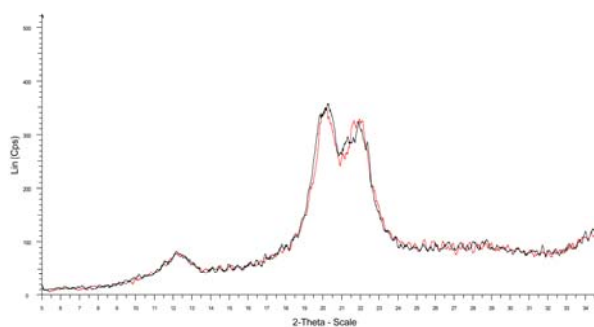
A: MCC 102 and **UICEL S**



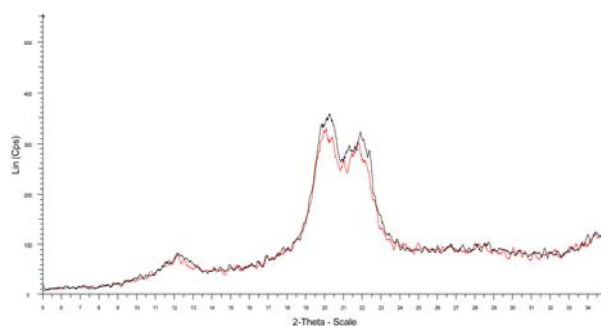
B: MCC 102 and **Type I**



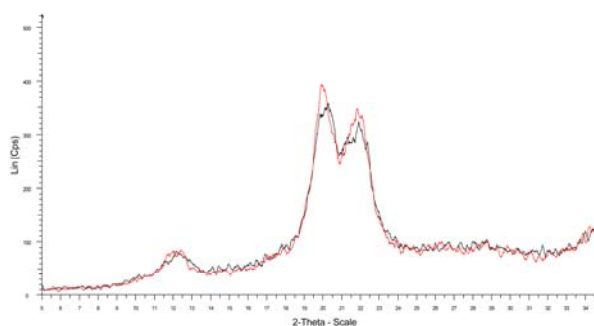
C: UICEL S and **Type II**



D: UICEL S and **UICEL B**



E: UICEL S and **UICEL SM**



F: UICEL S and **UICEL-XL**

Figure 15: X-ray diffractograms of all types of cellulose.

MATERIAL AND METHODS

4.1.4.2 Scanning Electron Microscopy (SEM)

Scanning electron microscopy pictures were done at the Centre of Microscopy at the University of Basel. (Scanning Electron Microscope, Philips XL 30 FEG ESEM, Philips, Eindhoven, NL). Before sputtering to achieve conductivity, the samples were dried over P₂O₅ (Art. 79609, Fluka, Buchs (SG), CH).

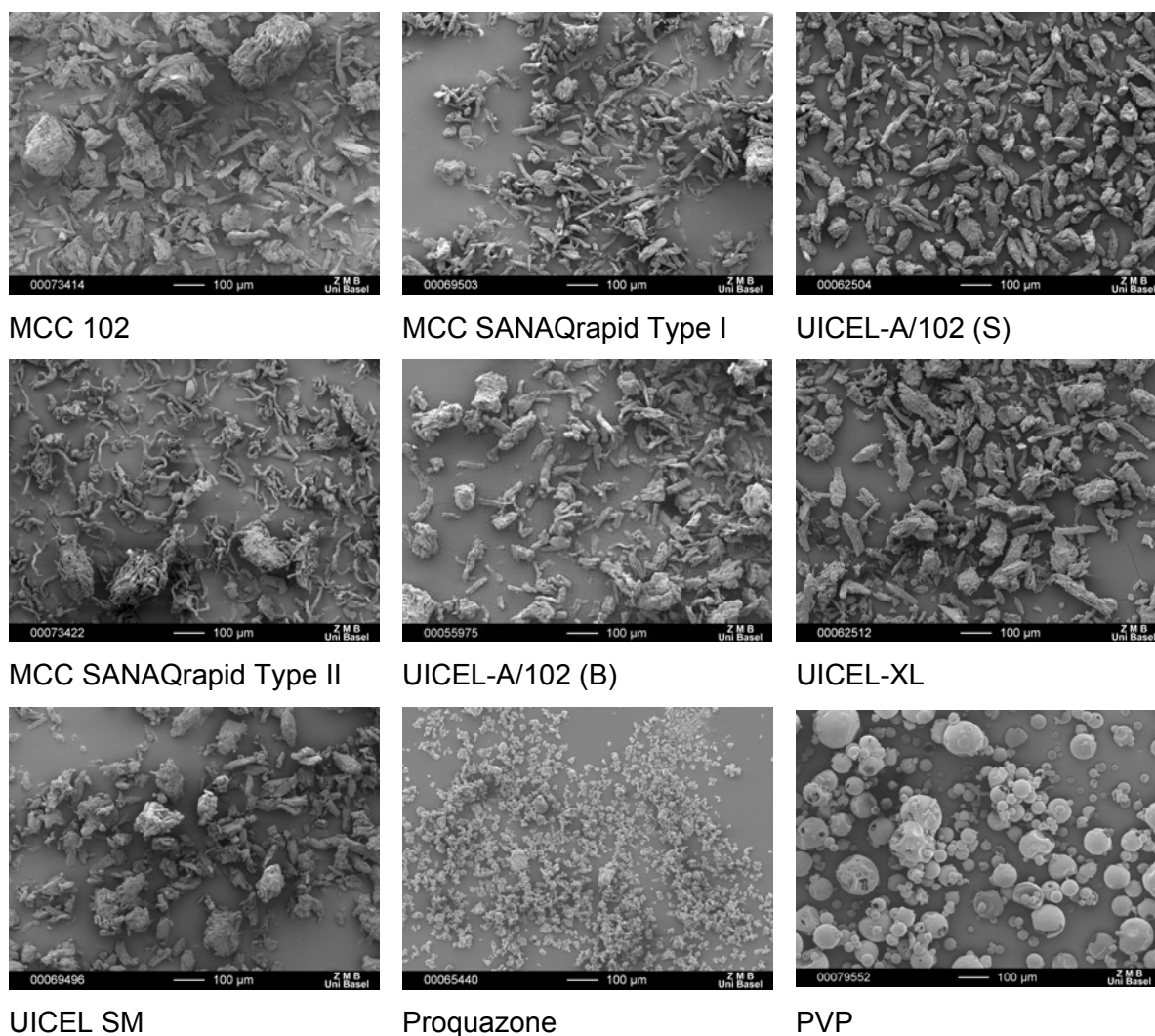


Figure 16: SEM pictures of powders (x 100).

4.1.4.3 Particle Size Determination

Particle size was determined with Mastersizer X (Malvern Instruments, Malvern, UK) and the MS-1-Small Volume Presentation Sample Units (Type MS519, Malvern Instruments,

Malvern, UK). Celluloses were dispersed in ethanol 96% (Et0007, Scharlau Chemie SA, Barcelona, E); proquazone was dispersed in water with Tween 80 (surf-24571, ICI Chemicals & Polymers, Middlesbrough, UK). The powders were sieved before (mesh size 180 μm). Five measurements per sample were performed after 30 seconds under constant stirring conditions for 30 seconds.

Table 9: Average and median particle size of celluloses.

	Average Particle Size [μm]		Median Particle Size [μm]	
	Average	SD	Average	SD
MCC 102	93.08	2.76	85.76	3.03
MCC SANAQrapid Type I	50.54	6.97	40.70	4.37
UICEL-A/102 (S)	73.27	3.24	66.08	2.57
MCC SANAQrapid Type II	109.97	23.94	86.27	19.92
UICEL-A/102 (B)	63.76	13.98	49.56	6.87
UICEL-XL	77.68	9.09	65.46	11.73
UICEL-A/102 (SM)	62.99	0.77	55.85	1.22

Table 10: Average and Median particle size of proquazone.

	Average Particle Size [μm]		Median Particle Size [μm]	
	Average	SD	Average	SD
Proquazone	15.60	0.50	15.09	0.51

The fibrous form of the particles and in some case fine powder can disturb the measurements and lead to a broad distribution of the particles.

MATERIAL AND METHODS

4.1.4.4 Densities

True density ρ_t was determined in triplicate with Helium Pycnometry (AccuPyc 1330, Micromeritics Instruments Corporation, Norcross, USA).

Bulk and tap density (ρ_{bulk} and ρ_{tap} , resp.) were determined according to the European Pharmacopoeia 5.0. [35] Due to the small sample size, the sample volume was reduced and the measurement was carried out in a 25 ml graduated cylinder. (Stampfvolumeter, STAV 2003, J. Engelsmann AG, Ludwigshafen am Rhein, D)

The relative bulk density ($\rho_{r \text{ bulk}}$) and the relative tap density ($\rho_{r \text{ tap}}$) were calculated according to following equation:

$$\rho_{r \text{ bulk}} = \frac{\rho_{\text{bulk}}}{\rho_t} \quad \text{respectively} \quad \rho_{r \text{ tap}} = \frac{\rho_{\text{tap}}}{\rho_t} \quad \text{Equation 26}$$

Table 11: Densities of celluloses.

n=3	ρ_t [g/cm ³]	ρ_{bulk} [g/cm ³]	ρ_{tap} [g/cm ³]	$\rho_{r \text{ bulk}}$	$\rho_{r \text{ tap}}$
MCC 102	1.5875 (0.0004)	0.369 (0.012)	0.467 (0.007)	0.233 (0.008)	0.294 (0.004)
MCC SANAQrapid Type I	1.5322 (0.0036)	0.414 (0.007)	0.615 (0.006)	0.270 (0.004)	0.401 (0.004)
UICEL-A/102 (S)	1.5476 (0.0082)	0.422 (0.015)	0.554 (0.007)	0.273 (0.009)	0.358 (0.005)
MCC SANAQrapid Type II	1.5461 (0.0023)	0.247 (0.0003)	0.448 (0.006)	0.160 (0.0002)	0.290 (0.004)
UICEL-A/102 (B)	1.5462 (0.0010)	0.421 (0.012)	0.616 (0.005)	0.273 (0.008)	0.398 (0.003)
UICEL-XL	1.5578 (0.0019)	0.394 (0.006)	0.528 (0.004)	0.253 (0.004)	0.339 (0.003)
UICEL-A/102 (SM)	1.5433 (0.0067)	n/a	n/a	n/a	n/a

Table 12: Densities of proquazone and magnesium stearate.

n=3	ρ_t [g/cm ³]
Proquazone	1.2517 (0.0002)
Magnesium stearate	1.0525 (0.0045)

4.1.4.5 Hausner Factor and Carr's Index

Hausner Factor and Carr's Index were calculated and classified according European Pharmacopoeia 5.3. [35]

Table 13: Hausner Factor, Carr's Index, and the classification of the powder flow properties.

n=3	Hausner Factor	Carr's Index	Classification
MCC 102	1.27 (0.02)	20.99 (1.54)	moderate
MCC SANAQrapid Type I	1.49 (0.01)	32.68 (0.47)	very poor
UICEL-A/102 (S)	1.31 (0.03)	23.83 (1.77)	moderate
MCC SANAQrapid Type II	1.81 (0.03)	44.88 (0.79)	insufficient
UICEL-A/102 (B)	1.46 (0.05)	31.56 (2.46)	very poor
UICEL-XL	1.34 (0.02)	25.38 (1.36)	moderate
UICEL-A/102 (SM)	n/a	n/a	n/a

4.1.4.6 Moisture Content

Loss on drying was determined thermogravically (Mettler-Toledo LP 16, Mettler-Toledo GmbH, Greifensee, CH). Before tableting, 1.0 – 1.7 g of the sample were heated at 105°C for 20 minutes.

MATERIAL AND METHODS

Table 14: Average moisture content (incl. standard deviation) and minimum and maximum moisture contents of powders used for direct compaction studies.

	Average MC [%]	Minimum MC [%]	Maximum MC [%]	n=
MCC 102	5.52 (0.73)	3.85	7.29	34
Type I	5.59 (0.91)	4.22	7.50	13
UICEL S	7.49 (0.56)	6.49	8.17	11
Type II	6.46 (0.75)	5.51	7.51	15
UICEL B	7.74 (0.65)	6.82	8.41	11
UICEL-XL	3.94 (n/a)	3.94	3.94	1
Proquazone	0.94 (0.76)	0.09	2.04	5

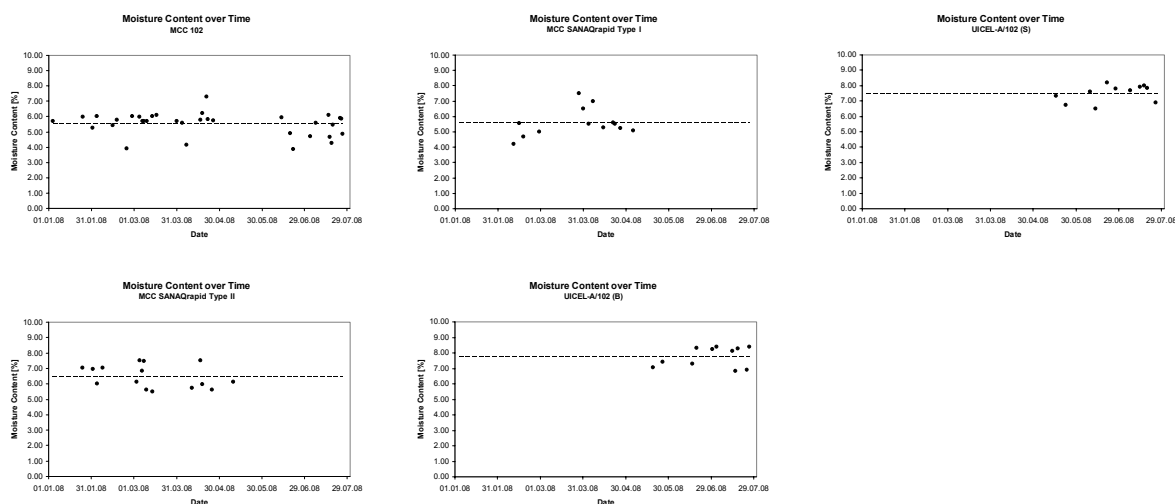


Figure 17: Moisture content over time of celluloses used in direct compaction studies (dotted line: average value).

Table 15: Average moisture content (incl. standard deviation) of powders used for granulation.

n=3	Average MC [%]
UICEL-A/102 (SM)	7.18 (0.79)
PVP	13.24 (0.14)

4.1.4.7 Solubility

Approximately 1 g proquazone was added to 100 ml HCl 0.1 M and stirred for 48 hours at $37 \pm 0.2^\circ\text{C}$. The magnetic stirrer (Variomag Telesystem Komet, Sterico, Wangen, CH) was placed in a water bath (Julabo, Julabo GmbH, Seelbach, D). Samples were taken after 90 minutes and 48 hours. The quantitative analysis was done as described in Chapter 4.4.8 (Dissolution) on page 62.

Table 16: Solubility of proquazone.

n=3	90 min	48 h
Solubility [g/l]	1.11	1.36
SD	0.12	0.03
RSD	10.55%	1.00%

4.1.4.8 Water Uptake Rate

Six tablets were compressed to approximately ρ_r 0.8. Water uptake rate was determined according to the method described in chapter 4.4.6.

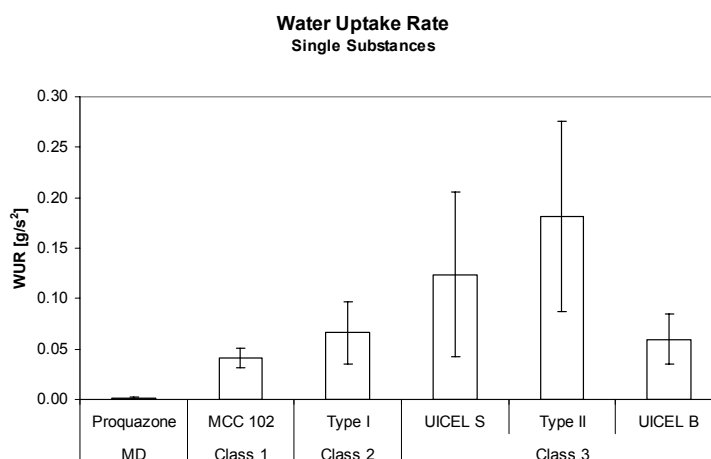


Figure 18: Water uptake rate of single substances.

4.2 Granulation

4.2.1 Preparation

Granulation was performed in a fluidised bed system (MiniGlatt, Glatt GmbH, Binzen, D). Approximately 80 g of powder mixture was mixed in Turbula (Type T2A, Willy A. Bachofen AG Maschinenfabrik, Basel, CH) for five minutes and then sieved (mesh size 355 μ m). This sieved mixture was transferred to the fluidised bed system, where it was mixed and heated up to a bed temperature of 33°C (Temperature probe, testo 925 (°C, °F, K), testo AG, Lenzkirch, D). The inlet temperature was set to 75°C. The binder liquid, PVP (5% (m/m)) in water, was sprayed in a rate of 6.3 g/min at the beginning and increased to 8.3 g/min when 50% was added. The spray rate was controlled by a peristaltic pump (Flocon 1003, Periflo, Loveland (Ohio), USA). The atomized air pressure was set to 0.04 MPa. After adding approximately 80 g of binder liquid, the granules were dried in the fluidised bed system until the bed temperature reached 33°C. The room temperature was about 23°C and the relative humidity varied from 36% to 40%. The process air pressure was maximally 0.15 bar.

Table 17: Composition of the granules.

Batch	Proquazone [g]	UICEL (SM) [g]	MCC 102 [g]	PVP [g]
UICEL-A/102 (SM)	16.0	60.0	0.0	4.0
MCC 102	16.0	0.0	60.0	4.0

4.2.2 Granules Characterisation

4.2.2.1 Scanning Electron Microscopy (SEM)

Analysis was performed according to the method used for powder characterisation. (4.1.4.2 Scanning Electron Microscopy (SEM), page 48)

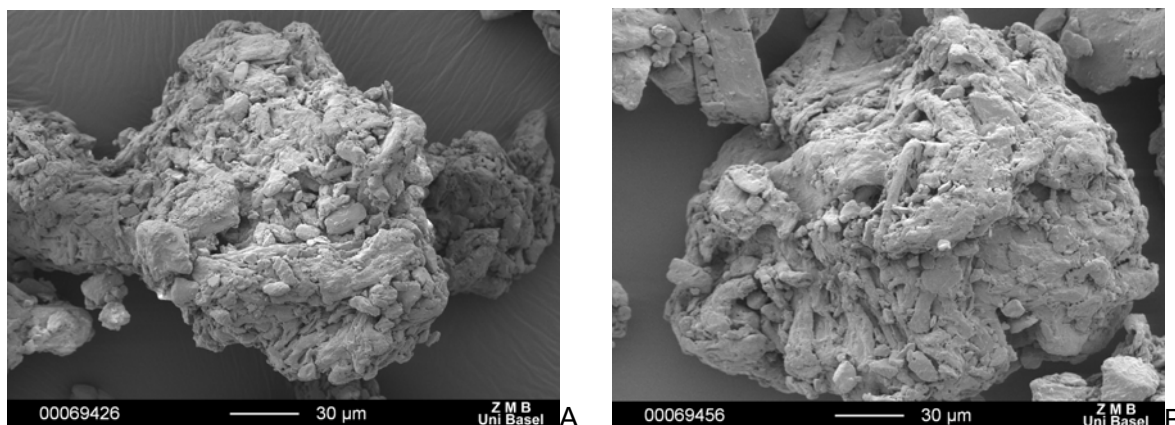


Figure 19: SEM pictures of the granules containing UICEL-A/102 (A) and MCC 102 (B) (x 500).

4.2.2.2 Particle Size Determination

Particle size determination of granules was done with Malvern Mastersizer X (Malvern Instruments, Malvern, UK) using the MS 64-Dry Powder Feeder (MSX 64, Malvern Instruments, Malvern, UK). Before measurement, the samples were sieved (mesh size 355 µm).

Table 18: Average and median particle size of granules.

n=5	Average Particle Size [µm]		Median Particle Size [µm]	
	Average	SD	Average	SD
UICEL-A/102 (SM)	97.28	3.78	83.42	2.03
MCC 102	127.42	0.91	122.66	1.08

MATERIAL AND METHODS

4.2.2.3 Densities

The densities were analysed as described for powder characterisation (4.1.4.4 Densities, page 50).

Table 19: Densities of granules.

n=3	ρ_t [g/cm ³]	ρ_{bulk} [g/cm ³]	ρ_{tap} [g/cm ³]	$\rho_{r\ bulk}$	$\rho_{r\ tap}$
UICEL-A/102 (SM)	1.4456 (0.0001)	0.402 (0.001)	0.518 (0.003)	0.278 (0.001)	0.358 (0.002)
MCC 102	1.4722 (0.0013)	0.367 (0.005)	0.472 (0.002)	0.249 (0.003)	0.321 (0.002)

4.2.2.4 Hausner Factor and Carr's Index

Hausner Factor and Carr's Index were calculated and classified as described in Chapter 4.1.4.5.

Table 20: Hausner Factor, Carr's Index, and the classification of the flow properties of granules.

n=3	Hausner Factor	Carr's Index	Classification
UICEL-A/102 (SM)	1.29 (0.01)	22.31 (0.54)	moderate
MCC 102	1.29 (0.01)	22.23 (0.65)	moderate

4.2.2.5 Moisture Content

The moisture content was determined as described for powder characterisation. (4.1.4.6 Moisture Content, page 51)

Table 21: Average moisture content (incl. standard deviation) of granules.

n=3	Average MC [%]
UICEL-A/102 (SM)	6.61 (0.21)
MCC 102	5.08 (0.26)

4.2.2.6 Drug Content

About 300 mg of the granules were weighed and dissolved in HCl 0.1 M. After 15 minutes in the ultrasonic bath (M. Scherrer AG Apparatebau, Wil, CH), the solution was centrifuged (Centrifuge, Sigma 302 K, Sigma Laborzentrifugen GmbH, Osterode am Harz, D). The excess was diluted and the absorption was determined at 230 nm. (General Purpose UV/VIS Spectrophotometer, DU 720, Beckman Coulter, Fullerton (CA), USA)

Table 22: Drug content (incl. standard deviation) of granules.

n=3	Content [%]
UICEL-A/102 (SM)	17.48 (1.13)
MCC 102	14.76 (1.08)

4.3 Tablet Compaction

4.3.1 Single Substance Compaction

Tablets were compressed using Zwick Universal Testing Instrument (Type 1478TM, Zwick GmbH, Ulm, D) equipped with an 11 mm flat-faced punch. The die was lubricated with magnesium stearate in advance. Approximately 300 mg of powder was weighed (Analytical balance, AT 460 Delta Range®, Mettler-Toledo GmbH, Greifensee, CH) and transferred manually to the die. Compaction force was set in a range of 0.5 kN to 35 kN. Compaction and ejection speed was set to 25 mm/min, load relieving speed to 100 mm/min.

4.3.2 Compaction of Binary Mixtures of two Excipients with a Constant Compaction Force

All powders were sieved (mesh size 355 μ m) before weighing and mixing (Turbula mixer, Type T2A, Willy A. Bachofen AG Maschinenfabrik, Basel, CH). After eight minutes mixing, sieved magnesium stearate 0.5% (m/m) (mesh size 180 μ m) was added and mixed for two additional minutes. The tablet weight was 300mg \pm 1mg. The mixtures were compacted using the Zwick Universal Testing Instrument equipped with an 11 mm flat-faced punch. Compaction occurred with a speed of 25 mm/min to the final compaction force of 7 kN, load relieving with 100 mm/min and ejection with 25 mm/min.

4.3.3 Compaction of Binary Mixtures of two Excipients to a Constant Relative Density

All powders were sieved (mesh size 355 μ m) before weighing and mixing them for seven minutes. Approximately 300 mg of the mixture were compacted using the Zwick Universal Testing Instrument equipped with an 11 mm flat-faced punch. The die was lubricated with magnesium stearate in advance. Compression, load relief, and ejection speed were set to 200 mm/min. The immersion depth of the punch was calculated according to Equation 1.

4.3.4 Ternary Mixture Compaction

The powder mixture was mixed for five minutes in a Turbula mixer, then sieved (mesh size 355 μ m) and mixed again for three minutes. After adding 0.5% (m/m) sieved magnesium stearate (mesh size 180 μ m), the mixture was finally sieved for two minutes. The tableting mass was individually weighed (approximately 300 mg) and transferred to the die. The powder was compacted using the Zwick Universal Testing Instrument equipped with an

11 mm flat-face punch to obtain tablets with a constant relative density. The method of calculation and compaction was equal to the method described in chapter 4.3.3, but with introduced dwell time of 10 ms.

4.3.5 Compaction for Granulation Studies

4.3.5.1 Tablets Made From Granules Compacted with a Constant Compression Pressure

After sieving (mesh size 355 μm) and adding magnesium stearate (0.5% [m/m]), the granules were mixed for two minutes in a turbula mixer. About 300 mg of this mixture were compressed on the Zwick Universal Testing Instrument equipped with an 11 mm flat-faced punch applying a constant compression force of 7 kN. Compression, load relief, and ejection speed were set to 200 mm/min.

4.3.5.2 Tablets Made From Powders

The powders were individually weighed and mixed for five minutes. After sieving (mesh size 355 μm), the mixture was mixed for further five minutes. Sieved (mesh size 180 μm) magnesium stearate (0.5% [m/m]) was added and mixed for the last two minutes. This mixture was then weighed (about 300 mg) and compressed on the Zwick Universal Testing Instrument equipped with an 11 mm flat-face punch to a defined relative density. Compaction settings were equal to the method described in Chapter 4.3.3. The target relative density was calculated to be identical to the relative density of the corresponding tablets made from granules.

4.3.5.3 Tablets Made From Granules Compacted to a Constant Relative Density

Tablets were prepared as described in Chapter 4.3.5.1, but compressed to a target relative density as described in Chapter 4.3.5.2.

4.4 Tablet Characterisation

4.4.1 Tablet Storage

All tablets were stored for three or four days in a desiccator over a saturated solution of potassium chloride. (see also 4.1.1)

4.4.2 Relative Density

The relative density ρ_r of the tablets was calculated according to Equation 1. The mass of the tablets was determined on an analytical balance (Mettler AT 460 Delta Range®, Mettler-Toledo GmbH, Greifensee, CH); tablet height and diameter were investigated with a digital calliper (Digit CAL SI, TESA SA, Rennens, CH).

4.4.3 Elastic Recovery

The elastic recovery was calculated according to Equation 27, where h is the tablet height after three or four days and h_{\min} is the tablet height under maximal load. h_{\min} was calculated from the Zwick raw data.

$$ER[\%] = \frac{h - h_{\min}}{h_{\min}} \cdot 100 \quad \text{Equation 27}$$

4.4.4 Crushing Strength and Tensile Strength

The crushing strength of the tablets was determined in triplicate with a tablet hardness tester (Tablet Tester 8M, Dr. Schleuniger, Pharmatron, Solothurn, CH).

Tensile strength σ_t (Equation 3) was calculated from the crushing strength F , the tablet diameter (D) and the tablet height (h).

4.4.5 Compaction Models

Compressibility was studied applying three different models such as Heckel equation (Equation 4, page 21), modified Heckel equation (Equation 7), and modified Van der Waals equation of the state (Equation 12). Compressibility and compactibility were investigated applying the Leuenberger equation (Equation 8).

Constant K from Heckel equation was determined with linear regression using Microsoft® Office Excel 2003 in a range of 21.05 to 84.18 MPa. The parameters ρ_c and C from the modified Heckel equation were received from non-linear regression on the data until 105.23 MPa using Mathematica® 5.2 (Wolfram Research, INC, Champaign, USA). The same method and data range was used to establish V_t , B_V , A_V , and C_V from the modified Van der Waals equation of the state. To evaluate the maximal tensile strength $\sigma_{t \max}$ and the pressure susceptibility γ_t from Leuenberger equation, the full data set was fitted using non-linear regression with Mathematica® 5.2.

Tablets were produced as described in Chapter 4.3.1 (Single Substance Compaction). Additionally, modified Heckel equation was applied on binary mixtures of proquazone and cellulose prepared according to 4.3.4. All measurements were done in triplicate.

4.4.6 Water Uptake Rate

Water uptake was determined with a Krüss K 100 MK Tensiometer (Krüss GmbH, Hamburg, D). The sample cell consisted of a glass tube and a bottom cap with a filter paper (Rufi 597, Schleicher & Schuell AG, Feldbach, CH; Rundfilter Grade 91 and Grade 1, Whatman plc, Maidstone, UK) which was fixed on a balance. The immersion depth of the sample cell was 0.5 mm; the maximal measurement time was set to 1200 seconds with two points per second. The endpoint was set to five consecutive identical values.

The water uptake, measured as mass^2 per time [g^2/s], was evaluated with linear regression in a range of 20 – 60% of the maximal water uptake.

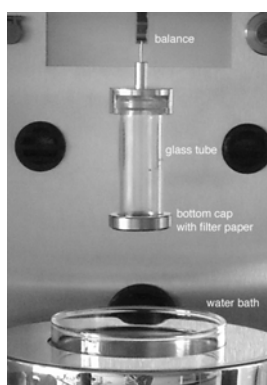


Figure 20: Sample cell for water uptake measurements consisting of a glass tube and a bottom cap.

MATERIAL AND METHODS

4.4.7 Disintegration Time

Disintegration time was determined with the manual disintegration tester SOTAX DT 3 (SOTAX AG, Basel, CH) according to European Pharmacopoeia 5.0 [35] in 700 ml purified water ($37 \pm 0.5^\circ\text{C}$) using disks. The average was calculated from 6 tablets.

Disintegration time in granulation studies was additionally determined under the same conditions but without disks.

4.4.8 Dissolution

Drug release was carried out in triplicate according European Pharmacopoeia 5.0. [35] The apparatus (Sotax AT6, Sotax AG, Allschwil, CH) was equipped with paddles. Hydrochloric acid (1000 ml, 0.1 M, $37 \pm 0.5^\circ\text{C}$) was used as medium. The paddle speed was set to 50 or 100 RPM. Samples of 5 ml were removed in defined intervals and either replaced with medium or included into calculations.

The removed samples were centrifuged (Sigma 302 K, Sigma Laborzentrifugen GmbH, Osterode am Harz, D) for five minutes with 3000 RPM at room temperature. The drug content of the sample was determined with HPLC. The HPLC was equipped with an autosampler (G1329A), thermostat (G13308B), degasser (G1322A), isocratic pump (G1310A), and a UV-detector (G1314A) from the Agilent Series 1100 (Agilent Technologies, Inc., Santa Clara (CA), USA). An MN Nucleosil Reversed Phase C8 ec 5 μm 125/5 column (Art. 7210795.20, Macherey-Nagel AG, Oensingen, CH) and a pre-column of the same type (Art. 7210805.30) with a diameter of 3 mm and a length of 8 mm was used as a stationary phase. The mobile phase was a volumetric mixture of 50% Ammonium acetate buffer 20 mM (Art. 09688, Fluka Chemie AG, Buchs (SG), CH), 40% Methanol (K37654007731, Merck KGaA, Darmstadt, D), and 10% Tetrahydrofuran (I360001 725, Merck KGaA, Darmstadt, D).

A stock solution of proquazone in DMSO (Dimethylsulfoxide, 41639, Fluka Chemie AG, Buchs (SG), CH) was stored at 4°C . A calibration curve of seven points was prepared from this stock solution and diluted in HCl 0.1 M.

4.4.8.1 Dissolution Models

All dissolution profiles were fitted to different dissolution models. The theoretical background on the different models is given in chapter 3.5.4.2 "Mathematical Models".

The amount dissolved M_t was given in percent [%] of the theoretical drug load. If M_0 was needed for the calculation, two different cases were applied:

Case A Plateau is achieved ($M_{90} - M_{75} \leq 1$) → M_0 = concentration at 90 minutes

Case B Plateau is not achieved ($M_{90} - M_{75} > 1$) → M_0 = theoretical load 100%

Difference factor f_1 (Equation 20) and similarity factor f_2 (Equation 21) were calculated according to the equation given including only one data point above 85% of the total drug amount dissolved.

The Weibull parameters a and b were established fitting the data sets to the Weibull equation (Equation 22). They were used to calculate $t_{90\%}$ according to Equation 23 assuming the lag time T equals zero for both equations. The same data sets were fitted to the first order equation (Equation 24) to obtain dissolution rate k_1 .

To evaluate the dissolution profiles according to the Hixson-Crowell equation (Equation 25), only data less than 85% of the maximum drug load M_0 were included. The evaluation according to the cubic root law was omitted when less than five points smaller than 85% were available. If the plot of the Hixson-Crowell equation showed a two-phase profile, the data were additionally analysed according to the Higuchi model (see Table 6) including all points up to approximately 60% of the maximum drug load M_0 .

Linear regression was executed with Microsoft® Office Excel 2003, non-linear regression was carried out with Mathematica® 5.2 (Wolfram Research, INC, Champaign, USA).

4.4.9 Statistical Analysis

Statistical analysis was performed using SPSS 15.0 for Windows (SPSS Inc., Chicago, USA). One-way ANOVA test followed by a Tukey post hoc analysis on a significance level $\alpha = 0.05$ was applied by default.

5 Results and Discussion

5.1 Compressibility and Compactibility

5.1.1 Single Substances

In a first step, compression characteristics of every powder were investigated using the Heckel equation (Equation 4) and the modified Heckel equation (Equation 7). The Leuenberger equation (Equation 8) was applied to quantify compressibility and compactibility. Finally, a new approach, the modified Van der Waals equation (Equation 12), was applied to the experimental data.

Figure 21 shows the linear part of the Heckel plot for all six types of cellulose. The measure of the compressibility K was derived from the slope. The corresponding values are given in Table 23. Experimental data and corresponding fits of the modified Heckel equation are depicted in Figure 22; the values for C and the critical relative density ρ_c are listed in Table 23.

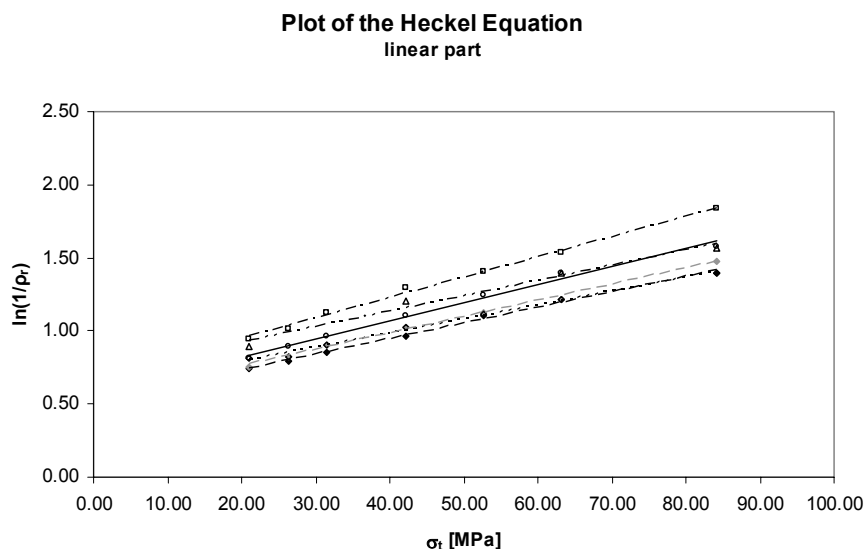


Figure 21: Linear part of the Heckel plot for all six types of cellulose.

Legend: Experimental (dots) and fitted values (lines) for MCC 102 (○, —), Type I (□, - - - -), UICEL S (◆, - - - -), Type II (◇, - - - -), UICEL B (◇, ·····), and UICEL-XL (△, ·····).

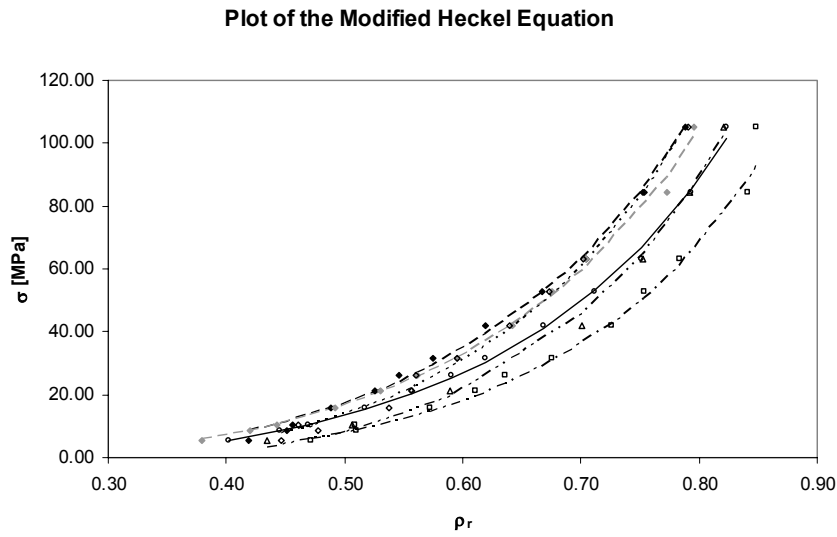


Figure 22: Modified Heckel plot of all six types of cellulose.

Legend: Experimental (dots) and fitted values (lines) for MCC 102 (○, —), Type I (□, -.-.-), UICEL S (◆, - - - -), Type II (◇,), UICEL B (△, - - - - -), and UICEL-XL (△,).

Table 23: Parameters K, σ_y , C, and ρ_c from the Heckel and the modified Heckel equation.

n=3	Heckel equation		modified Heckel equation	
	K [10^{-3} MPa^{-1}]	σ_y [MPa]	C [10^{-3} MPa^{-1}]	ρ_c
MCC 102	12.3 (0.45)	81.15 (2.957)	5.8 (0.27)	0.198 (0.0118)
Type I	14.0 (0.25)	71.61 (1.295)	6.2 (0.77)	0.253 (0.0257)
UICEL S	10.7 (0.25)	93.78 (2.223)	4.6 (0.21)	0.193 (0.0118)
Type II	11.1 (0.06)	89.82 (0.464)	5.2 (0.43)	0.177 (0.0193)
UICEL B	9.6 (0.42)	103.93 (4.411)	3.9 (0.19)	0.252 (0.0098)
UICEL-XL	10.6 (0.64)	94.28 (5.886)	4.1 (0.58)	0.307 (0.0285)

Plastic powders are characterized by larger values for K and C than brittle materials. As the mean yield pressure is the reciprocal of K (Equation 5), the ranking remains the same. The critical relative density ρ_c is defined as the relative density where rigidity starts to evolve and a negligible mechanical resistance is produced between the punches. [51]

RESULTS AND DISCUSSION

Analysing the Heckel parameter K, Type I showed the best compressibility followed by MCC 102. Both substances were significantly better compressible than the celluloses of Class 3 and 4. UICEL S which was used as standard cellulose for Class 3 did not differ significantly within this class. The compressibility of UICEL-XL is comparable to the substances of Class 3. Considering σ_y and C, the ranking for compressibility was the same as for K, but the differences between and within the classes was less explicit. Considering C from the modified Heckel equation, the compressibility of all fully converted cellulose II products was comparable. The compressibility ranking is listed in Table 26.

The conversion from solid particles dispersed in air to voids in a solid matrix takes place at the critical relative density ρ_c . This occurs between relative bulk density and relative tap density. [51] A schematic representation of this conversion is given in Figure 23. In this study, the critical relative density was very close to the relative bulk density $\rho_{r \text{ bulk}}$ (Figure 24). Due to gravitation discrete clusters of powder particles cannot be dispersed in air, the bulk density determined is hence close to the critical relative density calculated according to the modified Heckel equation.

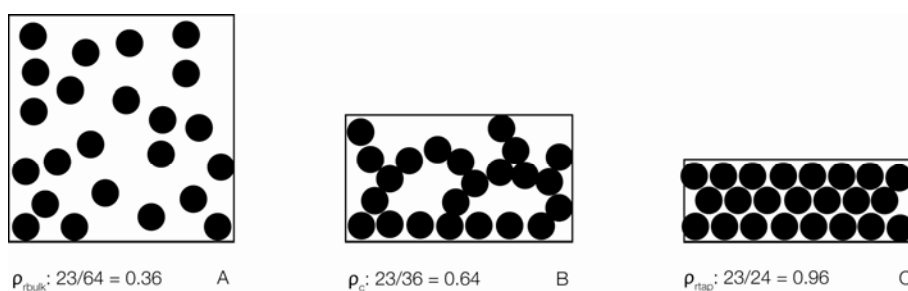


Figure 23: Schematic representation of the relative bulk density, critical relative density, and relative tap density; powder particles dispersed in air (A), voids in a solid matrix (B), and closest packing of particles(C).

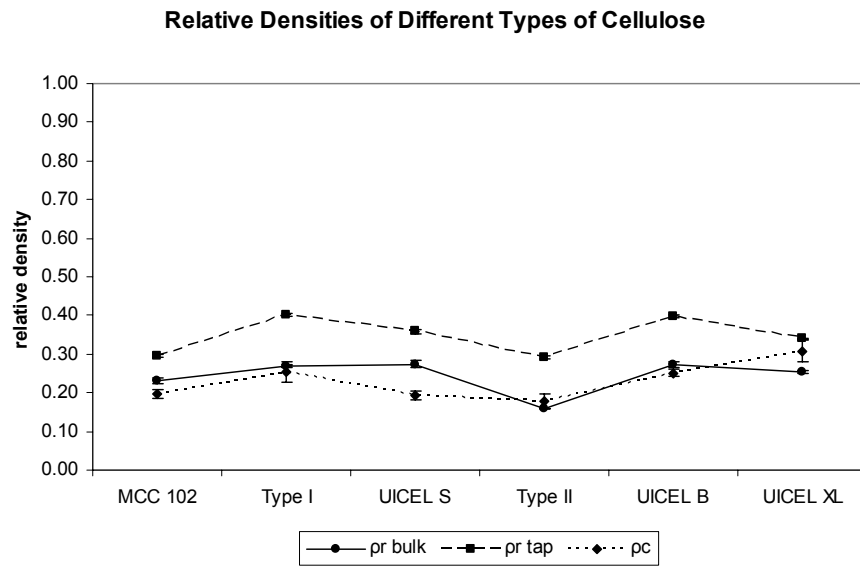


Figure 24: Relative bulk density, relative tap density, and critical relative density of six different types of cellulose; the corresponding values are given in Table 11 and Table 23. The points are connected by lines to improve the comprehensibility.

As presented in Figure 24, Type II showed the smallest relative bulk density, relative tap density, and critical relative density. This could be attributed to the fibrous structure of the powder (Figure 16). The percolation threshold for fibrous disintegrants is much smaller than for spherical particles. [94] Small critical relative density values can be advantageous in tablet compaction, since low relative densities already refer to a rigid structure.

Lanz [27] proposed a new approach to describe compressibility of a powder. The basic principle of this approach is based on the observation that gaseous as well as particulate systems are compressible. This new compression equation is derived from the Van der Waals equation of the state. Even though the equation should be applicable on the full compression range, the data were fitted only up to 105.23 MPa. Including higher compression pressures reduced the coefficient of determination considerably. The experimental and fitted data are depicted in Figure 25; the corresponding parameters are listed in Table 24.

RESULTS AND DISCUSSION

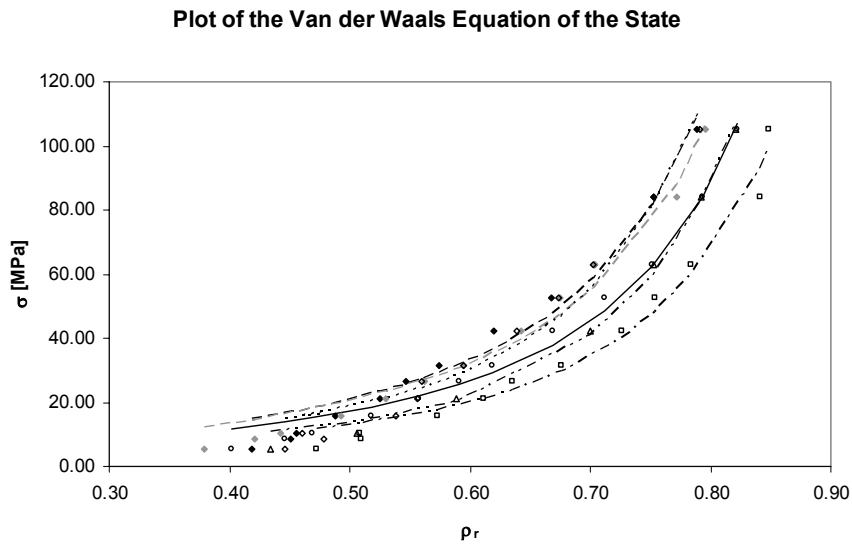


Figure 25: Plot of the modified Van der Waals equation of the state for all six types of cellulose.

Legend: Experimental (dots) and fitted values (lines) for MCC 102 (○, —), Type I (□, - - - -), UICEL S (◆, - - - -), Type II (◇, - - - -), UICEL B (◇, ·····), and UICEL-XL (△, ·····).

Table 24: Fitted values of the modified van der Waals equation.

	V_t [cm ³]	B_V [cm ³]	A_V [cm ⁶ ·MPa]	C_V [cm ³ ·MPa]
MCC 102	0.1894 (0.00006)	0.1936 (0.00169)	1.2150(0.53766)	4.7697 (0.68960)
Type I	0.1974 (0.00022)	0.1876 (0.00365)	3.2818 (1.22847)	7.2073 (1.72610)
UICEL S	0.1953 (0.00013)	0.2049 (0.00056)	1.5589 (0.27745)	5.7428 (0.22993)
Type II	0.1955 (0.00010)	0.2066 (0.00336)	0.6959 (0.18754)	4.5947 (0.09301)
UICEL B	0.1953 (0.00014)	0.2002 (0.00123)	3.4235 (0.19654)	7.8077 (0.15294)
UICEL-XL	0.1926 (0.00019)	0.1914 (0.00370)	3.9282 (0.71653)	7.7351 (0.88614)

Coefficient C_V theoretically correlates with the mean yield pressure σ_y of the Heckel equation. Small mean yield pressures correspond to small values for C_V , which is characteristic for ductile substances. The coefficient B_V has a clear physical meaning. It

equals the volume at infinite pressure and corresponds to the true volume of all particles (V_t). The coefficient A_V can also be related to the mean yield pressure. [27]

In this study, the correlation of the mean yield pressure σ_y , C_V , and A_V was ambiguous. The same rank order was found only for MCC 102. The correlation of C_V and σ_y was given for MCC 102, UICEL-XL, and UICEL B. C_V and A_V were, with the exception of UICEL-XL and UICEL B, in the same rank order. These two samples did not differ statistically ($p=1.000$).

Lanz describes a discrepancy between B_V and V_t and explains it by the in-die data analysis. He supposes, furthermore, to study the out-of-die data, which was done in this work. Unlike his assumptions, this discrepancy was found also with out-of-die data. It has to be said that in Lanz's studies V_t was calculated from the tablet mass and the true density ($V_t = m/\rho_t$). The same was done in these out-of-die studies, but since every run consisted of more than one tablet, an average V_t value per run was included. This reduced the confidence of the value.

The last equation applied on single powders was the Leuenberger equation. This model was preferred due the combination of compactibility and compressibility. Data points and fits are illustrated in Figure 26; the related fitting parameters are listed in Table 25.

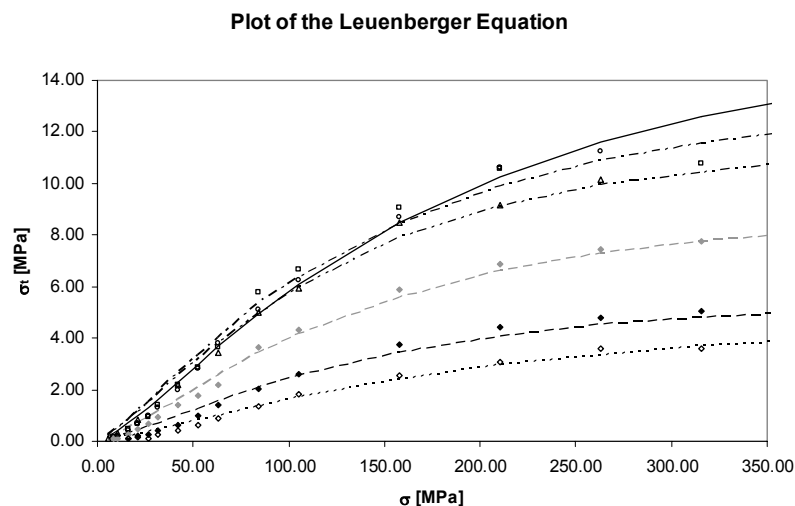


Figure 26: Plot of the Leuenberger equation for all six types of cellulose.

Legend: Experimental (dots) and fitted values (lines) for MCC 102 (○, —), Type I (□, - - - -), UICEL S (◆, - - - -), Type II (◇, - - - -), UICEL B (◇, ·····), and UICEL-XL (△, - - - -).

RESULTS AND DISCUSSION

Table 25: Maximal tensile strength and pressure susceptibility according to the Leuenberger equation.

	MCC 102	Type I	UICEL S	Type II	UICEL B	UICEL-XL
$\sigma_{t\max}$ [MPa]	16.68 (1.366)	17.44 (3.933)	5.48 (0.084)	8.85 (0.056)	4.82 (0.168)	11.62 (0.087)
γ_t [10^{-3} MPa $^{-1}$]	5.26 (0.524)	5.38 (1.881)	7.49 (0.223)	7.56 (0.052)	5.24 (0.302)	8.36 (0.154)

Type I showed the best compactibility closely followed by MCC 102. Class 1 and class 2 did not differ statistically ($p = 0.993$). UICEL-XL showed improved compactibility compared to UICEL-A/102 (S) ($p = 0.008$), but was still significantly reduced compared to MCC 102 ($p = 0.031$). The standard UICEL S showed comparable compactibility compared with both other substances from Class 3, UICEL B, and Type II. The full conversion from cellulose I to cellulose II reduced the compactibility distinctively.

The pressure susceptibility γ_t refers to the compressibility. Due to that parameter, UICEL-XL showed the best compressibility. The values were in the range of 5.24 to 5.38 10^{-3} ·MPa for MCC 102, Type I, and UICEL B, and between 7.49 and 8.36 10^{-3} ·MPa for UICEL S, Type II, and UICEL-XL. There was no systematic classification observed regarding pressure susceptibility. To bring together all values achieved by the different evaluation methods, the substances were ranked. The first position in Table 26 and Table 27 was related to the best compressibility or compactibility, respectively. Values for Carr's Index (CI) are listed in the materials and methods section (Table 13).

Table 26: Compressibility ranking (Rank 1 best compressibility).

Rank	CI	K [10^{-3} MPa $^{-1}$]	C [10^{-3} MPa $^{-1}$]	σ_y [10^{-3} MPa]	C_v [cm 3 ·MPa]	A_v [cm 6 ·MPa]
1	MCC 102	Type I	Type I	Type I	Type II	Type II
2	UICEL S	MCC 102	MCC 102	MCC 102	MCC 102	MCC 102
3	UICEL-XL	Type II	Type II	Type II	UICEL S	UICEL S
4	UICEL B	UICEL S	UICEL S	UICEL S	Type I	Type I
5	Type I	UICEL-XL	UICEL-XL	UICEL-XL	UICEL-XL	UICEL B
6	Type II	UICEL B	UICEL B	UICEL B	UICEL B	UICEL-XL

Table 27: Ranking of the compressibility and compactibility according to the Leuenberger equation (Rank 1 best compressibility or compactibility).

Rank	$\sigma_{t \max}$ [MPa]	γ_t [MPa ⁻¹]
1	Type I	UICEL-XL
2	MCC 102	Type II
3	UICEL-XL	UICEL S
4	Type II	Type I
5	UICEL S	MCC 102
6	UICEL B	UICEL B

Regarding compressibility and compactibility, no clear conclusion could be drawn from quantitative values of different models as well as from qualitative ranking. No correlation could be found between pressure susceptibility γ_t and compressibility K . Among those models, Heckel equation was selected to assess compressibility and Leuenberger principally to assess compactibility. The advantage of the Heckel equation compared to the modified Heckel equation is the ease of application, since evaluation can easily be performed with linear regression. Van der Waals equation of the state is an interesting model but the use of non-linear regression and the large amount of parameters to be identified push it into the background. Compactibility compared to compressibility is more important in the development of tablets; consequently Leuenberger equation was selected as the most appropriate model.

The compressibility and compactibility of cellulose is influenced by many factors as the degree of polymerisation, degree of crystallinity, particle size and shape, or moisture content. [98]

Crystallinity was not yet discussed and should therefore be assessed now. From literature it is known that MCC 102 is more crystalline compared to UICEL-A/102, UICEL-XL however shows increased crystallinity compared to the non cross-linked cellulose II. An overview about literature values is given in Table 1.

RESULTS AND DISCUSSION

Kumar and Kothari [99] measured the area under the peaks of hydrocellulose and amorphous cellulose, and physical mixtures of those two materials. Hydrocellulose was used as the 100% crystalline reference, amorphous cellulose was produced by ball milling this product. They describe a linear relationship between this area under the peaks and degree of crystallinity. This observation was used to study qualitatively the crystallinity of the celluloses used in this study. Regarding the X-ray diffractograms in Figure 15, MCC 102 and UICEL S (A) agreed with the curves described in literature. [7] Celluloses of class 3 and 4 were comparable to the standard UICEL S. Type II (C) showed decreased area under the peaks and consequently smaller crystallinity. UICEL B which was produced using the same procedure as the standard showed almost equal pattern and area under the curves, its crystallinity was considered as equal compared to the standard. UICEL SM which was milled showed decreased crystallinity, which could be expected since ball milling is used to prepare amorphous cellulose. The increased area under the peaks of UICEL-XL was also expected, since the two products were received from the group of Professor Kumar who already described this phenomenon. [10] Type I in Figure 15 B shows a different pattern compared to UICEL S. The typical two peaks at approximately 20 and 22 2θ merged to one peak which was shifted to the left side compared to the typical cellulose I peak at 23 2θ ; this observation lead to the assumption that Type I was only partially converted.

Reus Medina [34] studied the influence of the degree of polymerisation and the polymorphic form on the compressibility and compactibility of four different types of cellulose. Both crystal lattice II and high degree of polymerisation reduces the compressibility and compactibility. In this study, the influence of the polymorphic form was detectable from Heckel equation, modified Heckel equation, and Leuenberger equation. Further investigations should be done with regard to the degree of polymerisation.

The increased compactibility of UICEL-XL compared with UICEL-A/102, which was also described by Reus Medina [10], can be explained by the reduced mobility due to cross-linking and hence reduced elasticity which again leads to stronger compacts.

As discussed in the theoretical section, a low degree of crystallinity is related to poor compressibility and poor compactibility. Additionally to this, low crystalline substances tend to absorb more humidity. This again influences the mechanical properties of the tablets. According to Doelker [98] intermediate moisture content results in strongest tablets, whereas low moisture contents, as well as high moisture contents result in lower compactibility. The moisture content of the powders used in this study are listed in Table 14 and additionally depicted in Figure 17 as a result of the storage time. UICEL B showed the

highest moisture content ($7.74\% \pm 0.650$), UICEL-XL the smallest value (3.94%). European Pharmacopoeia [35] limits the moisture content to 7.0% for microcrystalline cellulose. This limit was exceeded only by the average of UICEL-A/102 (S and B), but also MCC 102, Type I, and Type II exceeded the limit with some measurements even though the samples were stored at constant relative humidity. From Figure 17 one can see that the moisture content did not follow a trend. The good compactibility of Type I and MCC 102 can furthermore be explained by the optimal moisture content.

The influence of particle size and shape seemed to be minor to the above mentioned findings since all types of cellulose exhibit plastic deformation. Obae and co-workers [100] conclude that long and narrow rod-shaped particles exhibit larger tensile strength than the round-shaped particles. In general, no correlation between particle shape and tensile strength was confirmed. However, within class 3, the increased compactibility of Type II compared with UICEL S and B could be explained by this phenomenon. SEM pictures of the celluloses used in this study are given in Figure 16. The association between particle shape and critical relative density ρ_c was already discussed above.

5.1.2 Binary Mixtures

5.1.2.1 Mixtures of Two Excipients

Prior to investigate binary mixtures of proquazone and cellulose, binary mixtures of MCC 102 and modified celluloses were investigated in two ways. First, binary mixtures were compressed with a constant compaction force of 7 kN.

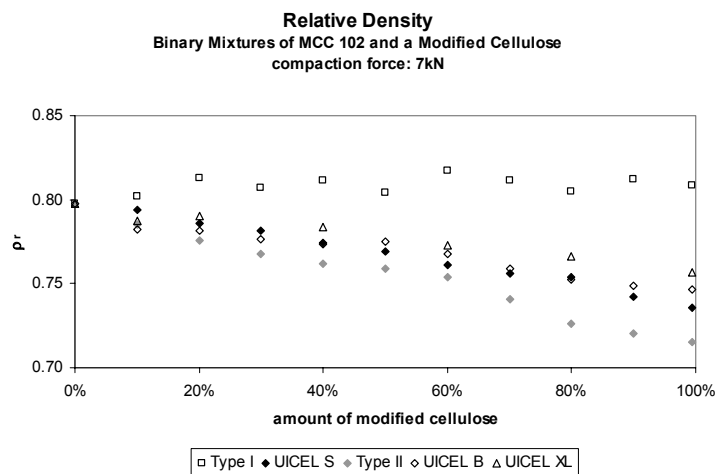


Figure 27: Relative density of MCC 102 – modified cellulose binary mixtures compressed with a constant force.

RESULTS AND DISCUSSION

Figure 27 shows the change of the relative density as a result of the modified cellulose load. As known from the Heckel equation, a poor compressible substance shows a smaller relative density compared to a well compressible substance when the same compaction pressure is applied. With this background and the results from Figure 27, the compressibility of the modified celluloses was assessed and rated as follows. Type I, independent of the quantity in the binary mixture, did not influence the relative density and showed the best compressibility. All modified celluloses of Class 3 and 4 tended to decrease the relative density with an increasing load; the strongest impact was found for Type II, followed by UICEL S, UICEL B, and then UICEL-XL. Comparing the resulting relative density of the single substances, i.e. a load of 0% modified cellulose for MCC 102 and 100% for modified celluloses, respectively, the compressibility showed a significant difference ($p < 0.05$) between all substances. The compressibility of Type I was improved compared to MCC 102, whereas the compressibility of cellulose II decreased as follows: UICEL-XL > UICEL B > UICEL S > Type II. These findings did not correlate with the findings of the Heckel equation.

The reduction of the relative density with increasing load of modified cellulose can be attributed to changes of ρ_t which was used to calculate ρ_r . The true density of class 3 and 4 substances decreased in the same order as the decrease of the relative density was found. This connection was not confirmed for Type I which showed in fact the smallest true density. An additional effect reduced the relative density of class 3 and 4 tablets. Increased elastic recovery of UICEL-A/102 compared to MCC 102 and UICEL-XL as described in literature was supposed to play a major role in compaction of cellulose II products. [10, 11] Elastic recovery will be discussed later in this work.

Tensile strength, the measure of tablet hardness, is important in the development and production and should therefore be investigated. Figure 28 illustrates the relation between the modified cellulose load in binary mixtures and the tensile strength.

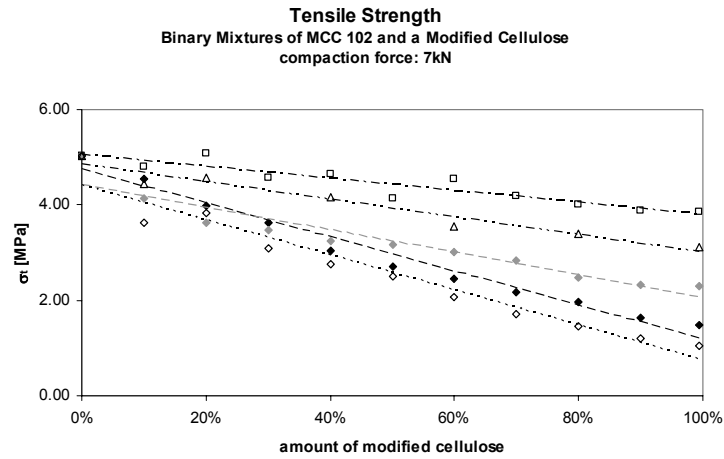


Figure 28: Tensile strength of MCC 102 – modified cellulose binary mixtures compressed with a constant force.

Legend: Experimental (dots) and fitted values (lines) for Type I (□, - - - -), UICEL S (◆, - - - -), Type II (◇, - - - -), UICEL B (◇, - - - -), and UICEL-XL (△, - - - -).

Table 28: Slopes and coefficients of determination of the correlation between tensile strength and load of modified cellulose; tablets compressed with a constant force.

	Slope	r^2
Type I	-1.2526	0.8675
UICEL S	-3.5673	0.9727
Type II	-2.3545	0.8994
UICEL B	-3.6667	0.9481
UICEL-XL	-1.8526	0.9513

An increased amount of modified cellulose reduced the tensile strength of all binary mixtures. The influence of the modified cellulose load on the tensile strength was evaluated by linear regression. Slopes and coefficients of determination of all samples are listed in Table 28. Tensile strength can be used to measure powder compactibility. A gentle slope was related to a small influence on tensile strength; the high compactibility of Type I

RESULTS AND DISCUSSION

compared to the fully converted cellulose II powders could be confirmed. The influence of the cellulose on the compactibility decreased as follows: UICEL-XL < Type II < UICEL S < UICEL B. These findings correlated with the results of the Leuenberger equation for single substances (Figure 26, Table 25) and supported the significance of this model. A deviation from the Leuenberger equation was found only for MCC 102 which showed better compactibility in binary mixtures than Type I.

It is known that the relative density is significantly involved in tablet strength and is therefore very important in solid dosage form design. In the previous investigations on compressibility and compactibility of binary mixtures, the relative density varied dependent on the formulation. One can not rule out the possibility that the decrease of the tensile strength was related to the decrease of the relative density. To exclude this factor, the same binary mixtures were compressed to a comparable relative density and the tensile strength was then evaluated again.

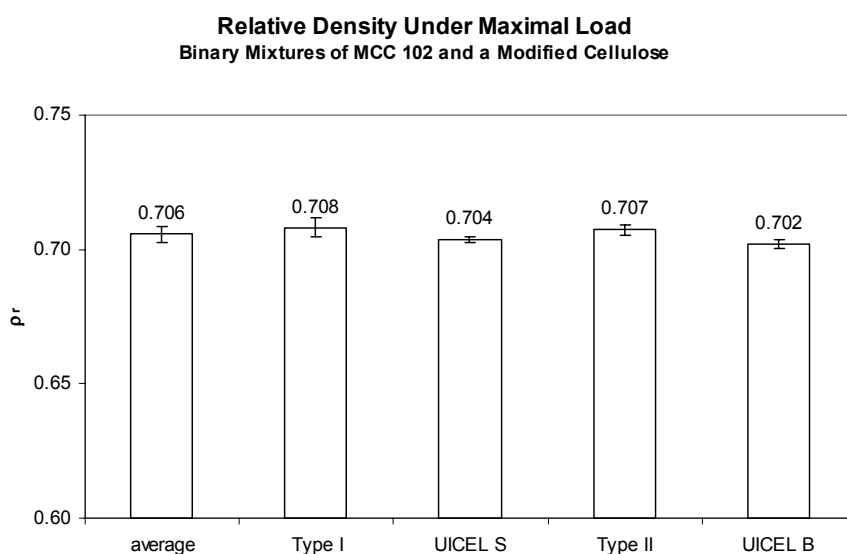


Figure 29: Average relative density under maximal load independent of the modified cellulose load.

Figure 29 represents the relative density under maximum load during compaction. For every substance, the relative density was determined over all binary mixtures. The bar representing the average, was calculated over all relative densities under maximal load.

Due to the very small variation between the different celluloses, the relative density under load was assumed as constant.

When a powder or a powder mixture is compacted to a defined relative density, a certain force will result from this process. In this study, this force is called the resulting compaction force RCF. The values were taken from Zwick raw data. As known from the Heckel equation, a good compressible substance stands out for low compression force needed to achieve a specified relative density. This correlation was used to assess the compressibility of the powders in binary mixtures of MCC 102 and modified celluloses.

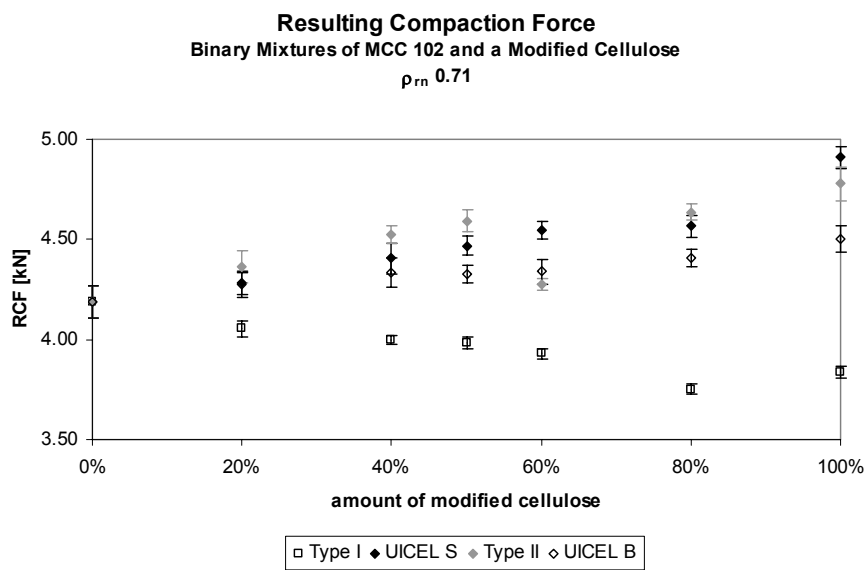


Figure 30: Resulting compaction force of MCC 102 – modified cellulose binary mixtures compressed to $\rho_{rn} 0.71$.

Figure 30 shows the influence of the modified cellulose load on the compressibility. UICEL-XL experiments were not performed due to small amount available for this study. With exception of Type I, the resulting compaction force increased with an increasing amount of modified cellulose. These findings were consistent with the general knowledge about reduced compressibility of the modified cellulose of class 3. According to the results from the Heckel equation, a higher compressibility was expected for Type I compared to MCC 102. The decrease of RCF with an increasing load of Type I confirmed the expectations.

RESULTS AND DISCUSSION

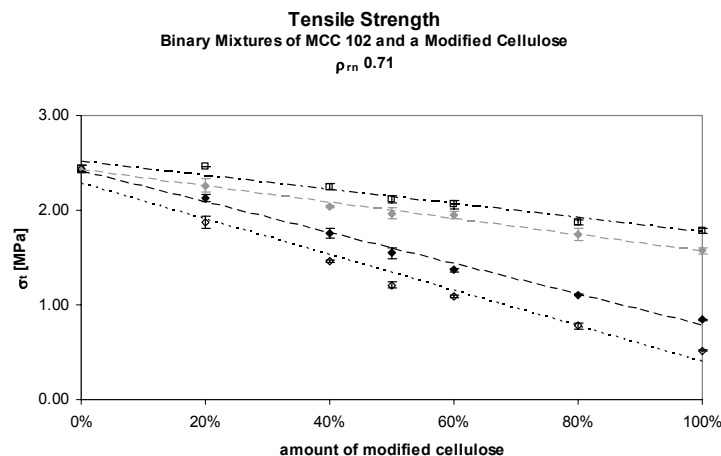


Figure 31: Tensile strength of MCC 102 – modified cellulose binary mixtures compressed to $\rho_m 0.71$.

Legend: Experimental (dots) and fitted values (lines) for Type I (□, - - - -), UICEL S (◆, - - - -), Type II (◇, - - - -), and UICEL B (◇, - - - -).

Figure 31 shows the more interesting and more meaningful tensile strength as a result of the modified cellulose load. To quantify the impact of the load of modified cellulose on the tensile strength, the decrease was determined by linear regression for every substance. Slopes and coefficients of determination are listed in Table 29. A small decrease of the tensile strength was assessed as good property of the modified cellulose and was related to high compactibility of the powder. The smallest decrease was found for Type I and with a small difference for Type II. Both types of UICEL-A/102 showed a clear reduction of the tensile strength with increasing load of modified cellulose.

Table 29: Slopes and coefficients of determination of the correlation between tensile strength and load modified cellulose; tablets compressed to $\rho_m 0.71$.

	Slope	r^2
Type I	-0.7398	0.9530
UICEL S	-1.6325	0.9931
Type II	-0.8501	0.9909
UICEL B	-1.8915	0.9747

To link the data from single substance compaction and binary mixture compaction following analysis was performed. The absolute value of the slope derived as described above (Table 28 and Table 29) was plotted against the reciprocal of the maximum tensile strength $\sigma_{t \max}$ derived from the Leuenberger equation (Table 25), the result is given in Figure 32.

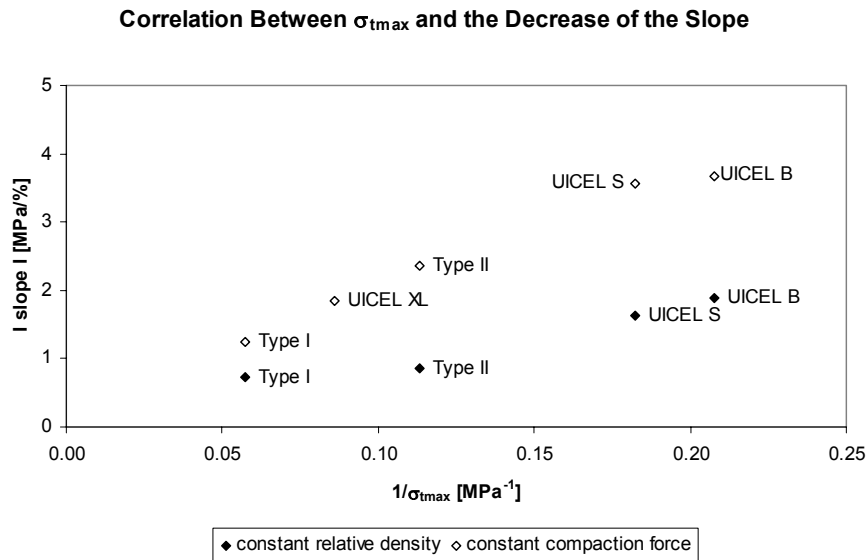


Figure 32: Correlation between the decrease of the tensile strength with increasing load of modified cellulose in binary mixtures with MCC 102 and the maximal tensile strength of the single substance according to the Leuenberger equation.

Figure 32 gives a nice overview on the compactibility of the different types of modified cellulose. A well compactable substance is localized close to zero, which signifies no influence of the load of modified cellulose on the tensile strength and a very high value for $\sigma_{t \max}$. On the opposite, a poorly compactable substance is localized in the right, upper corner. From this point of view, Type I could be confirmed as the best compactable substance amongst different types of modified cellulose. The ranking of the compactibility assessed by the Leuenberger equation was confirmed by the compaction of binary mixtures. More interesting than the rank order of the powders is the difference between the slopes of binary mixtures compressed with 7 kN (◇) compared to those compressed to a nominal relative density of 0.71 (◆). Tablets compressed with a constant compaction force showed steeper slopes compared to the tablets with comparable relative density. This can be explained by the influence of the relative density on the tensile strength.

RESULTS AND DISCUSSION

5.1.2.2 Mixtures of Proquazone and Excipients

As it is more interesting to study the compressibility and compactibility of excipients in combination with drugs, binary mixtures of proquazone and celluloses were studied.

As known from excipients mixtures, the resulting compaction force RCF can be used to evaluate compressibility of powder mixtures. Figure 33 shows this resulting compaction force of binary mixtures of proquazone and celluloses compressed to the nominal relative density of 0.8. Three different drug loads, 10%, 50%, and 90% were investigated.

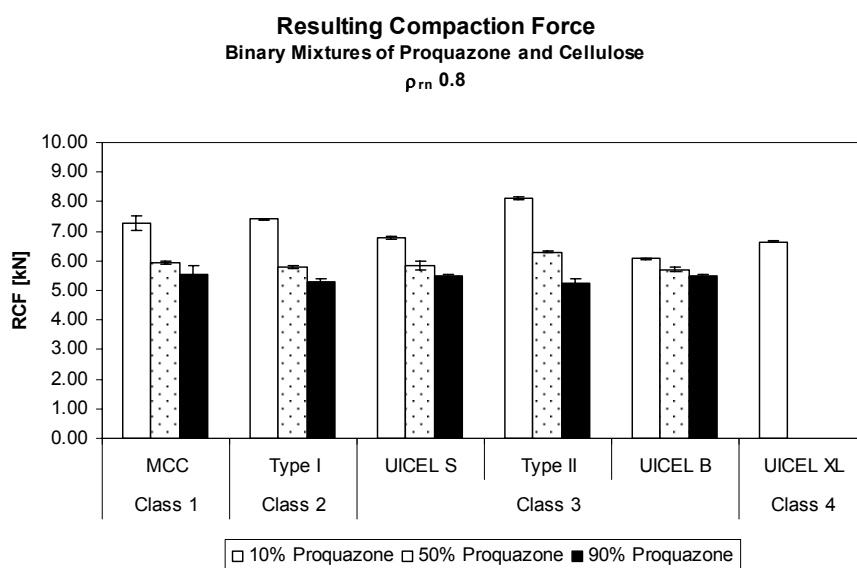


Figure 33: Resulting compaction force of proquazone – cellulose binary mixtures compressed to $\rho_{rn} 0.8$.

From the Heckel equation it is known that well compressible materials need less force to achieve a defined relative density. Considering the data from Figure 33, an increased drug load increased the compressibility of the powder mixtures. To show the influence of the drug load on the compressibility, the resulting compaction force was plotted against the drug load and the decrease was determined by linear regression (Figure 34, Table 30). If the binary mixture was strongly influenced by the drug, the slope was steep, whereas small values were a sign for robustness to drug load. To check if the influence was linear, the coefficient of determination r^2 was included as well.

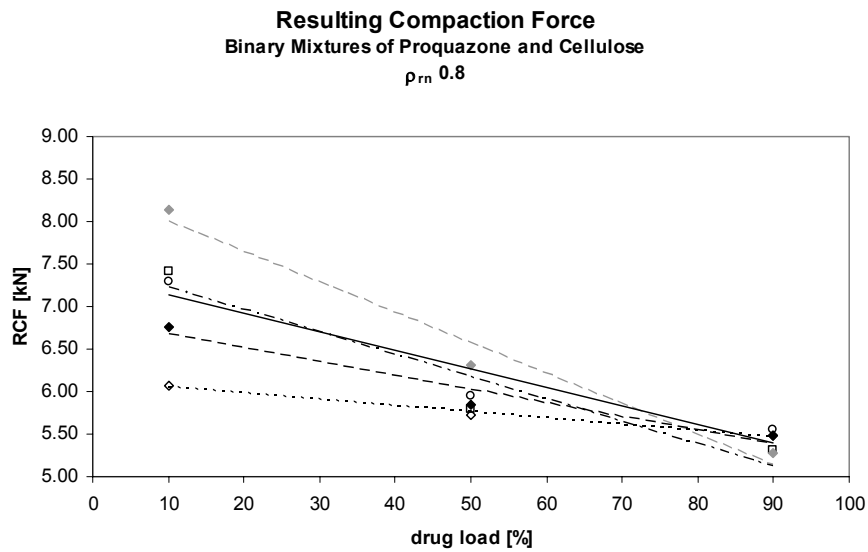


Figure 34: Resulting compaction force as result of the drug load of proquazone – cellulose binary mixtures compressed to $\rho_{rn} 0.8$.

Legend: Experimental (dots) and fitted values (lines) for MCC 102 (○, —), Type I (□, -.-.-), UICEL S (◆, -.-.-), Type II (◇, -.-.-), and UICEL B (◇,).

Table 30: Slopes and coefficients of determination of the correlation between RCF and drug load; tablets compressed to $\rho_{rn} 0.8$.

	Slope	r^2
MCC 102	-21.750	0.9068
Type I	-26.189	0.9125
UICEL S	-16.094	0.9435
Type II	-35.774	0.9750
UICEL B	-7.2371	0.9843

UICEL B showed a gentle slope and a very good coefficient of determination of 0.9843. One can say that UICEL B seemed to be very robust on drug load. Type II still showed a good coefficient of determination, whereas RCF of MCC 102 and Type I was not reduced linearly anymore. UICEL S showed an intermediate coefficient of determination but since only three values were included into evaluation, the linearity was not sufficient. A very

RESULTS AND DISCUSSION

steep slope was found for Type II. MCC 102 and Type I did not differ too much; UICEL S was located in the middle of Type I and UICEL B.

At 10% drug load, UICEL B showed the best compressibility, followed by UICEL-XL and UICEL S. Type II showed the poorest compressibility, followed by Type I and MCC 102. An increased drug load was accompanied by increased compressibility, but no tendency was found for celluloses. The ranking did not correlate with the findings of the Heckel equation (Table 26). It is difficult to explain these observations. Compared to the Heckel model, two parameters of the experimental set-up were changed for binary mixture compaction. First, the compaction speed was increased from 25 mm/min to 200 mm/min; secondly, a poor compressible model drug proquazone was introduced. Since speed was still very slow and constant within the experiments, this influence could be neglected. The introduction of the model drug on the other hand showed improved compressibility as shown in Figure 34. The poor result of this evaluation could be referred to ambient differences which influence the result. One can conclude that RCF is not a robust parameter to evaluate compressibility.

Since RCF did not seem to be a good compressibility measure, proquazone – cellulose binary mixtures were evaluated by the modified Heckel equation. Even though the Leuenberger equation was the preferred model, modified Heckel equation was necessary, because some tablets were too weak to determine the crushing force. Figure 35 shows the experimental data and the corresponding fits of the modified Heckel plots of binary mixtures with three different drug loads

From theory (see Chapter 3.4.5.1) it is known that high compressibility is related to high values of C. Figure 36 is a graphical representation of the values of Table 31 and Table 23. One can see that in most of the cases, compressibility expressed as C (Figure 36 A) was reduced when proquazone was added. These observations were expected because proquazone is known as a poorly compressible active ingredient. [40]. Considering the coefficient of determination, one has to keep in mind that the modified Heckel equation for binary mixtures was fitted only to three or four data points, whereas for single substances more experimental data were available. The modified Heckel equation of binary mixtures was applied on average values. Regarding the coefficients of determination, the poorest coefficient of determination was found for 90% proquazone and 10% MCC ($r^2 = 0.9906$), where only three points were included. All other formulations showed a coefficient of

determination above 0.9985. To improve expressiveness of the modified Heckel equation, more data should be included.

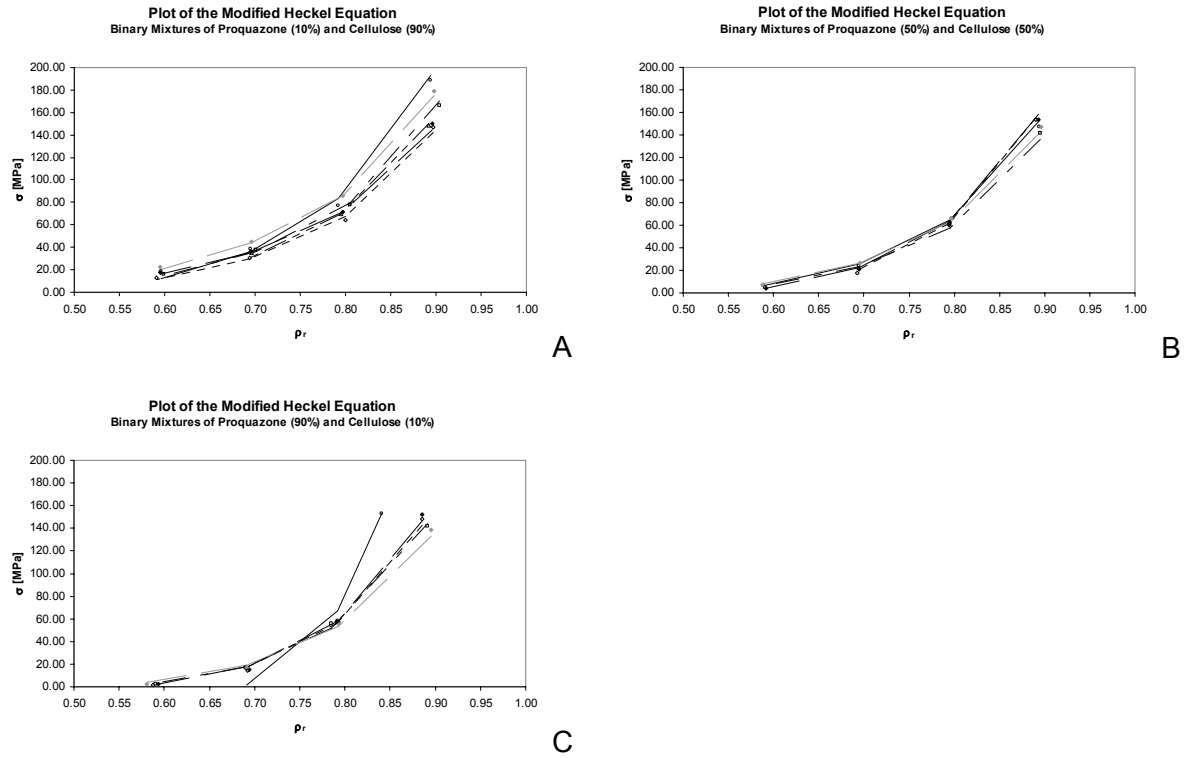


Figure 35: Modified Heckel plots of proquazone – cellulose binary mixtures at three levels of drug load: 10% (A), 50% (B), and 90% (C).

Legend: Experimental (dots) and fitted values (lines) for MCC 102 (○, —), Type I (□, - - - -), UICEL S (◆, - · - ·), Type II (◇, · · · ·), and UICEL B (◇, · · · ·).

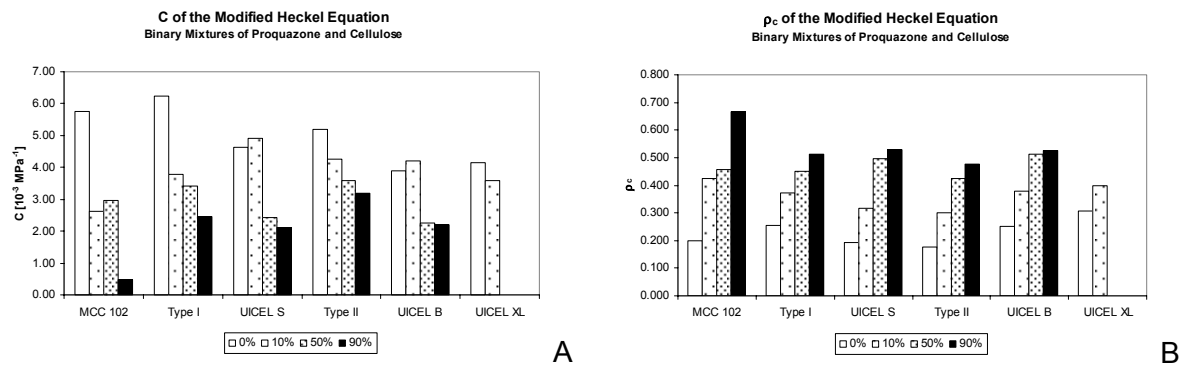


Figure 36: C (A) and ρ_c (B) of the modified Heckel plot of proquazone – cellulose binary mixtures as a result of the drug load.

RESULTS AND DISCUSSION

Considering the critical relative density as a measure for compressibility, small values can be advantageous in tablet compaction, since low relative densities already refer to a rigid structure. From Figure 36 B one can see that the critical relative density increased with an increasing load of the poorly compactable drug. This confirmed the poor compressibility of proquazone. As already seen before Type II showed the lowest critical relative density, which was referred to the fibrous particle shape. This advantage maintained also in binary mixtures, independent of the drug load.

Table 31: Parameters C and ρ_c from the modified Heckel equation applied on binary mixtures of proquazone and cellulose.

drug load	10%		50%		90%	
	C [10^{-3} MPa $^{-1}$]	ρ_c	C [10^{-3} MPa $^{-1}$]	ρ_c	C [10^{-3} MPa $^{-1}$]	ρ_c
MCC 102	2.61	0.424	2.96	0.456	0.47	0.667
Type I	3.79	0.373	3.43	0.451	2.46	0.511
UICEL S	4.90	0.316	2.44	0.495	2.12	0.530
Type II	4.26	0.301	3.59	0.425	3.18	0.476
UICEL B	4.21	0.379	2.26	0.513	2.20	0.526
UICEL-XL	3.59	0.398	n/a	n/a	n/a	n/a

As already noted above, the compressibility of binary mixtures did not correlate with the findings of the compressibility of single substances. With the experience from binary mixtures of two excipients, a better correlation between single substances and binary mixtures could be expected from compactibility studies. Therefore, the tensile strength of binary mixtures of proquazone and cellulose were investigated.

The influence of the drug load on the tensile strength of tablets compressed to a nominal relative density of 0.8 is given in Figure 37. Binary mixtures with MCC 102 resulted in the hardest tablets with an average tensile strength of $3.04 \text{ MPa} \pm 0.080$, followed by Type I ($2.22 \text{ MPa} \pm 0.023$) and Type II ($1.95 \text{ MPa} \pm 0.033$). Type II was the most compactable cellulose of class 3, both UICEL S and UICEL B resulted in weaker tablets

(0.90 MPa \pm 0.038 and 0.65 MPa \pm 0.034, respectively). The formulation with 10% proquazone and 90% UICEL-XL resulted in a tensile strength of 2.30 MPa \pm 0.019 (without figure). At a drug load of 10%, binary mixtures showed significantly different tensile strength with the exception of Type I and UICEL-XL. At a level of 50% proquazone, the compactibility was in the same rank order, also with significant differences. Only at a level of 90%, the tensile strength did not differ significantly anymore.

To quantify the influence of the drug load on tensile strength, the linearity was determined. Slopes and coefficients of determination are listed in Table 32.

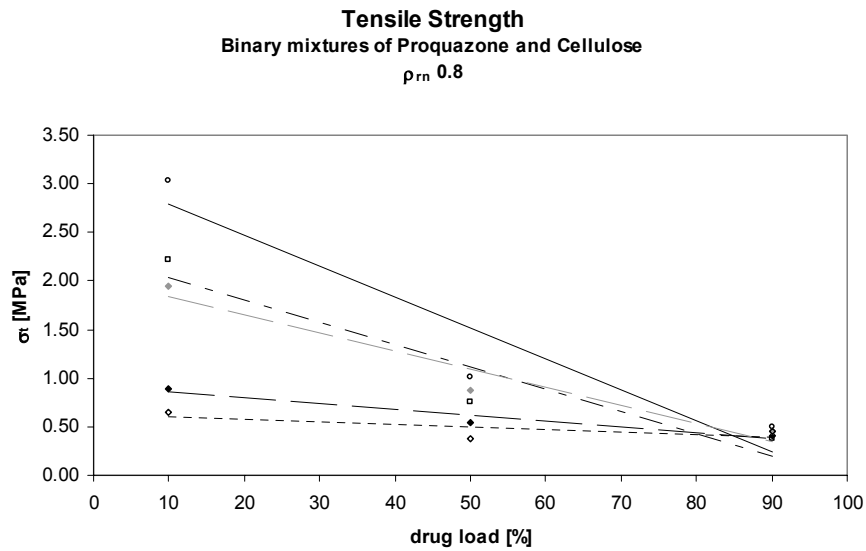


Figure 37: Tensile strength as result of the drug load of proquazone – cellulose binary mixtures compressed to $\rho_{rn} 0.8$.

Legend: Experimental (dots) and fitted values (lines) for MCC 102 (○, —), Type I (□, - - - -), UICEL S (◆, - - - -), Type II (◆, - - - -), and UICEL B (◇, ······).

RESULTS AND DISCUSSION

Table 32: Slopes and coefficients of determination of the correlation between tensile strength and drug load; tablets compressed to ρ_m 0.8.

	Slope	r^2
MCC 102	-0.0317	0.8962
Type I	-0.0230	0.8939
UICEL S	-0.0060	0.9387
Type II	-0.0187	0.9390
UICEL B	-0.0026	0.5265

Whereas at least a linear decrease of the RCF with increasing drug load was found for Type II and UICEL B, none of the substances showed linear change of tensile strength with increasing drug load, all coefficients of determination were smaller than 0.9400. However, drug load influenced tensile strength of the tablets. This non-linearity can be explained by dilution capacity, i.e. the phenomenon that the incorporation of a well compactable substance is limited to a certain mass fraction. This mass fraction is an excipient property. Dilution capacity of the celluloses used in study will be discussed later.

As known from Figure 32, tensile strength is strongly influenced by the relative density of the tablets. The tensile strength of binary mixtures of 10% proquazone and 90% celluloses is given in Figure 38 as a result of the nominal relative density.

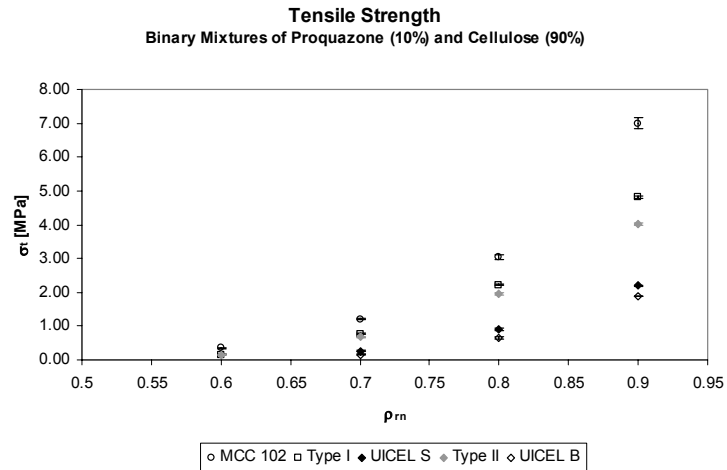


Figure 38: Tensile strength as result of the relative density of proquazone – cellulose binary mixtures.

It was detectable that reduced tensile strength was accompanied by increased porosity. The Leuenberger equation (Equation 8) connects relative density and the compaction pressure with the tensile strength. The described model was fitted to all binary mixtures of 10% proquazone and 90% cellulose. A minimum amount of four data points was needed to evaluate the compactibility. This was only possible for MCC 102, Type I, and Type II.

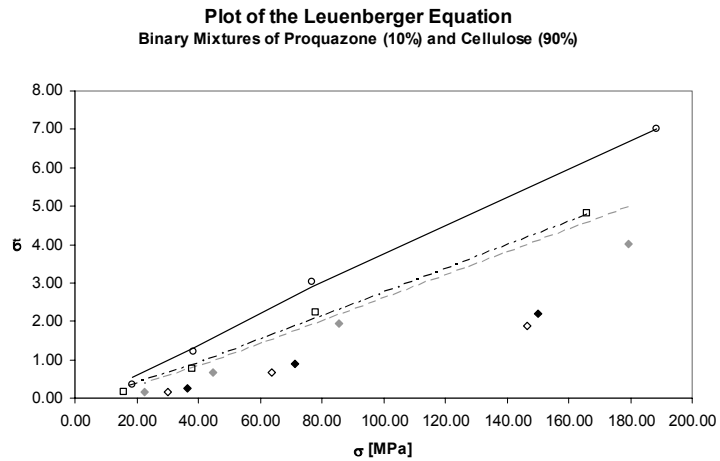


Figure 39: Plot of the Leuenberger equation for binary mixtures of proquazone and cellulose.

Legend: Experimental (dots) and fitted values (lines) for MCC 102 (○, —), Type I (□, - - - -), UICEL S (◆, ·····), Type II (◇, - · - ·), and UICEL B (◇, - - - -).

RESULTS AND DISCUSSION

Fitting of Leuenberger equation is poor due to the lack of data points. Four points are a minimum to fit.

Table 33: Maximal tensile strength and pressure susceptibility according to the Leuenberger equation.

	$\sigma_{t \max}$ [MPa]	γ_t [10^{-3} MPa $^{-1}$]	r^2
MCC 102	19.1367	0.0027	0.9989
Type I	42.2309	0.0008	0.9983
UICEL S	n/a	n/a	n/a
Type II	22.2729	0.0013	0.9961
UICEL B	n/a	n/a	n/a

The coefficients of determination in Table 33 showed that the model was applicable on four values. The highest compactibility was found for Type I; the maximal tensile strength for Type II and MCC 102 were reduced to half of the maximal value for Type I. Comparing $\sigma_{t \max}$ received from single substances (Table 25) and those obtained with this experiment, neither values nor ranking were comparable. Fitting to only four data points seemed to be possible and lead to good coefficients of determination, but the meaning of the values was low. To obtain useful results, more values have to be included in the evaluation.

5.1.3 Ternary Mixtures

Up to now, only combinations of proquazone and one cellulose were investigated. The studies of binary mixtures of MCC 102 and modified cellulose showed that the amount of modified cellulose influences the compressibility and compactibility. In a further step, ternary mixtures of proquazone (10%) and a mixture of MCC 102 and modified cellulose were investigated. Experiments with UICEL-XL were ignored due to the small amount of material available. The proquazone load was kept constant, while the amount of modified cellulose was gradually increased and MCC 102 was reduced.

As for binary mixtures, the resulting compaction force RCF was determined for ternary mixture too. Since the experimental set-up was similar to the compaction of MCC 102 and modified cellulose binary mixtures, comparable results were expected. The results of the mentioned experiments are given in Figure 30. With exception of Type I, an increasing amount of modified cellulose resulted in an increased compaction force, which can be related to decreased compressibility of the powder mixture. Evaluating ternary mixtures of Figure 40, the correlation between modified cellulose load and resulting compaction force could not be verified. This confirmed definitely the lack of robustness of the resulting compaction force and rejected this model to describe compressibility of powders and powder mixtures.

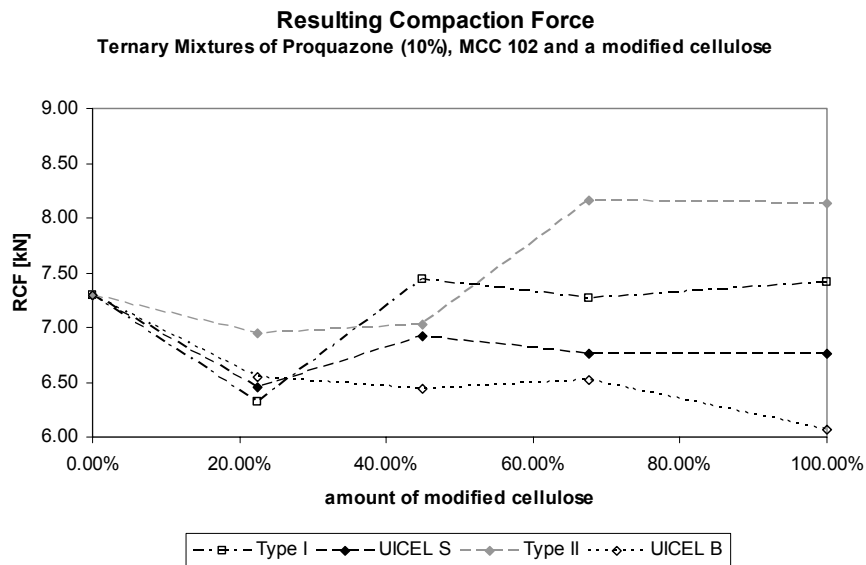


Figure 40: Resulting compaction force of ternary mixtures compressed to ρ_m 0.8. The points are connected by lines to improve the comprehensibility.

It was taken full advantage of the good experience with tensile strength as a tool to assess compactibility of ternary mixtures. In Figure 41, the tensile strength is given as a result of the amount of modified cellulose; slopes and coefficients of determination are listed in Table 34.

RESULTS AND DISCUSSION

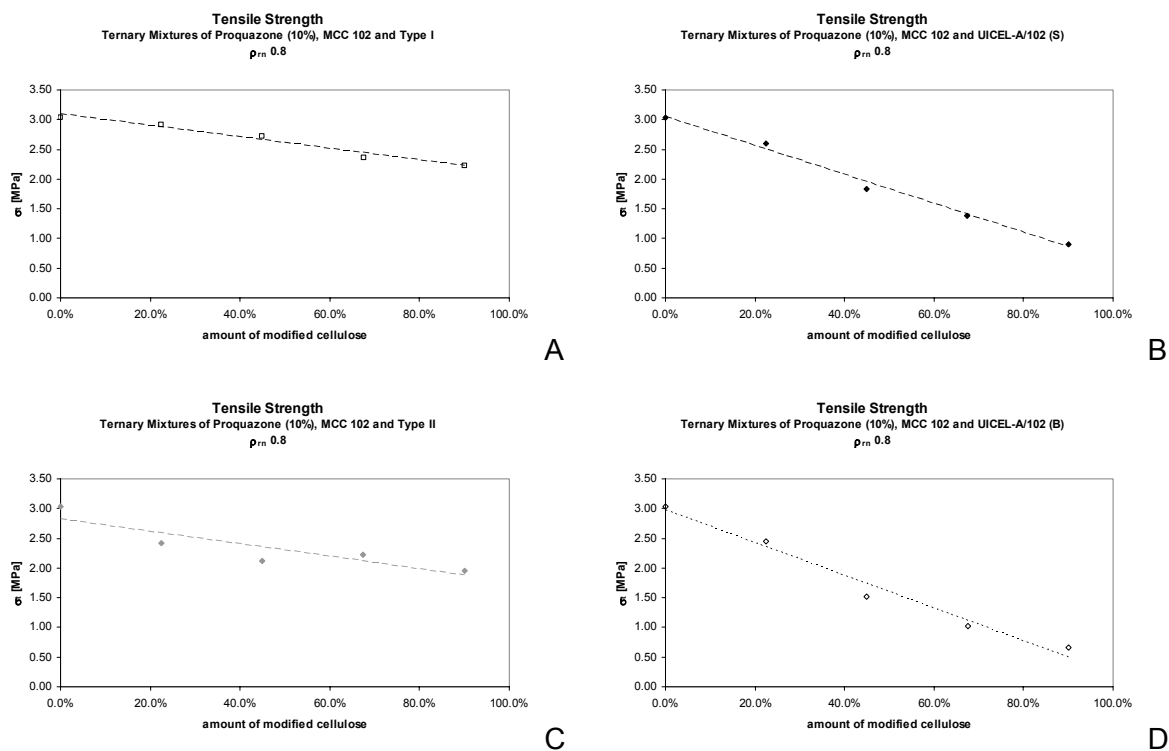


Figure 41: Linear regression of the tensile strength as a result of the amount of modified cellulose in ternary mixtures of proquazone (10%), MCC 102, and a modified cellulose; (A) Type I, (B) UICEL S, (C) Type II, and (D) UICEL B.

Table 34: Slopes and coefficients of determination of the correlation between tensile strength and amount of modified cellulose in ternary mixtures.

	Slope	r^2
Type I	-0.9659	0.9693
UICEL S	-2.4424	0.9916
Type II	-1.0511	0.7923
UICEL B	-2.7491	0.9768

A steep slope is related to a strong decrease of the compactibility. Assessing the slopes, UICEL B was found the poorest compactable substance followed by UICEL S. Type I showed a very gentle slope, which was accounted as a good property. The best

compactibility was found for MCC 102. This was expressed in the negative slopes with increasing amount of modified celluloses. The same results were found in binary mixture compaction and allowed to confirm MCC 102 as the best compactable substance. The deviation from the Leuenberger equation could be explained by the method. Tensile strength is only applicable when ideal fracture occurs. [41] The fracture of the tablet in Figure 42 shows that tensile strength was not properly used; this may have influenced the results of the Leuenberger equation.

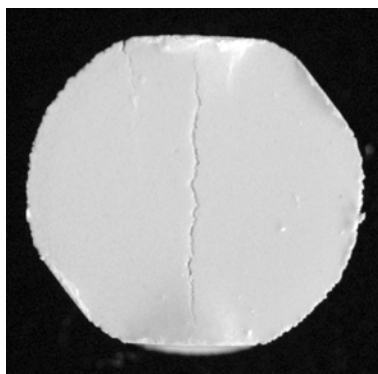


Figure 42: Tensile fracture of an MCC 102 tablet compressed with 20 kN.

5.1.4 Dilution Capacity

As mentioned above, every excipient can incorporate only a maximum mass fraction of a poorly compactable substance (B) in a well compactable substance (A). The term dilution capacity is related to the poorly compactable substance and equals the maximum amount of B that can be incorporated into A. Three different models were applied to calculate this mass fraction such as the model of Kuentz (Equation 13), the model of Lanz (Equation 14), and a simple rule of thumb (Equation 15). The models of Kuentz and Lanz required both the critical relative density which however was associated with the modified Heckel equation. Since it is very time consuming to estimate first this critical value, both relative bulk density ($\rho_{r \text{ bulk}}$) and relative tap density ($\rho_{r \text{ tap}}$) were included to estimate their suitability.

RESULTS AND DISCUSSION

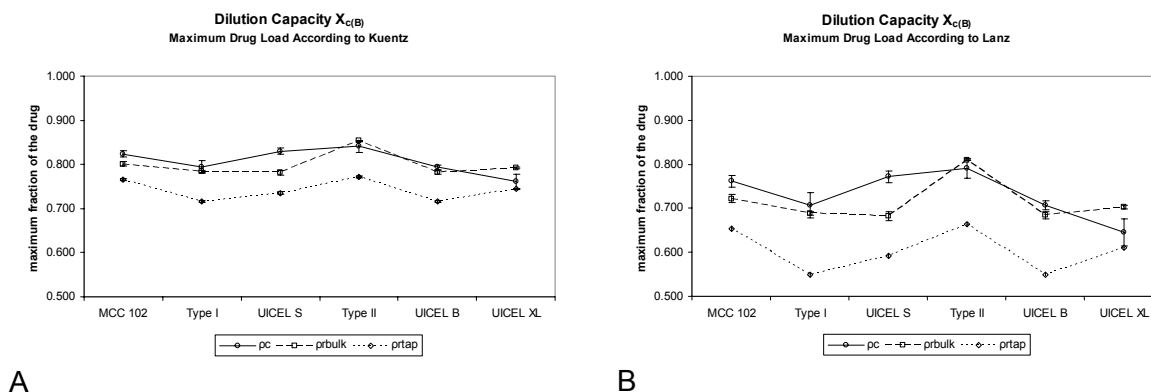


Figure 43: Influence of the relative density selected to calculate the dilution capacities according to Kuentz and Lanz, respectively. The points are connected by lines to improve the comprehensibility.

Figure 43 shows the dilution capacity of the poorly compressible proquazone for every excipient used in this study. For both models, i.e. Kuentz (A) and Lanz (B), the results calculated with the critical relative density and the relative bulk density were very close. From Figure 24 it is known that relative bulk density and critical relative density were very similar. Both models allow working with the relative bulk density, which is also suggested by Kuentz and Leuenberger [54]. The maximum mass fraction calculated with the relative bulk density was slightly below the values calculated with the critical density, only two exceptions were found, i.e. Type II and UICEL-XL. Compared to the model of Kuentz, the model of Lanz seemed to be more sensitive on the excipient properties. In general, the values calculated according to Lanz showed lower mass fractions for the poorly compressible drug and the differences between the different excipients were also more distinctive. Using the relative tap density resulted in the most conservative estimation of dilution capacity. Figure 43 was focussed on the relative density; to study the differences of the models Figure 44 was more suitable.

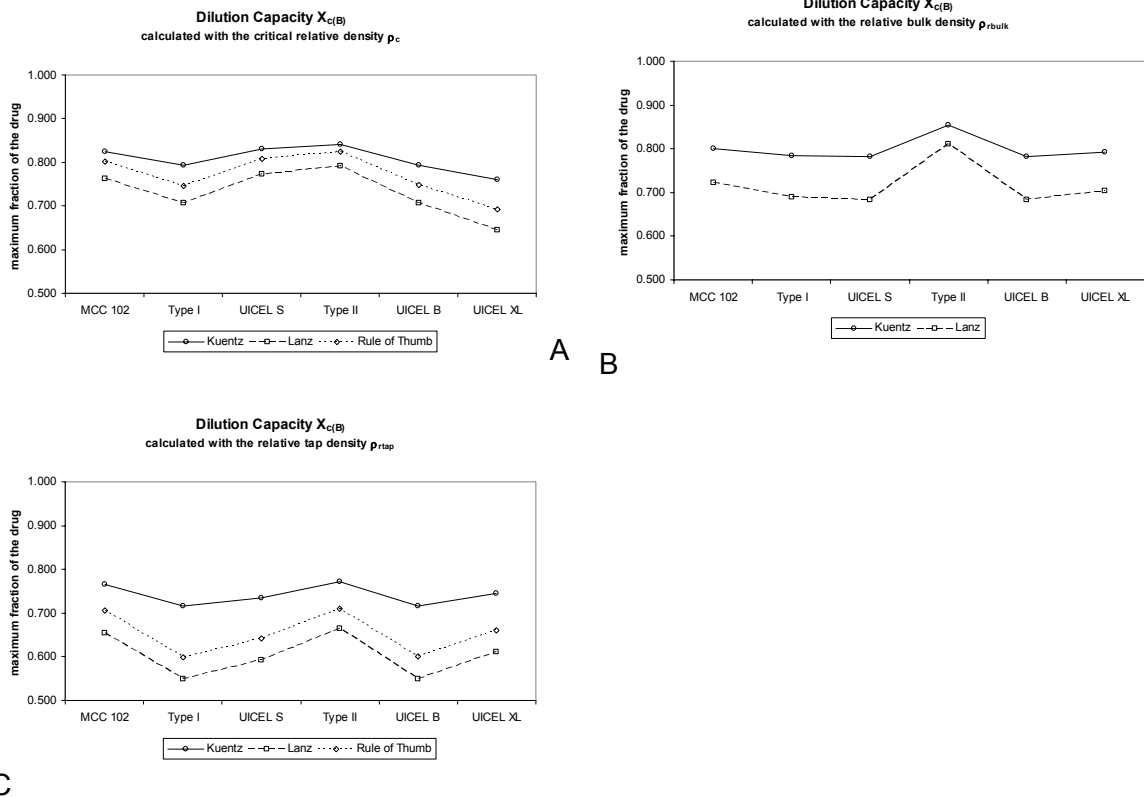


Figure 44: Influence of the model to calculate dilution capacities using three different densities. The points are connected by lines to improve the comprehensibility.

Figure 44 shows the dilution capacities ($X_{C(B)}$) calculated with different relative densities i.e. critical relative density ρ_c (A), relative bulk density $\rho_{r, bulk}$ (B), and relative tap density $\rho_{r, tap}$ (C). With this representation of the data differences between the models were better detectable. Independent of the density, the model of Lanz was the most conservative one. The model of Kuentz on the other hand resulted in very liberal dilution capacities. The rule of thumb ranged between the model of Kuentz and the model of Lanz and seemed to be a very useful tool to estimate the dilution capacity easily. According to Lanz [27], the rule of thumb is only applicable when the true density of both substances are very similar. In that case the dilution capacity equals approximately $1 - \rho_{c(A)}$. In Figure 44 A one can see that the rule of thumb is close to the model of Kuentz. The differences could be attributed to the differences in the true density ρ_t of the powders used in this study; true density of proquazone was 1.2517 g/cm^3 and true densities of the celluloses ranged between 1.5322 g/cm^3 for Type I and 1.5875 g/cm^3 for MCC 102.

Independent of the method Type II showed the best dilution capacity. The dilution potential of the other excipients was dependent on the relative densities used for the calculation.

RESULTS AND DISCUSSION

Since the model of Kuentz is valid without limits, the dilution capacity of the excipients was assessed according to Equation 13 using the critical relative density of the modified Heckel plot. The highest mass fraction of the poorly compressible substance could be incorporated in Type II, followed by UICEL S, MCC 102, Type I, UICEL B, and UICEL-XL.

One has to keep in mind that this critical mass fraction can only be attained at zero porosity. [54] As discussed before increased porosity in tablets reduces the tensile strength of them. For the model of Lanz it has to be pointed out that this equation is just strictly valid if the effect of B on the tensile strength can be neglected; i.e. only the matrix formed by substance A determines the strength of the tablets. [27]

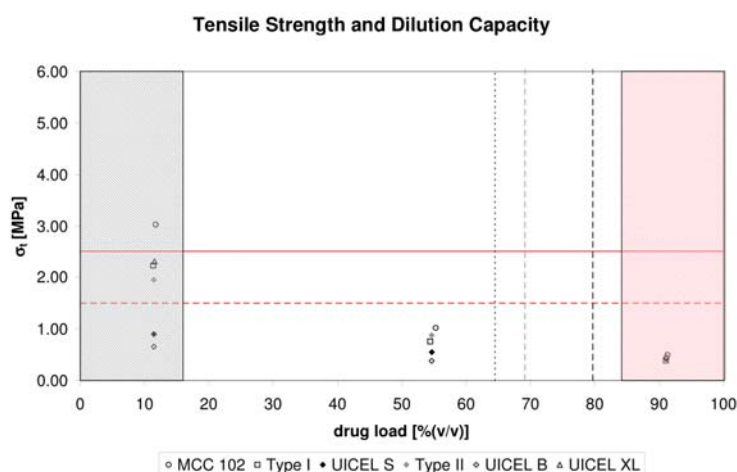


Figure 45: Link between dilution capacity and tensile strength of tablets compressed to ρ_{rn} 0.8.

Figure 45 tried to link tensile strength and dilution capacity. Dilution capacity is the maximum mass fraction of the poorly compactable ingredient which can be incorporated into a well compactable substance to produce “satisfactory tablets”. In this study, “satisfactory tablets” were defined as a tensile strength between 1.5 MPa and 2.5 MPa, which is proposed by Leuenberger. [38] The dashed red line shows the lower limit (1.5 MPa), the solid red line the upper limit (2.5 MPa). The minimal dilution capacity according to the rule of thumb using $\rho_{r\ tap}$ found for Type I (.....), the minimal dilution capacity according to Lanz using ρ_c (-----), and minimal value according Kuentz using ρ_c (-----), both found for UICEL-XL, are given as the vertical lines. At drug loads below this threshold, the tablets should be satisfactory. The shaded areas describe the maximum

possible fraction for spherical particles, where only one component is percolating. Below the first critical concentration ρ_{c1} (black shaded area), only cellulose contributes to the hardness of the tablet. Above the second critical concentration ρ_{c2} (red shaded area), the hardness of the tablet is entirely controlled by the poorly compressible drug. In the intermediate region, both ingredients are percolating and contribute to the mechanical resistance of the tablet. One could see from this figure that there is a discrepancy between the calculated dilution capacities (vertical lines) and the measured data points. At an approximate drug load of 55%(v/v), the tensile strength of all formulations was below the lower limit, but an influence of the cellulose was still detectable in the differences of the tensile strength. This effect entirely vanished above 90%(v/v) drug load, where the experimental data were very close. Even with the rule of thumb which was the most conservative model, no satisfactory tablets could be expected. From binary mixtures only formulations with 10% proquazone and UICEL-XL, Type I and Type II were in the range. One could criticize the high limit for tensile strength of 1.5 MPa, since all tablets with a drug load of 10% resulted in strong tablets.

The advice of Kuentz and Leuenberger [54] to use the relative tap density for the dilution capacity estimation is fully supported by the findings of this study. One could go even further and advice to use the easy rule of thumb. Since the theoretical dilution capacity and the real properties of binary mixtures differed much, the more sophisticated models overestimated the capacity. The use of dilution capacity given an idea of a maximum mass fraction, but in formulation development further parameters, e.g. relative density, influence the end product. Experiments should not be disregarded by the formulation scientist.

Wells and Langridge [53] studied microcrystalline cellulose in combination with dicalcium phosphate hydrate and found the best tablets were produced when they were composed of 66% - 99% of microcrystalline cellulose. This corresponds to a dilution capacity of 1% - 34%, which is much lower than the values found in this study.

5.1.5 Elastic Recovery

Elastic recovery is a property of a powder and is of a certain importance in pharmaceutical technology. Since elastic recovery after compaction increases the relative density of the tablet, the properties of the tablet itself will change. It was already shown in this work that the hardness of the tablet decreases with a decreased relative density. Hard tablets are

RESULTS AND DISCUSSION

primarily produced by materials possessing a low elastic component and having a high bonding surface area that could develop intermolecular forces. [46]

In this work, elastic recovery was evaluated from three experimental set-ups such as binary mixtures of two excipients compressed to a constant relative density, binary mixtures of proquazone (10%) and cellulose, and ternary mixtures.

Initially, elastic recovery was evaluated as a result of different compaction pressures. From literature it is known that the elastic recovery of MCC 102 and UICEL-A/102 increases with an increased compaction force until a plateau is reached. [11]

In this case, unexpected values were obtained, a decrease of the elastic recovery was found with an increasing compaction pressure. This difference between literature and experimental work given in Figure 46 could be attributed to the very soft tablets at lower compaction pressures, which made it almost impossible to determine the out-of-die thickness precisely. A second problem could be the equipment. The minimal tablet height was calculated from the maximum punch displacement during the compaction cycle and the maximum possible punch displacement when punch and lower die side were aligned. A minimal deviation of the true minimal height could therefore lead to differences in the elastic recovery. Due to the weakness of the tablets, evaluation was done without 50% and 90% proquazone.

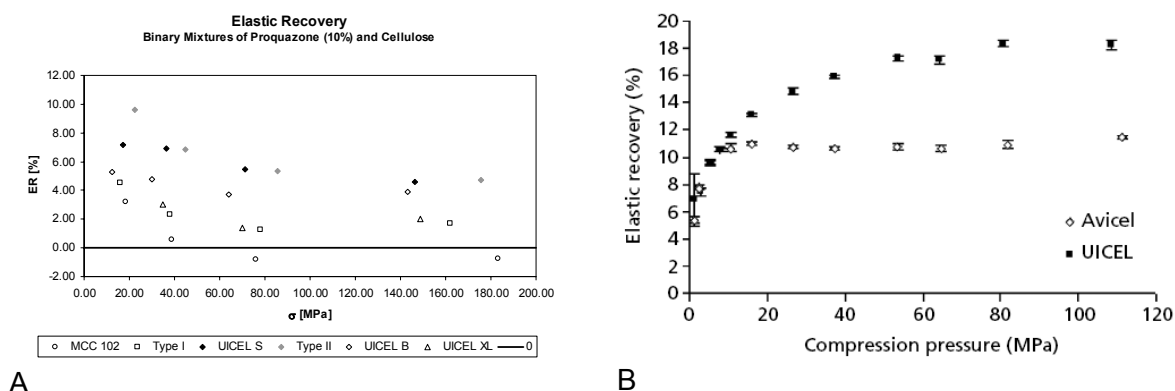


Figure 46: Elastic recovery as a result of the compaction pressure; experimental values (A), literature values for comparable substances (B) [11].

Even though a precise determination of the elastic recovery was difficult, the elastic recovery was studied as a result of the mass fraction of the modified cellulose. The elastic

recovery of MCC 102 – modified cellulose binary mixtures was plotted against the mass fraction of the modified cellulose (Figure 47). The influence was determined with linear regression; the corresponding values are listed in Table 35.

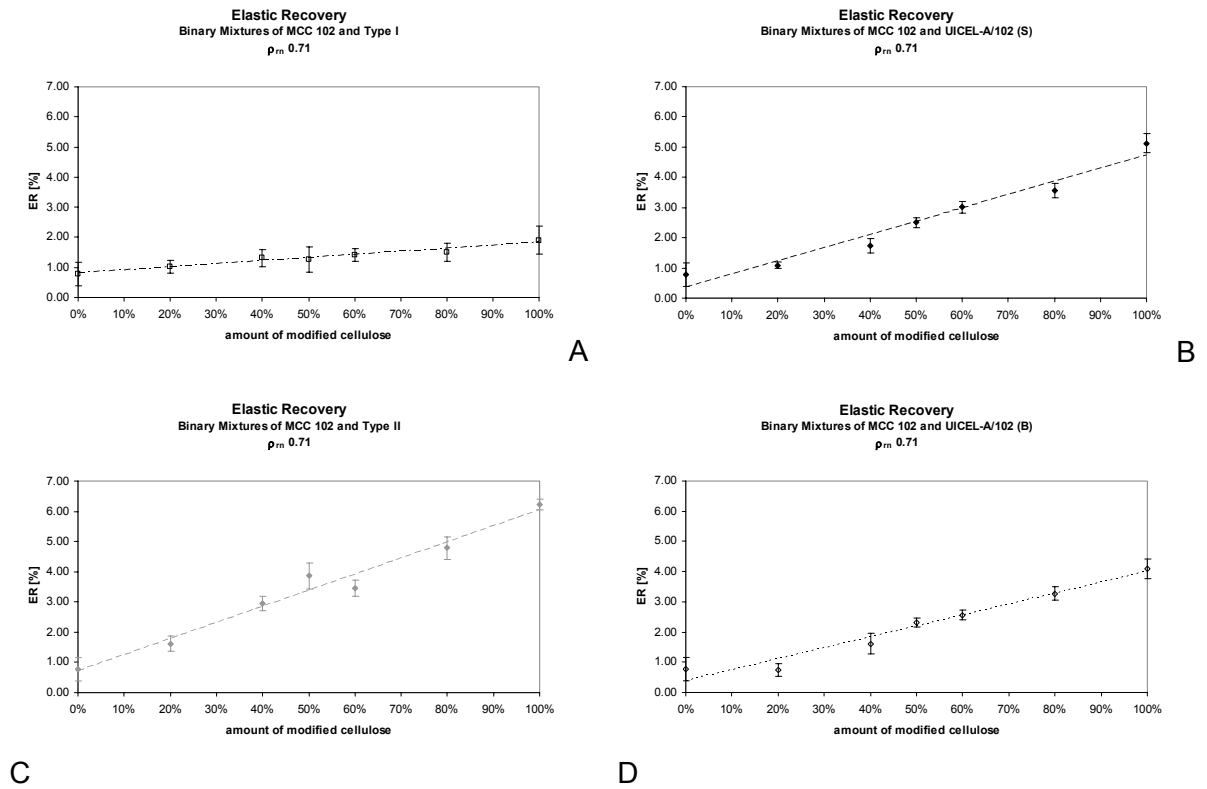


Figure 47: Correlation between elastic recovery and amount of modified cellulose in binary mixtures of MCC 102 and modified cellulose compressed to ρ_{rn} 0.71; (A) Type I, (B) UICEL S, (C) Type II, and (D) UICEL B.

Table 35: Slopes and coefficients of determination of the correlation between elastic recovery and amount of modified cellulose in binary mixtures of MCC 102 and a modified cellulose compressed to ρ_{rn} 0.71.

	Slope	r^2
Type I	1.0234	0.9599
UICEL S	4.3495	0.9571
Type II	5.3132	0.9728
UICEL B	3.5957	0.9606

RESULTS AND DISCUSSION

The relationship between the slope and the elastic recovery of the cellulose was assessed as follows. A positive slope signified increased elastic recovery compared to MCC 102; a steep slope was related to high elastic recovery. From this point, the increase of elastic recovery for all modified cellulose could be confirmed. The elastic recovery increased linearly with the load of modified cellulose. Type II showed the highest elastic recovery, followed by UICEL S and UICEL B. Type I, the partially converted cellulose, showed a clearly reduced effect. The same evaluation was also performed on ternary mixtures. The diagrams and values are given in Figure 48 and Table 36.

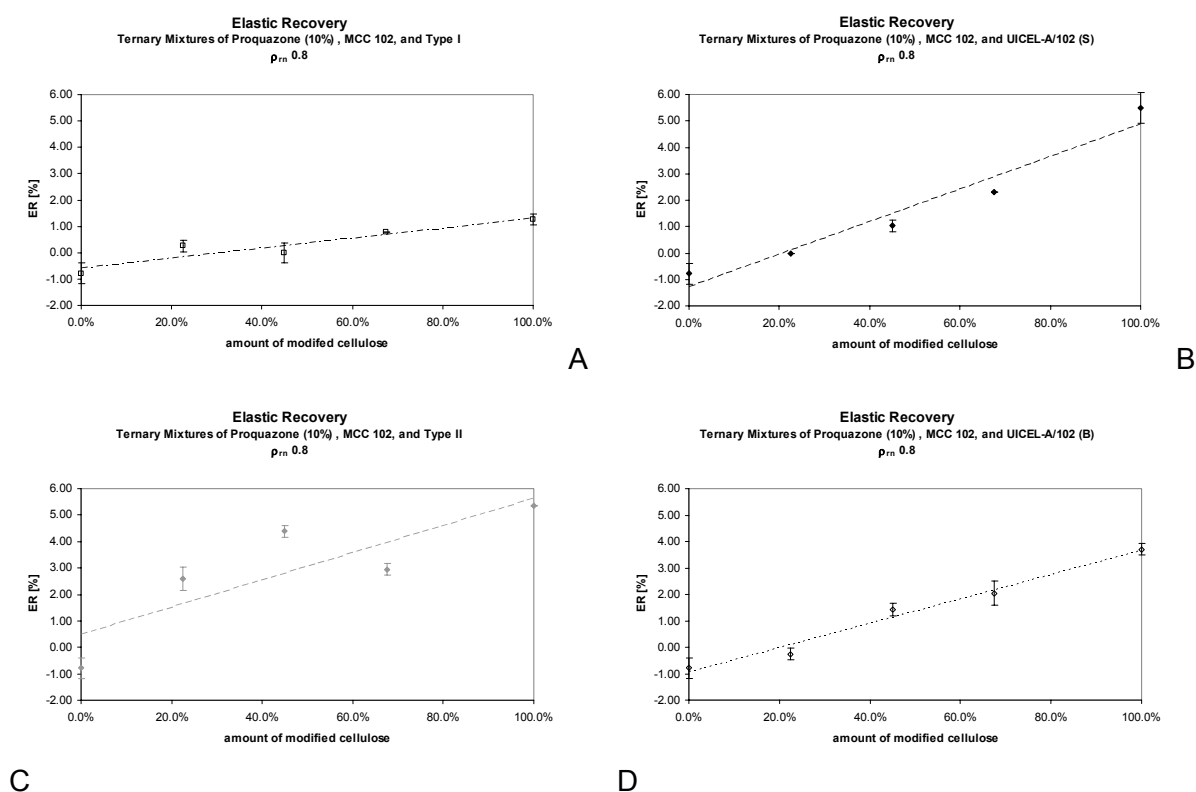


Figure 48: Correlation between elastic recovery and amount of modified cellulose in ternary mixtures; (A) Type I, (B) UICEL S, (C) Type II, and (D) UICEL B.

Before the results of ternary mixtures are discussed, it has to be noted that the elastic recovery of MCC 102 or more precisely the load 0% has a negative value. Reasons were already discussed before. Since the increase with increasing mass fraction was studied, the absolute elastic recovery was less important than the changes.

With the assumptions given above, Type I exerted the smallest elastic recovery, followed by UICEL B. This is in good agreement with the findings of the binary mixtures. UICEL S

and Type II, on the other hand, changed their position. All in all, it can be said that the elastic recovery increased with the degree of conversion. While the extent of elastic recovery of Type I was only a bit higher than for MCC 102, fully converted powders of class 3 recovered clearly more elastically. These results could confirm former studies investigating cellulose I and cellulose II polymorphs. [11, 27]

Table 36: Slopes and coefficients of determination of the correlation between elastic recovery and amount of modified cellulose in ternary mixtures.

	Slope	r^2
Type I	1.8403	0.8779
UICEL S	5.9388	0.9123
Type II	5.0605	0.7285
UICEL B	4.5139	0.9719

Considering the linearity of the fit it was detectable that the elastic recovery in ternary mixtures did not increase as linear as for binary mixtures. This could be referred to the smaller number of experimental data in ternary mixtures and the addition of the poorly compactable drug proquazone. For all substances, except for Type II and UICEL S, binary mixtures recovered more elastically.

Elastic recovery is important in the compaction process of tablets. Compressibility and compactibility can be reduced due to elastic recovery. To study this influence the extent of elastic recovery was plotted against the compressibility and compactibility of the single substances. Elastic recovery was expressed as the slope derived from the correlation between elastic recovery and mass fraction of binary mixtures which were selected due to the better correlation. Compressibility and compactibility were expressed in K from the Heckel equation and $\sigma_{t\max}$ from the Leuenberger equation, respectively.

RESULTS AND DISCUSSION

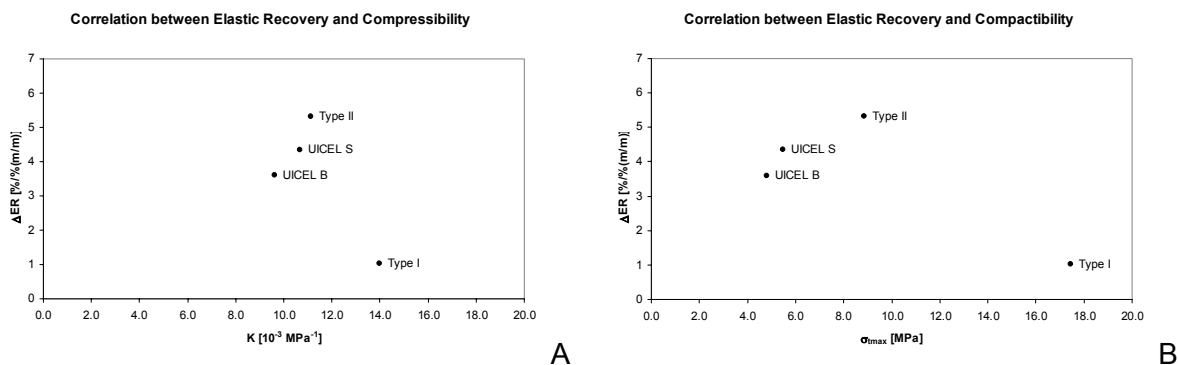


Figure 49: Correlation between the elastic recovery and the compressibility (A) and the compactibility (B).

Figure 49 shows the relation between decreased compressibility (A) and compactibility (B) with increased elastic recovery. Type I clearly showed a very high compressibility and compactibility at the same time a small elastic recovery. This is in good agreement with the theory. The fully converted celluloses UICEL S, Type II, and UICEL B showed decreased compressibility and compactibility accompanied by increased elastic recovery. Within class 3 this relationship between low elastic component and high compressibility or compactibility was not confirmed. The poorest compressibility and compactibility of UICEL B cannot only be ascribed to the elastic recovery, since UICEL S and Type II showed increased elastic recovery but also increased compressibility. The relatively poor compressibility and compactibility of UICEL B has therefore other reasons. Since starting material and method were comparable to UICEL S, it may be a factor of the process itself. Compressibility and compactibility of the single substances was detailed discussed before.

Due to the lack of material, elastic recovery of UICEL-XL could not be performed. From literature it is known that UICEL-XL exhibits less elastic recovery than UICEL-A/102. [10] This is reflected in the compactibility which is better for UICEL-XL than for the fully converted cellulose II powders (Table 25).

5.2 Liquid - Solid Interactions

5.2.1 Water Uptake

Water uptake is the pre-requisite for all further processes including disintegration, dissolution, and finally absorption of a drug. In this study, water uptake was investigated on binary and ternary mixtures containing proquazone, MCC 102 and/or modified celluloses of class 2, 3, and 4. Figure 50 shows the relationship between water uptake rate WUR and the relative density.

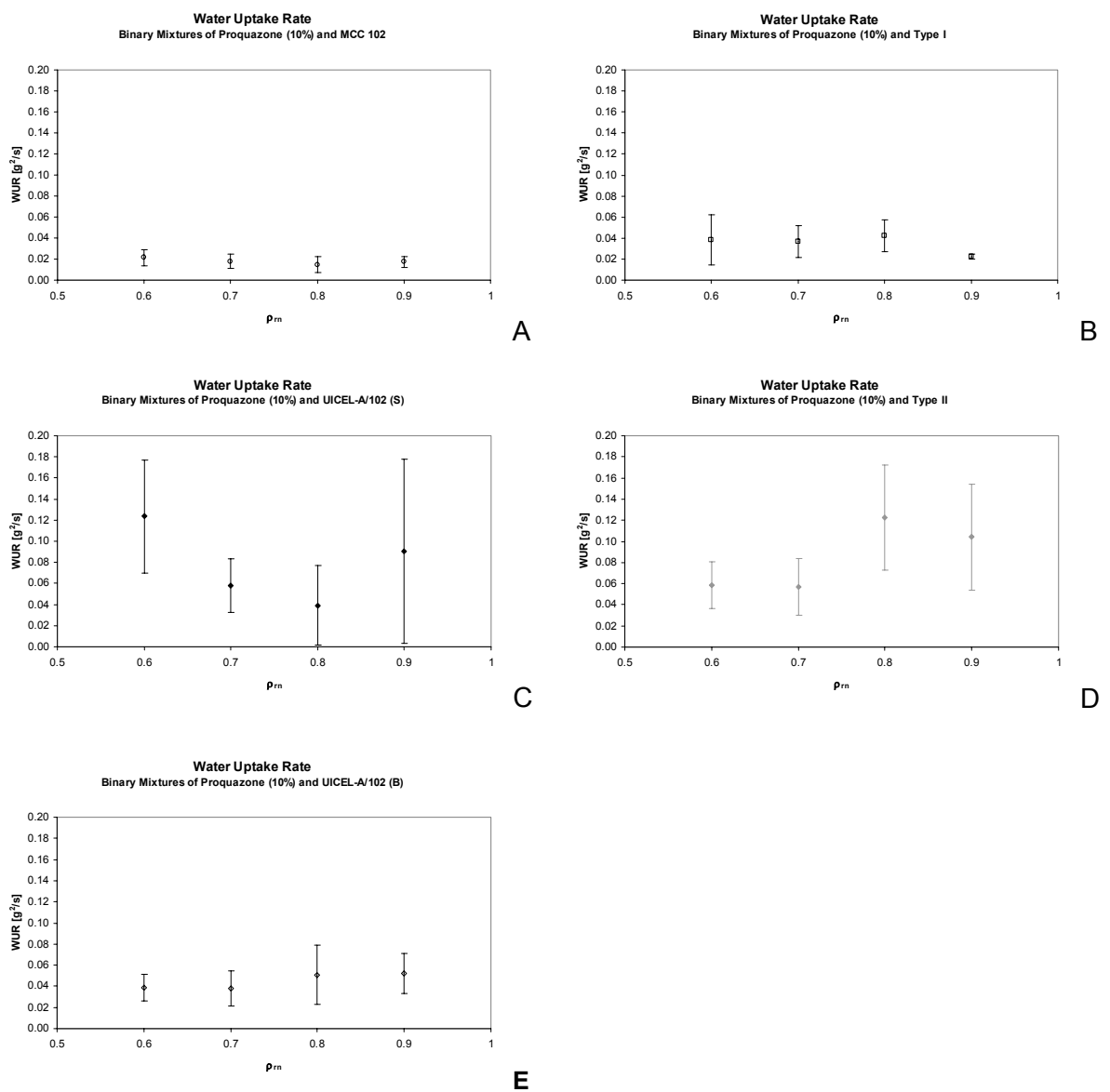


Figure 50: Water uptake rates of proquazone – cellulose binary mixtures at different nominal relative densities; (A) MCC 102, (B) Type I, (C) UICEL S, (D) Type II, and (E) UICEL B. The ordinates are not adjusted to facilitate the comparison between the different celluloses.

RESULTS AND DISCUSSION

Considering only the pore responsible for water uptake it becomes evident that a minimal relative density is required for the capillary effect described by the Washburn equation (Equation 16). With an increased compaction force, the powder is reduced to a minimum porosity. Above this threshold no continuous network of pores exists anymore. One could expect that differences of water uptake rate measurements are detected studying binary mixtures of proquazone and cellulose at different relative densities.

Statistical analysis with ANOVA disproved the influence of the relative density on the water uptake rate of binary mixtures. The only significant difference was observed in binary mixtures with Type II (D) between ρ_m 0.7 and 0.8 ($p = 0.0042$).

The second mechanism of action ascribed to water uptake is the promotion of the liquid throughout a network of disintegrant particles. The influence of the disintegrant was investigated studying binary mixtures of proquazone (10%) and cellulose at a nominal relative density ρ_m 0.8 (Figure 51).

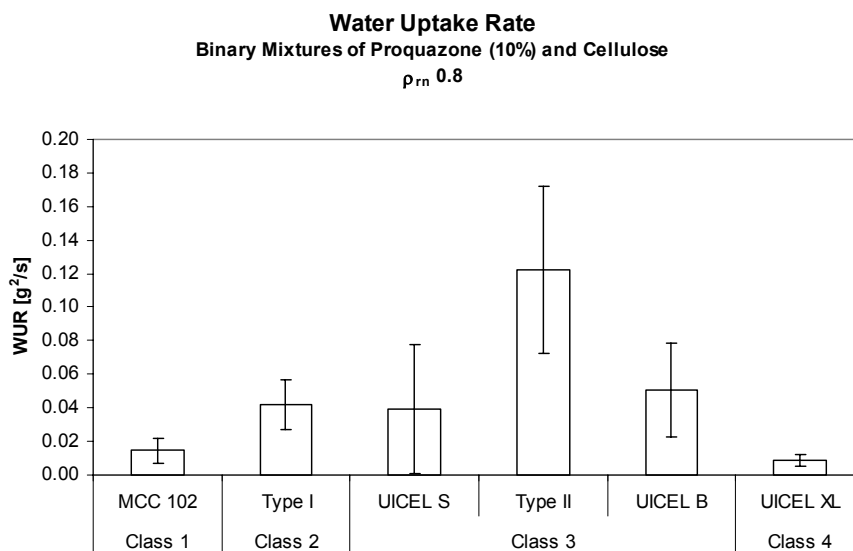


Figure 51: Water uptake rates of proquazone (10%) – cellulose binary mixtures compressed to ρ_m 0.8.

Type II binary mixture showed significantly faster water uptake rates compared to the other powder mixtures; amongst them, no differences were found. A clear advantage of the modified celluloses could not be established, but a trend of improved water uptake for class 2 and 3 was detected.

Comparing the water uptake rates found here with those of the powder characterisation (see Figure 18) the improved water uptake tendency of Type II was confirmed. This could be attributed to the fibrous structure of Type II (Figure 16), which is related to good wicking. [58]

In general, it could be shown that modification of the crystal lattice increased the water uptake rate. For single substance tablets, no difference was found for Type II and UICEL B compared to UICEL S, the standard of class 3. The slow water uptake rate for UICEL-XL was difficult to assess since only three measurements were included and no comparison of single substance and binary mixtures was possible. The very slow water uptake rate of proquazone shown in Figure 18 could be related to its poor wettability determined by von Orelli [40]. Comparing single substances and binary mixtures it became evident that a proquazone load of 10% slowed down the water uptake rate. To prove this influence two additional drug loads, 50% and 90%, were included.

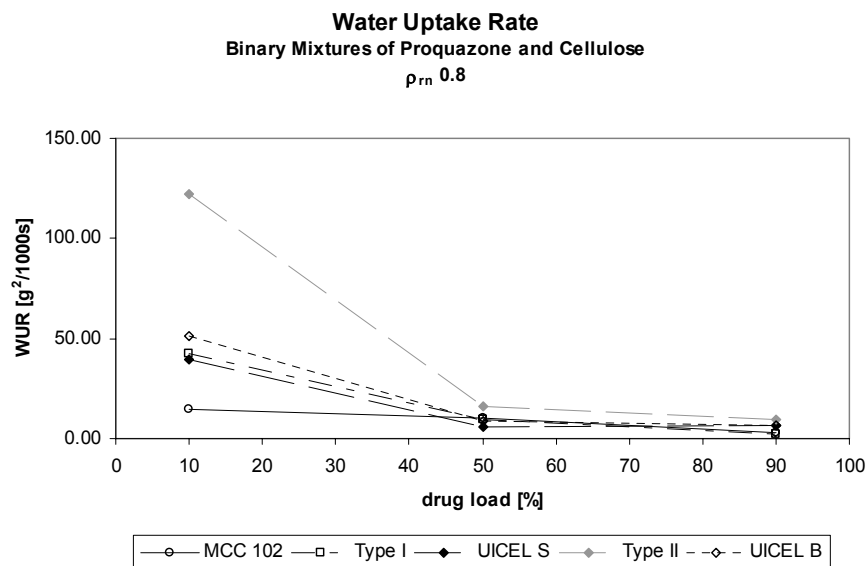


Figure 52: Water uptake rates of proquazone – cellulose binary mixtures at different drug loads. The points are connected by lines to improve the comprehensibility.

In Figure 52 it is detectable that increased drug load was accompanied by decreased water uptake rate. To keep the diagram clear, standard deviations were not shown; average values and corresponding standard deviations of six single determinations are given in Table 37. A statistical difference between 10% and 90% drug load was found for all binary mixtures except for UICEL S ($p = 0.051$). After 50% drug load the filler, except MCC 102

RESULTS AND DISCUSSION

($p = 0.041$), was not able to increase the water uptake rate. Compared to the water uptake rate of the pure proquazone, a statistically significant increase was found only for 90% Type II, 50% of a class 3 filler, and 10% MCC 102, Type I, Type II, or UICEL B.

Table 37: Average values and standard deviations of water uptake rates [$\text{g}^2/1000 \text{ s}$] as a result of the drug load.

	10%	50%	90%
MCC 102	14.55 (7.58)	9.90 (2.61)	2.65 (0.57)
Type I	42.22 (14.78)	9.18 (3.39)	2.22 (1.08)
UICEL S	39.28 (38.06)	5.57 (0.99)	6.37 (3.45)
Type II	122.28 (49.94)	15.78 (7.09)	9.22 (3.46)
UICEL B	50.95 (27.92)	8.80 (1.61)	6.62 (2.49)

In case of modified celluloses water uptake rate did not decrease linearly with increasing drug load. This may point to a critical amount of cellulose required for fast water uptake between 0% and 50%. The critical amount of spherical disintegrant particles is 16%(v/v); this fraction is reduced for fibrous particles. [94] After conversion of the 50%(m/m) modified cellulose fraction to %(v/v), it ranged from 44.04%(v/v) to 44.91%(v/v). The change of properties would have been expected at a drug load of 84%(v/v), this shift to smaller drug load can therefore not only be attributed to the disintegrant, but also to drug properties as poor wettability, or to the poor discriminative power of the method which could be seen in the very high standard deviations in Table 37.

Comparing those findings with the results of binary mixture studies, the impact of the filler on the water uptake decreased as follows: Type II >> UICEL B > Type I > UICEL S >> MCC 102.

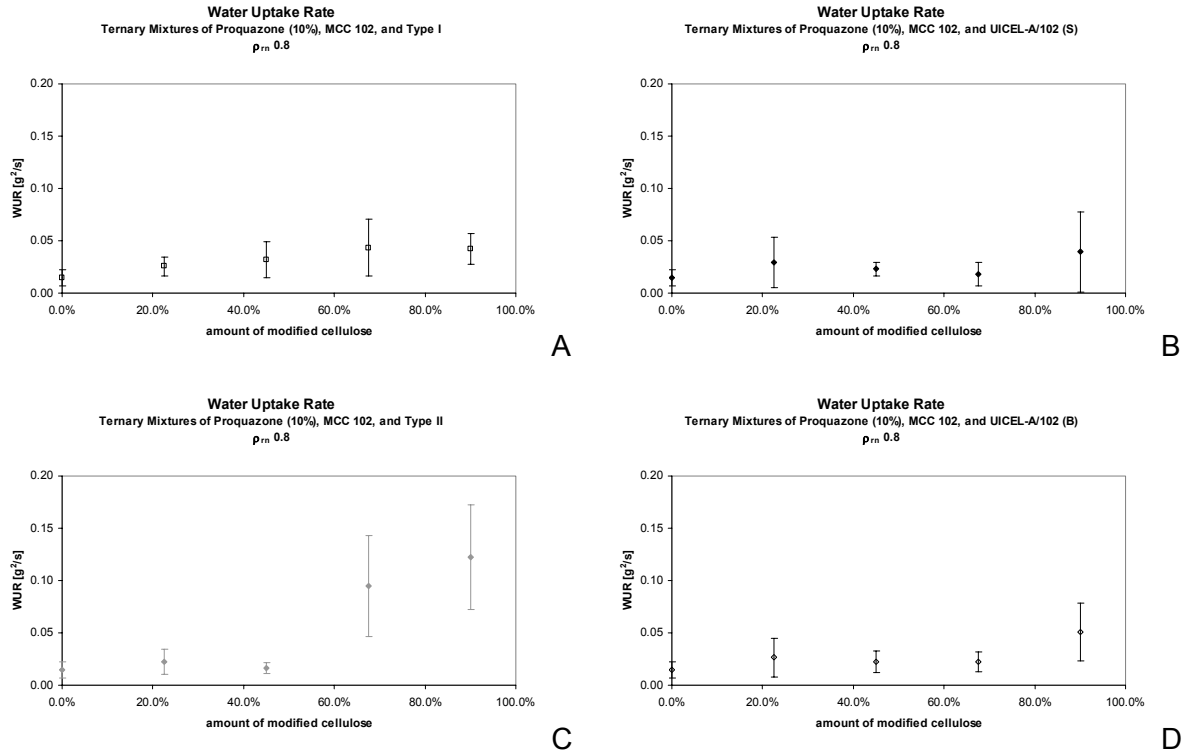


Figure 53: Water uptake rates of ternary mixtures; (A) Type I, (B) UICEL S, (C) Type II, and (D) UICEL B. The ordinates are not adjusted to facilitate the comparison between the different celluloses.

Studying the influence of the amount of modified cellulose in ternary mixtures, one could say that UICEL S (B) was not influenced by the load; Type II (C) showed a significantly increased water uptake rate above 67.5%(m/m) or 66.25%(v/v). Type I (A) and UICEL B (D) showed differences which could not be related to the load of modified cellulose; this differences were considered to be artefacts due to the imprecise method. The fastest water uptake rates were again found in formulations containing Type II.

From these results it can be concluded that adding cellulose improves liquid - solid interactions. Modified celluloses, independent of the degree of modification, show an increased tendency of water uptake rate compared to MCC 102. The suitability of water uptake rate determination to quantify liquid – solid interactions, as it was suggested by Luginbühl [68], has to be proved by disintegration and dissolution experiments.

5.2.2 Disintegration

Disintegration is the process by which a solid dosage form breaks up when it comes in contact with an aqueous medium. In order that the tablet can disintegrate, the bondings

RESULTS AND DISCUSSION

built during compaction have to be overcome. Since water uptake is a pre-requisite for disintegration (see also Figure 9: Mechanisms of disintegration.) a correlation between water uptake rate and disintegration time could be expected.

Initially, the influence of the relative density on the disintegration time was investigated. From water uptake experiments it is known that the relative density did not influence the water uptake rate.

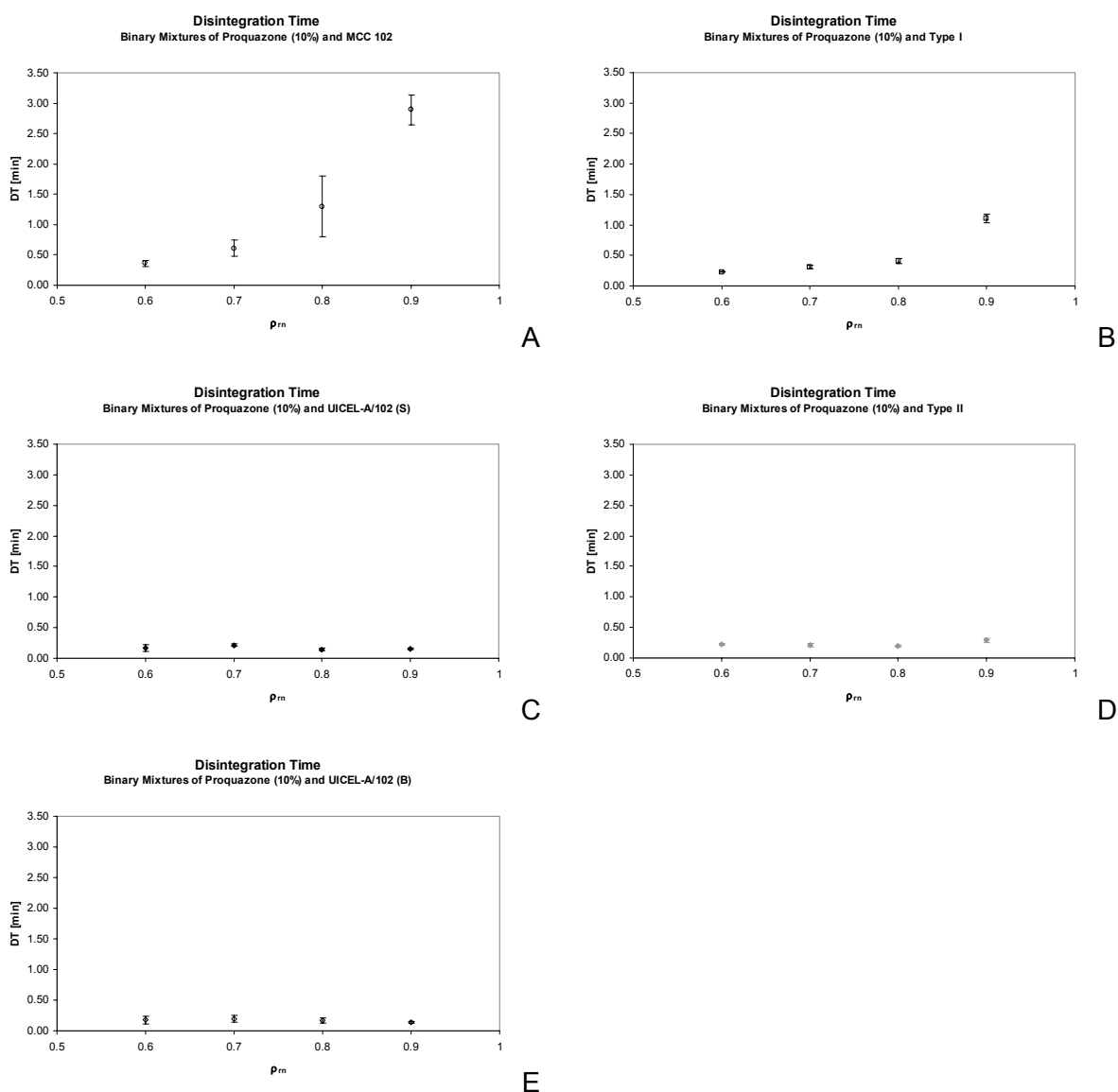


Figure 54: Disintegration times of proquazone – cellulose binary mixtures as a result of the relative density; (A) MCC 102, (B) Type I, (C) UICEL S, (D) Type II, and (E) UICEL B. The ordinates are not adjusted to facilitate the comparison between the different celluloses.

Figure 54 shows the relationship between the relative density and the corresponding disintegration time of binary mixtures with a 10% drug load. For binary mixtures containing MCC 102 (A) and Type I (B), the disintegration time increased significantly after a relative density of 0.7. The influence of the relative density on all class 3 substances was less explicit, but for Type II (D) a significant increase of the disintegration time was found for the relative density 0.9. UICEL B (E) was robust; for UICEL S (C), a significant increase of the disintegration time was found for the nominal relative density 0.7 compared to 0.8 and 0.9, but since these values were very short, statistical differences are not important.

Comparing the different fillers, MCC 102 showed significantly increased disintegration times independent of the relative density. Type I was clearly less efficient at a relative density 0.9 compared to the fully converted cellulose II products but still more efficient than MCC 102. The standard UICEL S showed no statistical proved advantage compared to the other substances of class 3 and 4.

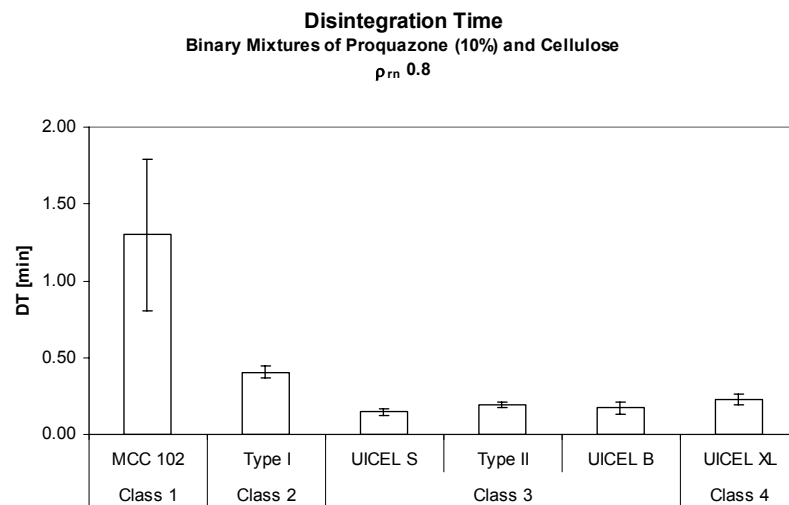


Figure 55: Disintegration time of proquazone (10%) – cellulose binary mixtures compressed to $\rho_{rn} 0.8$.

The comparison of the filler is given in Figure 55. The nominal relative density $\rho_{rn} 0.8$ was selected because of its important during the whole studies. The significantly increased disintegration time of MCC 102 compared to the other fillers was obvious. The modification of the cellulose increased the disintegrant efficiency. The partially modification of Type I decreased the disintegration time from 1.30 minutes to 0.41 minutes. Total conversion

RESULTS AND DISCUSSION

found in Class 3 and 4 decreased the disintegration time additionally. Conversion of the lattice structure can hence be considered as an important factor for the disintegrant development.

To study the relationship between water uptake rate and disintegration time, water uptake rates (Figure 51) and the reciprocal of the disintegration times (Figure 55) were combined (Figure 56). Since water uptake rate was not influenced by the relative density, binary mixtures of proquazone (10%) and cellulose compressed to ρ_{rn} 0.8 were investigated.

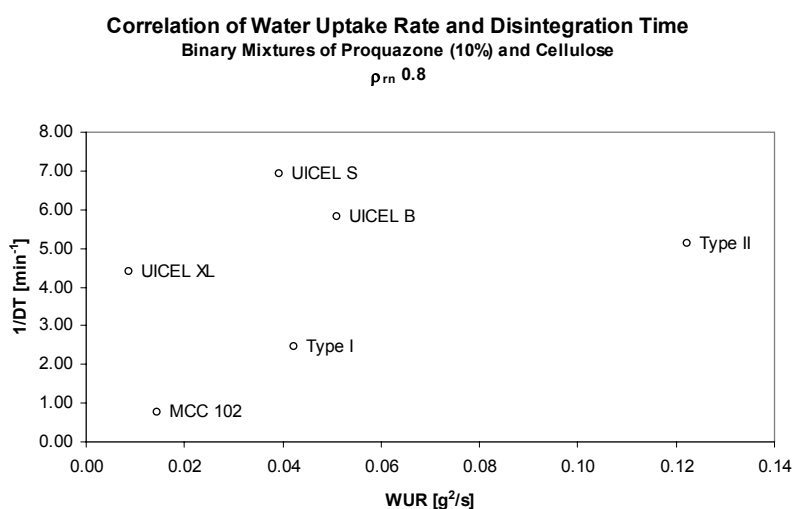


Figure 56: Correlation of water uptake rates and reciprocal disintegration times of proquazone (10%) – cellulose binary mixtures compressed to ρ_{rn} 0.8.

For MCC 102, Type I, and Type II, the expected decrease of the disintegration time with increasing water uptake rate was found. However, UICEL-XL showed an intermediate disintegration time with the slowest water uptake rate. One has to keep in mind that the water uptake rate of UICEL-XL was based on few data and was therefore less accurate. The disintegration efficiency of UICEL S and UICEL B was superior to Type I, even though their water uptake rates were comparable. The good disintegrant properties of UICEL-A/102 which were also described by Reus Medina et al. [9, 10] and Lanz [27] could not only be attributed to water uptake; other mechanisms seemed to have an influence on the effect. Beside water uptake, swelling is the most mentioned mechanism of action. From the work of Lanz [27] it is known that swelling capacity is not the main mechanism for UICEL and Avicel PH-102, but UICEL shows much higher swelling force and rate of force

development than Avicel. The improved disintegrant properties of UICEL-A/102 (S and B) could be attributed to this increased swelling force; a clear relationship between swelling force and disintegration time is described in literature. [65]

From water uptake measurements it was expected that disintegration time is influenced by the increase of drug load. The results of the disintegration time with respect to the drug load are given in Figure 57.

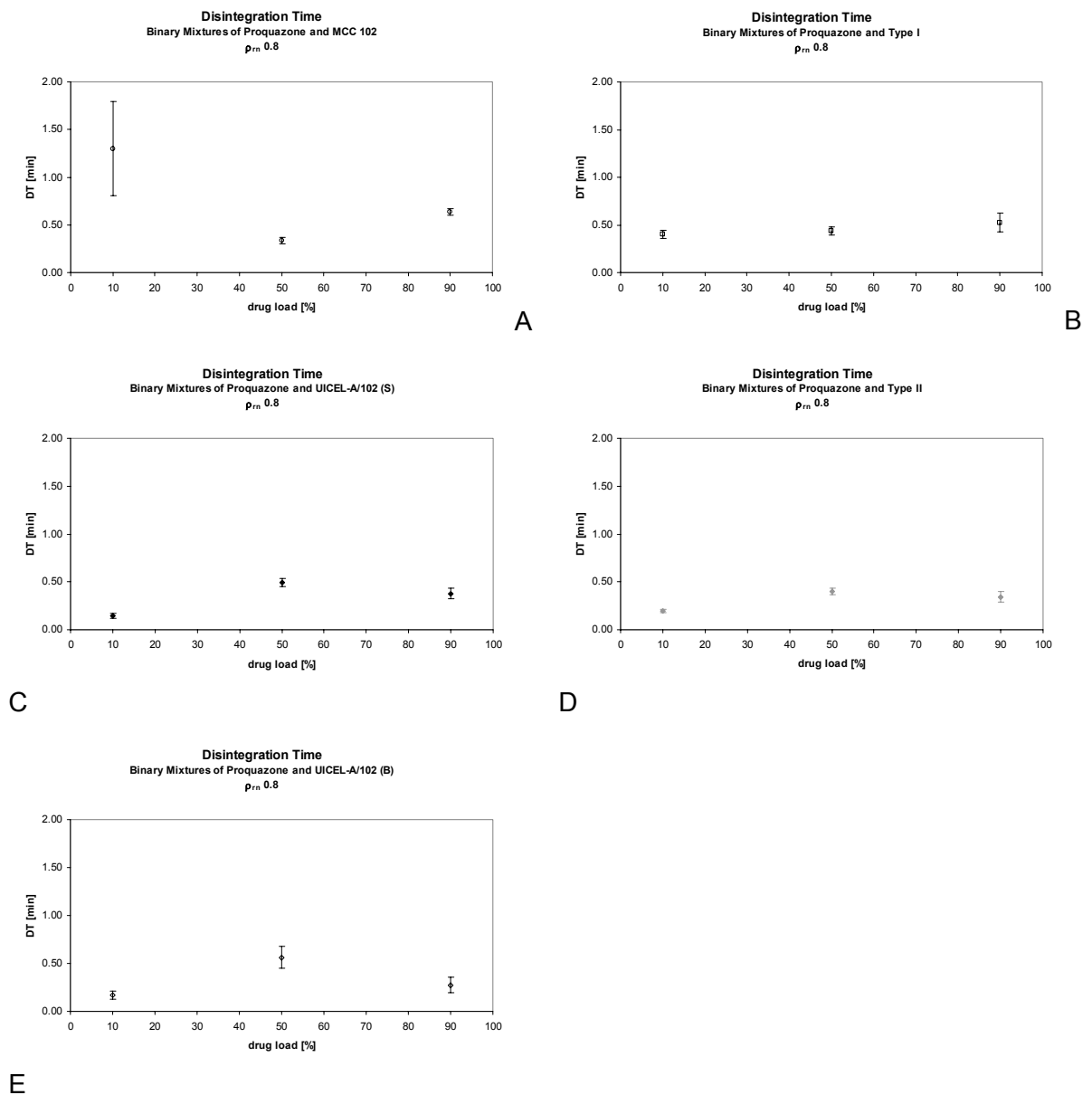


Figure 57: Disintegration times of proquazone – cellulose binary mixtures as a result of the drug load; (A) MCC 102, (B) Type I, (C) UICEL S, (D) Type II, and (E) UICEL B. The ordinates are not adjusted to facilitate the comparison between the different celluloses.

RESULTS AND DISCUSSION

From the individual plots in Figure 57 it was detectable that different classes showed different relationships between drug load and disintegration time. The minimum disintegration time of Class 1 (A) was found at a drug load of 50% and the maximum at a drug load of 10%. This confirmed the findings of Lanz [27], who studied binary mixtures of proquazone and Avicel 102 at different drug loads. The maximum disintegration time differed significantly compared to 50% and 90% which were similar ($p = 0.187$). The class 2 material Type I (B) showed the shortest disintegration time at 10% drug load and a maximum at 90% which was significantly slower. All class 3 substances, UICEL S (C), Type II (D), and UICEL B (E), showed minimal disintegration times at 10% drug load and maximum values at 50% drug load. For UICEL S, no statistical differences were found between all different levels of drug load, for Type II the difference vanished between 50% and 90% drug load, and for UICEL B the maximum was statistically proved. Even though differences were detected, disintegration times were very short (maximally $1.30 \text{ min} \pm 0.50$). Very short disintegration times of proquazone – UICEL binary mixtures independent of the amount of disintegrant are described by Lanz [27].

In the experiment above, the disintegrant efficiency was studied in binary mixtures. One has to keep in mind that disintegration is influenced by water uptake which, as shown above, is reduced by increased drug load. To study further disintegrant properties of modified celluloses ternary mixtures were prepared. The proquazone load was low (10%) to minimize the influence of its poor wettability. MCC 102 was used as filler in combination with modified cellulose. The results of these experiments are given in Figure 58.

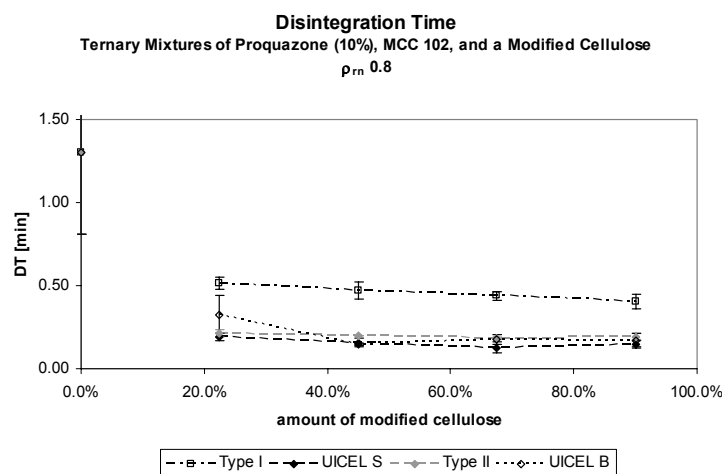


Figure 58: Disintegration times of ternary mixtures as a result of the amount of modified cellulose. The points are connected by lines to improve the comprehensibility.

One could see that a critical amount of modified cellulose between 0%(m/m) and 22.5%(m/m) reduced the disintegration time significantly; increasing the amount of modified cellulose, however, did not influence the disintegration time anymore. Disintegration of Type I formulations was independent of the load significantly slower than ternary mixtures with class 3 substances which were very similar. As discussed above for water uptake rates, a critical amount of disintegrant is required to obtain fast disintegration. For spherical particles this critical value is 16%(v/v); this fraction is reduced for fibrous particles. Conversion of 22.5%(m/m) to %(v/v) resulted in 22.50%(v/v) for Class 2 and 22.34%(v/v) for Class 3. To evaluate the critical value, ternary mixtures of Type II were studied with lower disintegrant loads. Figure 59 shows the disintegration times as a result of the load of modified cellulose in %(v/v).

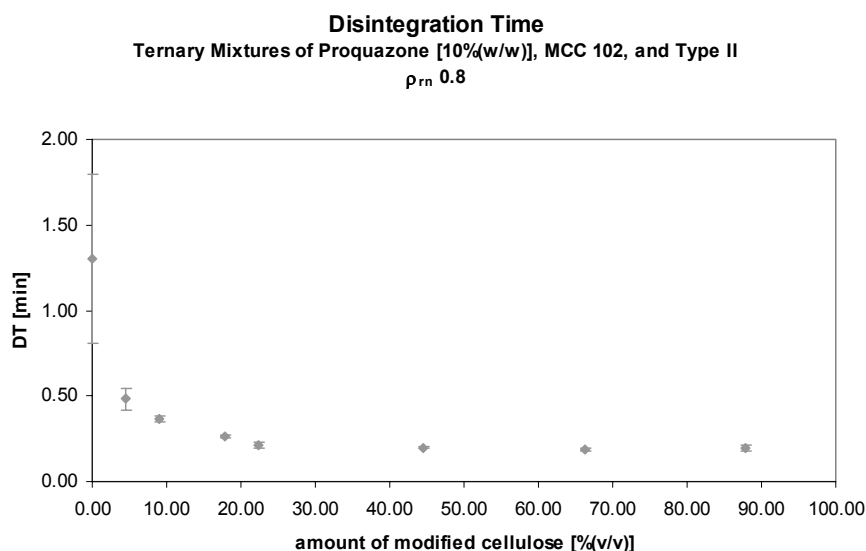


Figure 59: Disintegration times of ternary mixtures of proquazone, MCC 102, and Type II as a result of the amount of modified cellulose.

Even though disintegration time was reduced up to a load of 22.34%(v/v), statistically no difference was found after a load of 4.49%(v/v). The critical amount of modified cellulose in ternary mixtures is supposed to be between 0% and 4.49%(v/v). This is in good agreement with the theoretical considerations and the value is comparable to values used for Ac-di-Sol®. [94]

RESULTS AND DISCUSSION

Disintegrants that are efficient in an amount less than 5% are so called “super-disintegrants”. [71] Type II, and the similar class 3 substances UICEL S and UICEL B, can indeed be considered as superdisintegrants. To prove these assumptions, detailed investigations for UICEL-A/102 should be performed.

5.2.3 Dissolution

5.2.3.1 Influence of the Relative Density

Dissolution is the most important factor in solid dosage form design, since a drug can only be absorbed from solution. For a fast onset of action, a fast dissolution is required. This can be obtained by increasing the surface area from which the drug can dissolve. Disintegration is therefore a very important factor in immediate release dosage forms.

From disintegration studies it is known that relative density influences the disintegration time of MCC 102 and Type I, whereas class 3 celluloses seem more robust (Figure 54). UICEL-XL was studied only at one relative density, but similar results as for class 3 could be expected (Figure 55).

Initially, dissolution was studied on binary mixtures of proquazone (10%) and cellulose at three different relative densities. The dissolution profiles are given in Figure 60. Standard deviations of UICEL S (C), Type II (D), UICEL B (E), and UICEL-XL (F) were omitted for better clarity. After five minutes, relative standard deviations decreased below 2%, except Type II which showed slightly higher values, but still below 5%.

Regarding the dissolution profiles no influence of the relative density on dissolution was found for UICEL S (C), UICEL B (E), and UICEL-XL (F). This is in good agreement with disintegration times. Type II (D) showed significantly increased disintegration times at ρ_m 0.9; an influence of the relative density was also found in dissolution. For MCC 102 (A) and Type I (B) disintegration times as well as dissolution profiles were influenced by the relative density. The standard deviations found for MCC 102 (ρ_m 0.8) and Type I (ρ_m 0.7) were clearly higher compared to the other formulations. This was a problem of the tablet robustness. In case of MCC 102 the variation could be explained by the fact that two out of three tablets break into two or more pieces, and dissolved therefore faster than the third tablet.

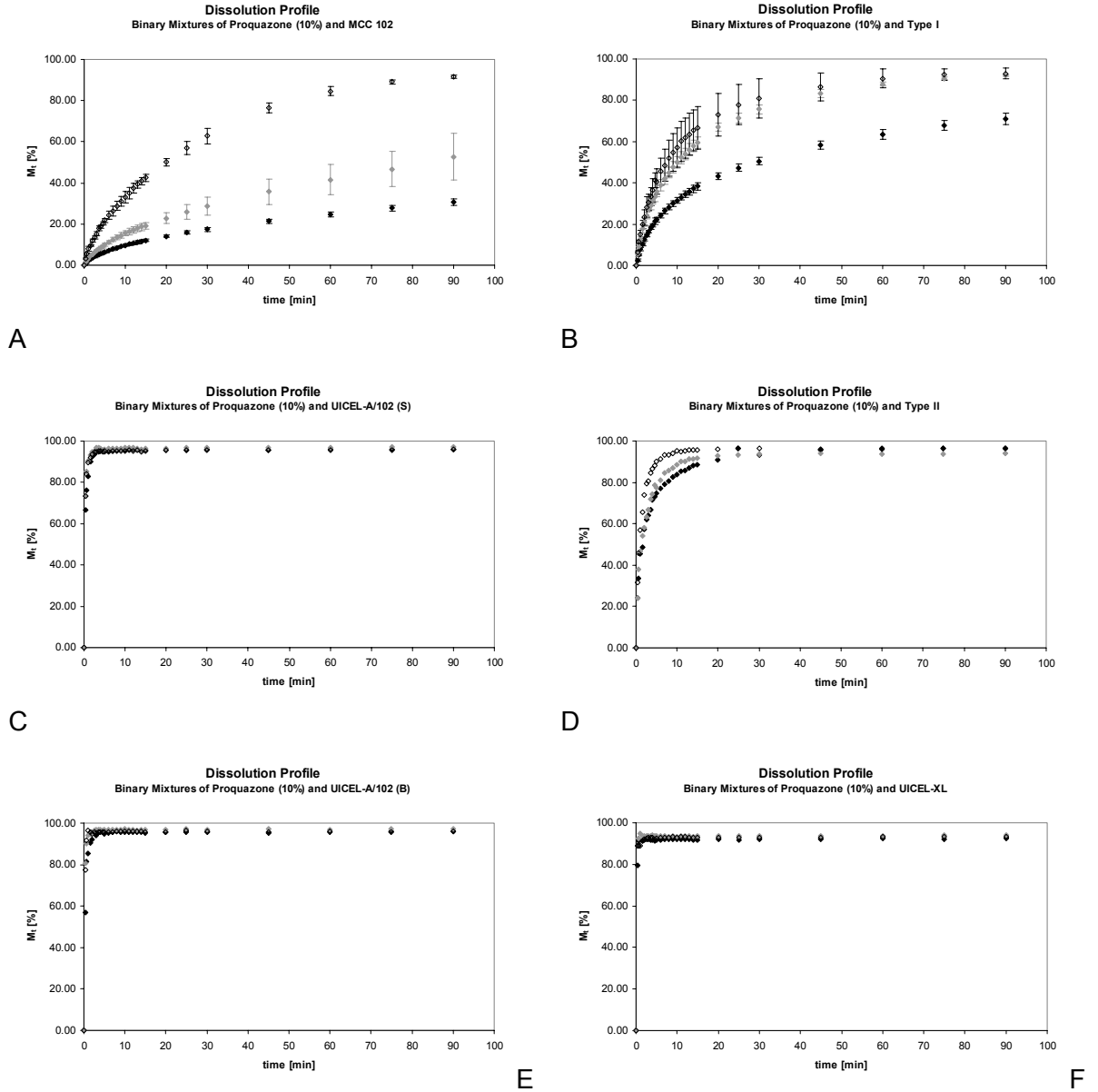


Figure 60: Dissolution profiles of proquazone – cellulose binary mixtures as a result of the relative density; (A) MCC 102, (B) Type I, (C) UICEL S, (D) Type II, (E) UICEL B, and (F) UICEL-XL.

Legend: ρ_{rn} 0.7 (\diamond), ρ_{rn} 0.8 (\blacklozenge), and ρ_{rn} 0.9 (\blacklozenge).

To quantify differences between dissolution profiles, all curves were tested with different models. To make comparison easier, the nominal relative density of 0.8 was selected as reference, the other two profiles were then compared to this standard curve and the differences were assessed. Model independent and model dependent approaches were studied.

RESULTS AND DISCUSSION

Model independent approach

The most simple model independent approach is statistical analysis with ANOVA. This was applied on $M_{30\text{ min}}$ data of Figure 61. The bars show the accumulated amount dissolved at 30 minutes ($M_{30\text{ min}}$), the dotted line corresponds to those 85% dissolved drug which are required for rapidly dissolving IR products according to FDA. [16] Using this diagram one could easily detect if the formulation met the requirements for rapidly dissolving immediate drug release.

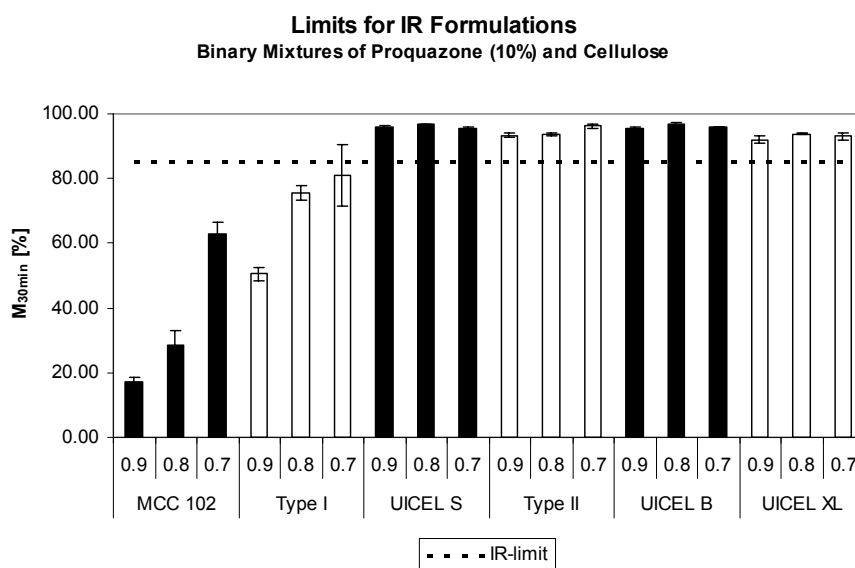


Figure 61: $M_{30\text{ min}}$ and IR limits for proquazone – cellulose binary mixtures as a result of the nominal relative density.

MCC 102 and Type I binary mixtures did not meet the requirements for rapid drug release, whereas all fully converted powders of class 3 and 4 were suitable. The clear differences between MCC 102 formulations were statistically proved ($p < 0.05$). As expected from the plot, no difference was found between ρ_m 0.7 and ρ_m 0.8 for Type I. However, statistically significant differences were found for UICEL S and Type II between ρ_m 0.7 and ρ_m 0.8. Both formulations with UICEL B, ρ_m 0.7 and ρ_m 0.9, were different compared to ρ_m 0.8.

Difference factor f_1 and similarity factor f_2 are concepts to compare two dissolution profiles promoted by FDA [82] and EMEA [83].

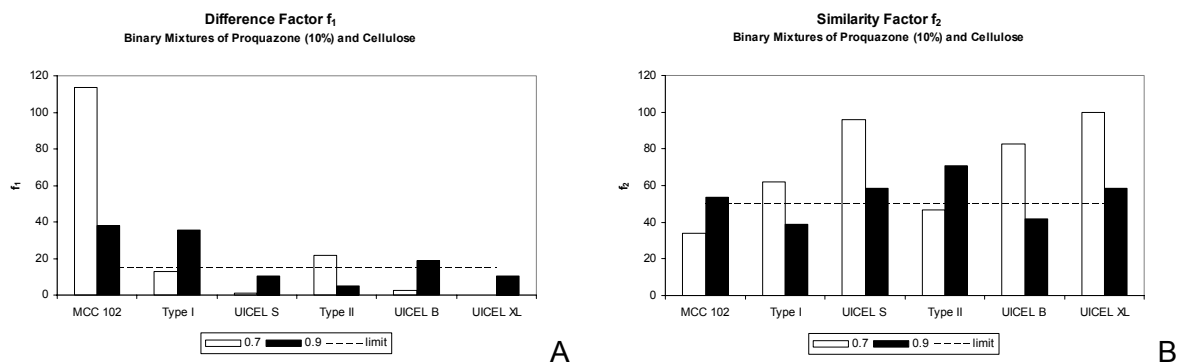


Figure 62: Difference factor f_1 (A) and similarity factor f_2 (B) for proquazone – cellulose binary mixtures with ρ_m 0.7 or ρ_m 0.9 compared to the reference formulation ρ_m 0.8.

Two curves are considered similar, when f_1 is close to 0 and f_2 is close to 100. f_1 values up to 15 as well as a minimal f_2 value of 50 are required to accept two curves as equal. These limits are given as the dotted line in Figure 62. Differences ($f_1 > 15$) between the dissolution profile of ρ_m 0.8 and at least one of the other dissolution profiles were found for MCC 102 (ρ_m 0.7 and ρ_m 0.9), Type I (ρ_m 0.9), Type II (ρ_m 0.7), and UICEL B (ρ_m 0.9); differences for MCC 102 (ρ_m 0.7), Type I and Type II and UICEL B were supported by the similarity factor f_2 . In case of MCC 102 (ρ_m 0.7), the difference factor was more rigorous. Formulations with UICEL S and UICEL-XL were found to be similar with both methods. Comparing these results to the dissolution profiles of Figure 60 differences of MCC 102, Type I, and Type II as well as similarity of UICEL S and UICEL-XL formulations were confirmed by this method. The difference between UICEL B ρ_m 0.8 and UICEL B ρ_m 0.9 was not found in the graph.

Comparing these three different model independent approaches it was evident that ANOVA resulted in the most rigorous results; similarity factor was the most liberal approach. Since these methods lack of scientific explanation, the use of model dependent methods were preferred.

The Weibull method is an ambiguous model, since it is indeed a model dependent approach, but based on statistics and without kinetic background. It is applicable on almost all kind of dissolution curves; therefore this approach was included in the evaluation. After fitting the data set to Equation 22 two parameters, a and b, were received, which were then used in Equation 23 to calculate the required time to dissolve a defined amount of drug. $t_{90\%}$ -values are given Table 38, the meaning of a and b will be discussed later.

RESULTS AND DISCUSSION

Table 38: $t_{90\%}$ -values [min] of proquazone – cellulose binary mixtures at different relative densities.

	ρ_m 0.7	ρ_m 0.8	ρ_m 0.9
MCC 102	84.62 (8.418)	626.90 (411.129)	2113.59 (244.112)
Type I	35.65 (13.982)	64.23 (6.175)	245.54 (31.844)
UICEL S	0.78 (0.099)	0.78 (0.168)	1.16 (0.062)
Type II	4.08 (1.200)	7.30 (0.383)	11.82 (1.279)
UICEL B	0.47 (0.106)	0.53 (0.098)	0.98 (0.039)
UICEL-XL	0.28 (0.210)	0.24 (0.037)	0.38 (0.058)

Weibull seemed to be a suitable model to describe dissolution profiles. The coefficients of determination r^2 were very high. The minimum coefficient of determination was 0.9976; only 7.3% of the fits were below 0.9990, but 46.3% of all fits were equal or greater than 0.9999.

The significantly slowest dissolution was found at ρ_m 0.9; differences between ρ_m 0.7 and ρ_m 0.8 were only found for Type II. Only UICEL-XL was not influenced by the relative density and can therefore be called robust. Comparing $t_{90\%}$ values with f_1 and f_2 , the similarity of UICEL-XL as well as the differences of Type I and UICEL B formulations were confirmed. In case of MCC 102 a similarity was found between ρ_m 0.7 and ρ_m 0.8; this was not found with model independent approaches neither was expected from qualitative analysis. In that case, $t_{90\%}$ determination with Weibull was obviously too liberal, whereas for UICEL S (ρ_m 0.9) and Type II (ρ_m 0.9) the model was more rigorous.

Since disintegration and dissolution are connected one could expect to find a correlation between these values; for that reason $t_{90\%}$ was plotted against the disintegration time DT (Figure 63). $t_{90\%}$ was selected because both, disintegration time and $t_{90\%}$ can be considered as endpoints of the process. A linear relationship between DT and $t_{90\%}$ was expected, therefore linearity was determined with linear regression. The individual plots and fits are given in Figure 63, the corresponding values in Table 39.

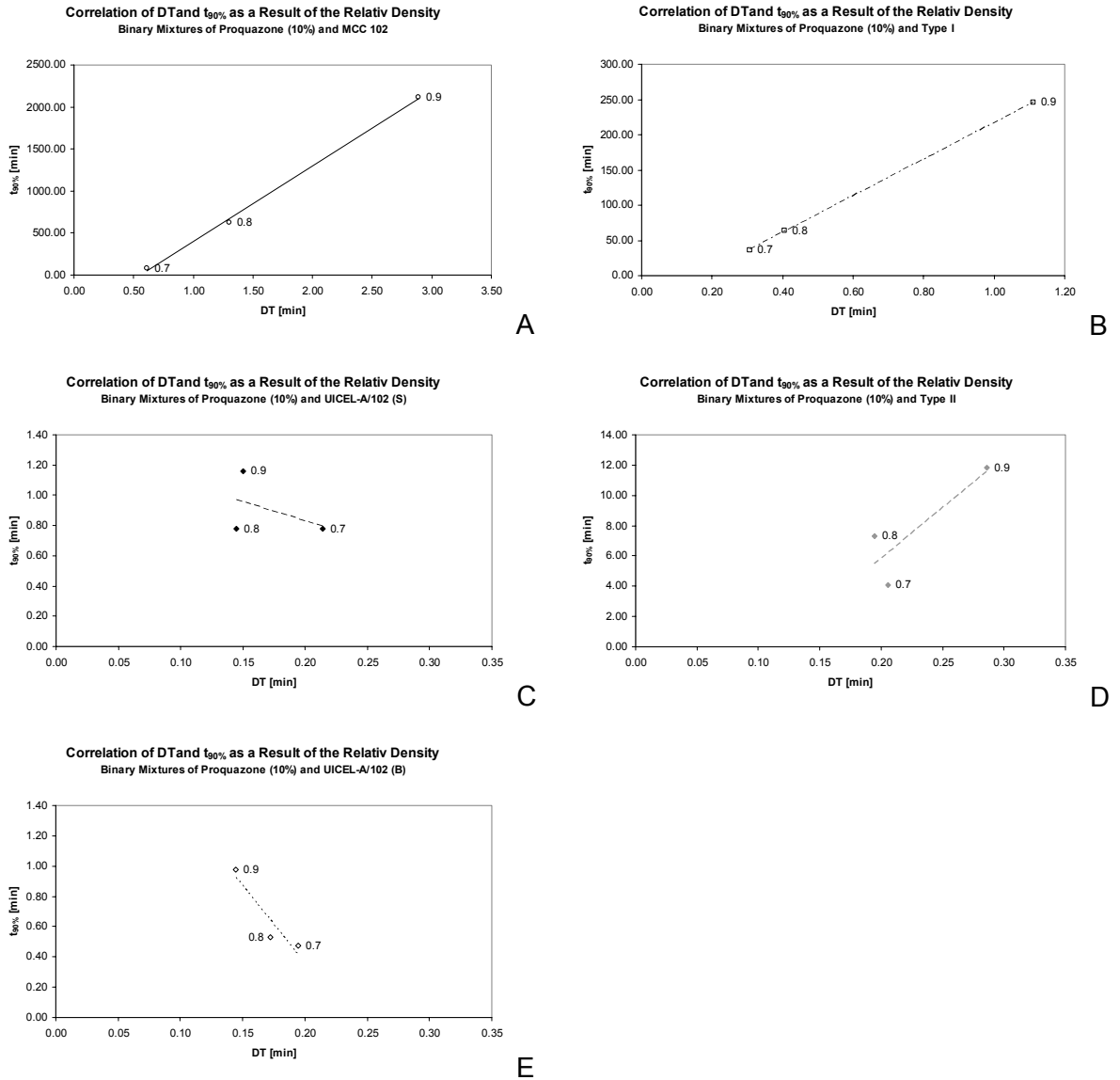


Figure 63: Correlation of the disintegration time and $t_{90\%}$ of proquazone – cellulose binary mixtures as a result of the relative density; (A) MCC 102, (B) Type I, (C) UICEL S, (D) Type II, and (E) UICEL B.

A clear correlation was found for MCC 102 and Type I binary mixtures, where with an increased relative density disintegration time as well as $t_{90\%}$ increased. This relation can be explained by significantly different disintegration times between the relative densities. An increase of disintegration time and $t_{90\%}$ was also found for Type II, even though the correlation was poor. This can be explained by disintegration times which were not clearly different. Since disintegration time of UICEL S and UICEL B formulations were independent of the relative density, it was not surprising that the results did not follow the rule and ended in a decrease of disintegration time.

RESULTS AND DISCUSSION

Table 39: Slopes and coefficients of determination of the correlation between disintegration time and $t_{90\%}$ as a result of the relative density.

	Slope	r^2
MCC 102	898.15	0.9986
Type I	259.78	0.9998
UICEL S	-2.4954	0.1922
Type II	66.771	0.7374
UICEL B	-10.322	0.8778

The meaning of the slope can be expressed as follows; an ideally, well soluble drug which is immediately released should reach $t_{90\%}$ at the same time as the tablet disintegrated, this results in a slope of 1. A steep slope can therefore be related to a hindered solubilization of the drug, either due to poor solubility or to physical hindrance by the formulation. Disintegration as it is determined according to the European Pharmacopoeia does not take into account the particle size after disintegration. When particles are smaller than 2 mm, they fall through the mesh and the tablet is counted as fully disintegrated. Particles of 2 mm can still contain embedded drug which is slowly released from this smaller particles. Even though disintegration times were all very short (< 5 min) one could see that this good disintegrant activity is not directly related to good dissolution properties. The property of a disintegrant to promote fast dissolution can be assessed by analysing the slope of the correlation between disintegration time and $t_{90\%}$. A gentle slope is related to good dissolution properties. From this point of view it was concluded that MCC 102 is the poorest disintegrant, followed by Type I and then Type II. Since it was possible for Type II formulations to meet the FDA requirements for rapidly dissolving immediate drug release, this material shows good disintegration properties.

The same problem was already summarized by Lowenthal [58]; he mentions the fact that disintegration does not distinguish between rapid and slow dissolution and tablets that disintegrate into fine particles show faster dissolution rates compared to large clumps.

First order kinetics and Hixson-Crowell model are appropriate to describe immediate release dosage forms. [85] Both models are based on a scientific background and make them more suitable to describe drug release. First, all dissolution profiles were fitted to the modified Noyes-Whitney equation (Equation 24) to establish dissolution rate k_1 . The corresponding values are listed in Table 40; fits with a coefficient of determination equal or greater than 0.9800 were considered as appropriately fitted, those below that value are plotted in Figure 64.

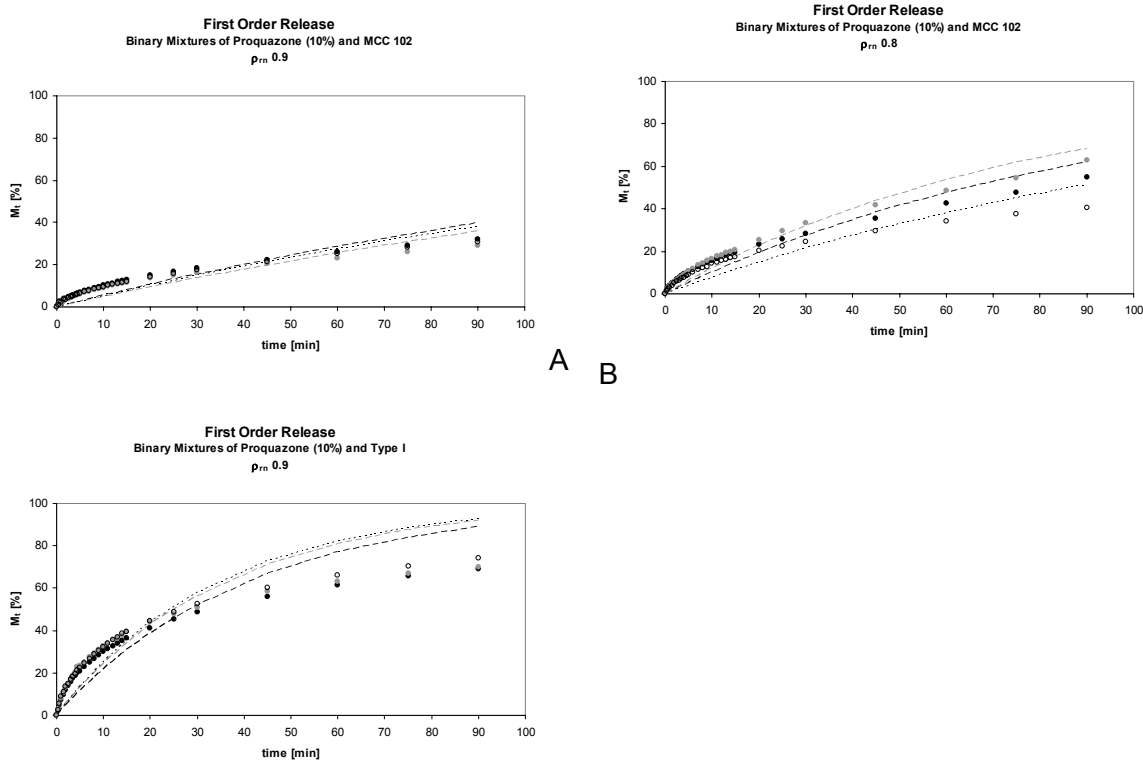
Table 40: Dissolution rate k_1 [min^{-1}] of proquazone – cellulose binary mixtures at different relative densities, incl. standard deviations in brackets.

	ρ_m 0.7	ρ_m 0.8	ρ_m 0.9
MCC 102	0.038 (0.002)	0.011 (0.002)	0.005 (0.0003)
Type I	0.102 (0.026)	0.068 (0.006)	0.027 (0.002)
UICEL S	3.952 (0.234)	3.964 (0.801)	2.841 (0.122)
Type II	0.804 (0.264)	0.467 (0.030)	0.363 (0.034)
UICEL B	4.992 (0.772)	5.145 (0.825)	2.718 (0.493)
UICEL-XL	44.614 (64.781)	8.840 (0.769)	6.112 (0.930)

From Figure 64 one could see that dissolution of MCC 102 (A and B) and Type I (C) formulations did not follow first order kinetics. They showed a faster dissolution rate at the beginning, which is slowed down in the later stage. An appropriate model to describe these two stages should be found.

Statistical analysis of the data of Table 40 confirmed the dependence of MCC 102 on the relative density. Robustness, as expected, was found for UICEL S and UICEL-XL. Type I showed similar profiles ρ_m 0.7 and ρ_m 0.8, which confirmed the findings of findings of the qualitative analysis as well as the model independent approaches and $t_{90\%}$ analysis. A difference was found for Type II only between ρ_m 0.7 and ρ_m 0.9. In general, it can be said that first order release rate is in good agreement with the qualitative analysis.

RESULTS AND DISCUSSION



C

Figure 64: Experimental and fitted data according to the modified Noyes-Whitney equation for profiles with $r^2 < 0.9800$; binary mixtures of proquazone and MCC 102 (A, B) or Type I (C) at different relative densities.

Legend: Experimental (dots) and fitted values (lines) for Run 1 (◆, - - - -), Run 2 (◆,) and Run 3 (◇, - · - ·).

A second model dependent approach applied was the Hixson-Crowell cubic root law, which accounts for the residual drug in the dosage form. The cubic root law (Equation 25) is only applicable when the dimensions of the solid diminish proportionally and the geometrical shape keeps constant. This model is applicable on very fast disintegrating tablets which appear immediately as powders after contact with the dissolution medium. Cubic root law was applied on mean dissolution profiles ($n=3$), including values $\leq 85.00\%$. The evaluation was only possible when minimally four points were available in this range. Dissolution rate k_2 , if available, and the coefficient of determination (r^2) are listed in Table 41.

The small amount of data made the cubic root law inappropriate for UICEL S, UICEL B, and UICEL-XL formulations. Slower releasing formulations with MCC 102, Type I, or Type II were analysed, but resulted in poorly described curves (compare r^2 values in brackets, and the non-randomly scattered deviations of experimental data and fitted values of MCC 102 (A), Type I (B), and Type II (C) in Figure 65).

Table 41: Dissolution rate k_2 [$\%^{1/3} \cdot \text{min}^{-1}$] of proquazone – cellulose binary mixtures at different relative densities, incl. r^2 in brackets.

	ρ_m 0.7	ρ_m 0.8	ρ_m 0.9
MCC 102	0.0361 (0.9785)	0.0110 (0.9637)	0.0058 (0.9386)
Type I	0.0747 (0.9301)	0.0479 (0.9063)	0.0172 (0.8853)
UICEL S	n/a (n=3)	n/a (n=2)	0.3582 (0.4557)
Type II	0.6072 (0.9346)	0.3127 (0.9202)	0.1940 (0.8581)
UICEL B	n/a (n=2)	n/a (n=2)	n/a (n=3)
UICEL-XL	n/a (n=1)	n/a (n=1)	n/a (n=2)

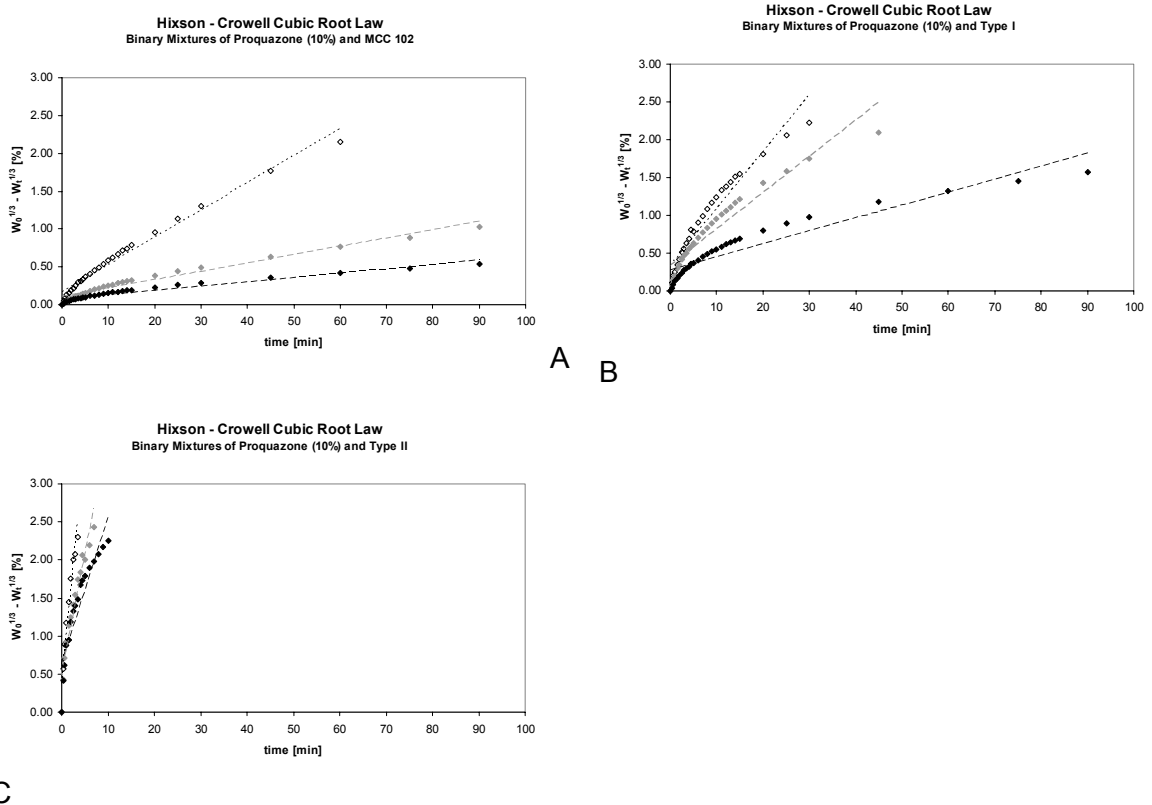


Figure 65: Experimental and fitted data according to the Hixson-Crowell equation for binary mixtures of proquazone and MCC 102 (A), Type I (B), or Type II (C), respectively.

Legend: Experimental (dots) and fitted values (lines) for ρ_m 0.7 (\diamond ,), ρ_m 0.8 (\blacklozenge , ----), and ρ_m 0.9 (\blacklozenge , -.-.-).

RESULTS AND DISCUSSION

Fitting to the cubic root law yielded in poor results; independent of the formulation, the model seemed not to describe dissolution profiles appropriately. Since neither first order kinetics nor cubic root law described the profiles of Figure 64 properly, these formulations had to be studied in more detail. The visible initial fast drug release with a later decrease is known from matrix systems which can be described by the Higuchi model (Table 6).

Additionally to the profiles of Figure 64, formulations with MCC 102 and a nominal relative density of 0.7 as well as Type I formulations of ρ_m 0.8 and ρ_m 0.7 were studied. Data until approximately 60% were included for this model. Plots including linear trend lines and the corresponding average dissolution rate k_3 , including standard deviation and r^2 values of every fit, are given in Figure 66 and Table 42, respectively.

Assessing the Higuchi model by the coefficient of determination, dissolution profiles of MCC 102 binary mixtures at all three investigated relative densities were appropriately described with a coefficient of determination > 0.985 . Type I formulations also fitted well to the model, but the correlation became smaller. In both cases increased relative density was accompanied by increased coefficient of determination. The differences between relative densities of MCC 102 were confirmed by statistical analysis. For Type I formulations, this model was not sensitive enough to detect differences. Connecting these results with the findings of the correlation between disintegration time and $t_{90\%}$, it was supposed that proquazone was still embedded in a matrix of MCC 102 or Type I after disintegration. This theory is strongly supported by the findings of the Higuchi model which describes the release from matrix systems.

Table 42: Average dissolution rate k_3 , standard deviation, and coefficients of determination of every fit of proquazone – cellulose binary mixtures at different relative densities.

	MCC 102			Type I		
	ρ_m 0.7	ρ_m 0.8	ρ_m 0.9	ρ_m 0.7	ρ_m 0.8	ρ_m 0.9
Av. k_3 [$\text{min}^{-1/2}$]	11.93	5.68	3.31	19.00	16.25	12.67
SD k_3 [$\text{min}^{-1/2}$]	0.44	1.12	0.17	3.86	0.78	5.79
r^2	0.9929	0.9970	0.9994	0.9906	0.9962	0.9955
	0.9874	0.9945	0.9989	0.9924	0.9956	0.9724
	0.9957	0.9967	0.9989	0.9955	0.9952	0.9892

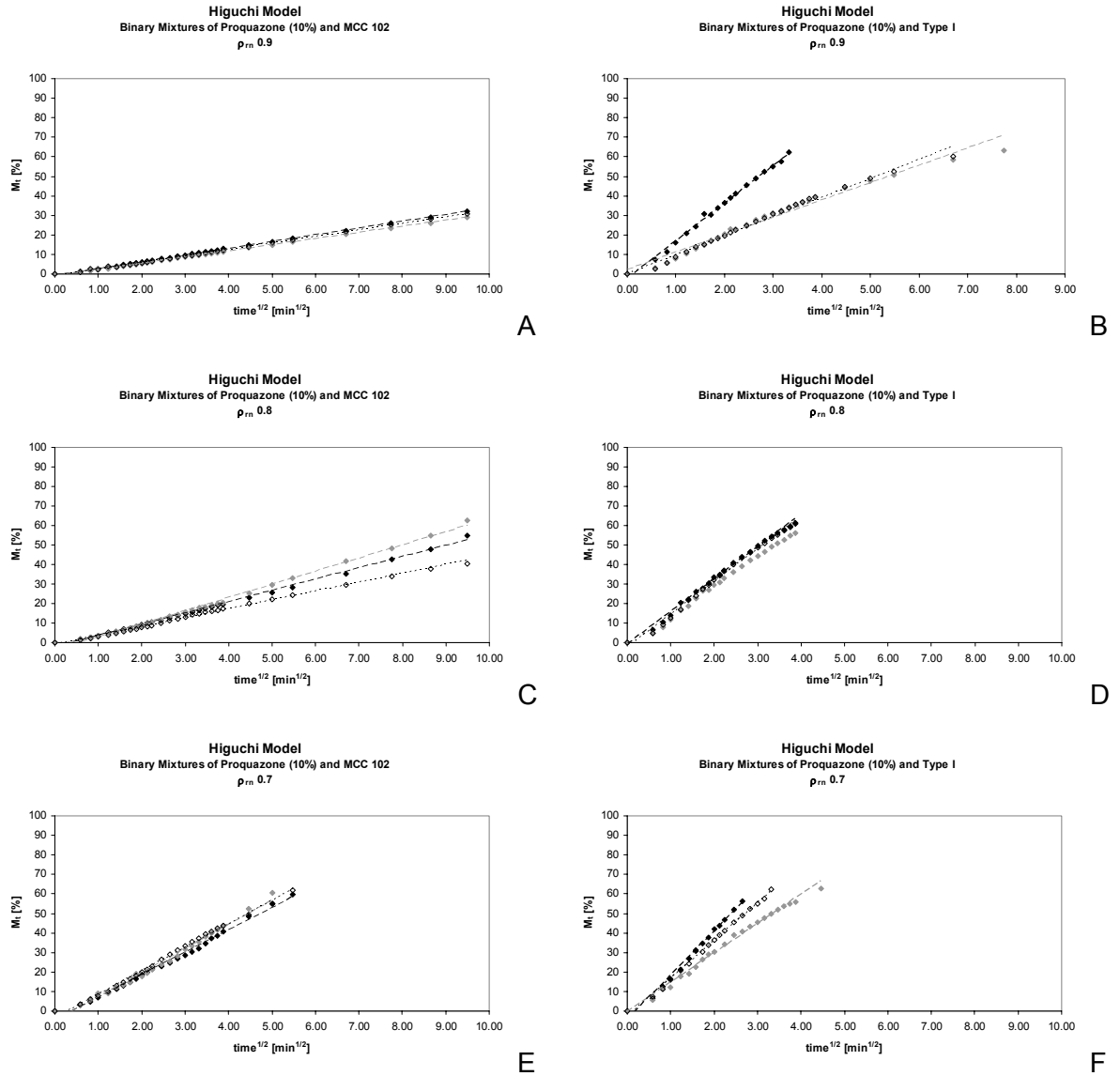


Figure 66: Experimental and fitted data according to the Higuchi equation for binary mixtures of proquazone and MCC 102 (A, C, E) and Type I (B, D, F) at different relative densities.

Legend: Experimental (dots) and fitted values (lines) for Run 1 (\diamond ,), Run 2 (\blacklozenge , -----), and Run 3 (\blacklozenge , -.-.-.-).

5.2.3.2 Influence of the Drug Load

The same approach as applied above was used to investigate the influence of the drug load on dissolution. First, dissolution profiles were presented graphically (Figure 67); relative standard deviations of UICEL S 10% and 50% decreased below 1.5% after five minutes and were therefore omitted.

RESULTS AND DISCUSSION

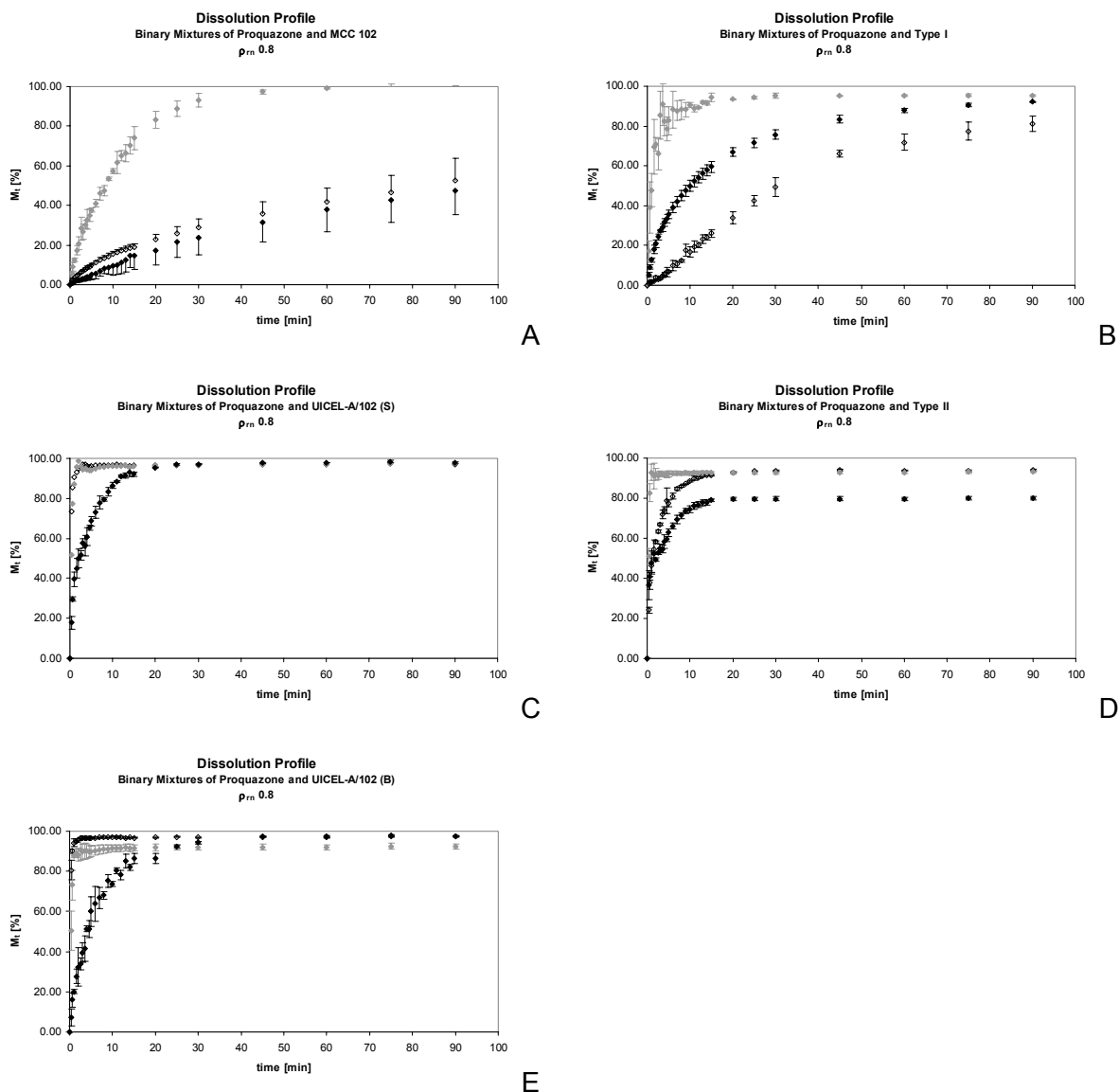


Figure 67: Dissolution profiles of proquazone – cellulose binary mixtures as a result of the drug load; (A) MCC 102, (B) Type I, (C) UICEL S, (D) Type II, and (E) UICEL B.

Legend: 10% proquazone (◆, - - - -), 50% proquazone (◇,), and 90% proquazone (○, ———).

MCC 102 showed a minimum disintegration time at a drug load of 50%, this was confirmed by the clearly faster dissolution rate given in Figure 67 A. A difference between 10% and 90% drug load was indeed detectable, but not as clear as expected from disintegration test. The decreased disintegration time of Type I 90% was also detectable in the dissolution profile (B), where it was the slowest formulation. 50% formulations released the drug fastest; this did not correlate with the disintegration time results. Class 3 substances showed fastest dissolution but slowest disintegration time at a drug load of 50%. To assess the influence of the drug load properly, quantitative analysis has to be performed.

The dissolution profile of Type II 90% reached its plateau below 80% drug released. Since this phenomenon appeared only once, it was regarded as an outlier and was referred to inappropriate handling during manufacturing, e.g. loss of drug. Amongst those formulations that reached the plateau within 90 minutes, this was the only formulation that was below 90%.

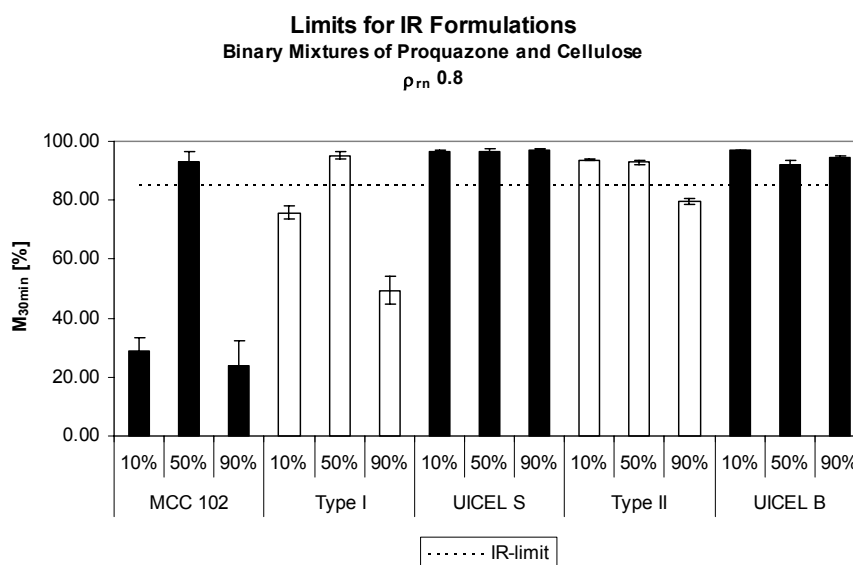


Figure 68: M_{30min} and IR limits for proquazone – cellulose binary mixtures as a result of the drug load.

Assessing only the limits for rapidly dissolving IR formulations given in Figure 68, one could see that all formulations with a drug load of 50% proquazone met the limits. Whereas formulations with MCC 102 (10% and 90%), Type I (10% and 90%), and Type II (90%) did not meet the requirements. Type II with a drug load of 90% missed the requirement because only 80% of the labelled drug amount was actually in the formulation. Recalculation of M_t with the actual endpoint set to 100% would result in a value for M_{30min} of $99.76\% \pm 0.13$; this would be clearly above the IR limits. Comparing M_{30min} values, no differences were found for MCC 102 between 10% and 90%, but 50% drug load was significantly faster. In formulations with Type I, the drug load decreased the dissolution rate significantly in the following rank order: 50% >> 10% >> 90%. No difference was found for UICEL S, whereas UICEL B showed a significantly increased dissolution rate for 10% drug load. Type II showed no differences between 10% and 50%, 90% was excluded due to the above mentioned problems.

RESULTS AND DISCUSSION

Difference factor and similarity factor were again applied on dissolution profiles. The most used formulation with 10% drug load was selected as reference, 50% and 90% drug load were then compared. The results are given in Figure 69.

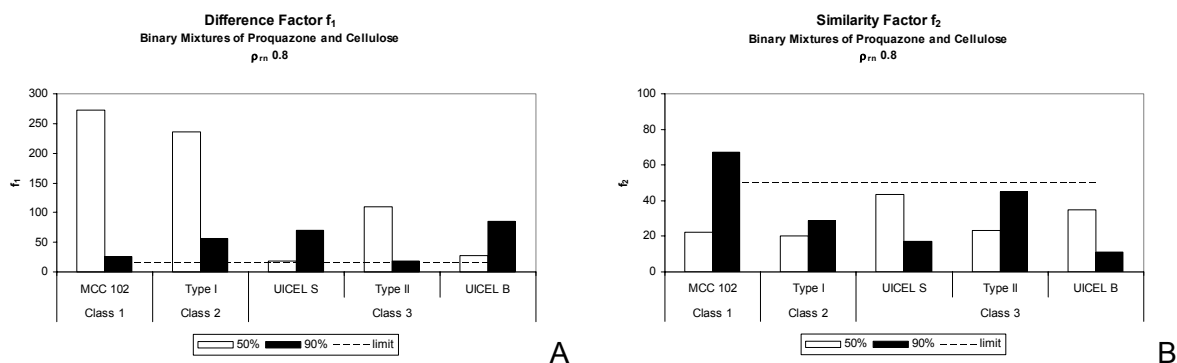


Figure 69: Difference factor f_1 (A) and similarity factor f_2 (B) of proquazone – cellulose binary mixtures with 50% and 90% drug load compared to the reference formulation with 10% drug load.

According to the difference factor f_1 none of the formulations with a higher drug load was similar to 10%, i.e. $f_1 < 15$. Similarity factor f_2 was slightly more liberal and resulted in a similarity ($f_2 = 67$) for MCC 102 90%. Comparing this with dissolution profiles given in Figure 67, it was detectable that similarity for these formulations could be expected. More surprisingly was the calculated difference of UICEL S 50% ($f_1 = 19$, $f_2 = 44$) and UICEL B 50% ($f_1 = 28$, $f_2 = 35$); regarding the profiles, they were expected to be similar. Compared to $M_{30\ min}$ f_1 and f_2 were more conservative and rejected similarity for UICEL S and Type II formulations.

Furthermore, all data were fitted to the Weibull model and the $t_{90\%}$ was then calculated to study curve properties and dissolution endpoints; the values are listed in Table 43.

Weibull seemed to be appropriate to describe dissolution profiles, since coefficients of determination r^2 were high. The minimal coefficient of determination of 0.9925 could be referred to the scattering of the data (compare dissolution profiles in Figure 67). An increased drug load reduced the fit of the model, but still more than 55% of all fits showed a coefficient of determination equal or greater than 0.9990.

Table 43: $t_{90\%}$ -values [min] of proquazone – cellulose binary mixtures at different drug loads, incl. standard deviations in brackets.

	10%	50%	90%
MCC 102	626.90 (411.13)	29.76 (3.08)	401.51 (136.62)
Type I	64.23 (6.18)	4.65 (0.72)	104.75 (15.83)
UICEL S	0.78 (0.17)	1.04 (0.25)	12.26 (1.32)
Type II	7.30 (0.38)	0.69 (0.12)	9.80 (1.13)
UICEL B	0.53 (0.10)	0.92 (0.15)	16.83 (1.46)

A correlation between disintegration time and $t_{90\%}$, where short disintegration times resulted in small $t_{90\%}$ -values, was detected for MCC 102 formulations. All other formulations did not correlate with the findings of disintegration time. The use of disintegration test to predict dissolution behaviour was already criticized above, but these findings here fully reject this method.

UICEL S and UICEL B were the only substances that showed fastest dissolution at a drug load of 10%, 50% was not significantly slower but $t_{90\%}$ increased with increasing drug load. Formulations with MCC 102, Type I, and Type II, however, showed smallest $t_{90\%}$ at a drug load of 50%.

This effect could be explained by the percolation theory considering binary mixtures of the poor wettable proquazone and the well wettable cellulose. At a drug load of 10%(m/m) proquazone is not percolating and can be considered as fully embedded in a percolating matrix of cellulose, i.e. drug-in-excipient or (D/E). In that case, dissolution is fully controlled by the cellulose. On the other side, at a drug load of 90% proquazone is percolating and the non-percolating cellulose is embedded in a matrix of proquazone, i.e. excipient-in-drug or (E/D). Cellulose can therefore no longer act as a disintegrant; this was also shown by the decreased water uptake rates of these formulations (Figure 52). Between these extrema both systems are percolating; cellulose can now ideally act as a disintegrant and promotes wetting of proquazone, this on the other hand goes freely into solution.

The fast dissolution of UICEL S and B and the similar $t_{90\%}$ values between 10% and 50% drug load could be referred to their good disintegrant properties. One could expect that these formulations follow first order kinetics.

RESULTS AND DISCUSSION

To study the influence of the disintegrant tablets of pure proquazone were compressed according to the method for ternary mixtures (Chapter 4.3.4), dissolution was performed, and $t_{90\%}$ was calculated ($2188.76 \text{ min} \pm 1087.10$). Compared to this value it was evident that a load of 10% disintegrant reduced $t_{90\%}$ distinctively, even MCC 102 was increasing dissolution rate.

In general, it could be said that dissolution profiles fitted very well to the first order release model. The coefficients of determination r^2 were mostly above 0.9900; profiles with a lower value are plotted in Figure 70.

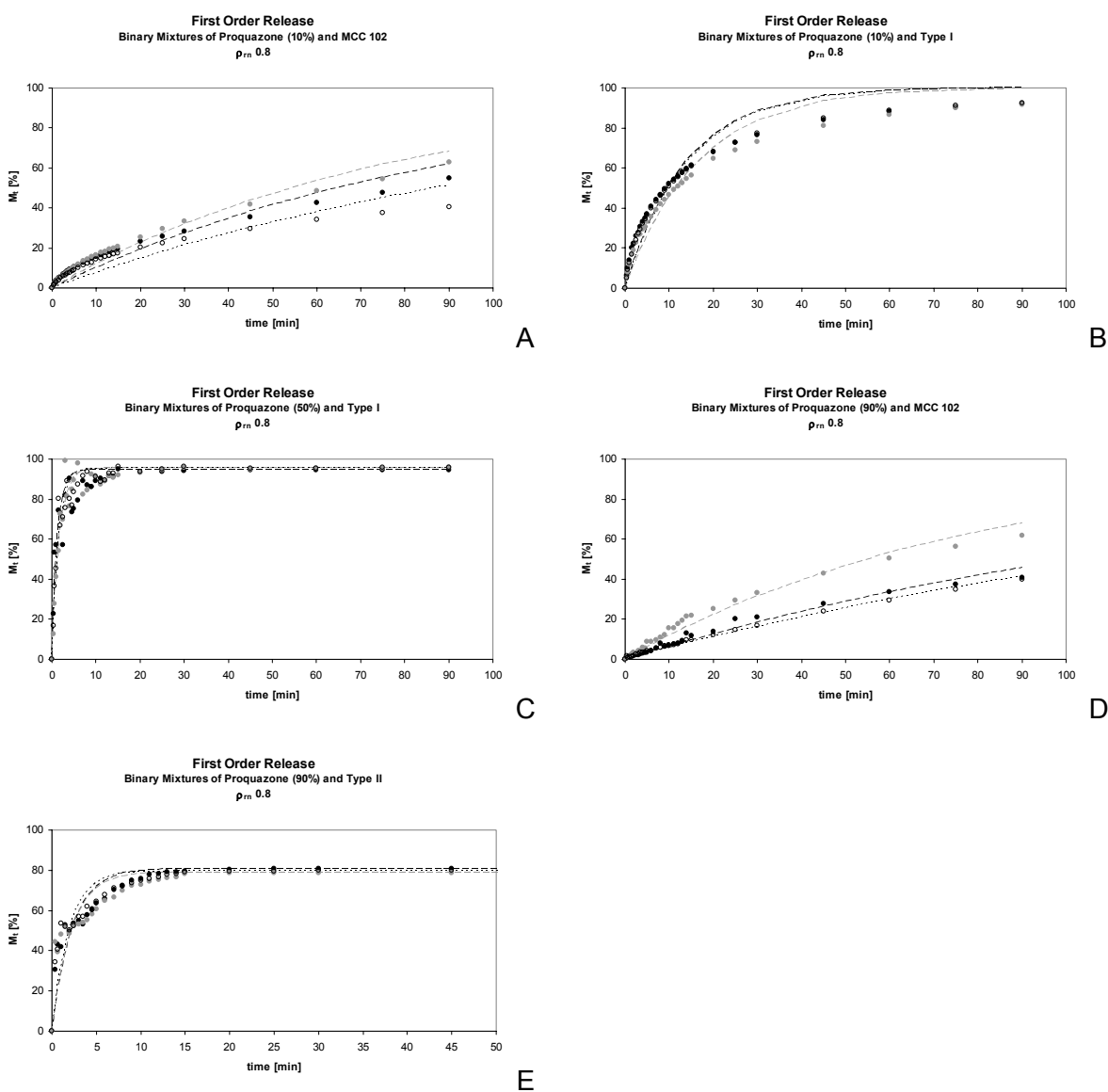


Figure 70: Experimental and fitted data according to the modified Noyes-Whitney equation for profiles with $r^2 < 0.9900$, binary mixtures of proquazone and cellulose at different drug loads; (A, D) MCC 102, (B, C) Type I, and (E) Type II. Legend: Experimental (dots) and fitted values (lines) for Run 1 (◆, —), 2 (◆, - - -) and 3 (○, ·····).

The profiles of binary mixtures with 10% drug load and Type I (B) or MCC 102 (A) were already discussed before (Figure 64). They were considered to follow Higuchi kinetics (Figure 66). The lower coefficients of determination of the profiles in picture (C) were related to the scattering of data points due to sampling problems. These profiles were considered to follow first order kinetics and were not studied more in detail. The clear deviation of MCC 102 binary mixtures with a drug load of 90% (D) from first order release required further investigations, especially with respect to Higuchi kinetics. The profiles of 90% proquazone and 10% Type II (E) showed a deviation from first order kinetics with a very fast initial increase and the reduced dissolution rate, fitting to the Higuchi model was advised.

Table 44 lists all dissolution rates k_1 derived from fitting to first order model, independent of the suitability of the model.

Table 44: Dissolution rate k_1 [min^{-1}] of proquazone – cellulose binary mixtures at different drug loads, incl. standard deviations in brackets.

	10%	50%	90%
MCC 102	0.011 (0.002)	0.090 (0.009)	0.008 (0.004)
Type I	0.068 (0.006)	0.667 (0.103)	0.021 (0.002)
UICEL S	3.964 (0.801)	2.326 (0.257)	0.271 (0.014)
Type II	0.467 (0.030)	2.816 (0.376)	0.474 (0.043)
UICEL B	5.145 (0.825)	2.508 (0.529)	0.166 (0.014)

Since the model seemed mostly appropriate to describe dissolution profiles, statistical analysis was performed on k_1 values; poor fitting of the above shown dissolution profiles was taken into consideration for the assessment. MCC 102, Type I, and Type II showed all a significantly faster dissolution rate at a drug load of 50%, but no difference between 10% and 90% drug load. This was in good agreement with the dissolution profiles given in Figure 67. Formulations containing UICEL-A/102 (S and B) showed a significant decrease of the dissolution rate with increasing drug load. To prove the linearity the decrease of dissolution rate k_1 was plotted against the drug load and linear regression was applied.

RESULTS AND DISCUSSION

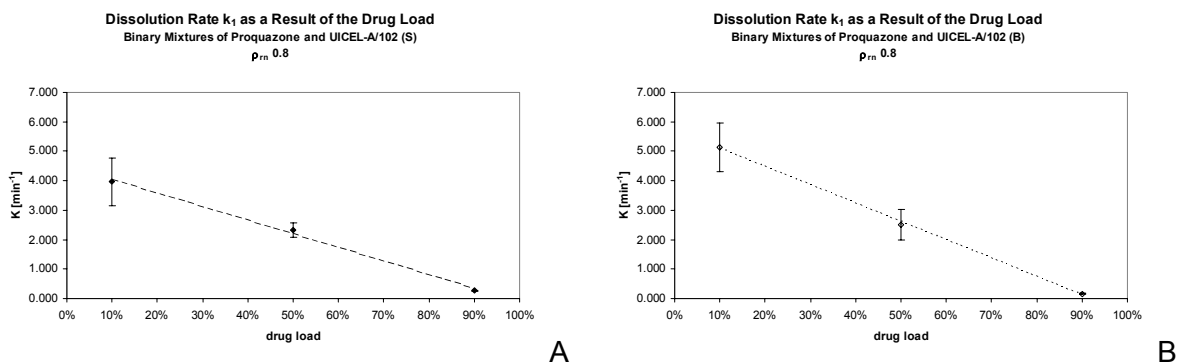


Figure 71: Proof of linearity between k_1 and drug load for binary mixtures of proquazone and UICEL S (A) and UICEL B (B), respectively.

A clear linear relationship could be detected for UICEL S ($-4.6170x$; $r^2 = 0.9958$) and UICEL B ($-6.2238x$; $r^2 = 0.9988$). At 10% drug load, UICEL B was significantly faster than UICEL S whereas at 50% drug load no difference was found. This resulted in a steeper slope for UICEL B. The comparison between both UICEL-A/102 samples was interesting since visually no differences were detectable at 10% drug load. Assessing $M_{30 \text{ min}}$ and $t_{90\%}$ both profiles were equal ($p = 1.000$). First order kinetics seemed to be very sensitive on small differences.

Before studying the dissolution profiles with Higuchi, all data sets, independent of the suitability of the first order kinetics, were studied with the Hixson-Crowell law. The results are listed in Table 45. Average dissolution profiles with a minimal amount of four data points below 85% M_t were included, in case of 90% proquazone and Type II, the plateau was reached below 85% due to drug loss during production. To make the evaluation possible, 85% of the plateau was selected to calculate k_2 .

Table 45: Dissolution rate k_2 [%^{1/3}·min⁻¹] of proquazone – cellulose binary mixtures at different drug loads, incl. r^2 in brackets.

	10%	50%	90%
MCC 102	0.0110 (0.9637)	0.1007 (0.9917)	0.0104 (0.9811)
Type I	0.0479 (0.9063)	0.4577 (0.7453)	0.0245 (0.9747)
UICEL S	n/a (n=3)	n/a (n=3)	0.2112 (0.9417)
Type II	0.3127 (0.9202)	n/a (n=3)	0.2223 (0.7733)
UICEL B	n/a (n=2)	n/a (n=3)	0.0263 (0.9724)

For MCC 102 and Type I, the maximum dissolution rate k_2 was, as expected, at 50% drug load, 10% was faster than 90%. For UICEL S and UICEL B, evaluation was possible only for 90% drug load due to the lack of data points. Type II showed a faster dissolution rate k_2 at 10% compared to 90%, 50% was not evaluated. In general, it could be said that the coefficient of determination was lower than for first order kinetic. Figure 72 shows the experimental data and fitted values according to the cubic root law. A detailed discussion of the curves with 10% drug load (A) was already given above in Figure 65. 50% drug load (B) was appropriately described by the model, MCC 102 with a coefficient of determination of 0.9917 and Type II still with 0.7453. The poorer correlation could be referred to wide distribution of the data points as described by the first order model. In case of 50% drug load, where Hixson-Crowell seemed the appropriate model, tablets did not really disintegrate into smaller particles, but the size of the tablet was reduced geometrically. This is one of the pre-requisite for the application of the cubic root law. All formulations with 90% drug load (C) were appropriately fitted to the cubic root law; only Type II which already needed a special treatment resulted in a coefficient of determination smaller than 0.9000.

RESULTS AND DISCUSSION

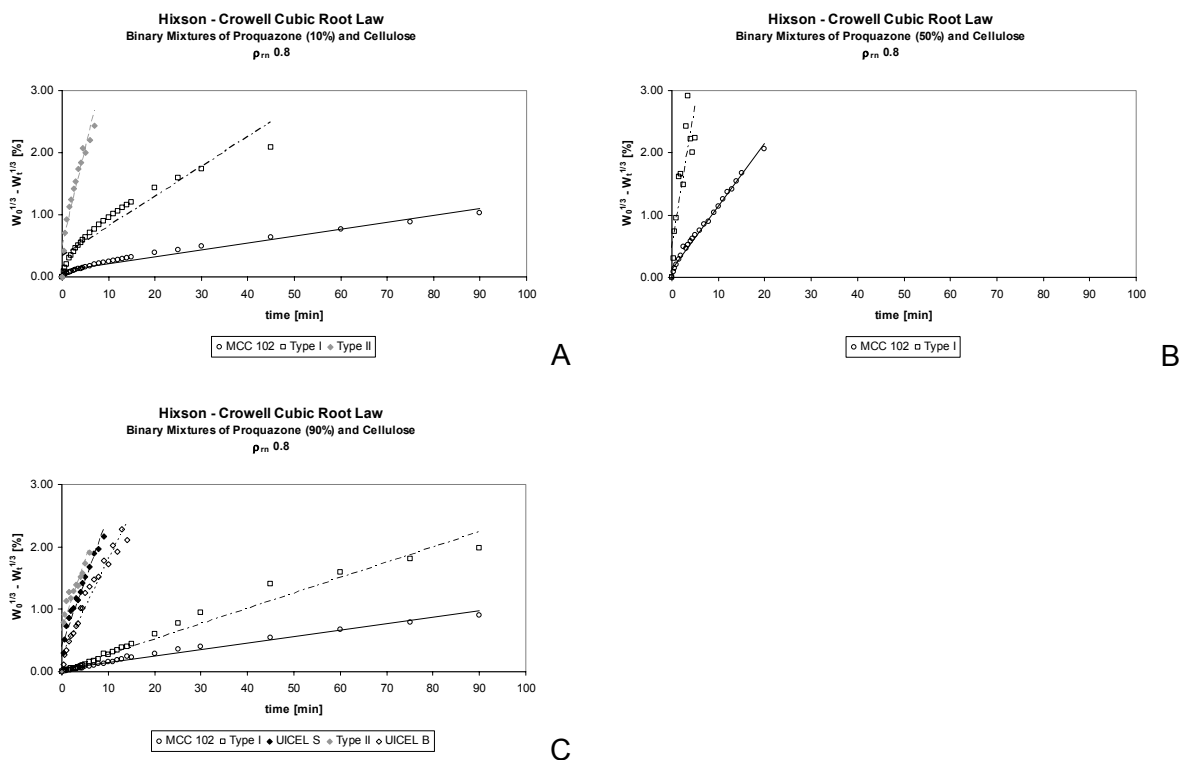


Figure 72: Experimental and fitted data according to the Hixson-Crowell equation for binary mixtures at different drug loads; (A) 10%, (B) 50%, and (C) 90%.

Legend: Experimental (dots) and fitted values (lines) for MCC 102 (○, —), Type I (□, - - - -), UICEL S (◆, - - - -), Type II (◇, - - - -), and UICEL B (◇, ······).

The Higuchi model was applied on those formulations which did not fit to first order kinetics, i.e. MCC 102 10% and 90% and Type II 90%. To evaluate the dissolution behaviour of all those formulations that did not meet the requirements for rapidly dissolving IR formulations (Figure 68), formulations with Type I 10% and 90% were included too.

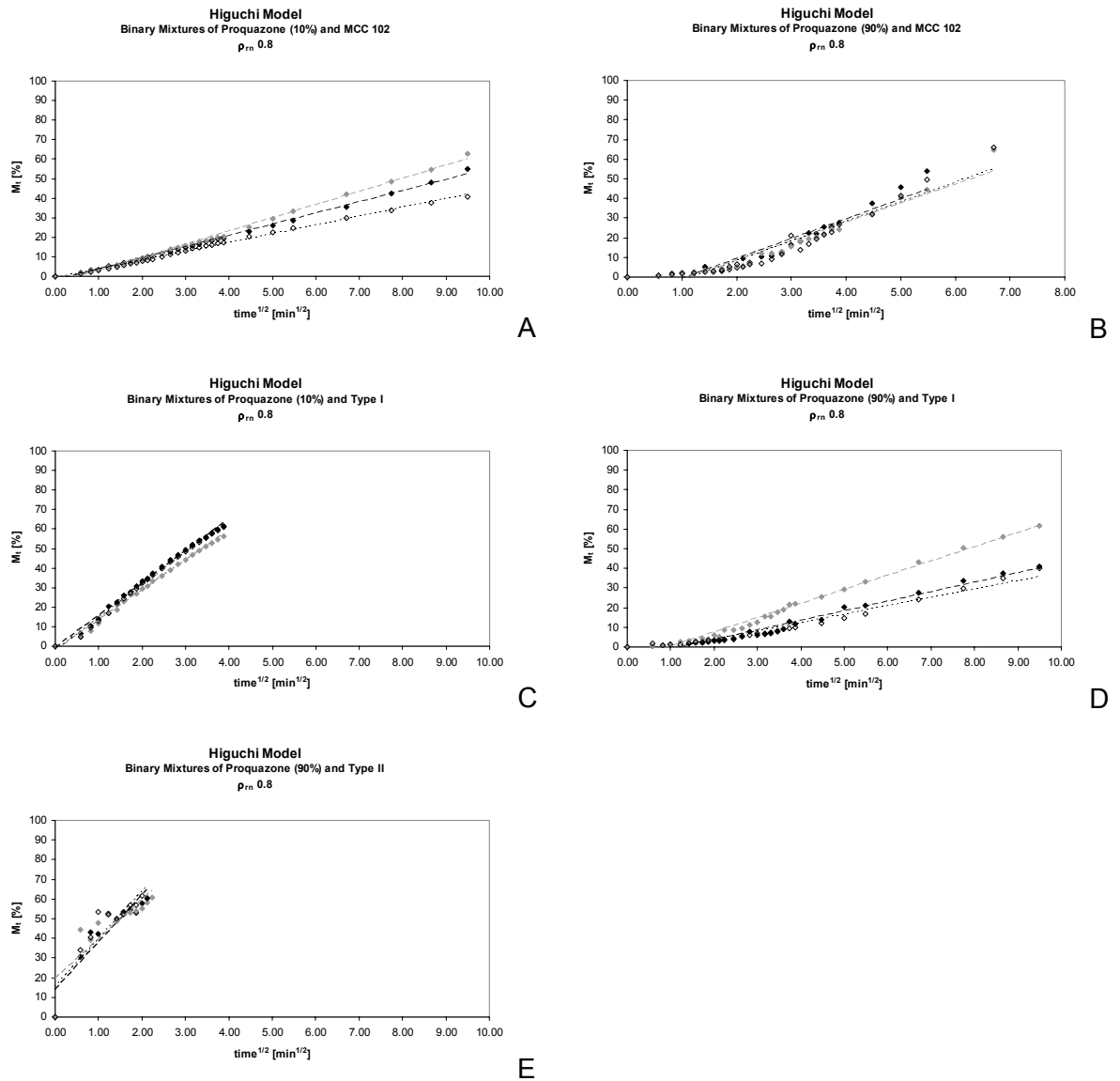


Figure 73: Experimental and fitted data according to the Higuchi equation for binary mixtures of proquazone and MCC 102 (A, C), Type I (B, D), or Type II (E) at different drug loads.

Legend: Experimental (dots) and fitted values (lines) for Run 1 (◇,), Run 2 (◆, ----), and Run 3 (◆, ----).

Transformation of time to its square root should result in a linear increase up to 60%, when the release follows Higuchi kinetics. From the investigated formulations, only two, proquazone (10%) and MCC 102 (A) and proquazone (10%) and Type I (C), followed Higuchi kinetics; they were already discussed in chapter 5.2.3.1. 90% drug load, independent of the filler, did not follow this model, since release was constant from beginning (compare Figure 67). Higuchi could not be expected, because the poorly soluble proquazone is the dominating component, for a matrix release, the drug has to be

RESULTS AND DISCUSSION

embedded in a non-soluble matrix, e.g. cellulose. The best model to describe those release profiles seemed to be Hixson-Crowell. To describe the dissolution profiles of 90% proquazone and Type II (E), Weibull was the most suitable model, but one has to keep in mind that two parameters, a and b , can be used to adjust the curve. Weibull is therefore not comparable to the other models, where only one parameter, the dissolution rate k , is fitted. For this formulation, first order kinetics was the most suitable method to describe the curve.

An explanation for the observed reduction of dissolution rate could be the exceeding of sink conditions. Noyes-Whitney equation is only applicable under sink conditions, i.e. 10% of the maximum solubility. [80] Solubility of proquazone after 90 minutes was 1.11 g/l (see Table 16, page 53). Sink conditions were therefore exceeded when more than 0.111 g/l were dissolved, this was the case at 50% and 90% drug load. Using dissolution rate k_1 (Table 44), a tablet weight of 300 mg, and a volume of 1l, sink conditions were calculated using the modified Noyes-Whitney equation (Equation 24), the results are given in Table 46.

Table 46: Time t in minutes to dissolve 0.111 g/l.

	50%	90%
MCC 102	15.36	62.78
Type I	2.06	25.92
UICEL S	0.59	1.97
Type II	0.49	1.13
UICEL B	0.55	3.22

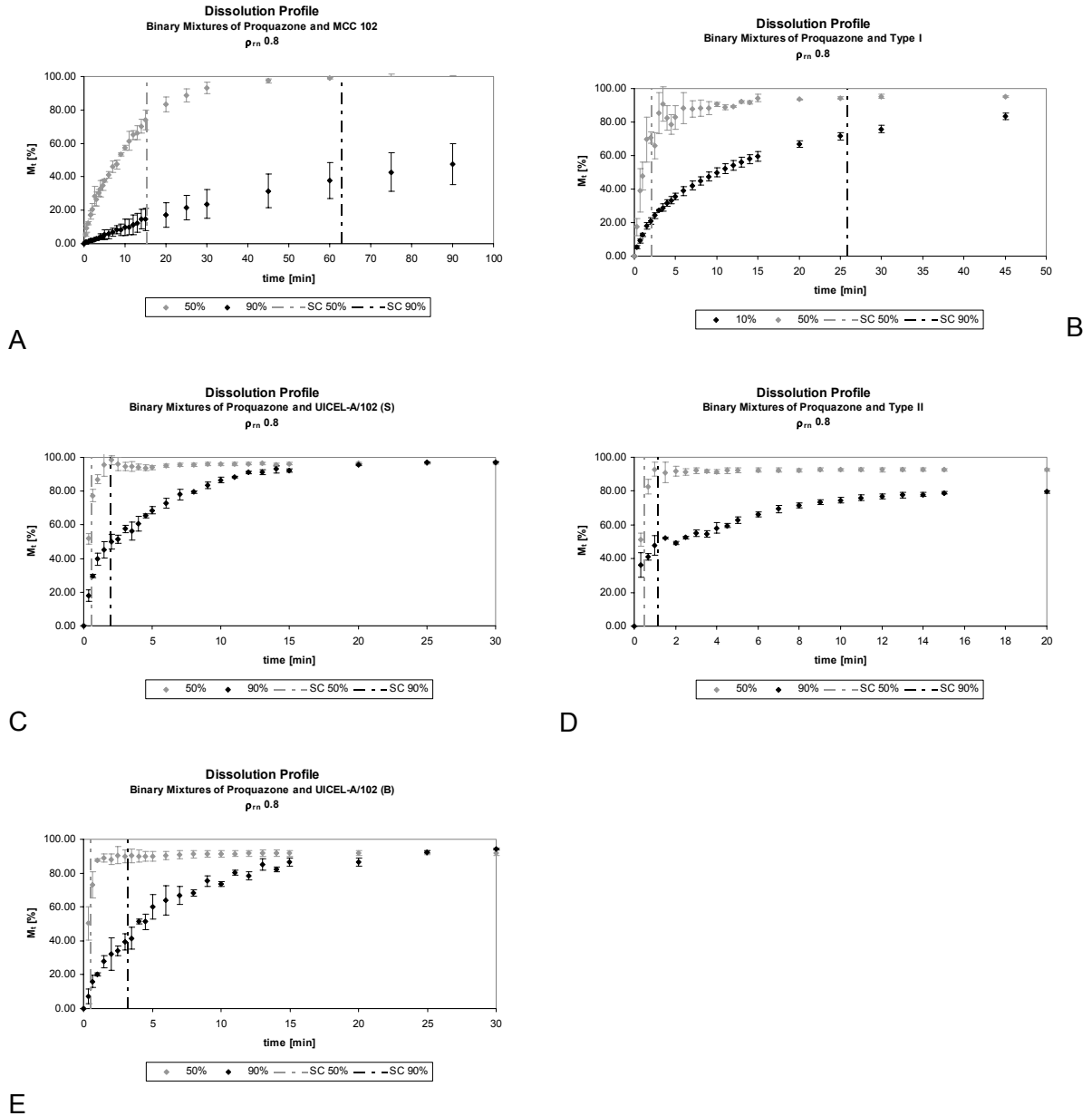


Figure 74: Dissolution profiles of proquazone – cellulose binary mixtures at 50% and 90% drug load, including the time (vertical line) when sink conditions were exceeded; (A) MCC 102, (B) Type I, (C) UICEL S, (D) Type II, and (E) UICEL B.

Table 46 lists the time required to reach the sink conditions limit; with the theoretical drug load and the tablet weight of 300 mg, the corresponding M_t was 74.7% for 50% formulations and 41.3% for 90% formulations. To prove the calculations above, M_t was qualitatively compared at the sink condition limit. All formulations, except 90% proquazone and Type I (Figure 74 B), agreed with the calculation.

RESULTS AND DISCUSSION

Sink conditions of 50% drug load formulations were exceeded very fast, in case of class 3 substances (Figure 74 C, D, and E) in less than one minute. In case where only two data points were available, no proper assessment was possible. But also formulations with MCC 102 (A) and Type I (B) which included more data points under sink conditions were difficult to weigh up, because profiles almost reached the plateau. The decreased dissolution rate could also be influenced by ending drug release. This problem could be neglected for 90% drug load formulations. MCC 102 (A) was very slow; only two points above sink conditions were measured, therefore it was difficult to see the influence. UICEL S (C), Type II (D), and UICEL B (E) showed a reduction of the dissolution rate after sink conditions, this is in good agreement with the theory. Type I (B) showed a different pattern. As mentioned above, the calculated limit was in general approximately 40%. The accumulated drug release at the time when the sink conditions were exceeded was approximately 70% for Type I 90%. This corresponded more to the release of the 50% drug load formulation. Regarding the dissolution profile, one could clearly see that the dissolution rate changed at approximately five minutes, which corresponds to M_t of approximately 40%. From the qualitative analysis, the influence of the sink conditions was indeed found for all formulations with 90% drug load.

5.2.3.3 Influence of the Load of Modified Cellulose

After studying influences of relative density and drug load on the dissolution profiles of binary mixtures, the influence of the disintegrant was studied in ternary mixtures. Proquazone was kept constant as a marker; the amount of modified cellulose was increased gradually, MCC 102 was used as filler. Dissolution profiles are given in Figure 75. Standard deviations were removed for better clarity when the relative standard deviations were less than 5% after five minutes.

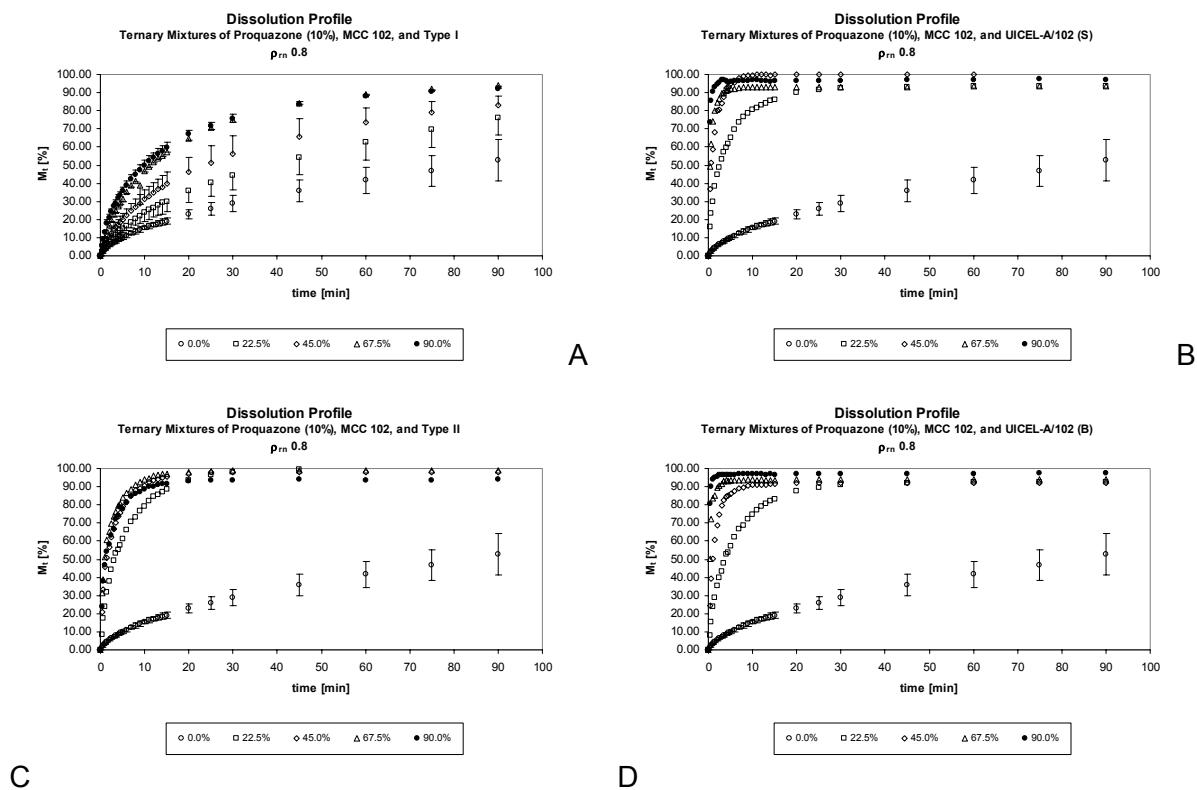


Figure 75: Dissolution profiles of ternary mixtures; (A) Type I, (B) UICEL S, (C) Type II, and (D) UICEL B.

Before dissolution profiles of ternary mixtures were evaluated with different models as known from prior experiments, they were assessed qualitatively. None of the ternary mixtures with Type I as disintegrant (A) reached the plateau within 90 minutes. Dissolution rate was increased with an increased disintegrant load up to 67.5%. UICEL S ternary mixtures (B) were clearly faster than those with Type I; all formulation with UICEL S reached the plateau easily. A load of more than 45% UICEL S did not clearly influence the profile anymore. The same was observed also for both other class 3 substances Type II (C) and UICEL B (D).

To study the quantitative differences between formulations, the same model independent and model dependent approaches were applied on the profiles as discussed before. At the beginning $M_{30\text{ min}}$ values and the suitability as rapidly dissolving immediate release formulations were assessed.

RESULTS AND DISCUSSION

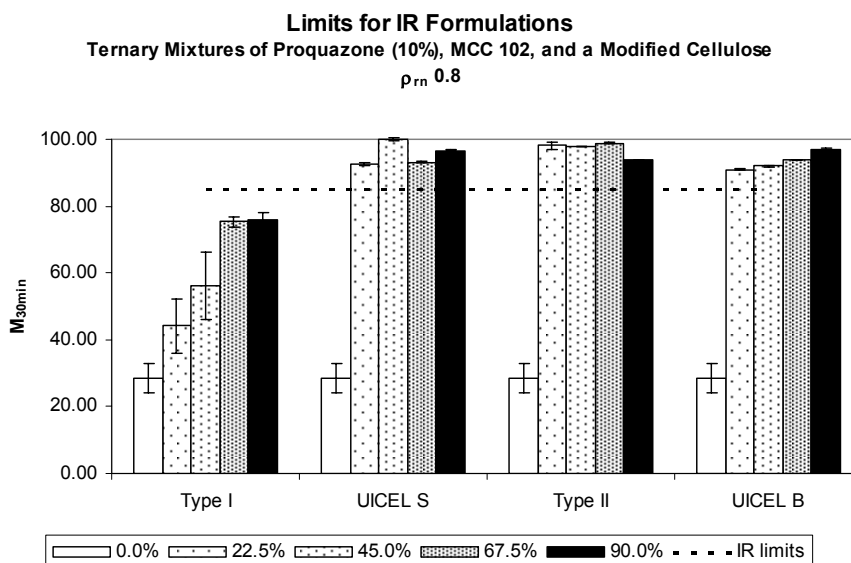


Figure 76: $M_{30 \text{ min}}$ and IR limits for ternary mixtures with proquazone (10%), MCC 102, and modified cellulose.

As expected, Type I formulations were not suitable for rapid drug release. From binary mixtures it was known that even the highest load of disintegrant (90%) was not sufficient to release 85% of the labelled drug amount within 30 minutes. However, binary mixtures with class 3 substances were suitable for rapidly dissolving IR formulations. As shown in Figure 76, even with a low amount of 22.5% disintegrant load, dissolution was very efficient and all formulations met the requirements. Studying $M_{30 \text{ min}}$ values, a significant increase of the release rate ($p = 0.000$) was found for UICEL S, Type II, and UICEL B. UICEL S and Type II formulations with a minimal load of 22.5% were similar compared to 90%. UICEL B showed similarity after a minimal load of 45% and Type I after 67.5%. Comparing the disintegrants at different loads, one could see that class 2 formulations were slower than class 3 formulations. All those findings agreed with the dissolution profiles of Figure 75.

Difference factor f_1 and similarity factor f_2 were used to prove similarity between dissolution profiles compared to 90% load of modified cellulose. When f_1 was smaller than 15 and / or f_2 was larger than 50, the curves were considered similar. Similarity is important since a maximum possible amount of MCC 102 should be included to increase mechanical resistance of the tablets. Figure 77 shows f_1 (A) and f_2 (B) and the corresponding limits.

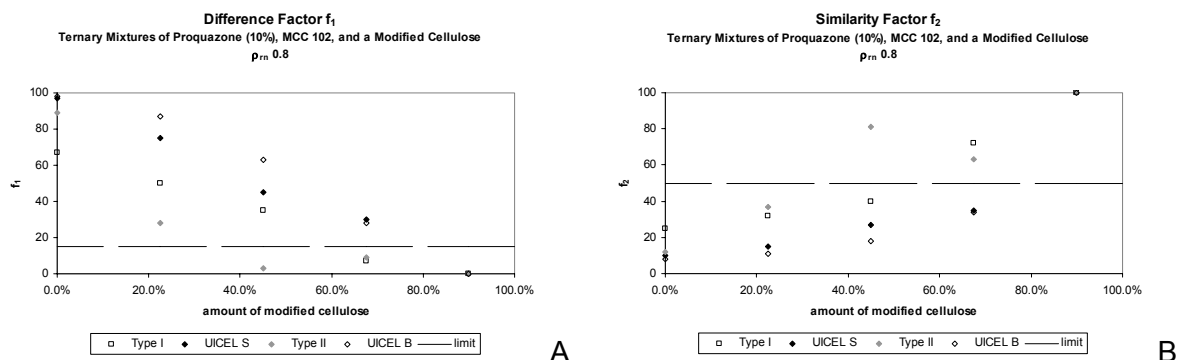


Figure 77: Difference factor (f_1) and similarity factor (f_2) for ternary mixtures, reference formulation with 90% load of modified cellulose.

No difference between difference factor and similarity factor was found. The similarity of Type I formulations with 67.5% compared to 90% load was confirmed by difference factor and similarity factor. In case of Type II formulations, these models were stricter, no similarity was found between 22.5% and 90% load. Interestingly in case of UICEL-A/102 formulations, difference and similarity factor found no similarity, even though qualitatively and with the evaluation of $M_{30 \text{ min}}$ values, similarity was found after 45% load of modified cellulose. This discrepancy can be explained by the small number of data included in the evaluation. For UICEL S and UICEL B only three data points were available including zero, whereas EMEA demands minimally three data points without zero. [83] One could say that difference factor and similarity factor are not a suitable to study similarity between profiles, but one has to keep in mind, that these models are not required when 85% of the drug is dissolved in less than 15 minutes.

To study the dissolution endpoint and to correlate dissolution with disintegration, $t_{90\%}$ was calculated using Weibull parameters. Average $t_{90\%}$ and standard deviations are listed in Table 47. Weibull seemed again to be appropriate to describe release profiles. 78.4% of all fits showed a coefficient of determination equal or greater than 0.9995. The minimum was 0.9962, which could be related to a clear outlier.

Dissolution was faster with an increased load of modified cellulose. No significant difference was found for $t_{90\%}$ of every substance after 22.5% drug load compared to 90%. Comparing the different disintegrants, Type I was always significantly slower than Class 3 substances, which were in general similar, with an exception at 67.5% disintegrant load where Type II was significantly slower compared to UICEL-A/102.

RESULTS AND DISCUSSION

Table 47: Average $t_{90\%}$ -values [min] of ternary mixtures, incl. standard deviations in brackets.

	Type I	UICEL S	Type II	UICEL B
0%	626.90 (411.13)	626.90 (411.13)	626.90 (411.13)	626.90 (411.13)
22.5%	201.39 (100.63)	12.86 (1.06)	16.53 (2.70)	15.07 (0.97)
45%	131.30 (51.30)	3.91 (0.11)	8.29 (0.56)	3.77 (0.34)
67.5%	60.06 (2.1)	1.95 (0.18)	7.10 (1.19)	1.26 (0.21)
90%	64.23 (6.18)	0.78 (0.17)	7.30 (0.38)	0.53 (0.10)

As already seen in chapter 5.2.3.1, $t_{90\%}$ can be used to study the correlation between disintegration time and dissolution rate. From Figure 58 it is known that a critical amount of modified cellulose less than 22.5% (m/m) reduced disintegration time significantly. To avoid distortion due to this critical amount, only formulations with minimally 22.5% modified cellulose were included.

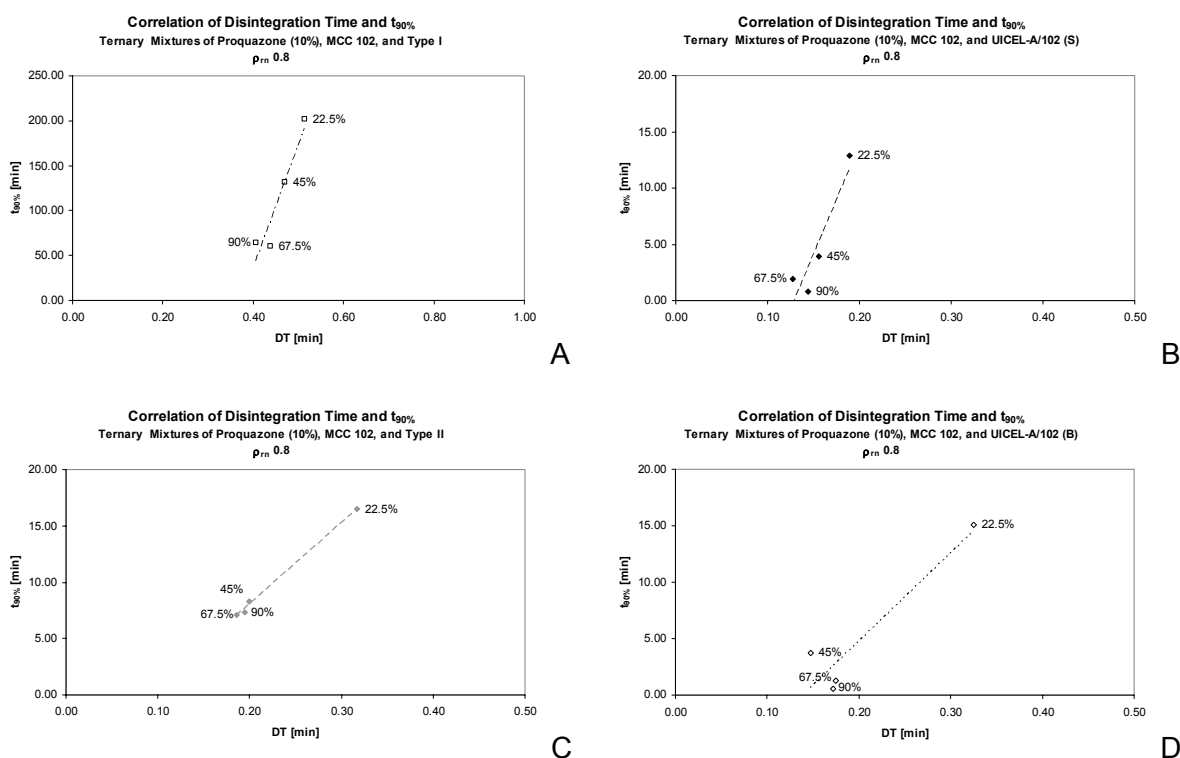


Figure 78: Correlation between disintegration time and $t_{90\%}$ as a result of the load of modified cellulose in ternary mixtures; (A) Type I, (B) UICEL S, (C) Type II, and (D) UICEL B.

Table 48: Slopes and coefficients of determination of the correlation between disintegration time and $t_{90\%}$ as a result of the modified cellulose load.

	Slope	r^2
Type I	1376.5	0.8964
UICEL S	196.58	0.8580
Type II	72.855	0.9970
UICEL B	78.022	0.8777

Neither disintegration time nor $t_{90\%}$ showed significant differences after 22.5% load of modified cellulose. A clear correlation between modified cellulose load, disintegration time, and dissolution rate was therefore not expected. Nevertheless, a correlation between disintegration time and dissolution rate could be discovered. All disintegrant types showed decrease of disintegration time and $t_{90\%}$ with increasing load (Figure 78); the accumulation of data points at higher disintegrant loads could be related to the small differences between these formulations which were confirmed by the similar dissolution profiles found in Figure 75. As already explained in chapter 5.2.3.1, the slope can be used to study release properties. A steep slope is related to a hindered solubilization of the drug, either due to poor solubility or to physical hindrance by the formulation. A gentle slope is related to good release properties since the drug is immediately dissolved. Studying the slopes of these correlations, poor disintegrant properties were found for Type I, whereas Type II and UICEL B showed an almost 20 times reduced slope. UICEL S, surprisingly, showed a steeper slope which was reduced only 7 times compared to Type I. This assessment was indeed supported in binary mixtures at different relative densities; in ternary mixtures it was not suitable to describe disintegrant properties. Similarity of disintegration times and $t_{90\%}$ of the formulations reduced the discriminative power of the model. Differences between dissolution profiles have therefore be to study with further models.

In summary can be said that fully modified celluloses showed improved disintegrant properties compared to the partially converted cellulose. The good release properties of Type II can be related to the fibrous structure that promotes water uptake and therefore solubilization.

RESULTS AND DISCUSSION

To confirm the critical amount of modified cellulose for fast disintegration as shown in Figure 59, $t_{90\%}$ was calculated for formulations with a smaller load of Type II. Figure 79 shows $t_{90\%}$ as a result of the load of modified cellulose in % (v/v).

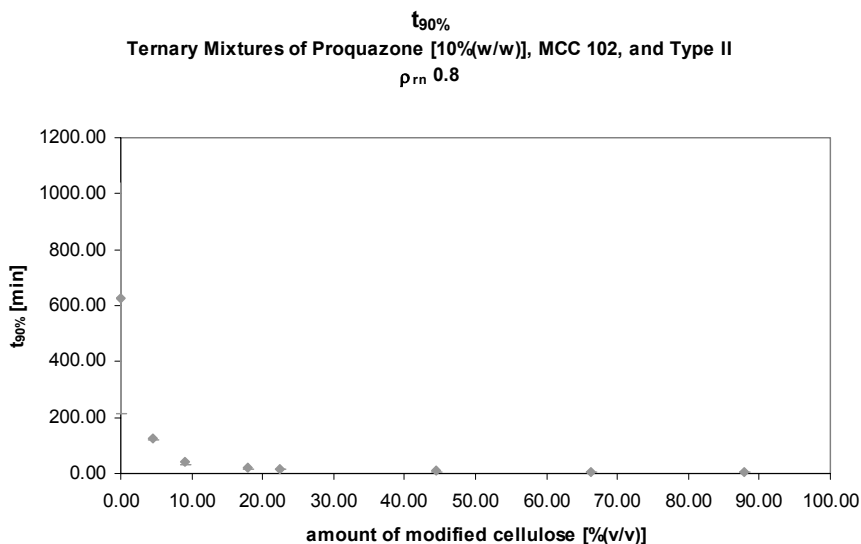


Figure 79: $t_{90\%}$ of ternary mixtures of proquazone, MCC 102, and Type II as result of the amount of modified cellulose.

Statistical analysis of $t_{90\%}$ values confirmed the critical amount between 0% (v/v) and 4.49% (v/v) which was already found in disintegration experiments. Increased disintegrant load did not significantly reduce $t_{90\%}$ anymore.

Form earlier discussions, it is known that first order model is very sensitive to detect differences. All dissolution profiles were therefore fitted to the modified Noyes-Whitney equation. First order kinetics were appropriate for UICEL S, Type II, and UICEL B formulations; the coefficient of determination was always greater than 0.9900. Type I formulations resulted, as expected from binary mixtures, in poorer results. The average dissolution rates k_1 with standard deviations are listed Table 49.

Table 49: Dissolution rate k_1 [min^{-1}] of ternary mixtures with proquazone (10%), MCC 102, and a modified cellulose.

	Type I	UICEL S	Type II	UICEL B
0%	0.011 (0.002)	0.011 (0.002)	0.011 (0.002)	0.011 (0.002)
22.5%	0.021 (0.005)	0.252 (0.014)	0.186 (0.026)	0.191 (0.013)
45%	0.032 (0.008)	0.790 (0.040)	0.396 (0.047)	0.717 (0.041)
67.5%	0.060 (0.002)	1.659 (0.129)	0.514 (0.088)	2.167 (0.167)
90%	0.068 (0.006)	3.964 (0.801)	0.467 (0.030)	5.145 (0.825)

At a load of 22.5% modified cellulose, UICEL S was significantly faster than Type II and UICEL B which again were significantly faster than Type I. At a load of 45% modified cellulose, both UICEL-A/102 were significantly faster than Type II and Type I. At a level of 67.5% all dissolution rates were significantly different. At a modified cellulose load of 90% two significantly different groups were found, the faster UICEL-A/102 substances and the slower SANAQrapid celluloses. This clear difference was not expected, but from Figure 75 it was possible to see that dissolution of SANAQrapid celluloses were slower than UICEL-A/102. However, it was surprising that no difference between Type I and Type II was found. This is contradictory to the $t_{90\%}$ results where a difference was found with $p = 0.000$. A significant increase of the dissolution rate between 0% and 22.5% load of modified cellulose was found only for Type II formulations. Compared to 90% modified cellulose load, no difference was found for Type I (67.5%) and Type II (45% and 67.5%). This is in good agreement with the results of difference factor and similarity factor as well as $M_{30 \text{ min}}$ values and $t_{90\%}$. UICEL S and UICEL B formulations with 90% modified cellulose load were significantly faster than all other formulations. This confirms the results of difference factor and similarity factor, where no similarity was found, but is contradictory to the findings of $M_{30 \text{ min}}$ and $t_{90\%}$.

As mentioned, UICEL S, Type II, and UICEL B showed coefficients of determination above 0.9900. Formulations with a lower value are given in Figure 80. Formulations with a Type I load of 67.5% or above showed coefficients of determination above 0.9800. The coefficient of determination decreased with decreased amount of Type I. Following formulations were already discussed above and are therefore not discussed anymore: proquazone (10%) and

RESULTS AND DISCUSSION

MCC 102 (90%) in Figure 64 B and Figure 70 A and proquazone (10%) and Type I (90%) in Figure 70 B.

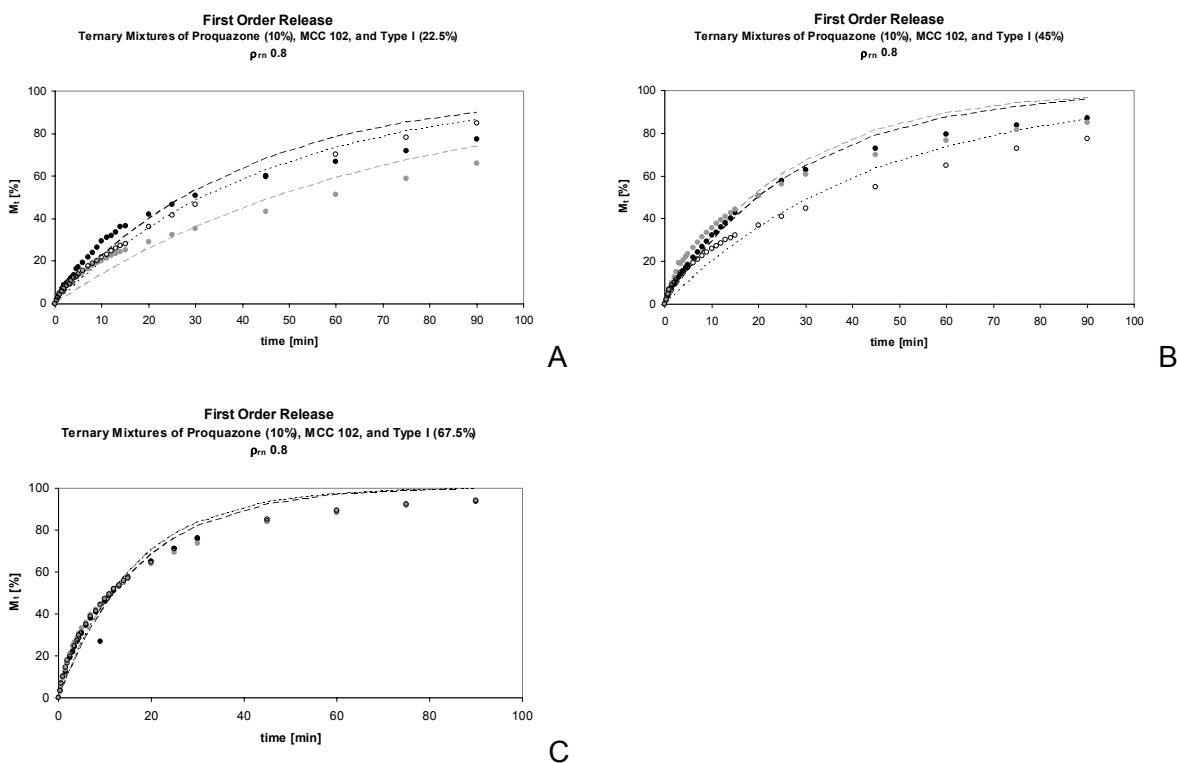


Figure 80: Experimental and fitted data according to the modified Noyes-Whitney equation for profiles with $r^2 < 0.9900$.

Legend: Experimental (dots) and fitted values (lines) for Run 1 (◆, - - - -), Run 2 (◆,) and Run 3 (◇,

Tablets with 22.5% Type I did not show a robust drug release since the profiles differed very much. However, an initially faster release compared to proquazone (10%) – MCC 102 binary mixtures (Figure 64 B) was detected. From the latter formulation it was known that Higuchi was appropriate to describe the curve, further investigations with regard to this model are applied later. For tablets with 45% modified cellulose load (Figure 80 B) still differences between the three profiles were found, whereas after 67.5% (Figure 80 C) the release was robust. The poor fitting of the latter formulation could be explained by the implementation. In case of the plateau was reached ($M_{90 \text{ min}} - M_{75 \text{ min}} < 1$), the accumulated amount at 90 minutes was selected as the endpoint. When the difference was greater than 1, the endpoint was assumed to be 100, which corresponds to the calculated drug load. In case (C) the difference was 1.78 and the plateau was therefore considered as not yet

reached. This limit of 1 was selected arbitrarily and was maybe too rigorous in this case. Fitting to $M_{90\ min}$ would have resulted in a higher coefficient of determination (r^2 : 0.9925, 0.9924, and 0.9950). The same could be expected for 90% and 45% modified cellulose load, even though the latter showed a difference of 3.93, which was considered as ongoing release. Due to the initially increased release rate of 45% Type I (B, Run 3) evaluation with the Higuchi model was anyway supposed.

Before the above mentioned profiles were fitted to the Higuchi model, all release profiles were fitted to the Hixson-Crowell cubic root law. The release rates are listed in Table 50.

Table 50: Dissolution rate k_2 [%^{1/3}·min⁻¹] of ternary mixtures, incl. r^2 in brackets.

	Type I	UICEL S	Type II	UICEL B
0%	0.0110 (0.9637)	0.0110 (0.9637)	0.0110 (0.9637)	0.0110 (0.9637)
22.5%	0.0193 (0.9702)	0.1729 (0.9392)	0.1659 (0.9560)	0.1540 (0.9637)
45%	0.0235 (0.9467)	0.6507 (0.9134)	0.3226 (0.9337)	0.6168 (0.9696)
67.5%	0.0496 (0.9343)	1.1515 (0.9060)	0.3733 (0.9143)	1.1515 (0.9060)
90%	0.0479 (0.9063)	n/a (n=2)	0.3127 (0.9202)	n/a (n=2)

From the coefficients of determination in brackets it was evident that those dissolution profiles did not fit to the cubic root law. Linearity was not found at the beginning where the release rate seemed faster than at the later stage. The release profiles and the corresponding fits are given in Figure 81.

RESULTS AND DISCUSSION

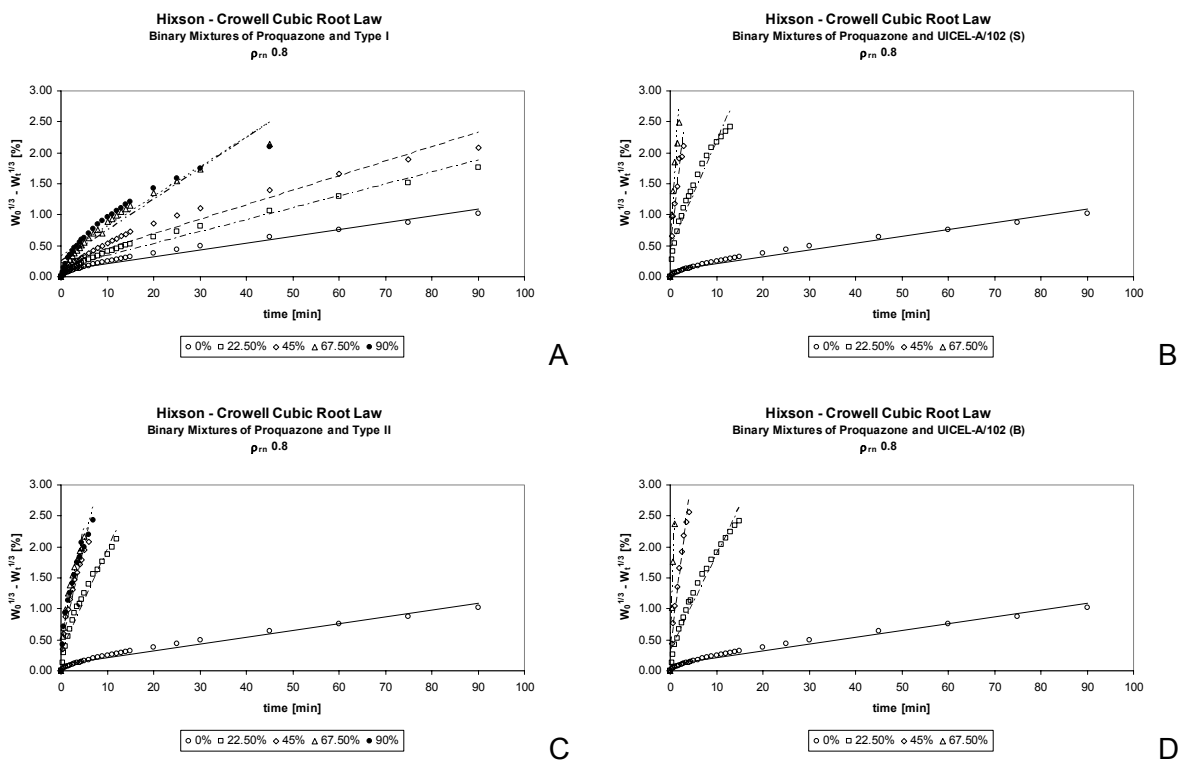


Figure 81: Experimental data (dots) and fitted values (lines) according to the Hixson-Crowell equation for ternary mixtures; (A) Type I, (B) UICEL S (C) Type II, and (D) UICEL B.

As promised above, release profiles of Type I formulations were fitted to the Higuchi model. The average dissolution rate k_3 and the coefficients of determination of every fit are given in Table 51; the profiles and the corresponding fits are shown in Figure 82. The profiles of the binary mixtures with MCC 102 and Type I are not depicted since they were already discussed above.

Table 51: Average dissolution rate k_3 , standard deviation, and coefficients of determination of every fit of ternary mixtures with proquazone, MCC 102, and Type I.

	0%	22.5%	45%	67.5%	90%
Av. k_3 [$\text{min}^{-1/2}$]	5.68	8.72	11.06	15.83	16.25
SD k_3 [$\text{min}^{-1/2}$]	1.12	1.63	2.18	0.20	0.78
r^2	0.9970	0.9877	0.9855	0.9916	0.9960
	0.9945	0.9983	0.9948	0.9633	0.9956
	0.9967	0.9840	0.9985	0.9946	0.9952

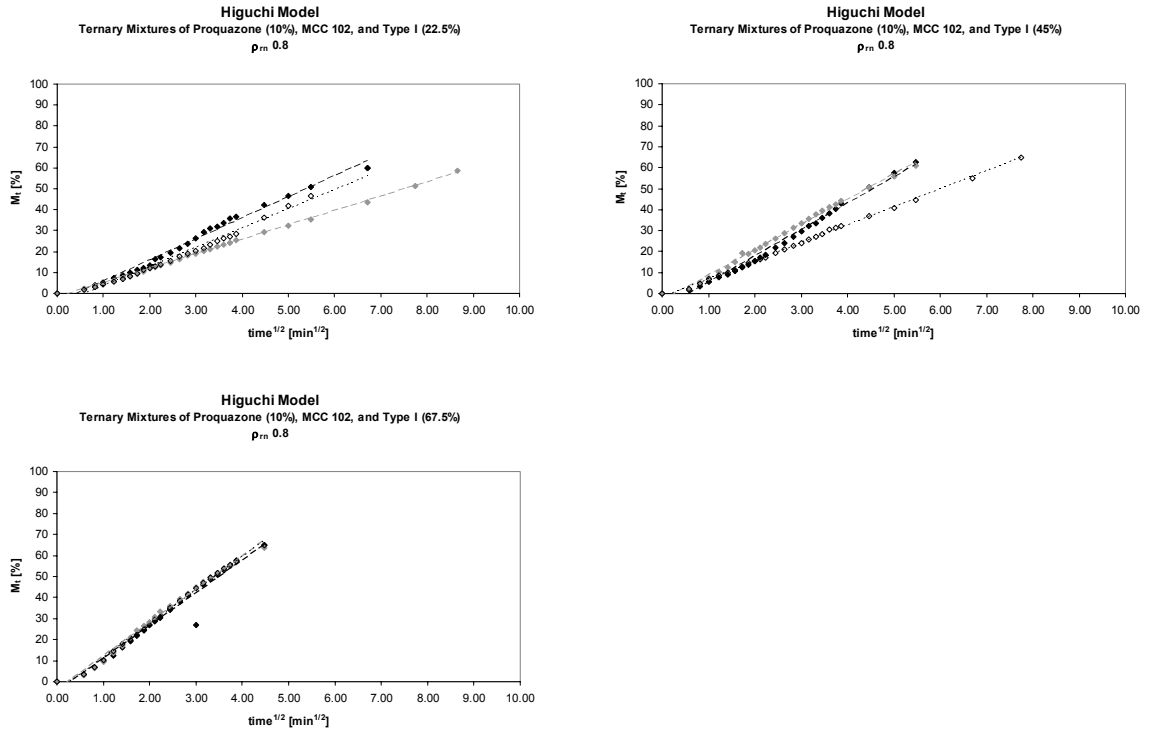


Figure 82: Experimental and fitted data according to the Higuchi equation for ternary mixtures with proquazone (10%), MCC 102, and Type I.

Legend: Experimental (dots) and fitted values (lines) for Run 1 (◇,), Run 2 (◆, ----), and Run 3 (◆, -----).

From the graphs as well as from the values it was evident that Higuchi was appropriate to describe drug release from Type I formulations. Dissolution rate increased with increasing amount of modified cellulose in the formulation. The formulation with 90% load was significantly faster, only compared to 67.5% load the difference vanished. Comparing the coefficients of determination, 0% and 90% were better described by Higuchi, all other formulations showed one run which was better described by first order kinetics. This may be a problem of the non robust formulations.

5.2.4 Dissolution Models

No clear favourite model to describe drug release was found after the evaluation of all experiments. Formulations influenced drug release; this again, influenced the suitability of every model. The next chapter is focussed now on this suitability of the models with the aim to describe advantages and disadvantages. Discussion is divided in model independent approaches and model dependent approaches.

RESULTS AND DISCUSSION

5.2.4.1 Model independent approach

Model independent approaches used in this study were IR limits proposed by the FDA [16], statistical analysis with ANOVA followed by a Tukey post hoc analysis on a significance level $\alpha = 0.05$ of $M_{30 \text{ min}}$ values, difference factor f_1 , and similarity factor f_2 .

The FDA defines a product to be rapidly dissolving when no less than 85% of the labelled amount of drug dissolves within 30 minutes under given conditions as paddle speed 50 RPM and a 900 ml of HCl 0.1 N. This definition was used to justify biowaivers for highly soluble and highly permeable drug substances. In this study, the FDA's definition was expanded to poorly soluble drugs as proquazone. Also medium volume and paddle speed were changed. The volume was increased to 1000 ml, but since all experiments with a drug load of 10% were implemented under sink conditions, the volume should not influence the result; formulations with 50% and 90% drug load exceeded sink conditions anyway. The faster paddle speed of 100 RPM had an influence on the result; details will be discussed later in chapter 5.4. Increased paddle speed increases the dissolution rate and can therefore reduce the discriminative power of the method. [101] Formulations which reached the limits by a narrow margin could fail the requirements when paddle speed is reduced. Since only one data point is required, no further information about release can be obtained.

The FDA IR limit approach is nothing else than a single-point measurement, where the accumulated amounts dissolved at 30 minutes are compared. As it was shown, disintegration time and dissolution rate do not have to correlate. Using only disintegration test in quality control without checking dissolution rate or at least its extent false positive results could be expected. In this study, this would have been the case in following formulations: 10% proquazone and MCC 102 or Type I at all three different relative densities and mixtures of those two fillers at ρ_m 0.8, as well as formulations with 90% drug load and MCC 102 or Type I at a relative density of 0.8. They all showed indeed disintegration times less than 3.50 minutes but did not meet the requirements for rapidly dissolving immediate release dosage forms. Careful observation of the disintegration process showed that tablets disintegrated in smaller particles, but the size of the particles was different. Very efficient disintegrants as UICEL S, UICEL B, and UICEL-XL resulted in very fine powders, whereas the above mentioned formulations with 10% drug load resulted in coarser particles which passed the test indeed, but dissolution was not very efficient. One could see that disintegration is not an appropriate tool to predict dissolution behaviour, but careful implementation, including observation of particle size, combined with a single-

point measurement could be an interesting method in quality control of immediate release dosage forms.

To compare single-point measurements, analysis of variance using ANOVA is proposed. [80, 85] Including post hoc analysis as applied in this study allows determining differences also between individual groups. The comparison of more than two curves at the same time is a big advantage of this statistical method compared to the pair-wise procedure as difference factor f_1 and similarity factor f_2 . Polli [85] criticized ANOVA tests as too discriminating; an increased sensitivity of ANOVA compared to f_1 / f_2 methods was found only for the relative density experiments, in general, ANOVA tended to be more liberal than the other two models.

Application of difference factor f_1 and similarity factor f_2 is a user-friendly approach, since it can be easily implemented using spreadsheet analysis or even a calculator, no further knowledge about statistics is required. Originally, these methods were proposed by the FDA to compare dissolution profiles after major changes. A reference batch before change is compared to a post-change batch. [82] In this study, these approaches were used to compare different dissolution profiles. For every experimental set-up, a reference formulation was selected and the other formulations were then compared. In general, f_1 and f_2 assessed curves similar, when differences were found between these two approaches, f_2 was more liberal. The application of these models was not suitable in case of ternary mixtures with UICEL S and UICEL B (Figure 77), where profiles were compared to the reference curve UICEL-A/102 90%. It was problematic that a minimal number of three data points excluding zero was required, but only two data points were available. [83] One has to keep in mind that EMEA rejects the use of these models when 85% of the drug is dissolved within 15 minutes. Those formulations which passed the IR limits were tested then evaluated with regard to this higher limit. Two formulations that passed the IR limits did not pass these EMEA similarity limits, 50% proquazone and MCC 102 and 10% proquazone, MCC 102, and 22.5% UICEL B.

Regarding the small amount of data points for UICEL S (n=3), UICEL B (n=3), and UICEL-XL (n=2) including zero, it was not surprising that difference factor f_1 accepted similarity of 10% proquazone and UICEL S (ρ_m 0.7) and the same formulation with UICEL B, whereas ANOVA of $M_{30\ min}$ refused it. The same was found in drug load experiments. Deviations of f_1 compared to $M_{30\ min}$ were accompanied by a maximal number of data points of four including zero. Whereas in case of relative densities f_1 was more

RESULTS AND DISCUSSION

liberal compared to $M_{30 \text{ min}}$, the opposite was found in drug load experiments. Independent of the number of data points included in analysis, f_1 was more sensitive in finding differences between the curves compared to $M_{30 \text{ min}}$ in ternary mixtures. No similarity was found when only three data points were included, even though $M_{30 \text{ min}}$ confirmed it. Additional differences which were not related to the number of data points point to increased sensitivity of this approach. Except in two cases, MCC 102 10% compared to 90% drug load and MCC 102 ρ_m 0.8 compared to ρ_m 0.9, where f_2 was less conservative, no differences were found between f_1 and f_2 .

Freitag [79] listed some points with respect to f_2 which should be discussed. She sympathizes with the fixed similarity level of 50 which was established in recent years. With respect to the results of this study, this level could be criticised. The formulation with 50% proquazone and UICEL S resulted in a difference of $f_2 = 44$ compared to 10% drug load, even though $M_{30 \text{ min}}$ confirmed their similarity. Indisputably, the number of data points could have influenced the result, but one has to keep in mind that the limit is not based on a scientific background, but is based on former experience. Furthermore, she criticized the high liberality in deciding for similarity. This has to be refused by the findings of ternary mixtures, where it was more rigorous compared to $M_{30 \text{ min}}$ values which were already criticized to be too sensitive by Polli [85]. Finally, she mentioned the sensitivity to amount of included data points, especially after the plateau has been reached. To avoid this problem, the recommendation of the FDA to include only one value above 85% dissolution was followed, and all dissolution profiles were made under the exact same conditions as medium type and volume, stirring rate, and sampling schedule.

5.2.4.2 Model dependent approach

Model independent approaches compare either only single-point measurements by ANOVA or release profiles by means of differences in multi-point measurements between two curves. Release properties of formulations, i.e. the kinetic background, are not involved. Model dependent approaches are focussed on the description of the release profile. From the models applied in this study, Weibull was a special case, since it is based on statistics and not on kinetics as Noyes-Whitney, Hixson-Crowell, and Higuchi.

The advantage of Weibull is the successful application to different release profiles. [84] Since two parameters were available, the model was very suitable to describe profiles precisely. This was confirmed by the evaluation of r^2 values which were very in general

very high (63% ≥ 0.9995). Up to now, the Weibull model was only used to calculate $t_{90\%}$, but parameters a and b were not discussed. The scale parameter a defines the time scale of the process, the shape parameter b characterizes the curves. [84]

Before these parameters were compared with parameters of other models, the correlation between those two parameters were assessed.

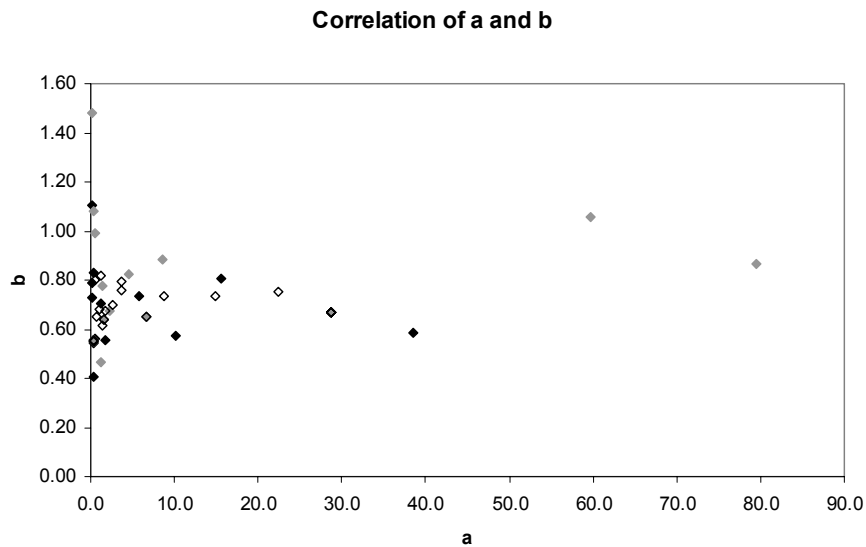


Figure 83: Correlation between the Weibull parameters a and b .

Legend: Binary mixtures with different relative densities (◆), binary mixtures with different drug loads (◈), and ternary mixtures (◇).

Figure 83 shows no correlation between a and b , this allowed to study the influence of these two parameters separately. Since scale parameter a is related to the time, a correlation between a and k_1 was expected. A decreased value for a was accompanied by increased k_1 ; a plot of this correlation is given in Figure 84.

A correlation was found for binary mixtures at different relative densities ($r^2 = 0.9072$) and different drug loads ($r^2 = 0.8373$), but also for ternary mixtures with different disintegrant loads ($r^2 = 0.9664$). Parameter a could indeed be used to detect differences in dissolution rates. Compared to statistical analysis of k_1 , a was more liberal in accepting similarity between curves.

RESULTS AND DISCUSSION

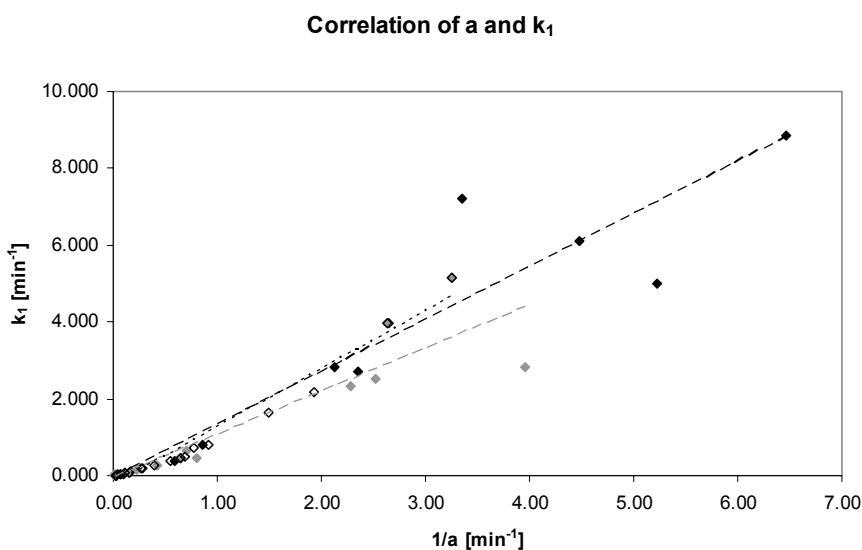


Figure 84: Correlation between scale parameter a and first order dissolution rate k_1 .

Legend: Experimental (dots) and fitted values (lines) for binary mixtures with different relative densities (◆, - - - -), binary mixtures with different drug loads (◇, - · - ·), and ternary mixtures (◇, ·····).

The shape parameter b is related to the curve shape. Langenbucher [84] refers to three different cases: (1) the curve is exponential with $b = 1$, (2) the curve is S-shaped ($b > 1$), or (3) the curve is first steeper, then consistent with the exponential curve. In case (1), Weibull corresponds to the modified Noyes-Whitney equation for first order release. In this study, most of the curves followed (3). Only four formulations showed greater b values, but those findings could not be related to a kinetic background and were therefore considered as artefacts.

The Weibull model was indeed an interesting approach to describe dissolution profiles, but drug release could not be characterized. Models with a kinetic background are therefore preferred. Initially, first order release by Noyes-Whitney should be discussed. The advantage of this model is the application on disintegrating tablets, whereas Hixson-Crowell was limited to tablets which decrease in size geometrically. From the evaluation of the shape factor it was known that most of the curves followed an almost exponential release. First order kinetics could therefore be considered as suitable to describe release profiles. This was confirmed by the evaluation of the coefficients of determination, where, with a few exceptions, first order was suitable to describe the release profiles ($r^2 \geq 0.9800$).

The next approach was the Hixson-Crowell model which as mentioned above is only applicable when the tablet size decreases geometrically. Disintegrating tablets with 10% drug load, even when they disintegrate immediately in fine powder, were poorly described by this model. With increasing drug load and an increased impact of drug properties, Hixson-Crowell was suitable to describe release profiles. A small number of data points resulting from very fast dissolving formulations, especially with UICEL-A/102 as disintegrant, refused the proper application of this model. At least four data points below 85% drug released should be included.

A correlation between first order dissolution rate and Hixson-Crowell dissolution rate was described by Polli. [85] To prove this correlation, k_2 was plotted against k_1 (Figure 85). Dissolution rates of UICEL S ρ_m 0.9 were removed from analysis, because k_2 was qualified as an outlier, since only four data points were available and the coefficient of determination was very poor ($r^2 = 0.4557$).

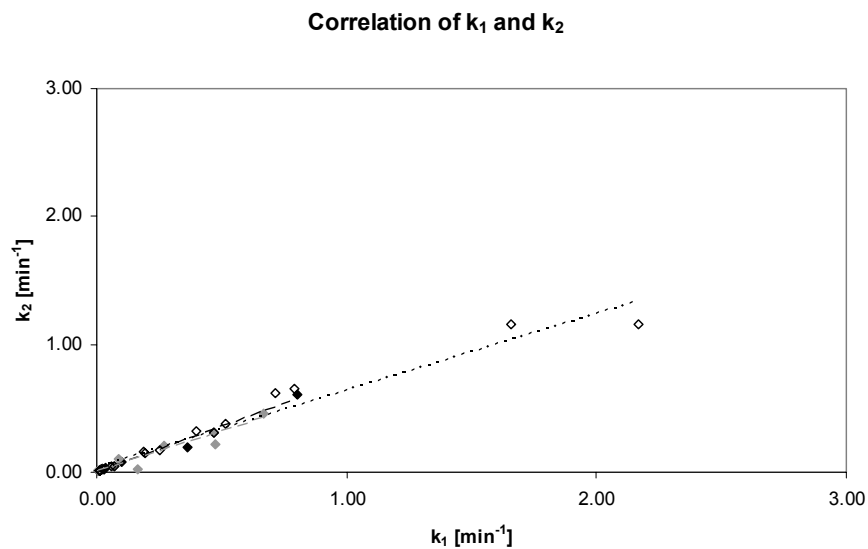


Figure 85: Correlation between dissolution rates obtained by first order and Hixson-Crowell analysis.

Legend: Experimental (dots) and fitted values (lines) binary mixtures with different relative densities (◆, - - - -), binary mixtures with different drug loads (◇, - - - -), and ternary mixtures (◇,

The slopes and coefficients of determination from linear regression are given in Table 52.

RESULTS AND DISCUSSION

Table 52: Slopes and coefficients of determination of the correlation between k_1 and k_2 .

	Slope	r^2
relative density	0.7172	0.9823
drug load	0.6252	0.9178
disintegrant load	0.6024	0.9567

A clear correlation between k_1 and k_2 was found; the slopes which ideally should be 1 were in this case smaller, this is referred to a faster dissolution described by first order kinetics. The different experimental set-up, relative density, drug load, and disintegrant load did not influence the correlation; both models were indeed suitable to describe different release profiles.

Unexpected was the suitability of the Higuchi model to describe drug release from MCC 102 and Type I formulations with a low drug load. Higuchi in general is used to describe drug release from matrix systems. [102] These formulations with their short disintegration times were supposed to release drug according to first order kinetics. Analysis showed that a more complex process occurred. The initial faster increase followed by later dropping off and the almost linear release in the second stage pointed to drug release according to Higuchi. Transformation of the time t to its square root resulted in a linear increase up to 60%. This is in good agreement with the theoretical considerations. This phenomenon was explained by percolation theory, where the small amount of drug was fully embedded in the not dissolving matrix of cellulose. Type I resulted in faster release rates, this might be related to the better disintegrant properties of this partially converted cellulose II product.

5.2.5 Disintegrant Comparison based on a Model Independent and a Model Dependent Approach

After studying different approaches and different models, it was difficult to select two appropriate models to assess differences between celluloses. Every method showed advantages and disadvantages. Due to the ease of application, similarity factor would have

been the model of choice amongst model independent approaches. Due to the small number of data points available, this approach was rejected and statistical analysis of $M_{30\text{ min}}$ was preferred.

Indeed a correlation between k_1 and a and between dissolution rates k_1 and k_2 was found (Figure 84 and Figure 85), but the values themselves differed between the models. To assess properties of a disintegrant, comparable values are required. This leads now to the main problem of the model dependent approaches; in case that drug release follows different kinetics, a comparison of the rates is no longer possible. A kinetic independent approach has to be select to avoid distortion by different models. This is an advantage of the Weibull approach. Independent of the release kinetics, the curves were described very well and for that reason, Weibull was selected as the model dependent approach.

After selection of the models, the experiments to assess disintegrant properties were carefully selected. Ternary mixtures with 10% drug load and increasing amount of modified cellulose are considered to show the impact of the disintegrant on the dissolution; UICEL-XL which was studied only in binary mixtures was included into evaluation.

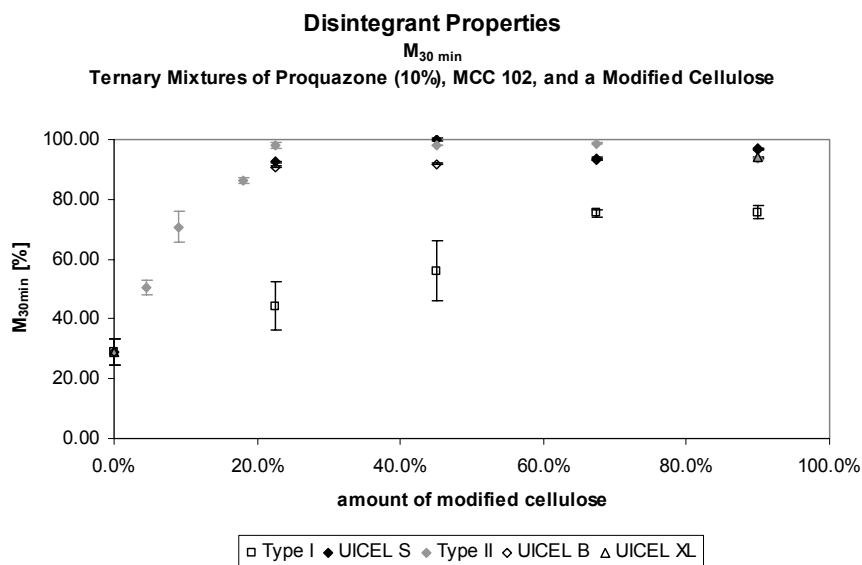


Figure 86: $M_{30\text{ min}}$ as result of the amount of modified cellulose.

Figure 86 shows $M_{30\text{ min}}$ values as a result of the amount of modified cellulose. Compared to MCC 102, $M_{30\text{ min}}$ was significantly increased after a 4.5% Type II, 22.5% UICEL S or UICEL B, and 45% Type II; smaller amounts of UICEL S and UICEL B were not

RESULTS AND DISCUSSION

investigated. The difference between MCC 102 and UICEL-XL was statistically proved ($p = 0.000$). Independent of the load of modified cellulose, class 2, the partially converted cellulose Type I, was always significantly less efficient than class 3 and class 4 substances. No difference between UICEL B and UICEL S, the standard cellulose of class 3, was found; Type II was more effective at a level of 67.5% but less effective at 90%. UICEL-XL which was studied only at a level of 90% showed no difference to the class 3 substances.

The next step was the evaluation with the Weibull model, where two parameters a and b were determined. Even though a was related to the release rate (Figure 84) and b was independent (Figure 83), both parameters were included into assessment by calculating $t_{90\%}$. The results are graphically shown in Figure 87.

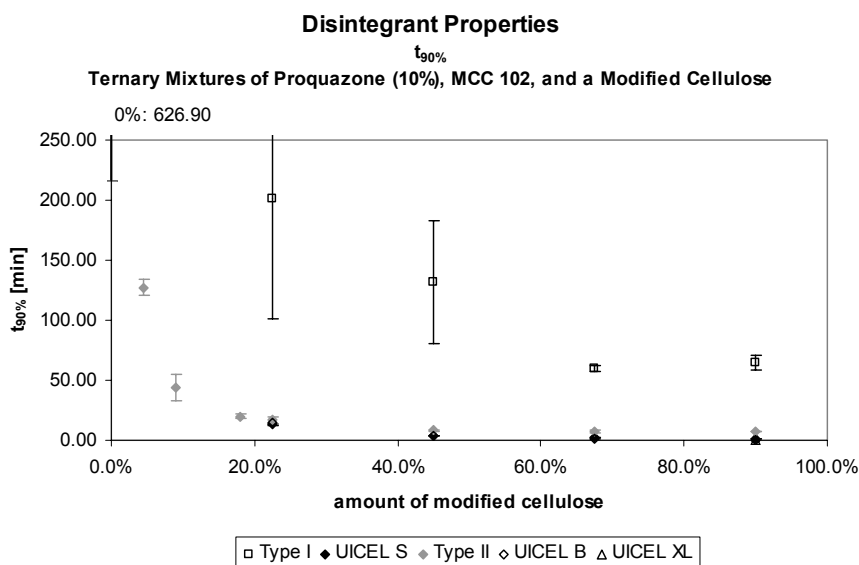


Figure 87: $t_{90\%}$ as result of the amount of modified cellulose.

A statistical reduction of $t_{90\%}$ ($p = 0.012$) was reached with a minimal Type II load of 4.5%. Further load of Type II did not reduce $t_{90\%}$ anymore. Type I showed independent of the load of modified cellulose statistically increased $t_{90\%}$ values compared to substances of class 3 and 4. Differences between UICEL S and UICEL B were not found. $t_{90\%}$ of UICEL-XL, class 4, was equal to class 3 ($p = 1.000$). Type II showed a statistically increased $t_{90\%}$ at a load of 67.5% compared to UICEL S and UICEL B with $p = 0.004$ and $p = 0.002$, respectively. This difference vanished at a load of 90% and was therefore not considered as very important

fact. Comparison of $t_{50\%}$ values resulted in the same order, $t_{10\%}$ showed a clear advantage of class 3 and 4 compared to class 2 at all levels of modified cellulose.

These clear advantages of cellulose II powders compared to cellulose I were already described by Reus Medina and Kumar [9] and Lanz [27]. Lanz found a minimal amount of 5% UICEL-A/102 in binary mixtures with proquazone sufficient to increase dissolution rate clearly and make dissolution more efficient than with 50% Avicel PH-102. He further described increased drug release with increased load of UICEL-A/102. These findings could be confirmed with this study. Reus and Kumar [9], furthermore, ascribe the good dissolution properties to the cellulose II structure. This could also be confirmed comparing the degree of conversion of the investigated celluloses. The fully converted celluloses showed very similar dissolution properties, whereas the partially converted cellulose was somewhere between cellulose I with the standard MCC 102 and cellulose II with the standard UICEL S. The degree of conversion is therefore very important for the quality of the product.

5.3 Relation between Mechanical Resistance and Liquid - Solid Interactions

Water uptake rate is not directly influenced by the strength of the tablet. The Washburn equation (Equation 16) includes indeed porosity, but tensile strength is also a result of the porosity. Additionally, water uptake rate determination was not suitable to detect differences. Both parameters were already discussed as a result of the porosity, no further information is expected from water uptake, therefore it will be excluded from further studies.

More interesting are correlations between tensile strength and disintegration times. Lowenthal listed different publications where disintegration was either affected by tablet hardness or the opposite was found. [58] Lanz supposed that the increase of the disintegration time is a result of the increase in the cohesive energy which is given by the tensile strength. [27] To prove this assumption, disintegration time was plotted against the tensile strength. Disintegration time of class 3 substances was not influenced by the relative density; UICEL B and Type II were therefore not further investigated. UICEL S was included as the standard for fully converted celluloses. Disintegration time of UICEL-XL was determined only at ρ_m 0.8; this point was also included for comparison. The correlation

RESULTS AND DISCUSSION

between disintegration time and tensile strength of binary mixtures with proquazone (10%) and MCC 102, Type I, or UICEL S was assessed with Figure 88.

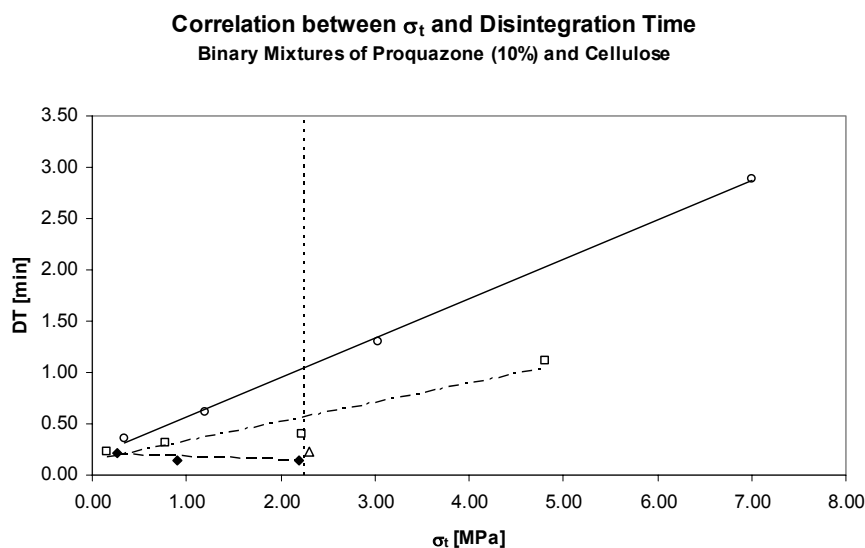


Figure 88: Correlation between tensile strength and disintegration time as a result of the relative density.

Legend: Experimental (dots) and fitted values (lines) for MCC 102 (○ —), Type I (□ - - - -), UICEL S (◆ - - - -), and UICEL-XL (△).

A linear relationship between tensile strength and disintegration time was found for MCC 102 ($r^2 = 0.9985$) and Type I ($r^2 = 0.9354$). The disintegration time of UICEL S was not affected by the tensile strength; Type I and MCC 102, on the other hand, showed increased disintegration times with increased hardness. This confirmed the hypothesis of Lanz. Furthermore, disintegrant properties of the cellulose could be assessed. MCC 102 showed the poorest disintegrant efficiency, Type I, obviously, released more energy to break up bondings. Since tensile strength did not influence the disintegration time of UICEL-A/102, it can be concluded, that the disintegration force developed in contact with water is very strong and effective. The influence of the tensile strength on UICEL-XL could not be determined, but a comparison between the different classes was anyway possible. At a comparable tensile strength of approximately 2.25 MPa (the vertical line in Figure 88), UICEL S showed the shortest disintegration time, closely followed by UICEL-XL, then Type I. Disintegration times of MCC 102 formulations were much higher. In this study, UICEL S showed shorter disintegration times compared to UICEL-XL; this contradicts the findings of Reus Medina who ascribed better disintegrant properties to UICEL-XL than

UICEL-A/102 at comparable tensile strength. [10] The statement of Lowenthal [58] that various celluloses increase tablet strength without adversely affecting disintegration time could be confirmed considering the still very short disintegration times compared to the very high tensile strength of the MCC 102 formulations.

In case of drug load experiments, no relationship between disintegration time and tensile strength was expected; increased drug load reduced tensile strength, disintegration followed a more complex pattern (Figure 57). This was attributed to drug properties. The evaluation of ternary mixtures was neither very informative, since disintegration times were significantly reduced with 22.5% disintegrant, but further load did not reduce them anymore.

Dissolution is dependent on the disintegration and the extent of disintegration. The extent of disintegration, i.e. the resulting particle size after contact with water, is a property of the disintegrant. As discussed in the previous section, especially MCC 102 but also Type I disintegrated rapidly but did not release the drug very fast. Those fast disintegration times could be explained by the method. Moving disks exert external stress on tablets which let them disintegrate without disintegrant action. In dissolution studies, this external stress was not present and as described, tablets did not disintegrate in fine particles but resulted in lamination or coarse particles. This could be attributed to the strong cohesion force which has to be overcome. To study the disintegrant properties without the influence of the disks, it may be interesting to assess $t_{90\%}$ as a result of the tensile strength. All used formulations contained 10% proquazone, this constant load allowed to assess the properties of the disintegrant without the influence of the drug. Figure 89 shows the correlation between tensile strength and $t_{90\%}$, and additionally, disintegrations times as a result of the tensile strength.

RESULTS AND DISCUSSION

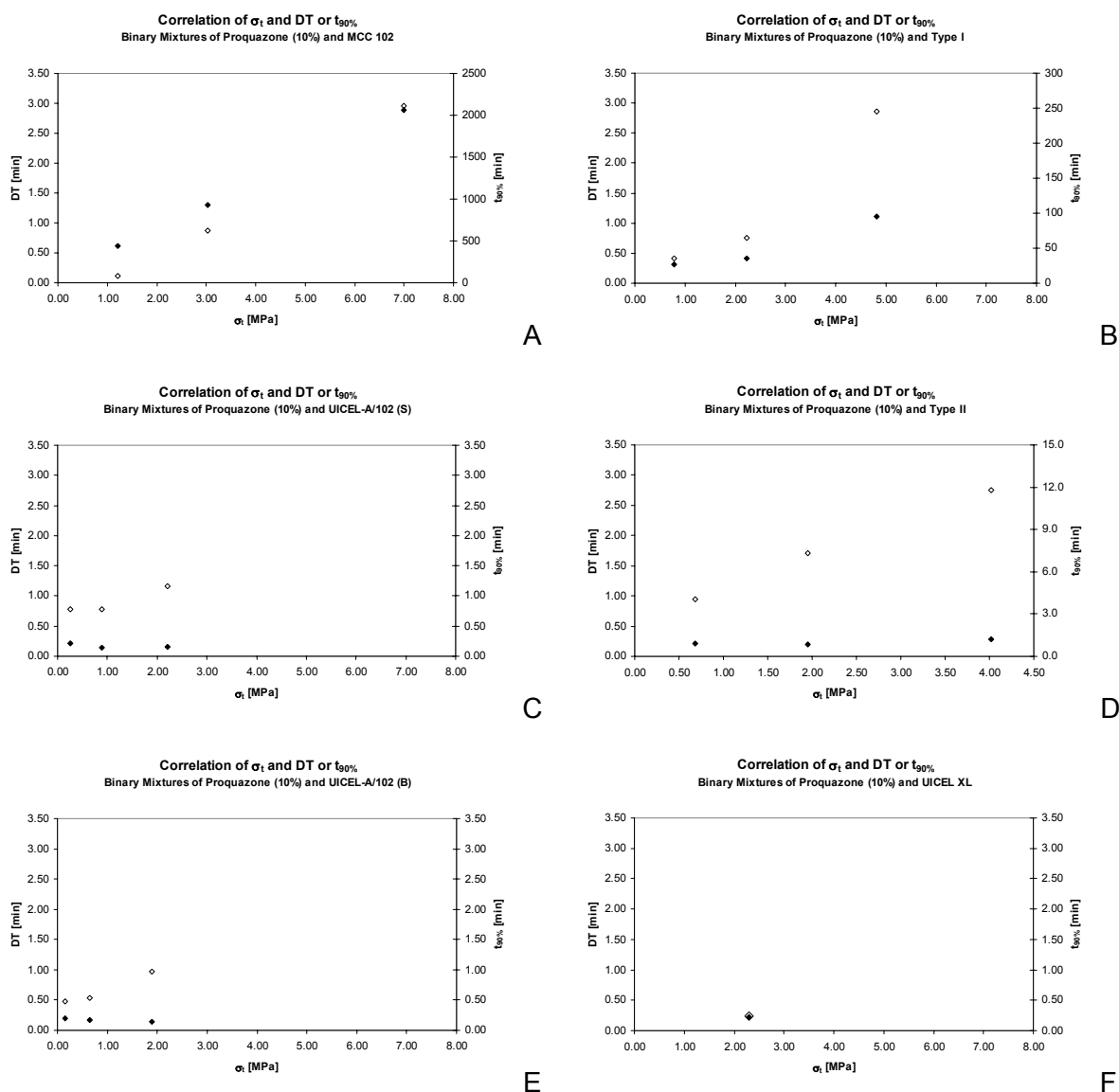


Figure 89: Correlation between tensile strength and the disintegration time or $t_{90\%}$ as a result of relative density; (A) MCC 102, (B) Type I, (C) UICEL S, (D) Type II, (E) UICEL B, and (F) UICEL-XL. The ordinates (disintegration time) are not adjusted to facilitate the comparison between the different celluloses.

Legend: $t_{90\%}$ (\diamond) and disintegration time (DT) (\blacklozenge).

Studying disintegration times in Figure 89 A, one could clearly see that disintegration was related to the external stress, the increase of $t_{90\%}$ (cave: time scale) with increasing mechanical resistance is therefore a real property of the filler MCC 102. The same pattern with a smaller extent was also found for Type I (B). Type I can be considered as the better disintegrant. As discussed, disintegration of class 3 substances was not influenced by the cohesive forces; $t_{90\%}$ of UICEL-A/102 formulations, on the other hand, showed a tendency

to increase between 1 and 2 MPa tensile strength (C, E). Cohesive forces seemed to influence the release properties. The disintegrant properties of Type II (D) were smaller compared to the other class 3 substances, since dissolution was prolonged with increasing mechanical strength of the tablets. The energy released in contact with water was therefore not as sufficient to break the tablets as for UICEL-A/102. UICEL-XL (F) was difficult to assess since only one value was available, very interesting in this case was the accordance of disintegration time and $t_{90\%}$, this showed the very good disintegration and dissolution properties of UICEL-XL, where no physical or chemical hindrance occurred.

A further relation between compaction behaviour and disintegrant properties was set up by Kanig and Rudnic; they related high elastic accommodation to poor disintegration behaviour. [67] To prove this, the difference between disintegration time of MCC 102 formulations and modified cellulose formulations were plotted against the slope of the elastic recovery of ternary mixtures. The difference between MCC 102 and modified celluloses was selected, since elastic recovery was also only a relative value compared to MCC 102. A large difference between disintegration times of MCC 102 and the modified cellulose was considered as a good disintegrant property of the later substance. Elastic recovery of ternary mixtures are listed in Table 36 and discussed there.

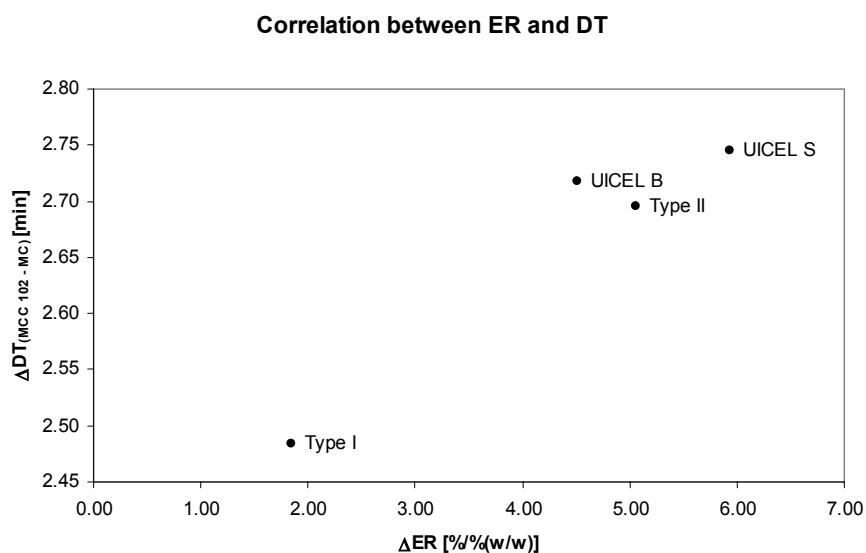


Figure 90: Correlation of the elastic recovery of ternary mixtures (Table 36) and the disintegration times expressed as the difference between binary mixtures of proquazone (10%) and MCC 102 or a modified cellulose, respectively, at a ρ_{rn} 0.8.

RESULTS AND DISCUSSION

The supposed reduction of disintegration efficiency with increased elastic recovery was not found in this study, on the contrary, substances with increased elastic recovery showed shorter disintegration times in comparison to MCC 102. It was supposed that elastic recovery played a minor role in this process, since the evaluation was done three to four days after compaction to allow the tablets greatest possible elastic recovery.

5.4 Granulation versus Direct Compaction

5.4.1 Compressibility and Compactibility

Direct compaction is a simple and fast method, no wetting and drying of the powder mixtures is required, this reduces time and saves costs, but direct compaction also shows disadvantages and sometimes granulation cannot be avoided. Advantages and disadvantages of wet granulation, dry granulation, and direct compaction are compared in Table 3.

Investigations on wet granulation of celluloses are interesting since reduced compactibility of MCC was found after wet granulation. [103] Furthermore, a reduction of the superdisintegrant performance is described. [104] UICEL-A/102 (S) might be considered as a superdisintegrant; this was described in literature and confirmed in this study. [27]

Initially, compressibility and compactibility were studied. Two types of cellulose were included, MCC 102 and UICEL SM which was a milled fraction of UICEL S. Ball milling did not change the polymorphic form, but the smaller area under the peaks in Figure 15 E could be related to a reduced crystallinity. Granules were first compressed applying 7 kN with a resulting relative density ("granules"); to allow comparison with direct compaction, a powder mixture of identical composition was compressed to the relative density of these tablets ("powder"). Additionally, granules were also compressed to this relative density ("granules rd").

Tablets made from granules with 7 kN resulted in a relative density of 0.81 for MCC 102 formulations and 0.77 for UICEL SM formulations. To compare powder mixtures with these tablets, they were compressed to the same relative density. Detailed values including standard deviations are given in Table 53.

Table 53: Relative densities of tablets made from granules or powder, incl. standard deviations in brackets.

	MCC 102	UICEL SM
Granules	0.81 (0.003)	0.77 (0.003)
Granules rd	0.80 (0.003)	0.74 (0.006)
Powder	0.81 (0.007)	0.75 (0.002)

Formulations with MCC 102 showed almost similar relative densities three to four days after ejection. UICEL SM formulations showed a deviation of the aimed values of 0.77. This could be explained by imprecise adjustment of Zwick, but rather by elastic recovery.

Figure 91 shows the elastic recovery which was calculated with the height of the tablet directly after ejection and the height after three or four days. As already discussed in a previous section, the height of the tablet under maximal load was difficult to determine precisely. To show the tendency of elastic recovery, the applied method was suitable.

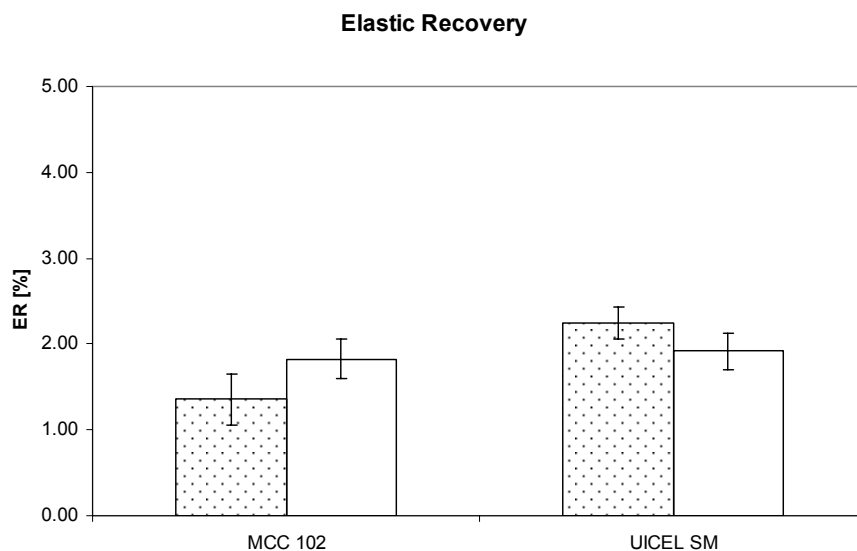


Figure 91: Elastic recovery calculated with height after ejection and after three or four days.

Legend: Granules rd (▨) and powders (□).

RESULTS AND DISCUSSION

Since no significant difference was found between granules and powders, the groups were compared without respect to the formulation; UICEL SM was significantly more elastic than MCC 102. This effect was already discussed before and is consistent with literature. [11] Additionally, the differences of the relative densities of Table 53 could be explained by this fact.

An evaluation of compressibility using the resulting compaction force was not really suitable in previous experiments; nevertheless, the results were studied to get an idea of compressibility. Table 54 lists those values.

Table 54: (Resulting) compaction force in [N] of tablets made from granules or powder, incl. standard deviations in brackets.

	MCC 102	UICEL SM
Granules	6981.62 (2.175)	6984.51 (1.670)
Granules rd	5736.17 (125.769)	4634.99 (59.979)
Powder	6977.06 (226.352)	4951.52 (51.292)

Regarding the compaction force in Table 54, nearly similar compaction forces with only a very small standard deviation were found for tablets compressed with a constant compaction pressure. A small deviation from those 7 kN was attributed to the inaccuracy of Zwick. Since these values were set in advance, similarity and precision were not surprising. However, more interesting was the resulting compaction force when tablets were compressed to a defined relative density, these values are directly related to the compressibility of the material. From the Heckel equation (Equation 4) it is known that high compressibility is accompanied by small compaction pressures to achieve a specified relative density. In both cases, significantly less compaction force was required to reach the aspired relative density for granules than for powders, i.e. granulation increased compressibility of MCC 102 and UICEL-A/102.

The poorer compressibility of MCC 102 compared to UICEL SM here was contradictory to the findings of the Heckel equation (Table 23), but confirmed the lack of suitability of the RCF to assess compressibility. The increased compressibility of MCC 102 and UICEL SM

has therefore to be judged critically, especially because reduced plasticity of MCC after wet granulation is described in literature. [32]

More suitable to characterise substances is the evaluation of tensile strength, i.e. compactibility. Therefore, powders were compressed to the relative density of granules compressed with 7 kN. The results are shown in Figure 92.

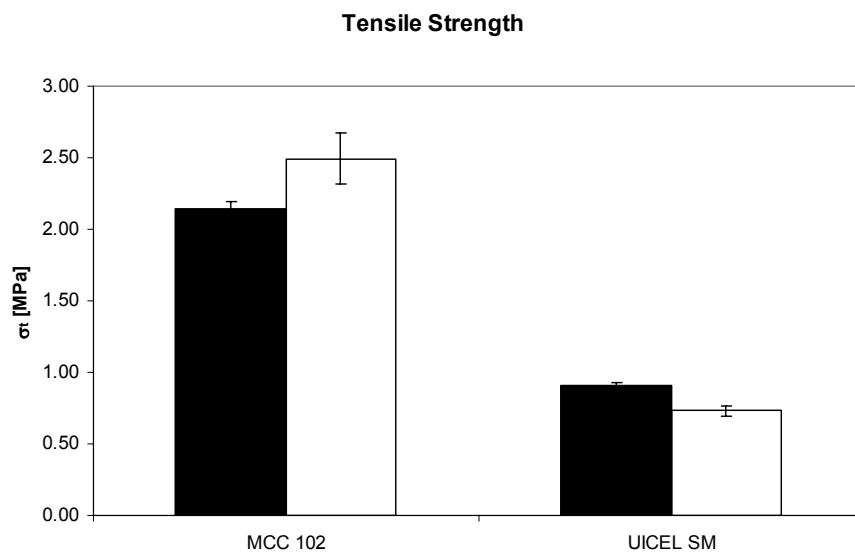


Figure 92: Tensile strength of tables made from granules and powders with comparable relative density.

Legend: Granules 7 kN (■) and powders ρ_m (□).

Tensile strengths of UICEL SM formulations were clearly lower than for MCC 102 formulations. This could be referred to the smaller relative density, which was explained in Figure 32, but also to the reduced compactibility of UICEL SM, a fraction of UICEL S, according to the Leuenberger equation (Table 25). More interesting was the influence of granulation on the compactibility. Wet granulation of MCC 102 formulations decreased the hardness, whereas for UICEL SM it was increased. This is in good agreement with literature. Badawy et al. described a decrease in compactibility of MCC after granulation. [103] No negative impact of UICEL SM on hardness after granulation was found in this study. Even though wet granulation might decrease hardness of tablets, considering the still appropriate hardness of the tablets given in Table 55, wet granulation with UICEL may be possible.

RESULTS AND DISCUSSION

Direct comparison of MCC 102 and UICEL SM formulations were difficult since relative densities as well as compaction forces differed between the fillers but also between the procedures. Compaction force of UICEL SM formulations was decreased about 2 kN for powder compaction compared to compressed granules. This clearly lower compaction force could additionally influence hardness of the tablets, since not enough bondings were built.

Table 55: Crushing force [N] of tablets made from granules or powders, incl. standard deviations in brackets.

	MCC 102	UICEL SM
Granules	98.0 (2.12)	43.8 (0.84)
Powder	112.3 (7.37)	36.0 (1.73)

Not discussed was the importance of the flow properties. An advantage of granulation is the improvement of them. Comparing the values of Table 13 (powders) and Table 20 (granules), no improvement of the flow was found. To assess this important fact, compendial flowability studies using the funnel should be done.

5.4.2 Liquid - Solid Interactions

In previous experiments water uptake was inappropriate to detect differences between formulations. Nevertheless, water uptake rates of tablets made from granules and from powders, compressed to the same nominal relative density, were evaluated. The water uptake rates are graphically shown in Figure 93.

Granulation did not influence the water uptake rate, but a significant difference was found between MCC 102 and UICEL S. The improved water uptake tendency of UICEL S was already discussed earlier (Figure 51).

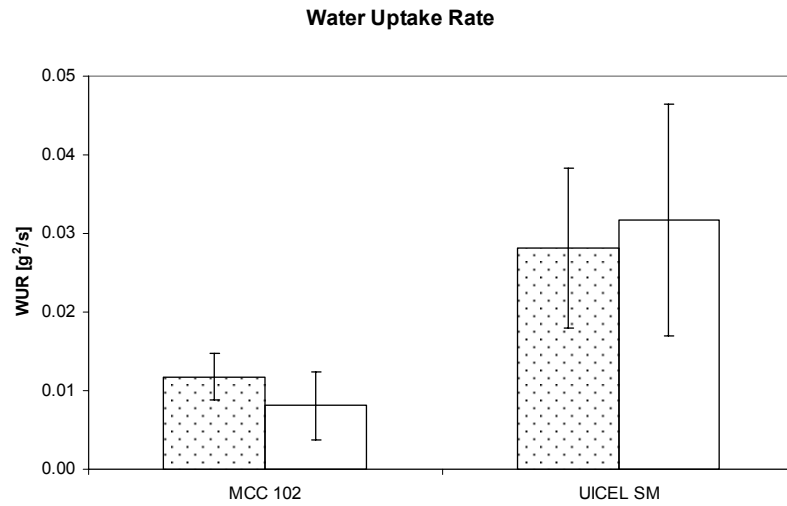


Figure 93: Water uptake rates of tablets made from granules (▨) or powder (□) compressed to the same nominal relative density.

A better discriminative power was expected of disintegration time measurements. Therefore, two different methods were applied. Tablets made from granules were tested without disk, while tablets made from powder were determined with and without disks. Testing without disks allowed investigating the impact of external stress on disintegration times.

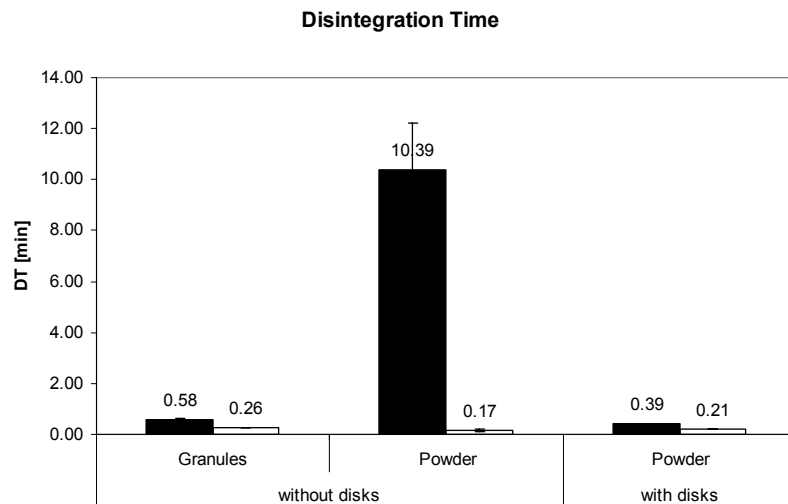


Figure 94: Disintegration times of tablets produced from granules or powders.

Legend: MCC 102 (■) and UICEL SM (□).

RESULTS AND DISCUSSION

The fast water uptake rate and the knowledge of previous experiments raised the expectations of short disintegration times of UICEL SM; this could be confirmed independent of composition and method (white bars in Figure 94). Tablets containing MCC 102, on the other hand, were very sensitive on the method. Tablets made from powder showed a tremendous reduction in disintegration time when disks were used. This could be related to the external forces exerted from disks. Without disks MCC 102 tablets were floating and swelling at the beginning and disintegrated in bigger flakes which did not pass the sieve of the disintegration basket. Tablets made from granules were less sensitive on the method; they disintegrated very fast into small particles even without disks. This could be referred to the good disintegrant properties of UICEL S. The reduced disintegration time of MCC 102 granules compared to powder gave rise to the assumption that granulation improves disintegration properties. This contradicts the findings of Zhao and Augsburger, who found increased disintegration times after granulation. [104] Increased water uptake rate however could not be found. It was supposed that PVP which was sprayed from solution was uniformly distributed on the surface of the particles and hence improves wettability. This distribution of binder on the surface is described in literature. [37] SEM pictures of the surface of granules are given in Figure 19. The fibrous structure of the cellulose was still visible, but the smoother surface could be related to the binder on it.

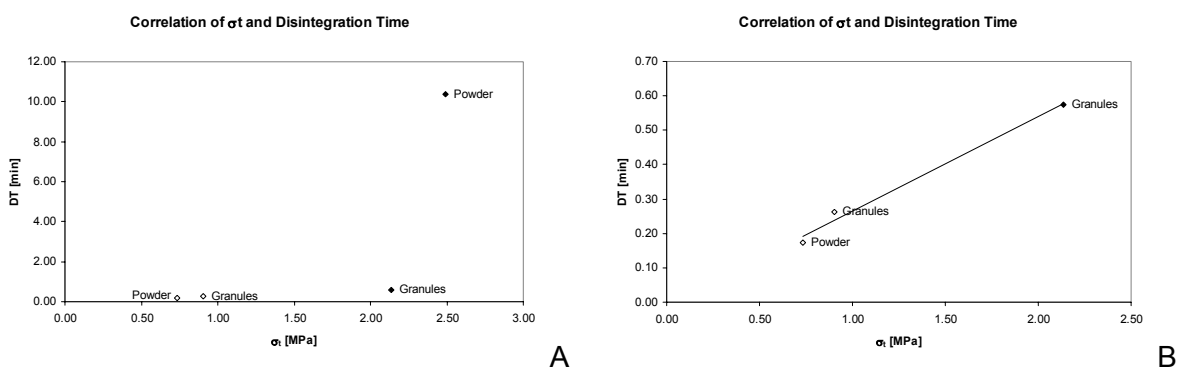


Figure 95: Correlation between tensile strength and disintegration times of tablets produced from granules or powders, disintegration times determined without disks; all experimental data(A), MCC 102 (B) powder formulation excluded.

Legend: MCC 102 (◆) and UICEL SM (◇).

Disintegration time is reduced when water uptake or disintegration force is increased. An increase of water uptake rate could not be found and a direct increase of the disintegration

force is not expected, since the disintegrant amount was constant. However, reduced cohesive forces may increase disintegration time, since less force is required to overcome these forces. Figure 95 shows the correlation between the cohesive forces expressed in the tensile strength and the disintegration times. Figure 95 B shows a nice correlation of tensile strength and disintegration times ($r^2 = 0.9901$), whereas in (A), where all experimental data were included, the linearity vanished. This slow disintegration process of MCC 102 powder formulations could not fully be explained by cohesive forces. The granulation process may play a major role, to prove this assumption, tablets of different hardness should be produced from granules and powders and disintegration should be studied without disks.

From earlier experiments it is known that dissolution is the most discriminative method to find differences between formulations. In the first step, dissolution profiles of compressed granules and compressed powders were compared. Figure 96 shows the accumulated amount of proquazone dissolved at a paddle speed of 50 RPM.

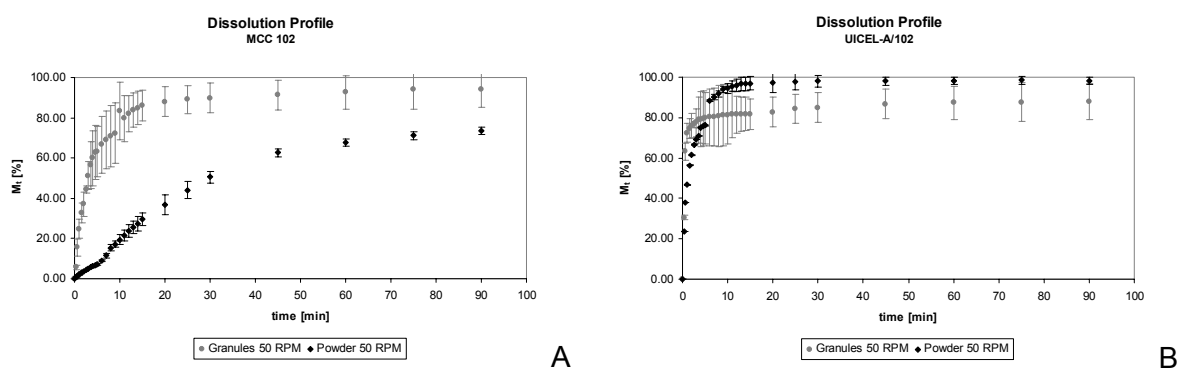


Figure 96: Dissolution rate profiles of granules and powder formulations at 50 RPM; (A) MCC 102 and (B) UICEL SM.

The production showed an influence on the dissolution profile of MCC 102 formulations (Figure 96 A); tablets made from granules showed a faster drug release than those made by direct compaction. This could be expected from disintegration test without disks. A small dissolution rate increase was found for granulated UICEL SM formulations compared to powders (B). Beside the dissolution rates it should be pointed to the quality of the profiles. It was clearly detectable that granulated tablets resulted in less robust dissolution profiles. The very high standard deviations until 90 minutes might be a result of poor content uniformity of the granules. The values of Table 22 showed smaller standard deviations and

RESULTS AND DISCUSSION

could not fully explain them. The differences might be traced back to poor sampling for both tests. Directly compacted powders, on the other hand, showed fairly small standard deviations; dissolution seemed more robust. Dissolution profiles of compacted powders in Figure 96 showed a kink after five minutes. Dissolution performed with 50 RPM might lead to inadequate mixing of the drug in the acceptor medium and a reduced drug load at the sampling position. Substitution of the medium which was generally done after five minutes improved mixing. This could explain the immediate increase of the drug released after five minutes. To prove the influence of the stirring rate, dissolution of compacted powders was determined at 50 and 100 RPM.

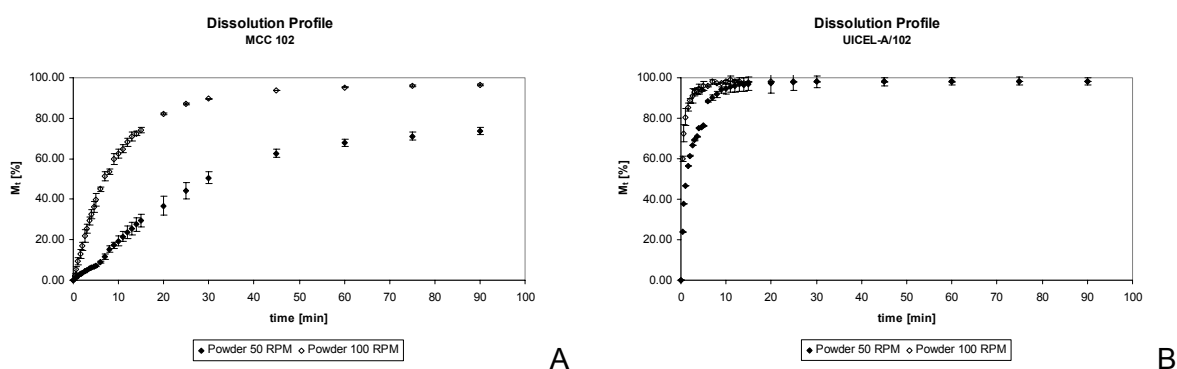


Figure 97: Dissolution rate profiles of compacted powders at 50 RPM or 100 RPM; (A) MCC 102 and (B) UICEL SM.

In case of MCC 102 formulations (Figure 97 A), the increased paddle speed resulted in faster and complete drug release, UICEL SM formulations (B) showed an increased release profile, but the shape of the curve was only slightly smoothed. To quantify differences between formulations and to prove the impact of stirring speed, all profiles were studied with different model independent and model dependent approaches.

Initially, formulations were checked for their suitability as rapidly dissolving IR formulations (Figure 98). MCC 102 formulations met the requirements only after granulation, whereas UICEL SM was not influenced by the method. UICEL SM granules were slightly below the limit ($84.95\% \pm 5.43$), but with respect to the maximum possible drug release of $87.82\% \pm 3.3$ and after adjustment of the data as described before (Figure 68), formulations would clearly meet the requirements. The MCC 102 powder formulation met the requirements when the paddle speed was increased to 100 RPM. In that case, it was

clearly detectable that the experimental set-up, e.g. stirring rate, might have a great impact on the results.

This diagram shows clearly the limits of in vitro testing and the prediction of in vivo behaviour. One could see that only one parameter, i.e. the stirring rate, rejected a formulation as rapidly dissolving. [16] Considering all the parameters that can be changed in vivo, e.g. biorelevant dissolution media or gastric juice composition and volume, feeding state, or gastric hydrodynamics, a prediction of the extent of drug release is difficult from in vitro data. [76, 77]

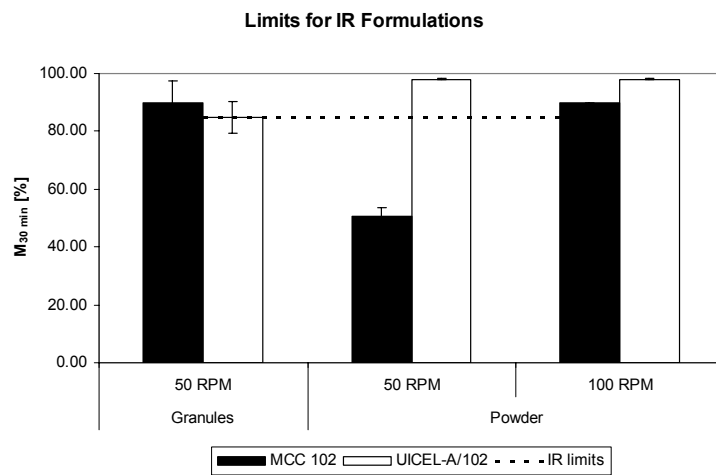


Figure 98: M_{30 min} and IR-limits for tablets made from granules or powder.

To compare dissolution profiles, the concept of difference factor and similarity factor seemed favourably, since this method supported the comparison of dissolution profiles after major changes, e.g. granulation. [82]

Table 56: Difference factor f_1 and similarity factor f_2 of formulations with MCC 102 or UICEL SM; reference formulation: powder 50 RPM.

	MCC 102		UICEL SM	
	granules	100 RPM	granules	100 RPM
f_1	401	213	18	81
f_2	16	24	44	26

RESULTS AND DISCUSSION

According to the values in Table 56, no similarity was found between powder dissolution and granules dissolution independent of the filler. Granulation was a major change in formulation which requires further investigations. Paddle speed changed the dissolution profile in an extent that no similarity was detectable anymore. These findings were in good agreement with the qualitative analysis of the curves in Figure 96 and Figure 97. The small differences between the reference and UICEL SM “granules” can be related to the similarity of the curves at the initial part.

Weibull equation was used to calculate $t_{90\%}$, the minimum coefficient of determination of 0.9879 was found for the MCC 102 powder formulation. Table 57 shows the values for $t_{90\%}$. Granulation reduced $t_{90\%}$, but a significant influence was only found for the MCC 102 powder formulation. A relation between fast drug release and short disintegration times could be found, but disintegration times were still clearly faster than total drug release, disintegration test could therefore not be used to predict it. Both fillers showed significantly reduced $t_{90\%}$ with increasing paddle speed. A clear delayed $t_{90\%}$ of MCC 102 powder tablets could be expected from the slower disintegration test without disks.

Table 57: $t_{90\%}$ values [min] of tablets made from granules or powder, incl. standard deviations in brackets.

	Powder		Granules
	50 RPM	100 RPM	50 RPM
MCC 102	128.38 (11.19)	23.04 (1.13)	13.83 (3.77)
UICEL SM	7.22 (1.56)	1.94 (0.31)	4.81 (3.30)

Influences of the formulations and the process as well as the analytical set-up were qualitatively described in Figure 96 and Figure 97, model independent approaches as well as Weibull implementation proved differences. With further model dependent approaches the release kinetics were studied.

Table 58 lists the dissolution rates fitted according to the first order model. Coefficients of determination below 0.9900 were related to non robust drug release. All experimental data fitted adequately to first order model. Independent of the filler, dissolution rate at 100 RPM was significantly faster compared to 50 RPM. At 50 RPM, UICEL SM granules formulation

released significantly faster compared to the powder formulation. No statistical difference was found for MCC 102 formulations. Comparison between powders showed no statistical difference, whereas the UICEL SM granules formulation was significantly faster than the corresponding MCC 102 tablets.

Table 58: Dissolution rate k_1 [min^{-1}] of tablets made from powder or granules at different stirring rates, incl. standard deviations in brackets.

	Powder		Granules
	50 RPM	100 RPM	50 RPM
MCC 102	0.020 (0.002)	0.103 (0.007)	0.220 (0.029)
UICEL SM	0.450 (0.099)	2.090 (0.197)	1.496 (0.522)

The correlation between the reciprocal of the first order dissolution rate k_1 and $t_{90\%}$ ($r^2 = 0.9986$) as well as between $1/k_1$ and the Weibull parameter a ($r^2 = 0.9976$) is shown in Figure 99. Faster dissolution rate k_1 was accompanied by reduced $t_{90\%}$ as well as reduced shape parameter a . This was expected since a correlation between a and k_1 was found and discussed earlier (Figure 84), the steeper slope of the correlation of k_1 and $t_{90\%}$ was related to the influence of b , which was included to calculate $t_{90\%}$.

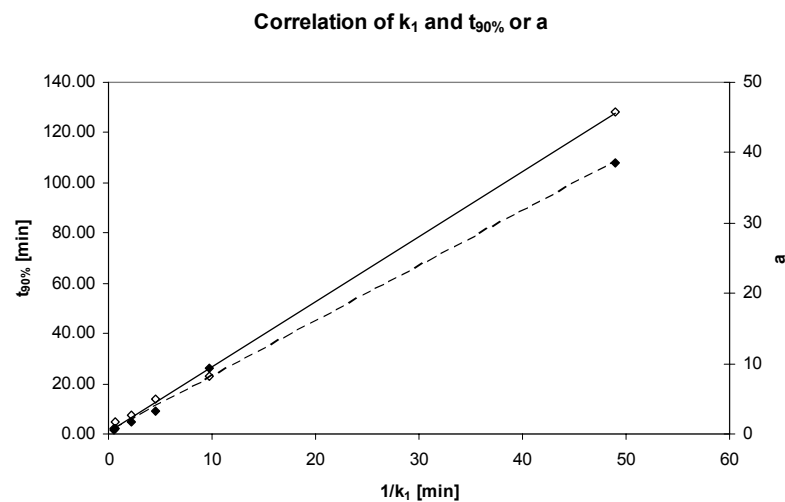


Figure 99: Correlation between the reciprocal of k_1 and $t_{90\%}$ (\diamond) or a (\blacklozenge), respectively.

RESULTS AND DISCUSSION

Furthermore, the experimental data were fitted to the Hixson-Crowell cubic root law, but the model was not adequate to describe drug release; the maximum coefficient of determination was found for MCC 102 powder formulations at 50 RPM ($r^2 = 0.9398$). This formulation was further fitted to the Higuchi model, but the model was neither appropriate to describe the profile since the kink appeared also here.

The idea of fitting the MCC 102 powder formulation to the Higuchi model was appropriate since directly compacted MCC 102 formulations with a low drug load are known to follow Higuchi kinetics (Figure 66). However, these formulations here contained approximately 70%(v/v) cellulose, this was not enough to embed proquazone in a non soluble matrix. Higuchi could therefore not be expected. This could be proved by comparing this formulation at 100 RPM in Figure 97 A, where the release followed ideally first order kinetics (minimal $r^2 = 0.9993$), and the formulation with 10% proquazone and MCC 102 at comparable relative density (ρ_m 0.8) and the same stirring rate (Figure 60 A). The slow release from this MCC 102 powder formulation was therefore only related to stirring rate. This influence was also described by Costa and Sousa Lobo [105] and Röst and Quist [106], and can be explained with respect to the model of Noyes-Whitney.

First order release described by the Noyes-Whitney equation requires a gradient between solubility (C_s) and the concentration (C) in the medium at time t . The thickness of the diffusion layer (h) is stagnant and inverse proportional to the dissolution rate. High drug concentration in the dissolution medium (above sink conditions) or poor mixing due to a slow stirring rate may lead to increased thickness of the boundary layer; a decrease in dissolution rate results. This could be shown here and in a previous section at high drug loads.

5.5 Quality of Fit

To compare the suitability of different models to describe experimental data, very often the dimensionless coefficient of determination r^2 is used. This is so far not correct, especially when a transformation of the data occurred before analysis, and was also criticized. [107] This chapter wants to focus now on the difficulties of model comparison, respectively model discrimination and the problems of the coefficient of correlation.

For this study, two model curves were selected; (1) 10% proquazone and Type I, compressed to ρ_m 0.7 and (2) 90% proquazone and Type I compressed to ρ_m 0.8. Four different model dependent approaches were used to describe drug release of formulations. The Weibull equation and the first order kinetics were determined with non-linear regression; therefore, no data transformation was required. The Hixson-Crowell and the Higuchi approach were determined by linear regression after data transformation. The correlation of determination was calculated as shown in Equation 28. Both values required were directly taken from Mathematica® print-out. The r^2 -value of the linear regression was directly received from Excel®.

$$R^2 = \frac{SQ_{\text{model}}}{SQ_{\text{total}}} \quad \text{Equation 28}$$

Table 59: Models, fitted parameters and their signification, coefficients of determination and residual sum of squares.

Model	Fitted parameters and their signification	Formulation 1		Formulation 2	
		R ²	SQ _{res} /no	R ²	SQ _{res} /no
Weibull	Scale parameter a which accounts for the time and shape parameter b which accounts for the curve shape	1.0000	0.15	0.99538	4.48
First order	k ₁ : dissolution rate constant	0.9971	11.47	0.99535	4.50
Hixson-Crowell	k ₂ : dissolution rate constant	0.9751	96.09	0.9959	1.97
Higuchi	k ₃ : dissolution rate constant	0.9921	24.59	0.9302	85.87

The residual sum of squares was considered as the square of the difference between the experimental data (◆, ◇) and the fitted value (—,). A high quality of fit is accompanied by a minimal residual sum of squares. When a transformation of the data was done, these sums of squares were transformed back to the non-transformed data set. Since not all models included the same number of data, the residual sum of squares was divided by the number of data included. Table 59 shows the not adjusted r^2 values and the residual sum of squares divided by the number of data points. From these data, one could

RESULTS AND DISCUSSION

clearly see that a reduction of the r^2 value is accompanied by an increase of the residual sum of squares.

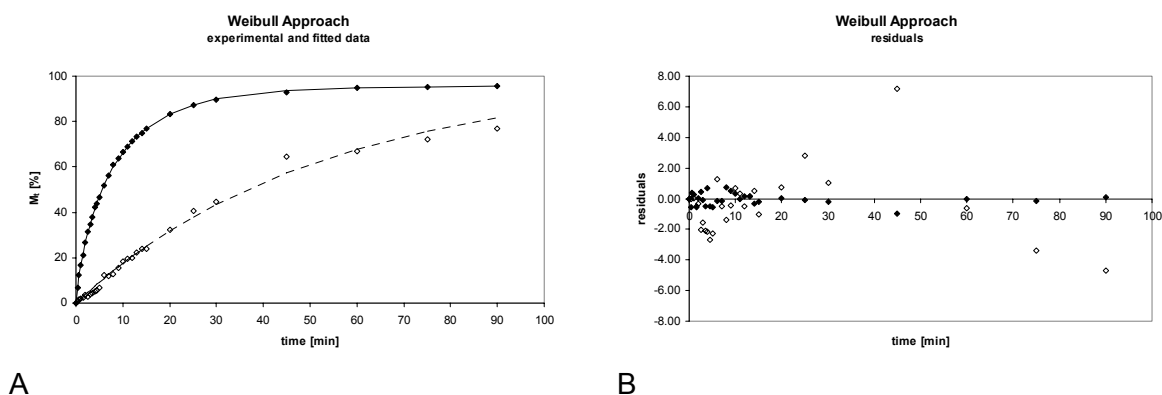


Figure 100: Experimental and fitted data according to the Weibull equation (A) and the distribution of the residuals (B).

Legend: Experimental (dots) and fitted values (lines) for formulation 1 (◆, ----) and formulation 2 (◇,).

Figure 100 A shows the experimental and fitted data according to the Weibull approach. The excellent quality of fit is clearly visible from the data plotted in Figure 100 A and could be expected from the values of Table 59. The most important information concerning the quality of fit is, however, the evaluation of the residuals in Figure 100 B. The residuals scattered randomly around zero, this is regarded as a sign the selection of a suitable model and a high quality of fit.

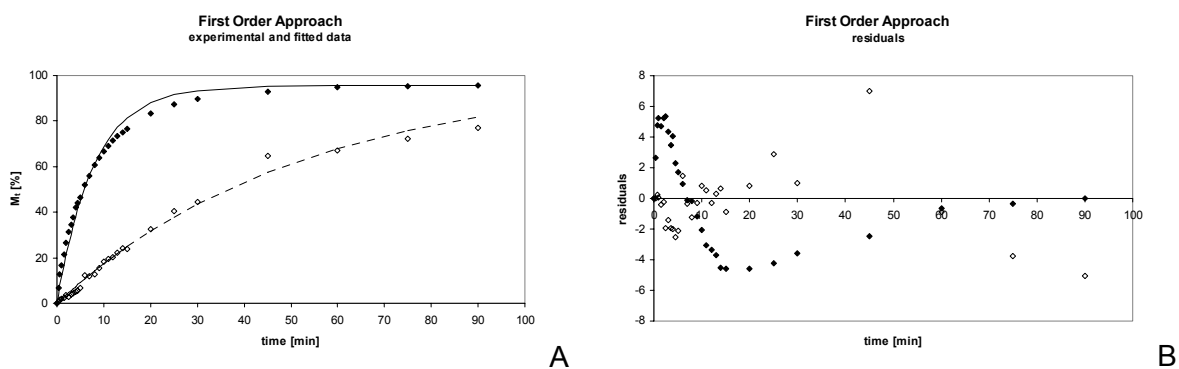


Figure 101: Experimental and fitted data according to the modified Noyes-Whitney equation (A) and the distribution of the residuals (B).

Legend: Experimental (dots) and fitted values (lines) for formulation 1 (◆, ----) and formulation 2 (◇,).

Regarding the plot of the residuals in Figure 101 B, one could see that the fitted curve of formulation 1 deviated in two phases from the experimental data, whereas the residuals of formulation 2 scattered around zero without trend. The trend of (B) could also be detected in (A). The experimental data of formulation 1 showed an initial faster release than expected from the model. The scattering of the residuals of formulation 2, on the other hand, is a good sign that the curve fits well the data.

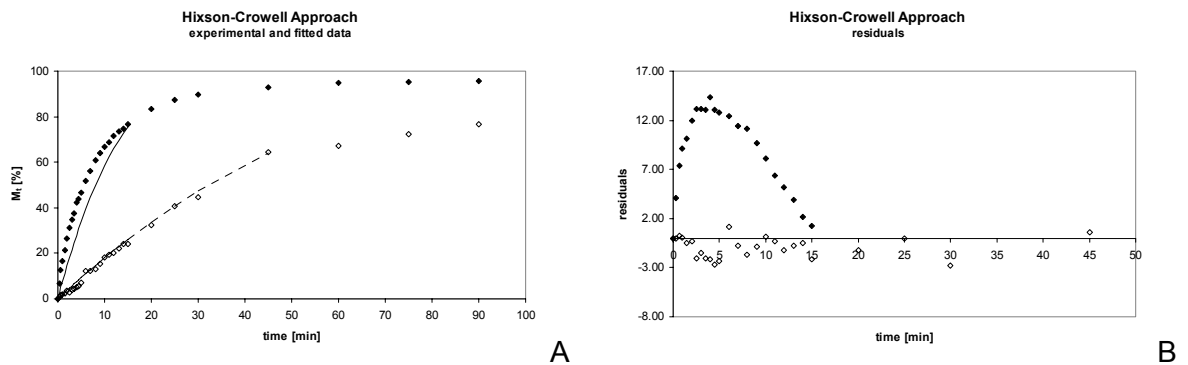


Figure 102: Experimental and fitted data according to the Hixson-Crowell equation (A) and the distribution of the residuals (B).

Legend: Experimental (dots) and fitted values (lines) for formulation 1 (◆, - - - -) and formulation 2 (◇,).

The Hixson-Crowell approach fitted fairly well to the data of formulation 2. The residuals shown in Figure 102 B were small and scattered around zero. The horseshoe-shaped distribution of the residual of formulation 1 already gave an impression on the fit of the curve. The experimental data in (A) showed a distinctive curvature compared to the fit.

The Higuchi approach was a special case since no back transformation was required. The residual sum of squares accounts for the differences on the y-axis. Since the transformation was done on the x-axis, it did not influence the result. Figure 103 shows the fit of Higuchi equation to the experimental data of formulation 1 and formulation 2. The poor quality of fit was clearly visible from the experimental data and the fitted curve in (A) and was proved by the analysis of the residual in (B).

RESULTS AND DISCUSSION

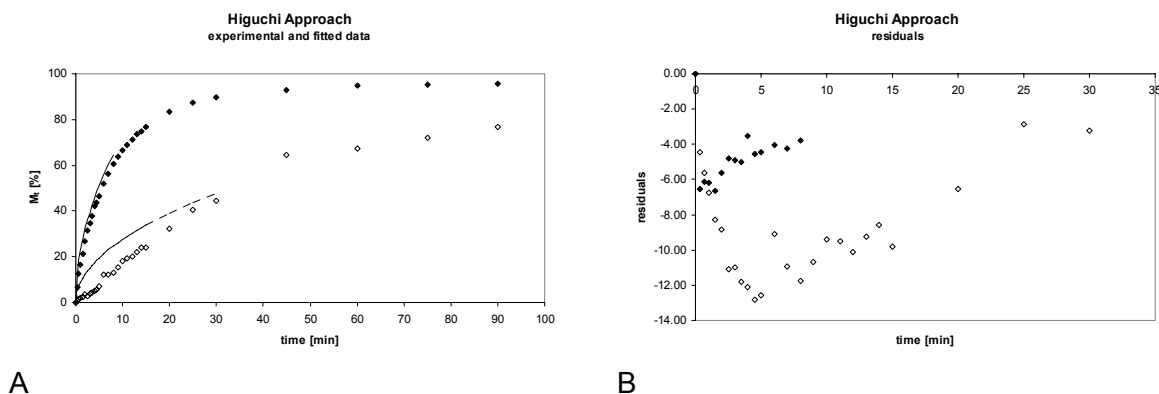


Figure 103: Experimental and fitted data according to the Higuchi equation (A) and the distribution of the residuals (B).

Legend: Experimental (dots) and fitted values (lines) for formulation 1 (◆, - - - -) and formulation 2 (◇,).

In case of formulation 1, the Weibull equation showed the best result. A minimal sum of squares and a regular scatter of the residuals confirmed the maximum r^2 value. Formulation 2 showed a minimal sum of squares for the Hixson-Crowell model; the distribution of the residuals showed no trend.

In conclusion, one could say that the analysis of the sum of squares, especially the analysis of the residuals, improves the meaningfulness of the fitting. Every fitted curve should be accompanied by the representation of the analysis of residuals. They should randomly scatter around zero without showing a trend.

In this context, it has to be kept in mind, that the wide applicability of the Weibull equation and the high quality of fit is not surprisingly, since two parameters, a and b , are available to adjust the curve to the data. This fact has been taken into account in a separate column of Table 59, describing the parameters of the different models available for adjustment of the data. In the additional column the meaning of the parameter is described. A model equation can be described as optimal if the number of parameters available for the fit can be kept at a minimum. Ideally the model is not an empirical equation but the meaning of the parameter is clearly based on a physical model such as Fick's law of diffusion.

6 Conclusions and Outlook

6.1 Selection and Comparison of Models

The implementation of an experiment results in a set of data, such as the resulting relative density after compaction with a defined compaction pressure or the accumulated drug amount at a certain time t . This data can give already an idea of the behaviour of a substance, e.g. compressibility or dissolution behaviour, but a comparison of different formulations is only possible with methods based on statistics, such as ANOVA, MANOVA, or difference and similarity factor. Sometimes, the comparison of single values is already enough, but to get a deeper insight in the behaviour of materials, it is advised to use different models to evaluate the experimental data. This was done in this study with respect to compressibility and compactibility and dissolution. Details on the evaluation of the models are given in the following sections; this section focuses on general consideration.

The comparison of compressibility and compactibility as well as dilution capacity are based on the results and the significance, the confidentiality, and feasibility of the model. This will be discussed and assessed later.

More interesting was the evaluation of the dissolution, where the same data were fitted to different models to obtain information about release kinetics. Therefore, a model with physical background such as the Fick's law of diffusion is preferred. But which is the suitable model to describe the drug release? Initially, it might be useful to assess the experimental data to exclude models, which are contradictory to the results, e.g. sustained-release models in case of rapidly dissolving immediate release formulations. Furthermore, an adequate number of data should be available and the number of fitted parameter should be minimal. After selection of appropriate models, the data set is fitted to them. But how to compare them now? Very common is the use of the coefficient of determination (r^2). This value is either directly available from the software or can easily be calculated as done in this study. The comparison of this value may be misleading, when no further investigations are done. This is particularly the case if transformed data, e.g. in case of the Hixson-Crowell approach, are fitted. An alternative strategy is required in that case. The use of the residual sum of squares might be a solution. High quality of fit is accompanied by minimal residual sums of squares. If transformed data are used, the sum of squares just has to be transformed back and can be used for comparison. To avoid distortion by different numbers of data points which may influence the residual sum of squares it is advised to divide the

CONCLUSIONS AND OUTLOOK

residual sums of squares by the number of data points. Beside the assessment of the quality of fit by the residual sums of squares, the model can also be studied based on the distribution of the residuals. Ideally, the residuals are randomly scattered around zero without showing a tendency.

For further studies, where data are fitted to different models, it is advised to evaluate the residual sum of squares and plot the experimental and fitted data as well as the distribution of the residuals.

6.2 Compressibility and Compactibility

Common methods to assess compressibility of powders are Heckel equation and modified Heckel equation. Both models are well established in pharmaceutical technology and many substances were already investigated. New materials are therefore preferentially assessed using one of those models, since comparison with well known substances may be possible. The clear advantage of the Heckel equation is the simple evaluation with linear regression. The modified Heckel equation, which gave the same results in this study, requires non-linear regression. The increased sensitivity and mainly the ease of application support the use of the Heckel equation.

The recently introduced modified Van der Waals equation of the state was found to be an interesting tool to evaluate the compressibility of powders. The concept is based on the idea that powder systems can behave like a gas, like a liquid and/or like a solid, and powders can hence be compressed like a gas. [108] in both cases compression leads to a phase transition, i.e. from the gaseous to the liquid state or from a disperse particulate state to a solid such as a tablet. The clear findings from Lanz [27], including correlation between mean yield pressure and van der Waals parameters C_V and A_V , could not be proved since the characteristics of the different samples were maybe too similar. Disadvantages of this model are clearly the complex evaluation of the data, where with only two input variables, compaction pressure σ and corresponding relative density ρ_r , three parameters are received, A_V , B_V , and C_V . Additionally to the fairly high number of parameters, the true volume V_t is already an average value and therefore also afflicted with an error. This contradicts the demands on a model as discussed above. Furthermore, it was not possible to include the full range of data, as it was proposed by Lanz [27]. In the data range of the modified Heckel equation, i.e. up to 105 MPa, this new model was applicable.

Further models to describe compressibility were evaluated. Carr's Index, even though it is called compressibility index, is not suitable to characterise compressibility behaviour of powders. The findings made in this study did not correlate with more scientific approaches as Heckel equation and modified Heckel equation. Carr's index, comparable to the Hausner factor, may be suitable to estimate powder flow properties as intended by the European Pharmacopoeia 5.3. [35] The use of the resulting compaction force RCF is neither a satisfying model. Inaccuracy of the tablet press, ambient differences, and the small number of values gave poor results. In development, RCF seems not to be appropriate, whereas later, when the machine parameters are well established and the process is validated, the control of the resulting compaction force can be a useful tool to ensure quality with respect to the principles of PAT.

Considering the different methods, the Leuenberger equation was assessed as the most appropriate model. Heckel equation and modified Heckel equation are, as discussed, very common to describe compressibility, i.e. the volume reduction under pressure. However, information about the hardness of a tablet, i.e. mechanical resistance, is more important for further steps as tablet coating, storage, transport, and packaging.

The Leuenberger equation is very useful to assess material properties, especially because it includes the mechanical resistance of a tablet. Furthermore, pressure susceptibility γ_t can be used to establish compressibility. The meaningfulness of γ_t is limited as no correlation between γ_t and K from Heckel was found. The compactibility of materials assessed using the maximum possible tensile strength $\sigma_{t \max}$, could be confirmed by MCC 102 – modified cellulose binary mixtures and ternary mixtures. Only one exception was detected. A higher $\sigma_{t \max}$ value was found for Type I compared to MCC 102, tensile strength determination on the other hand showed the opposite. This inconsistency can be attributed to the method of hardness determination. The use of tensile strength is indeed only allowed when ideal fracture occurs. [41] Since this was not the case in this study, a more appropriate method to determine hardness, e.g. Brinell hardness, may result in a better agreement. It was possible to show that tensile strength can be used to assess compactibility simply and fast, without expenditure of time and material, but limits were found in case of drug load. Binary mixtures of proquazone and cellulose were not suitable since abrupt changes in the compaction behaviour appeared with increasing drug load. This is attributed to the dilution capacity of an excipient.

CONCLUSIONS AND OUTLOOK

Three different models to calculate dilution capacity were investigated using three different relative densities. After careful evaluation, the rule of thumb (Equation 15) was selected as the most appropriate model. The advantage of this rule of thumb is the easy application using the relative tap density $\rho_{r\text{ tap}}$ supposed by Lanz [27]. The model of Kuentz and the model of Lanz are certainly closer to the theoretical background of percolation theory, but the investment of time in contrast with the return of information is not balanced. With respect to the theory, the most accurate results are expected from using the critical relative density ρ_c . Since determination of this value is related to time and material consuming determination of the modified Heckel equation, a replacement value is proposed. Both authors suggest using the relative tap density $\rho_{r\text{ tap}}$ to be on the safe side. [27, 54] From the experience gained during these studies it may be more appropriate to use the relative bulk density $\rho_{r\text{ bulk}}$, since these values were very close to ρ_c . Discrete clusters of powder particles dispersed in air, as it is assumed for the relative bulk density, cannot exist due to gravitation. The relative bulk density determined is hence close to the critical relative density established using the modified Heckel equation.

Safety should not be overestimated, since all models are based on the assumption that the tablet shows 0% porosity, which is not found in reality. A decrease of the tensile strength was accompanied by the increase of the porosity. Keeping this in mind, it is evident that dilution capacity is useful to roughly estimate the maximum possible fraction of the drug; therefore, a rough estimation using the rule of thumb is sufficient.

Finally, some general considerations on compressibility and compactibility and the related parameters should be discussed. It was shown in this work that the relative density has an influence on the tensile strength and has therefore to be considered. To compare materials or formulations it is not appropriate to compress tablets with constant compaction pressure, since this may result in different relative densities. Alternatively, tablets should be compressed to a specific relative density. This may be difficult, if minimally one component shows high elastic recovery, which influences the final tablet porosity. In this work linearity between elastic recovery and amount of modified cellulose was found. In case that this linearity can be confirmed with further studies, it can be taken into considerations and allows an estimation of the effect on the final product. The same approach can be used for tensile strength, where linearity was found at low drug loads, i.e. the cellulose was dominating the system.

6.3 Liquid - Solid Interactions

Liquid – solid interactions were studied with different methods. Water uptake rate which is the first step in all liquid – solid interactions was not very suitable to evaluate the different celluloses. The method was indeed easy to apply, but the shapes of the water uptake profiles were fairly variable, hence proper evaluation was difficult and the average water uptake rates of the different formulations showed high standard deviations. The correlation of water uptake rate and disintegration time and dissolution rate, which is described in literature [68], was not confirmed. Short disintegration times were independent of the water uptake rate; this allows the conclusion that a further parameter, e.g. the swelling force, may be responsible for disintegration. These swelling forces have to be stronger than the cohesive binding forces in tablet for efficient disintegration. The disintegration of UICEL S formulations was very fast independent of the cohesive forces; this confirms the assumption that swelling forces exist. However, disintegration times of MCC 102 and Type I, the substances which were not as efficient as Class 3 and 4 excipients, were influenced by the cohesive forces of the tablets. Increased swelling forces in cellulose II products are known [27], but should be investigated in further studies to prove if differences between the types of cellulose can explain differences in the disintegration behaviour of them. The application of water uptake rate can not be proposed to predict disintegration and dissolution behaviour.

Disintegration test is well established and often used in routine quality control. Limits of this method were found in this study. The European Pharmacopoeia requires the use of disks in case of non coated tablets. [35] It could be shown that disintegration time is strongly influenced by the use of disks. One has to keep in mind that the movement of the disks act like external forces that can destroy the tablet. A better correlation between disintegration time and $t_{90\%}$ was found when no disks were used, but also then, a delay between complete disintegration and complete drug release was found. A direct statement on release properties after disintegration test is hence only reduced permissible.

The problem of the disintegration test as given by the European Pharmacopoeia is the lack of sensitivity. First, the measurement is based on a single-point determination, where after 15 minutes all six tablets have to be disintegrated. Qualitative differences between tablets are not considered, even though differences in drug release can be expected when the disintegration time is shifted, for instance, from 1 to 14 minutes. Furthermore, it was shown in this study that disintegration times shorter than five minutes do not have to be related to IR formulations. Beside the determination of the exact endpoint, the compendial method neither takes into account the particle size when particles pass the mesh of the

CONCLUSIONS AND OUTLOOK

disintegration basket. Poor drug release properties of MCC 102 and Type I were related to the inclusion of the drug in coarse cellulose particles. The final particle size may depend on cohesive forces as well as on disintegration forces, and may be accounted as a quality parameter. It may be interesting to study critical formulations, such as low drug load formulations with MCC 102 at different relative densities with respect to dissolution. In general, it is advised to investigate on the final particle size to estimate drug release and, furthermore, to prove a possible correlation between disintegration and drug release efficiency.

Compared to water uptake rate measurements, disintegration time determination was slightly more decisive, but the best discriminative power was found with dissolution studies. The main advantages of dissolution are, beside the discriminative power, also the significance in product development with respect to bioavailability and the wide variety of evaluation methods. Dissolution testing is clearly accompanied by increased investment of time and material, but in the development of dosage forms, a careful analysis of the drug release profile can expand the knowledge of drug and excipient properties. Later, in routine control, the work can be reduced to a more simple process as single-point or multi-point determinations. Important is also the proper evaluation of the method; apparatus, medium volume and composition, and, as shown, paddle speed may influence the drug release massively and lead to different results. This was shown in the example of the MCC 102 powder formulation which met the requirements of rapidly dissolving IR formulations only with an increase of the paddle speed to 100 RPM. In vitro studies are performed under constant conditions which cannot be taken as granted in vivo. Feeding state, content composition, and gastrointestinal motility may influence the drug release. As it is not yet possible to mimic the in vivo situation completely, it is advised to do it as much as possible, e.g. by performing studies in different media, at different pH values, with different volumes, and, especially, at different paddle speeds. A robust formulation should be independent of those factors.

To evaluate and compare drug release profiles, various approaches are possible. It was an aim of this study to evaluate different methods and, based on their advantages and disadvantages, to select the most appropriate one. Three main approaches were applied, (1) qualitative analysis, (2) model independent approaches, and (3) model dependent approaches.

Qualitative assessment of release profiles requires no further tools, but the meaningfulness, particularly in similar curves, is poor.

Model independent approaches are fairly simple to use and do not need knowledge on release kinetics; this on the other hand can also be criticized. In this study, three different model independent approaches were used. Initially, all formulations were tested on their suitability as rapidly dissolving IR formulations according to the FDA. [16] This method provides information about pass or fail, but gives no information about the time required to reach the limits. This is hence comparable to the compendial disintegration test. Based on the same data, $M_{30\text{ min}}$, ANOVA analysis was performed. ANOVA is very interesting when more than two formulations are compared. It can furthermore be used to compare release constants derived from model dependent approaches. As proposed for routine quality control, multi-point determination may be advantageous; the analysis can be done with MANOVA. The FDA favours the use of difference factor or similarity factor. [82] These methods are fairly unsuitable in development. A clear advantage of these approaches is the analysis which can be done by spread sheet analysis or even with a calculator. The problems are the limitation to only two curves that can be compared and the reference curve which has to be defined first. Both models may be useful in quality control, and, as supposed by the FDA, to quantify differences after changes. Furthermore, difference factor and similarity factor are only significant when drug release is slower than 85% in 15 minutes. Beside the mentioned advantages and disadvantages, the models showed often contradictory results.

After studying the different models, it can be concluded that ANOVA is very suitable to compare profiles, but the parameters to compare have to be properly selected and evaluated and in case that three or four formulations are compared, it may be advised to perform post hoc tests to prove differences between the formulations.

Four model dependent approaches were studied; three of them showed kinetic background, the fourth, the Weibull equation, is based on statistics. Fitting to this Weibull equation showed clearly the best results. This is not surprising since two parameters, a and b , are available to fit the curve. The advantage of Weibull, this was also useful in this study, is the wide applicability to different types of release kinetics. Negative arguments are certainly the lack of the kinetic background and the need of non-linear regression which requires special software and knowledge. As indicated, the release profiles followed different kinetics. Most of the formulations released the drug with first order kinetics. It is a very suitable model, since disintegration of the tablet did not show a negative impact. Furthermore, enough data were available since they were fitted using non-linear regression. However, an influence of the stirring rate and the exceeding of the sink conditions which both resulted in decreased dissolution rate was found. This is in good

CONCLUSIONS AND OUTLOOK

agreement with the theoretical considerations of the Noyes-Whitney equation and the layer model. [38] Cubic root release after the model of Hixson-Crowell was observed for 90% proquazone formulations, where the tablets did not break up but reduced the size proportionally. This is in good agreement with the theory. 50% proquazone formulations released the drug very fast; therefore, not enough data points were available for a proper evaluation according to the Hixson-Crowell approach. It is supposed that also these formulations may follow the cubic root law as long as the tablets do not break up. This is difficult to predict, since both, drug and excipient, are percolating the system. Further studies should be performed including more data points in the initial stage of drug release to prove this assumption. A special case was detected in 10% proquazone formulations. MCC 102 and in a smaller extent also Type I, both not very efficient disintegrants, showed a release kinetic which was best described using the square root law of Higuchi, which is valid for matrix release. Also this effect may be explained with percolation theory. At a drug load below the critical concentration, the drug is fully embedded into the matrix of non-soluble cellulose (D/E-formulation). The tablet may disintegrate in coarse particles from which the drug is then slowly released. To prove if this effect is influenced by the compaction pressure, it may be interesting to study the relation between compaction pressure and drug release on a critical formulation as 10% proquazone and MCC 102.

The difficulty of the selection of an appropriate model was discussed in the first part of this chapter. It is difficult to propose one model as the most appropriate one, with keeping in mind the lack of physical background and the insignificance of the fitted parameters a and b , the use of Weibull may be advised since all release kinetics may be described and furthermore compared.

6.4 Granulation

Influences of granulation were studied on two formulations and two preparations. No general conclusion with respect to compactibility can be drawn. MCC 102 formulations showed reduced tensile strength after granulation; UICEL SM, however, showed increased plasticity. Badawy [103] related the reduced compactibility to the primary particle porosity; this plays a minor role in this study, where the tablets were compressed to a comparable relative density. This observation may rather be explained by the smoothing effect of PVP on the particle surface, which again reduces the cohesive forces between the particles. This effect seems less important in case of UICEL SM, where the difference in tensile strength can also be related to the differences in relative density. The elastic recovery was not influenced by granulation, and showed higher values for UICEL SM. The reduction of

compactibility in case of MCC 102 should not be overestimated since the tablets still showed very high mechanical resistance.

More important effects were found concerning liquid – solid interaction. A reduction of the superdisintegrant performance as described by Zhao [104] was not found in this study; moreover, a clearly reduced disintegration time was established for MCC 102 formulations after granulation. A clear effect of granulation on UICEL SM formulations was not detected, since disintegration times were anyway very short ($15.7 \text{ s} \pm 1.03$) and the effect of the relative density could not be excluded. Water uptake rate was not influenced by granulation. The best discriminative results were also here determined by dissolution testing. Granulation promoted dissolution. In case of MCC 102 formulations, directly compacted powders did not even meet the requirements for rapidly dissolving IR formulations.

While water uptake rate was not positively influenced by granulation, a further effect influencing disintegration and dissolution must exist. On one hand, reduced cohesive forces are responsible; on the other hand, PVP may influence wettability of the drug. PVP is well distributed over all particles after granulation. Water which is transported via the cellulose network into the tablet can better dissolve the drug when PVP acts as a hydrophilizer. It is now the question why PVP has a positive effect after granulation, but not after direct compaction. The volume fraction of PVP, 5.99%(v/v) for UICEL SM and 6.12%(v/v) for MCC 102 direct compacted formulations, is below the critical fraction of 16%(v/v) for spherical particles. PVP which is fairly spherical as shown in Figure 16 does not percolate the tablet. Solubilization of PVP before spraying leads to better distribution and hence better dissolution.

Regarding the release kinetics, all formulations followed the first order model. This could be expected from the studies of binary mixtures, where UICEL S formulations fitted, independent of the drug load, to this model, whereas MCC 102 formulations were influenced by that. Above the theoretical critical drug concentration of 16%(v/v), the sole control of MCC 102 vanishes. This was clearly the case in granulation studies where the drug load was greater than 20%(v/v).

It is difficult to give evidence on a process based on only four formulations. The problem is that the formulations do not show the same relative density. However, this is a prerequisite for a reliable comparison. To assess the influence of granulation, further studies are required. To confirm the effect of the binder, it is advised to use different amounts of binder

CONCLUSIONS AND OUTLOOK

and even different types of binders, but it may also be interesting to study formulations at different relative densities to assess the influence on the cohesive forces. To prove the effect of the cellulose, it is recommended preparing formulations with a drug load below the critical concentration.

6.5 Evaluation of Cellulose Types

The assessment of different celluloses with respect to their suitability as excipient in rapidly dissolving immediate release formulations was one of the main scopes of this work. Based on the different models discussed before, all six celluloses were evaluated.

Class 1 (MCC 102) showed slow drug release and is therefore not suitable as pure filler in rapidly dissolving immediate release formulations. Class 2 (Type I) was a little faster, but as MCC 102, the drug release was slow and dependent on the relative density and the drug load. The advantages of Class 1 and 2 fillers are certainly the high bonding strength and the resulting strong tablets. According to the Leuenberger approach, no statistical difference was found between MCC 102 and Type I concerning the maximum tensile strength $\sigma_{t,max}$. This fact and the limits of the Leuenberger equation for very plastic materials may explain the findings of binary and ternary mixtures, where MCC 102 resulted in even stronger tablets than Type I. Class 2, obviously, shows only little differences compared to Class 1. The question is now, which role could this new partially converted product play in formulation design. It was shown in this work, that formulations with Type I, compared to MCC 102, showed first order release at least at lower relative densities. This excipient could hence be used as filler in slow dissolving IR formulations, preferably at smaller relative densities, which still show appropriate mechanical resistance. Furthermore, it may be appropriate to add Type I in mixtures to increase the mechanical resistance of a tablet accompanied by a small disintegrating effect. On the other, one should keep in mind that the development of this material requires high investment of knowledge and costs to achieve a robust product with a reproducible degree of conversion. Prior to invest more efforts in the production of this material, it may be advantageous to prove alternative materials on the market.

The clear advantages of Class 3 (UICEL S, Type II, and UICEL B) are worth this investment. The good properties of fully converted cellulose II products found in earlier studies could be confirmed. All three tested materials were clearly suitable for rapidly dissolving immediate release formulations independent of the relative density and the drug load. The compactibility of all three materials was significantly reduced compared to Class

1 and 2. According to the Leuenberger approach, both samples, Type II and UICEL B, did not differ significantly compared to the standard UICEL S. The best compactibility within class 3 was found for Type II, this may be related to the fibrous structure; no negative impact of the reduced crystallinity was found because the reduced crystallinity. UICEL S formulations resulted in harder tablets than those made with UICEL B. The original idea was to develop an all-in-one filler/binder/disintegrant. [9] Based on the experience of this study, modified cellulose may be used as a multifunctional excipient, but with respect to the reduced compactibility, mixtures of Class 1 and 3 fillers may be favourable. It could be shown that an amount of 22.5% modified cellulose already results in rapidly dissolving immediate release formulations, with Type II, furthermore, the critical load was 4.5%. Since UICEL S and UICEL B behaved comparable to Type II, the same critical amount can also be expected. Since this is only an assumption, it is recommended proving this. Mixtures of Class 1 and 3 show advantageous in mechanical resistance, which can be a critical point in formulation design. If a relationship between the load of modified cellulose and the tensile strength can be established, it can furthermore be used to estimate the mechanical resistance in mixtures. Class 3 substances can additionally be used in granulation processes which promote dissolution. A common feature of all class 3 celluloses is the increased elastic recovery which did not negatively influence compactibility and disintegration. Furthermore, improved liquid – solid interactions were found and confirmed. Type II shows the fastest water uptake rate, which can be related to the fibrous structure. Class 4 (UICEL-XL) seemed to be the cellulose which is best suitable as an all-in-one filler/binder. Compared to Class 3, compactibility was increased retaining comparable disintegration times. As already discussed before, one should not forget the costs of such a product, where production includes many steps as conversion and cross-linking. UICEL-XL is clearly advantageous compared to UICEL-A/102 or comparable materials, but with respect to the expenditure, a simple fully converted cellulose II in mixture with the strong binding microcrystalline cellulose may be favourable in formulation design.

A common feature of all discussed modified celluloses is the high moisture content which exceeds the already high moisture content of MCC 102. This may lead to stability problems in formulations with moisture sensitive drugs.

To reduce time and cost of product development, different tools were introduced during the last few years. A major role plays clearly Quality by Design (QbD). In early steps, especially when novel excipients are introduced, the knowledge space should carefully be evaluated.

CONCLUSIONS AND OUTLOOK

This includes preformulation, where the drug properties are studied, as well as first formulations studies. Within this space of knowledge, more detailed investigations are required to identify the design space where material attributes, e.g. origin and production procedure of raw materials, formulation parameters, e.g. drug load or amount of disintegrant, and process parameters, e.g. relative density, assure quality. Including in silico knowledge based on databases or simulation may simplify and speed up the process of development and reduce time and costs to market.

6.6 Outlook

In previous studies as well as in this work, UICEL-A/102 was mainly used in very small to small scale. Direct transfer of this knowledge to large scale production would certainly result in non robust processes. To gain more information about process parameters, product properties, and evaluation methods further investigations should be done.

The use of modified celluloses was intended for direct compaction. First, trials of wet granulation using UICEL-A/102 (S) were done in this and a previous study [40]. Since this material also showed beneficial properties after wet granulation, further investigations may be interesting with respect to the binder type and amount. Furthermore, formulations may be compared at different relative densities to assess the influence of the cohesive forces. To prove the effect of the cellulose, it is recommended preparing formulations with a drug load below the critical concentration. Furthermore, the use of modified cellulose in dry granulation should be proved. To get additional information about the process, it may be favourable to use instrumented lab scale equipment of the same type as later used in production. The compaction process is a crucial parameter for the quality of the final product; the use of a compaction simulator to study powder or granules compaction in a small scale but mimicking large scale conditions can save material and time and may already give important knowledge about critical parameters. The risk of non robust processes can be reduced by the early implementation of PAT and the proper definition of the design space.

A critical drug load which is related to dilution capacity was determined in this work. Further experiments with additional drug loads may enclose the design space. The knowledge of the interplay between active ingredient and excipient is based on only one active principle. The use of further drugs with different physical-chemical properties, e.g. different solubility and wettability, ionized drugs, etc., should be studied. In ternary mixtures, a critical mass

fraction of Type II was found at 4.5%, the same mass fraction was assumed for UICEL S and UICEL B. To confirm this, further studies with even lower mass fraction should be performed. These ternary mixtures were only implemented using proquazone and celluloses. It may be interesting to investigate also the interplay between modified celluloses and other excipients, e.g. starch, lactose, or calcium hydrogen phosphates. At the same time, modified celluloses may be differentiated from those excipients. This differentiation may be important with respect to the above mentioned processes and process parameters. To increase the knowledge about critical parameters of modified celluloses, it is advised to determine quantitatively the crystallinity and the degree of polymerisation. The high moisture content of modified celluloses might be problematic in case of moist sensitive drugs; at the same time, one could take advantage of that and use it in the stabilization of a hydrated active ingredient. Furthermore, modified cellulose may be applied in other fields of pharmaceutical technology or food industry.

Expanded investigations of certain methods used in this study are proposed. The use of the resulting compaction force RCF which was not useful in this study may be suitable as a control tool in large scale production; proper analysis of these data derived from instrumented lab scale equipment should be included. Even though the results of the modified Van der Waals equation of the state were not fully satisfactory, further experiments should be performed including plastic, elastic, and brittle materials. Moreover, flowability of modified celluloses should be tested using the funnel method with respect to the conditions in scale up and production.

For a better correlation of all liquid – solid interactions, water uptake rate, disintegration test, and dissolution method have to be improved. If water uptake rate determinations are required in future experiments, a proper method development and validation has to be done. The determination of the swelling force may be more useful since this is an important property of a good disintegrant. It is advised to study disintegration additionally, or even only, without disks, since their movements may destroy tablets and distort the results. It may be interesting to study critical formulations, such as low drug load formulations with MCC 102 at different relative densities with respect to the final particle size, cohesive and disintegration forces, and dissolution. To increase the power of dissolution models, more data points in the first few minutes should be generated. Therefore, it may be useful to measure dissolution continuously. Furthermore, when different model should be compared, it is advised to study the residuals of the model in the non-transformed space to assess the quality of fit.

7 References

- [1] W. Forth, D. Henschler, W. Rummel, U. Förstermann, K. Starke, Allgemeine und spezielle Pharmakologie und Toxikologie, Urban & Fischer Verlag, München - Jena, 2001.
- [2] I. Zimmermann, Galenik oder wie aus einem Wirkstoff ein Arzneimittel wird. Teil I: Einführung und chemische sowie physikalisch-chemische Prinzipien. Chemie in unserer Zeit 23(4) (1989) 114-120.
- [3] I. Zimmermann, Galenik oder wie aus einem Wirkstoff ein Arzneimittel wird. Teil II: Entwicklung eines Arzneimittels in der Praxis. Chemie in unserer Zeit 23(5) (1989) 161-169.
- [4] G.L. Amidon, H. Lennernäs, V.P. Shah, J.R. Crison, A Theoretical Basis for a Biopharmaceutic Drug Classification: The Correlation of in Vitro Drug Product Dissolution and in Vivo Bioavailability. Pharmaceutical Research 12(3) (1995) 413-420.
- [5] K.H. Bauer, K.-H. Frömmling, C. Führer, Lehrbuch der Pharmazeutischen Technologie: mit einer Einführung in die Biopharmazie, Wissenschaftliche Verlagsgesellschaft mbH, Stuttgart, 2002.
- [6] A.H. Kibbe, Handbook of Pharmaceutical Excipients, Pharmaceutical Press, London, 2000.
- [7] V. Kumar, M.d.I.L. Reus-Medina, D. Yang, Preparation, Characterization, and Tableting Properties of a New Cellulose-based Pharmaceutical Aid. International Journal of Pharmaceutics 235(1-2) (2002) 129-140.
- [8] V. Kumar, M.d.I.L. Reus Medina, H. Leuenberger, Cross-linked Powered/Microfibrillated Cellulose II, Application: US Patent, 29.12.2005, 2005.
- [9] M.d.I.L. Reus Medina, V. Kumar, Evaluation of Cellulose II Powders as a Potential Multifunctional Excipient in Tablet Formulations. International Journal of Pharmaceutics 322(1-2) (2006) 31-35.
- [10] M.d.I.L. Reus Medina, V. Kumar, Modified Cellulose II Powder: Preparation, Characterization, and Tableting Properties. Journal of Pharmaceutical Sciences 96(2) (2007) 408-420.
- [11] M.d.I.L. Reus Medina, M. Lanz, V. Kumar, H. Leuenberger, Comparative Evaluation of the Powder Properties and Compression Behaviour of a New Cellulose-based Direct Compression Excipient and Avicel PH-102. Journal of Pharmacy and Pharmacology 56(8) (2004) 951-956.
- [12] P. Suresh, P.K. Basu, Improving Pharmaceutical Product Development and Manufacturing: Impact on Cost of Drug Development and Cost of Goods Sold of Pharmaceuticals. Journal of Pharmaceutical Innovation 3 (2008) 175-187.
- [13] FDA, Guidance for Industry - PAT - A Framework for Innovative Pharmaceutical Development, Manufacturing, and Quality Assurance. in: F. D. A. U.S. Department of Health and Human Services, Center for Drug Evaluation and Research (CDER) (Ed.), 2004.

- [14] J.F. MacGregor, M.-J. Bruwer, A Framework for the Development of Design and Control Spaces. *Journal of Pharmaceutical Innovation* 3 (2008) 15-22.
- [15] R. Nosal, T. Schultz, PQLI Definition of Criticality. *Journal of Pharmaceutical Innovation* 3 (2008) 69-78.
- [16] FDA, Guidance for Industry - Waiver of In Vivo Bioavailability and Bioequivalence Studies for Immediate-Release Solid Oral Dosage Forms Based on a Biopharmaceutics Classification System. in: F. D. A. U.S. Department of Health and Human Services, Center for Drug Evaluation and Research (CDER) (Ed.), 2000.
- [17] P.H. Karpinski, Polymorphism of Active Pharmaceutical Ingredients. *Chemical Engineering & Technology* 29(2) (2006) 233-237.
- [18] D.J.W. Grant, in: H. G. Brittain (Ed.), *Polymorphism in Pharmaceutical Solids*, Vol. 95, Marcel Dekker, Inc., New York, 1999, pp. 1-33.
- [19] A.T. Florence, D. Attwood, *Physicochemical Principles of Pharmacy*, Palgrave, New York, 1998.
- [20] D. Singhal, W. Curatolo, Drug Polymorphism and Dosage Form Design: A Practical Perspective. *Advanced Drug Delivery Reviews* 56(3) (2004) 335-347.
- [21] J. Bauer, S. Spanton, R. Henry, J. Quick, W. Dziki, W. Porter, J. Morris, Ritonavir: An Extraordinary Example of Conformational Polymorphism. *Pharmaceutical Research* 18(6) (2001) 859-866.
- [22] A.J. Aguiar, J. Krc, A.W. Kinkel, J.C. Samyn, Effect of Polymorphism on Absorption of Chloramphenicol from Chloramphenicol Palmitate. *Journal of Pharmaceutical Sciences* 56(7) (1967) 847-853.
- [23] D. Giron, Le polymorphisme des excipients. *S.T.P. Pharma* 6(Hors-série) (1990) 87-98.
- [24] W. Blaschek, Cellulose, ein interessanter Grundstoff für die pharmazeutische Nutzung. *Pharmazie in unserer Zeit* 19(2) (1990) 73-81.
- [25] A.C. O'Sullivan, Cellulose: The Structure Slowly Unravels. *Cellulose* 4(3) (1997) 173-207.
- [26] V. Kumar, Powdered/Microfibrillated Cellulose, Application: WOWO Patent 6.821.531, 23.05.2002, 2002.
- [27] M. Lanz, *Pharmaceutical Powder Technology: Towards a Science Based Understanding of the Behaviour of Powder Systems*. Philosophisch-Naturwissenschaftliche Fakultät, Universität Basel, Basel, 2006.
- [28] D. Klemm, H.P. Schmauder, T. Heinze, in: S. de Baets, E. J. Vandamme and A. Steinbuechel (Eds.), *Biopolymers*, Vol. 6, Wiley-VCH Verlag GmbH, Weinheim, 2002, pp. 275-319.
- [29] S.H. Kothari, V. Kumar, G.S. Banker, Comparative Evaluations of Powder and Mechanical Properties of Low Crystallinity Celluloses, Microcrystalline Celluloses, and Powdered Celluloses. *International Journal of Pharmaceutics* 232(1-2) (2002) 69-80.

REFERENCES

- [30] Y. Nakai, E. Fukuoka, S. Nakajima, J. Hasegawa, Crystallinity and Physical Characteristics of Microcrystalline Cellulose. *Chemical & Pharmaceutical Bulletin* 25(1) (1977) 96-101.
- [31] R. Huettenrauch, I. Keiner, Wie kristallin sind "mikrokristalline" Cellulosen? *Pharmazie* 31(3) (1976) 183-187.
- [32] E. Doelker, R. Gurny, J. Schurz, A. Janosi, N. Martin, Degrees of Crystallinity and Polymerization of Modified Cellulose Powders for Direct Tableting. *Powder Technology* 52(3) (1987) 207-213.
- [33] G. Shlieout, K. Arnold, G. Müller, Powder and Mechanical Properties of Microcrystalline Cellulose With Different Degrees of Polymerization. *AAPS PharmSciTech* 3(2) (2002) 1-10.
- [34] M.d.I.L. Reus Medina, V. Kumar, Comparative Evaluation of Powder and Tableting Properties of Low and High Degree of Polymerization Cellulose I and Cellulose II Excipients. *International Journal of Pharmaceutics* 337(1-2) (2007) 202-209.
- [35] E. Pharmakopöekommission, European Pharmacopoeia. Deutscher Apotheker-Verlag, Stuttgart, 2005.
- [36] G.K. Bolhuis, Z.T. Chowhan, in: G. Alderborn and C. Nyström (Eds.), *Pharmaceutical Powder Compaction Technology*, Vol. 71, Marcel Dekker, Inc., New York, 1996, pp. 419-500.
- [37] M. Summers, M. Aulton, in: M. E. Aulton (Ed.), *Pharmaceutics: The Science of Dosage Form Design*, Churchill Livingstone, Oxford, 2002, pp. 364-378.
- [38] H. Leuenberger, *Physikalische Pharmazie: pharmazeutisch angewandte physikalisch-chemische Grundlagen* / Martin, Wissenschaftliche Verlagsgesellschaft mbH, Stuttgart, 2002.
- [39] H. Sucker, P. Fuchs, P. Speiser, *Pharmazeutische Technologie*, Georg Thieme Verlag, Stuttgart, 1991.
- [40] J.C. von Orelli, *Search for Technological Reasons to develop a Capsule or a Tablet Formulation*. Philosophisch-Naturwissenschaftliche Fakultät, Universität Basel, Basel, 2005.
- [41] H. Leuenberger, The Compressibility and Compactibility of Powder Systems. *International Journal of Pharmaceutics* 12(1) (1982) 41-55.
- [42] D. Train, An Investigation into the Compaction of Powders. *The Journal of Pharmacy and Pharmacology* 8(10) (1956) 745-761.
- [43] E.M. Rudnic, J.B. Schwartz, in: D. Troy (Ed.), *Remington: The Science and Practice of Pharmacy*, Lippincott Williams & Wilkins, Baltimore, Maryland, USA, 2005.
- [44] H. Rumpf, Basic Principles and Methods of Granulation. I. II. *Chemie Ingenieur Technik* 30 (1958) 144-158.
- [45] C. Führer, Substance Behavior in Direct Compression. *Labo-Pharma - Problemes et Techniques* 25(269) (1977) 759-762.

- [46] C. Nyström, G. Alderborn, M. Duberg, P.-G. Karehill, Bonding Surface Area and Bonding Mechanism - Two Important Factors for the Understanding of Powder Compactibility. *Drug Development and Industrial Pharmacy* 19(17-18) (1993) 2143-2196.
- [47] J.N. Israelachvili, *Intermolecular and Surface Forces*, Academic Press, London, 1985.
- [48] G. Bolhuis, N.A. Armstrong, Excipients for Direct Compaction-an Update. *Pharmaceutical Development and Technology* 11(1) (2006) 111-124.
- [49] R.W. Heckel, Density-Pressure Relationship in Powder Compaction. *Trans. Metall. Soc. AIME* 221 (1961a) 671-675.
- [50] R.W. Heckel, An Analysis of Powder Compaction Phenomena. *Trans. Metall. Soc. AIME* 221(1001-1008) (1961b).
- [51] M. Kuentz, H. Leuenberger, Pressure Susceptibility of Polymer Tablets as a Critical Property: A Modified Heckel Equation. *Journal of Pharmaceutical Sciences* 88(2) (1999) 174-179.
- [52] D. Blattner, M. Kolb, H. Leuenberger, Percolation Theory and Compactibility of Binary Powder Systems. *Pharmaceutical Research* 7(2) (1990) 113-117.
- [53] J.I. Wells, J.R. Langridge, Dicalcium Phosphate Dihydrate - Microcrystalline Cellulose Systems in Direct Compression Tableting. *International Journal of Pharmaceutical Technology & Product Manufacture* 2(2) (1981) 1-8.
- [54] M. Kuentz, H. Leuenberger, A New Theoretical Approach to Tablet Strength of a Binary Mixture Consisting of a Well and a Poorly Compactable Substance. *European Journal of Pharmaceutics and Biopharmaceutics* 49(2) (2000) 151-159.
- [55] J. Krämer, L.T. Grady, J. Gajendran, in: J. Dressman and J. Krämer (Eds.), *Pharmaceutical Dissolution Testing*, Taylor & Francis Group, LLC., Boca Ration, FL, USA, 2005, pp. 1-37.
- [56] C.D. Melia, S.S. Davis, Mechanisms of Drug Release from Tablets and Capsules .1. Disintegration. *Alimentary Pharmacology & Therapeutics* 3(3) (1989) 223-232.
- [57] E. Krausbauer, M. Puchkov, G. Betz, H. Leuenberger, Rational Estimation of the Optimum Amount of Non-Fibrous Disintegrant Applying Percolation Theory for Binary Fast Disintegrating Formulation. *Journal of Pharmaceutical Sciences* 97(1) (2008) 529-541.
- [58] W. Lowenthal, Disintegration of Tablets. *Journal of Pharmaceutical Sciences* 61(11) (1972) 1695-1711.
- [59] O. Enslin, Über einen Apparat zur Messung der Flüssigkeitsaufnahme von quellenden und porösen Stoffen und zur Charakterisierung der Benetzbarkeit. *Chem Fabrik* 6 (1933) 147-148.
- [60] H.V. Van Kamp, G.K. Bolhuis, A.H. De Boer, C.F. Lerk, L. Lie-A-Huen, The Role of Water Uptake on Tablet Disintegration. *Pharmaceutica Acta Helveticae* 61(1) (1986) 22-29.
- [61] W. Weibull, A Statistical Distribution Function of Wide Applicability. *Journal of Applied Mechanics* 18 (1951) 293-297.

REFERENCES

- [62] F. Ferrari, S. Rossi, M. Bertoni, C. Caramella, M. Geddo, Modeling of Water Penetration Into Fast Disintegrating Tablets. *S.T.P. Pharma Sciences* 1(2) (1991) 137-144.
- [63] E.W. Washburn, Dynamics of Capillary Flow. *The Physical Review* 17(3) (1921) 273-283.
- [64] F. Ferrari, M. Geddo, A. Gazzaniga, C. Caramella, U. Conte, Water Uptake to Fast Disintegrating Tablets and Weibull Function. *S.T.P. Pharma* 4(6) (1988) 481-484.
- [65] A.M. Guyot-Hermann, Tablet Disintegration and Disintegrating Agents. *S.T.P. Pharma Sciences* 2(6) (1992) 445-462.
- [66] R. Luginbühl, Anwendung der Perkolationstheorie zur Untersuchung des Zerfallsprozesses, der Wasseraufnahme und der Wirkstofffreisetzung von binären Tablettensystemen. Philosophisch-Naturwissenschaftliche Fakultät, Universität Basel, Basel, 1994.
- [67] J.L. Kanig, E.M. Rudnic, The Mechanisms of Disintegrant Action. 8(4) (1984) 50-63.
- [68] R. Luginbühl, H. Leuenberger, Use of Percolation Theory to Interpret Water Uptake, Disintegration Time and Intrinsic Dissolution Rate of Tablets Consisting of Binary Mixtures. *Pharmaceutica Acta Helvetiae* 69(3) (1994) 127-134.
- [69] P.H. List, U.A. Muazzam, Swelling - The Force That Disintegrates. *Drugs made in Germany* 22(4) (1979) 161-170.
- [70] R. Huettenrauch, I. Keiner, Neues hochwirksames Sprengmittel für Komprimat. *Pharmazie* 28(2) (1973) 137.
- [71] W.A. Ritschel, A. Bauer-Brandl, Die Tablette: Handbuch der Entwicklung, Herstellung und Qualitätssicherung., ECV - Editio Cantor Verlag, Aulendorf, 2002.
- [72] A. Dokoumetzidis, P. Macheras, A Century of Dissolution Research: From Noyes and Whitney to the Biopharmaceutics Classification System. 321(1-2) (2006) 1-11.
- [73] E. Pharmakopöekommission, Pharmacopoea Helvetica. Eidgenössische Drucksachen- und Materialzentrale, Bern, 1953.
- [74] E. Pharmakopöekommission, Pharmacopoea Helvetica, Eidgenössische Drucksachen- und Materialzentrale, Bern, 1986.
- [75] S. Azarmi, W. Roa, R. Loebenberg, Current Perspectives in Dissolution Testing of Conventional and Novel Dosage Forms. *International Journal of Pharmaceutics* 328(1) (2007) 12-21.
- [76] J.B. Dressman, G.L. Amidon, C. Reppas, V.P. Shah, Dissolution Testing as a Prognostic Tool for Oral Drug Absorption: Immediate Release Dosage Forms. *Pharmaceutical Research* 15(1) (1998) 11-22.
- [77] J. Dressman, B., C. Reppas, In Vitro - In Vivo Correlations for Lipophilic, Poorly Water-Soluble Drugs. *European Journal of Pharmaceutical Sciences* 11(Suppl. 2) (2000) S73-S80.
- [78] E. Galia, E. Nicolaidis, D. Hörter, R. Löbenberg, C. Reppas, J.B. Dressman, Evaluation of Various Dissolution Media for Predicting In Vivo Performance of Class I and II Drugs. *Pharmaceutical Research* 15(5) (1998) 698-705.

- [79] G. Freitag, Guidelines on Dissolution Profile Comparison. *Drug Information Journal* 35(3) (2001) 865-874.
- [80] P. Costa, J.M. Sousa Lobo, Modeling and Comparison of Dissolution Profiles. *European Journal of Pharmaceutical Sciences* 13(2) (2001) 123-133.
- [81] A. Rescigno, Bioequivalence. *Pharmaceutical Research* 9(7) (1992) 925-928.
- [82] FDA, Guidance for Industry - Dissolution Testing of Immediate Release Solid Oral Dosage Forms. in: F. D. A. U.S. Department of Health and Human Services, Center for Drug Evaluation and Research (CDER) (Ed.), 1997.
- [83] EMEA, Note for Guidance on the Investigation of Bioavailability and Bioequivalence. in: T. E. A. f. t. E. o. M. Products and E. o. M. f. H. Use (Eds.), London, 2001.
- [84] F. Langenbucher, Linearization of Dissolution Rate Curves by the Weibull Distribution. 24(12) (1972) 979-981.
- [85] J.E. Polli, G.S. Rekhi, L.L. Augsburger, V.P. Shah, Methods to Compare Dissolution Profiles and a Rationale for Wide Dissolution Specifications for Metoprolol Tartrate Tablets. *Journal of Pharmaceutical Sciences* 86(6) (1997) 690-700.
- [86] A.A. Noyes, W.R. Whitney, On the Rate of Solution of Solids In Their Own Solutions. *Z Phys Chem* 23 (1897) 689.
- [87] A.W. Hixson, J.H. Crowell, Dependence of Reaction Velocity Upon Surface and Agitation. I. Theoretical Considerations. *Journal of Industrial and Engineering Chemistry* 23 (1931) 923-931.
- [88] P.J. Flory, Molecular Size Distribution in Three Dimensional Polymers. I. Gelation. *Journal of the American Chemical Society* 63 (1941) 3083-3090.
- [89] W.H. Stockmayer, *Theory of Molecular Size Distribution and Gel Formation.*, Taylor & Francis, London, 1943.
- [90] S.R. Broadbent, J.M. Hammersley, Percolation Process. I. Crystals and Mazes. *Proc Camb Philos Soc* 53 (1957) 629-641.
- [91] D. Stauffer, A. Aharony, *Introduction to Percolation Theory*, CRC Press LLC, Boca Raton, FL, USA, 1994.
- [92] H. Leuenberger, The Application of Percolation Theory in Powder Technology. *Advanced Powder Technology* 10(4) (1999) 323-352.
- [93] R. Leu, H. Leuenberger, The Application of Percolation Theory to the Compaction of Pharmaceutical Powders. *International Journal of Pharmaceutics* 90(3) (1993) 213-219.
- [94] E. Krausbauer, *Contributions to a Science Based Expert System for Solid Dosage Form Design*. Philosophisch-Naturwissenschaftliche Fakultät, Universität Basel, Basel, 2007.
- [95] P.H. Stahl, *Feuchtigkeit und Trocknen in der pharmazeutischen Technologie*, Dr. Dietrich Steinkopff Verlag, Darmstadt, 1980.
- [96] A. Roos, P.H. Hinderling, Protein Binding and Erythrocyte Partitioning of the Antirheumatic Proquazone. *Journal of Pharmaceutical Sciences* 70(3) (1981) 252-257.

REFERENCES

- [97] S. Sweetman, Martindale: The Complete Drug Reference, Pharmaceutical Press, London, 2007.
- [98] E. Doelker, Comparative Compaction Properties of Various Microcrystalline Cellulose Types and Generic Products. *Drug Development and Industrial Pharmacy* 19(17&18) (1993) 2399-2471.
- [99] V. Kumar, S.H. Kothari, Effect of Compressional Force on the Crystallinity of Directly Compressible Cellulose Excipients. *International Journal of Pharmaceutics* 177(2) (1999) 173-182.
- [100] K. Obae, H. Iijima, K. Imada, Morphological Effect of Microcrystalline Cellulose Particles on Tablet Tensile Strength. *International Journal of Pharmaceutics* 182(2) (1999) 155-164.
- [101] K. Knop, Wirkstofffreisetzung aus festen Arzneiformen - Prüfmethoden, Auswertung, Einflussparameter. *Pharmazie unserer Zeit* 28(6) (1999) 301 - 308.
- [102] T. Higuchi, Rate of Release of Medicaments from Ointment Bases Containig Drugs in Suspension. *Journal of Pharmaceutical Sciences* 50 (1961) 874-875.
- [103] S.I.F. Badawy, D.B. Gray, M.A. Hussain, A Study on the Effect of Wet Granulation on Microcrystalline Cellulose Particle Structure and Performance. *Pharmaceutical Research* 23(3) (2006) 634-640.
- [104] N. Zhao, L.L. Augsburger, The Influence of Granulation on Super Disintegrant Performance. *Pharmaceutical Development and Technology* 11 (2006) 47-53.
- [105] P. Costa, J.M. Sousa Lobo, Influence of Dissolution Medium Agitation on Release Profiles of Sustained-Release Tablets. *Drug Development and Industrial Pharmacy* 27(8) (2001) 811-817.
- [106] M. Röst, P.-O. Quist, Dissolution of USP prednisone calibrator tablets Effects of Stirring Conditions and Particle Size Distribution. *Journal of Pharmaceutical and Biomedical Analysis* 31 (2003) 1129-1143.
- [107] J.M. Sonnergaard, On the Misinterpretation of the Correlation Coefficient in Pharmaceutical Sciences. *International Journal of Pharmaceutics* 321(1-2) (2006) 12-17.
- [108] H. Leuenberger, M. Lanz, Pharmaceutical Powder Technology - From Art to Science: The Challenge of the FDA's Process Analytical Technology Initiative. *Advanced Powder Technology* 16(1) (2005) 3-25.

8 Curriculum Vitae

Personal Information

Name Franziska Simone Müller
 Date of Birth 14.07.1980
 Place of Origin Oberhofen, AG

Education

2005 - 2008 PhD-Thesis under supervision of Prof. H. Leuenberger and Dr. G. Betz at the Institute of Pharmaceutical Technology at University of Basel
 09. 2004 Diploma in Pharmaceutical Sciences
 2000 - 2004 Studies in pharmaceutical sciences at the University of Basel
 1996 - 1999 Kantonales Gymnasium Liestal, Baselland

Teaching Experience

2005 - 2008 Assistant in practical courses on solid dosage forms for bachelor students in pharmaceutical sciences
 01. – 06. 2008 Supervision of the master thesis of M. von Moos with the topic “Modifizierte Cellulosen als multifunktionelle Hilfsstoffe in schnell zerfallenden Tabletten”
 03. – 07. 2007 Supervision of the master thesis of K. Gloor with the topic “UICEL als innovativer Hilfsstoff in schnell zerfallenden Tabletten”

Poster and Presentations

09. 2008 Poster presentation “Modified Celluloses as Excipients in Fast Dissolving Tablets”, 68th FIP World Congress of Pharmacy and Pharmaceutical Sciences, Basel, Switzerland
 08. 2008 Oral presentation “Excipients in Fast Disintegrating Tablets”, IPS Workshops pre-satellite to the 68th FIP World Congress of Pharmacy and Pharmaceutical Sciences, Basel, Switzerland
 04. 2008 Poster presentation “Compressibility and Compactability of Different Batches of Modified Cellulose”, 6th World Meeting on Pharmaceutics, Biopharmaceutics and Pharmaceutical Technology, Barcelona, Spain

CURRICULUM VITAE

During my studies I attended lectures given by

Aebi, U., Anselmetti, D., Arber, S., Beier, K., Berger Büter K., Betz, G., Bickle, T.A., Bienz, K.A., Boelsterli, U., Boller, Th., Bongartz, G., Brenner, A., Brenner, H.R., Dopfer, O., Drewe, J., Eberle, A., Engel, A., Engel, J., Engel, T., Erb, P., Ernst, B., Folkers, G., Gehring, W.J., Gescheidt, G., Grzesiek, S., Guentert, T.W., Güntherodt, H.-J., Hauri, H.-P., Hauser, P., Hersberger, K., Huber, H., Huwyler, J., Im Hof, H.-C., Imanidis, G., Jenal, U., Keller, W., Kessler, M., Kiefhaber, T., Körner, Ch., Krähenbühl, St., Kunz, D., Leuenberger, H., Lüdin, E., Lüthi, A., Marrer, St., Mayans, O., Meier, B., Meier, Chr., Meier, Th., Melchers, F., Meyer, J., Meyer, U.A., Monard, D., Mühlebach, St., Müller, Hj., Müller, J., Müller, S., Neri, D., Otten, U., Pfeleiderer, G., Rehmann-Sutter, Ch., Reichert, H., Rogers, S., Rolink, A., Rüegg, M., Schaffner, W., Schirmer, T., Schlienger, R., Schmid, B.J., Schmid, V., Scholer, A., Schönenberger, Ch., Seelig, J., Seelig-Löffler, A., Séquin, U., Sick, I., Spiess, M., Spornitz, U.M., Stoeckli, E., Strazewski, P., Vedani, A., Wessels, H.-P., Wormser, R., Zaugg, Ch., Zuberbühler, A.